University of Strathclyde

Department of Naval Architecture and Marine Engineering

"Performance-Based Damage Survivability of Passenger Ships and Design Implications"

PhD Thesis

Nikolaos Tsakalakis

2012

Copyright statement

This thesis is the result of the author's original research. It has been composed by the author and has not been previously submitted for examination which has led to the award of a degree.

Signed: *Date:*

Acknowledgements

Nothing is possible without help so I would like to thank, first of all, Professor Dracos Vassalos for assigning me with this task, trusting that I could and would bring this matter to a conclusion and guiding me throughout the process. The University of Strathclyde and the Department of Naval Architecture and Marine Engineering for the opportunity and funding to undertake this task and the administration staff for all their help throughout the years of study. Special thanks to my colleagues at the Ship Stability Research Centre and the Department for their guidance, support, compassion and friendship. I would also like to thank my dear Kalliopi for believing in me when needed the most. Last but certainly not least, the biggest gratitude I owe to my parents and brother for their support and understanding through turbulent times and for their guidance and sacrifice so I could make this true. This thesis is dedicated to them.

Abstract

The introduction of the probabilistic framework for damage stability, namely SOLAS 2009, introduced in 1st of January 2009 was a step change in regulation history and subsequently in Naval Architecture as a whole industry. The industry, as well as the academia though, was caught unprepared for such a ground breaking change, leading to confusion and retrospectively wrong decisions and misconceptions. It has been proven that survivability is not predicted accurately by the SOLAS s-factor and that harmonisation could not actually work. Furthermore it is believed, and thus still dealt with by deterministic means, that the water on deck problem has not been resolved. To this end, the focus in this study is on passenger vessels. An attempt has been made to highlight not only the shortcomings of the probabilistic framework but also the sheer benefits from utilising such a method. SOLAS 2009 has been benchmarked against conventional methods so as to prove the later. More specifically it has been shown how the survivability of a given damage scenario can be accurately predicted and how time to capsize can actually be related to survivability in waves. In order to achieve this, established concepts like the critical significant wave height have been revised. Moreover, the proposed modifications of the s-factor can link it directly to performance-based standards such as Safe-Return-to-Port. Finally, it has be demonstrated how, when freed of its "childhood" illnesses, the probabilistic framework can provide with an irreplaceable, handy tool with which to make goal-based design and really exploit all the hidden potential leading to safer and more functional ships.

Table of Contents

List of Figures

List of Tables

Chapter 1 – Preamble

1 Preamble

Ship design seems to be evolving. In the past few years, it has changed to incorporate innovation at the highest possible degree. In such a competitive market, the industry is keen on applying new technologies even if they're still in an experimental stage of development. The race is on towards finding the tools that would provide the means to measure the performance of each and every component of the ship in order to optimise it. Production, operation, cost, everything has gone under the designer's magnifying glass. Fortunately, so has safety. Following a considerable campaign from major players in the past decade, safety is now considered to be another design objective and not a constraint. In other words, there are now safety goals. Inevitably, questions like "what is the state of the art?", "are the tools available accurate?", "what should be considered as safe enough?" are common among others. There is great effort being done towards answering all these and this work is bound to provide a more accurate tool for measuring safety in the design level, hopefully supplementing an effort that started in the 1960s with Wendel's introduction of the probabilistic framework for ship subdivision [48].

"Subdivision of ships" evolved into SOLAS 2009, a regulation that all new ships would have to comply with as from 1st of January 2009. It is a probabilistic framework for ship subdivision and stability unlike Wendel's framework that was designed to address only subdivision. In its current form it is essentially a goal-based framework according to which the ship's Index-A need to meet a required standard. The fact that it is named an "index", conveniently hides its true nature from an industry that seems would rather not know the truth. Index-A is a summation of the products of

the probability of a damage event to occur times its expected consequences. Thus, this is by definition risk [34], which makes Index-A a measure of the ship's risk to flooding or, as more recently named, vulnerability to flooding [14]. Although a huge leap forward from previous regulations that dealt with safety in an immature, deterministic manner, SOLAS 2009 does not come without flows of its own. To begin with, components that contribute to overall risk to flooding are omitted, most notably grounding. It has been observed that grounding is 4 times more frequent [18] than flooding thus, although probability of loss due to grounding is not as high as collision it could as well prove to be just as onerous. In addition to omitting grounding it is arguable whether what is indeed represented by Index-A is done so correctly. Studies carried out just before SOLAS 2009 was to come to force, revealed a number of misconceptions and deficiencies in its components [45] and more are still revealed to this day. It is a very complicated concept and even the very people that promoted SOLAS 2009 are only just beginning to scrape the surface of its potential. From the two components of Index-A, probability and consequences, the latter turned out to be unable to deal with the complexity of problems associated with modern passenger vessels. Not only it could not represent survivability accurately but also what it stands for is vague, to say the least.

The s-factor (the survivability or consequences component) is measured in a scale of 0 to 1. While 0 means no survivability at all, 1 means nothing robust. The way it has been formulated, s=1 means that if the ship suffers the given damage scenario, it has a 50% probability to survive in sea-states of at least 4m for 30 minutes [30]. Considering the ensuing link between survival (or critical) wave height and time to capsize that has been modelled in this thesis, expressing all damages with the s-factor without any explicit reference

to survival wave height, is hiding a lot of information from the designer, or indeed, the regulator and the operator.

To this end, this work is aiming at overcoming these shortcomings as well as identifying any other potential drawbacks in the way SOLAS 2009 has been constructed and proposing viable alternatives.

Chapter 2 – Objectives

2 Objectives

- To evaluate the available first principles and analytical performance-based assessment methods towards identifying the most appropriate for use in this study.
- To estimate the level of safety imposed by previous and current regulatory instruments and specifically the adequacy of the required index –R– of SOLAS 2009.
- To develop and validate a generalised and consistent analytical formulation for evaluating explicitly the vulnerability of passenger ships (Ro-Pax and cruise ships) to collision and grounding damage and to WOD-problem by adopting a Unified Approach that accounts for key design and operational parameters within a probabilistic framework.
- To elucidate this vulnerability in the design and operation of typical ship designs and operational profiles.
- To undertake parametric studies to develop passive (design) and active means (operational practice) to risk-manage damage vulnerability.
- To make suitable recommendations for the design, operation and regulation of passenger ships.

Chapter 3 – Critical review

3 Critical review

From a basic Naval Architecture perspective, the most fundamental goal to be achieved is for a ship to remain afloat and upright, especially so after an accident involving water ingress and flooding. Regulations to address the former focus on subdivision and the latter on damage stability, even though more recent regulatory instruments tend to cater for both issues concurrently. The first Merchant Shipping Act of 1854 is the first known legal requirement addressing safety at sea concerning watertight bulkheads, leading eventually and after heavy loss of life (notably the sinking of the Titanic on 14 April 1912 and the loss of some 1,500 lives providing the catalyst for the adoption on 20 January 1914 of the first International Convention for the Safety Of Life At Sea), wars and other “ills” to the adoption of the first internationally agreed system of subdivision in SOLAS 1929. The first damage stability requirements, on the other hand, were introduced following the 1948 SOLAS Convention and the first specific criterion on residual stability standards at the 1960 SOLAS Convention with the requirement for a minimum residual GM of 0.05m. This represented an attempt to introduce a margin to compensate for the upsetting environmental forces. It is worth mentioning that a regulation on "Watertight Integrity above the Margin Line" was also introduced reflecting the general desire to do all that was reasonably practical to ensure survival after severe collision damage by taking all necessary measures to limit the entry and spread of water above the bulkhead deck.

The first probabilistic damage stability rules for passenger vessels, deriving from the work of Kurt Wendel on “Subdivision of Ships” [48] were introduced in the late sixties as an alternative to deterministic requirements

of SOLAS '60, in the belief that this represented a more rational approach to addressing damage stability. However, there's evidence to suggest that common sense is hardly the driving force behind rule making for damage stability, with accidents continuing to provide the main motivation. Emphasis has primarily been placed on reducing the consequences, i.e., on cure rather than prevention. The prevailing situation can be drastically improved through understanding of the underlying mechanisms leading to vessel loss and to identification of governing design and operation parameters to target risk reduction cost-effectively. This, in turn, necessitates the development of appropriate methods, tools and techniques capable of meaningfully addressing the physical phenomena involved but it was not until the early 90s when dynamic stability pertaining to ships in a damaged condition, was addressed by simplified numerical models, [38]. The subject of dynamic ship stability in waves with the hull breached and also of the probability of surviving such scenarios (damage survivability), only received the deserved attention following once again a tragic accident, this time the one of Estonia in 1994. Repercussions of that led to a step change in the way damage stability and survivability are being addressed, namely by assessing the performance of a vessel in a given environment and loading condition on the basis of first principles.

In parallel, motivated by the compelling need to understand the impact of the then imminent introduction of probabilistic damage stability regulations on the design of cargo and passenger ships and the growing appreciation of deeply-embedded problems in both the rules and the harmonisation process itself (achieving unified rules for all types of vessels), an in-depth evaluation and re-engineering of the whole probabilistic framework was launched through the EC-funded project HARDER, [4]. In this respect, HARDER

became an IMO vehicle carrying a major load of the rule development process and fostering international collaboration at its best – a major factor contributing to the eventual success in achieving harmonisation and in proposing a workable framework for damage stability calculations in IMO SLF 47. Deriving from developments at fundamental and applied levels in project HARDER as well as other EU projects such as NEREUS [20], ROROPROB [24] and SAFEVSHIP [10] and other international collaborative efforts (work by the Stability in Waves Committee at the International Towing Tank Conference from 1996 onwards, e.g., [13]), a clearer understanding of damage stability and survivability started to emerge together with confidence in the available knowledge and tools to address the subject matter effectively and with sufficient engineering accuracy. All these efforts provided the inspiration and the foundation for SAFEDOR [26], which offered the opportunity for consolidating contemporary developments on damage survivability, thus rendering implementation possible even at concept design level. The knowledge gained can now be used to address critically all available regulatory instruments and to foster new and better methodologies to safeguard against known design deficiencies in the first instance, until safer designs evolve to reflect this knowledge, [40], [45], [33].

However, adopting probabilistic rules in the maritime industry has had a more profound effect, the results of which are yet to be fully appreciated. Surprisingly, the biggest influence so far is seen at the birth place of prescription: "The future is Risk-Based" was proclaimed at the International Maritime Organization (IMO) post-HARDER (2002) and goal-setting-performance-based approaches are claimed to be the new face of safety. What is known as Safe Return to Port (SRtP) of SOLAS 2009, enforceable on every passenger vessel newbuilding and on special primrose ships over

120m in length, will challenge everything known and done about safety. The new regulations represent a step change from the current deterministic methods of assessing subdivision and damage stability. The old concepts of floodable length, criterion numeral, margin line, 1 and 2 compartment standards and the B/5 line are disappearing whilst contemporary developments adopt a more holistic approach to addressing damage survivability. This entails design and operational measures ranging from consideration of all conceivable (statistical, experiential, judgemental) damage scenarios to deal with subdivision, dynamic damage stability in all feasible loading conditions and environments, residual functionality of essential systems onboard post-damage, evacuation and rescue and onboard decision support systems. Moreover, such considerations encompass the principal hazards (flooding and fire) over the life-cycle of the vessel, targeting cost-effective safety as a key design objective, alongside other conventional design objectives.

Clearly, the obvious need for a holistic approach using knowledge in all its forms became all too compelling, driving industry and academia into an unprecedented frenzy of activity and developments that could only stop with a credible solution to the damage stability problems, particularly for passenger ships. With monumental effort over the past two decades, the end of this tunnel is considered to be within reach.

3.1 Damage Ship Stability Fundamentals

The approach that has attracted considerable research interest over the recent past is based on rigid body dynamics, aiming at achieving a balance between simplicity and meaningful representation of physics. Here, the mass of floodwater in the ship hull is treated as a pendulum attached to the ship, with its mass located at the centre of the fluid volume, which in turn is found from the intersection between tank geometry and fluid free surface, the latter assumed to be flat. The fluid free surface is either assumed to remain parallel to the sea level, e.g. Vassalos et al [37], [36], de Kat [17] or to be moving in accordance with some basic motion mechanism, e.g. Papanikolaou et al, [21], [49] and Jasionowski, [15]. This section offers a brief overview of the mathematical model deriving from this approach, including the generalised ship motions and floodwater motion mechanism with some discussion on validation and benchmark studies and focus on issues remaining unresolved.

3.1.1 Ship motions

The equations describing damaged ship behaviour are derived from fundamental motion principles: the law of conservation of linear and angular momentum. The law initially applied to rigid bodies, has also been extended to the internal fluid mass, resolved in a body-fixed system of reference, as shown in Figure 3-1. Rigorous derivation leads to a set of 6 scalar equations for linear and angular motions. Of these, the three equations for angular motions are presented here in vector form (3-1). A detailed explanation of all the relevant terms and of the model itself can be found in Jasionowski, [15].

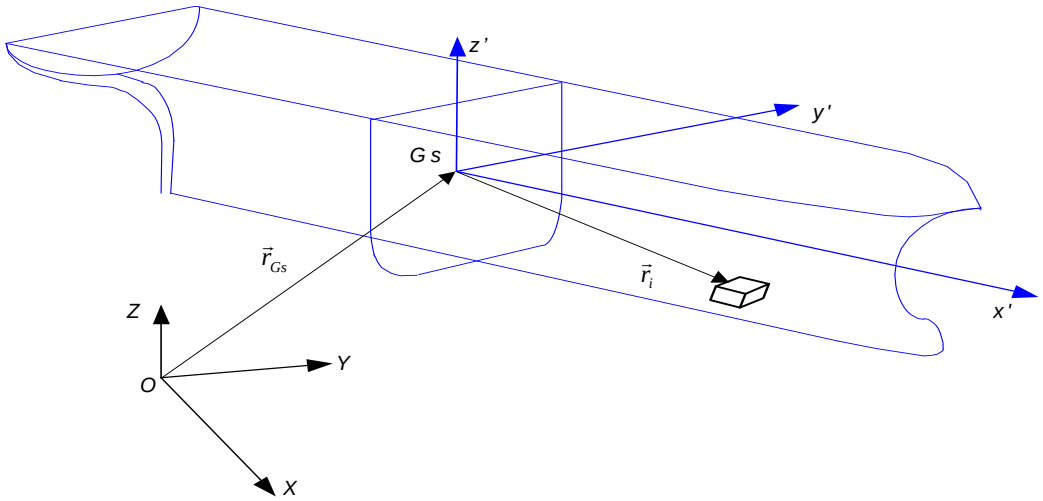

Figure 3-1: Coordinate system of the intact vessel

Coordinate system is fixed to the centre of gravity of the intact vessel

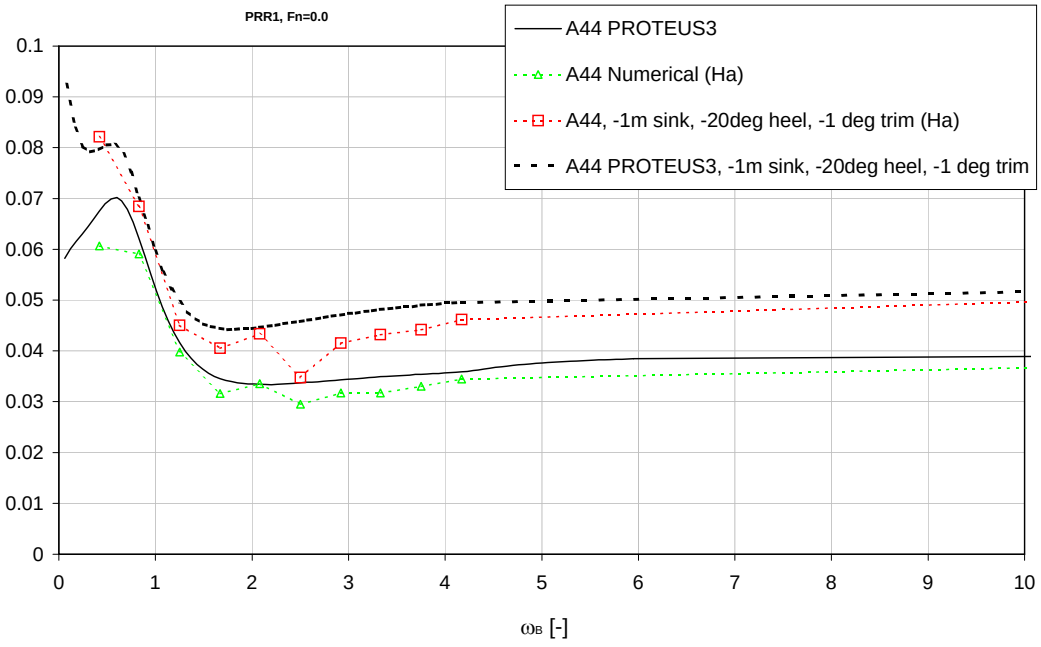

Figure 3-2: Dimensionless roll added moment

For 3D hull form - PRR1 from HARDER [4]; effect of –1m sinkage, -20deg heel and –1deg (aft) trim, derived by strip theory and 3D panel methods at Fn=0.0

$$(I'_s + I'_w) \cdot \frac{d}{dt}\vec{\omega} + M_w \cdot \left[\vec{r}'_w \times \left[\frac{d}{dt}\vec{v}'_{Gs}\right]\right] +$$

$$+M_w \cdot [(\vec{\omega}' \cdot \vec{r}'_w) \times \vec{v}'_w] +$$

$$+M_w \cdot \left[\vec{r}'_w \times \left[\frac{d}{dt}\vec{v}'_w + \vec{\omega}' \times (\vec{v}'_{Gs} + \vec{v}'_w)\right]\right] + \qquad (3\text{-}1)$$

$$+\frac{d}{dt}M_w \cdot [\vec{r}'_w \times (\vec{v}'_{Gs} + \vec{v}'_w)] +$$

$$+\left(\frac{d}{dt}I'_w\right) \cdot \vec{\omega}' + \vec{\omega}' \cdot [(I'_s + I'_w) \cdot \vec{\omega}'] = \vec{M}'_{Gs}$$

$$\vec{F}, \vec{M}'_{Gs} = \vec{F}_{Gravity} + \vec{F}_{F-K,Restoring} + \vec{F}_{Radiation} + \vec{F}_{Diffraction} + \vec{F}_{Manoeuvring,Rudder} + \vec{F}_{Drift,Current,Wind,Viscous}$$

Where:

$\vec{F}_{F-K,Restoring}$	Direct integration of static pressures on actual geometry
$\vec{F}_{Radiation}$	Convolution techniques
$\vec{F}_{Diffraction}$	Spectral techniques
$\vec{F}_{Manoeuvring,Rudder}$	Empirical formulae
$\vec{F}_{Drift,Current,Wind,Viscous}$	Empirical formulae

The right hand side of the equation, $\vec{M}'_{Gs}$, and the respective force vector $\vec{F}$ of the rectilinear motions, represent all the external forces and moments acting on the vessel, expressed in a body-fixed system of reference, $G_S xyz$, located at the ship centre of mass. These forces/moments are predicted with conventional Naval Architecture methods. The Froude-Krylov and restoring forces and moments are integrated up to the instantaneous wave elevation; the radiation and diffraction forces and moments are derived from linear potential theory and expressed in time domain using convolution and spectral techniques, respectively. The hull asymmetry due to floodwater is taken into account by a database approach, whereby the hydrodynamic coefficients are predicted beforehand, and then interpolated during the simulation, as illustrated in figure 3-2.

The second order drift forces, wind and current effects and other forces of viscous origin are also catered for, at present based on parametric formulations. Naturally the gravity force and moment vectors correspond to ship and floodwater weights. A correction for viscous effects on roll motion is applied based on an established empirical method proposed in [5], where the viscous damping moment is divided into several components: friction, eddy shedding, lift, wave and bilge keel and the total force is obtained by a superposition of all these components. However, the proposed method, representing the non-linear viscous damping as an equivalent linear coefficient at the roll natural frequency, remains a function of roll amplitude, which cannot be known a priori and hence not suitable for application to time-domain simulation in random seas. In this respect, an engineering approximation has been proposed in [15], whereby a discrete piece-wise constant treatment of the linearised coefficient is used with the coefficient evaluated at the wave spectrum peak frequency and for an amplitude

corresponding to the amplitude of the last half-roll cycle. In this approach the viscous roll damping will vary with time, constantly adjusting to roll amplitude. The whole system (3-1), after re-arranging into a matrix form as a set of twelve differential equations of the first order, is solved for position in space of the centre of gravity of the intact ship $\vec{r}_{Gs} = \int \vec{v}_{Gs} \cdot dt$ and three rotations through a 4th order Runge-Kutta-Feldberg integration scheme with a variable step size.

3.1.2 Flood water sloshing

Undetermined in equations (3-1), remain the relevant vectors for floodwater location, velocity and acceleration, $\vec{r}'_w$, $\vec{v}'_w$ and $\frac{d}{dt}\vec{v}'_w$, respectively. These are the quantities that must be derived from a model representing the sloshing water phenomenon. When CFD techniques are used, these vectors and related forces and moments can be derived from integration of pressure due to fluid motion. Here, however, a simplification mentioned in the foregoing, has been adopted – see figure **3**-3. According to this, a lumped mass model, the initial concept of which was presented by Papanikolaou et al [21], has been developed treating the floodwater as a free point-mass moving due to the acceleration field and restrained geometrically by predetermined potential surfaces of the centre of buoyancy for given amounts of floodwater, FMPS (Free Mass in Potential Surface), as shown in figure **3**-3 and figure **3**-4. This model, derived from simple rigid body motion consideration, similar to the one leading to equations (3-1), is presented as a set of equations (3-2).

$$\begin{cases} \frac{d}{dt}\vec{r}'_w = \vec{v}'_w - (\vec{v}'_w \cdot \vec{n}') \cdot \vec{n}' \\ \frac{d}{dt}\vec{v}'_w = \vec{a}'_f - (\vec{a}'_f \cdot \vec{n}') \cdot \vec{n}' \end{cases} \tag{3-2}$$

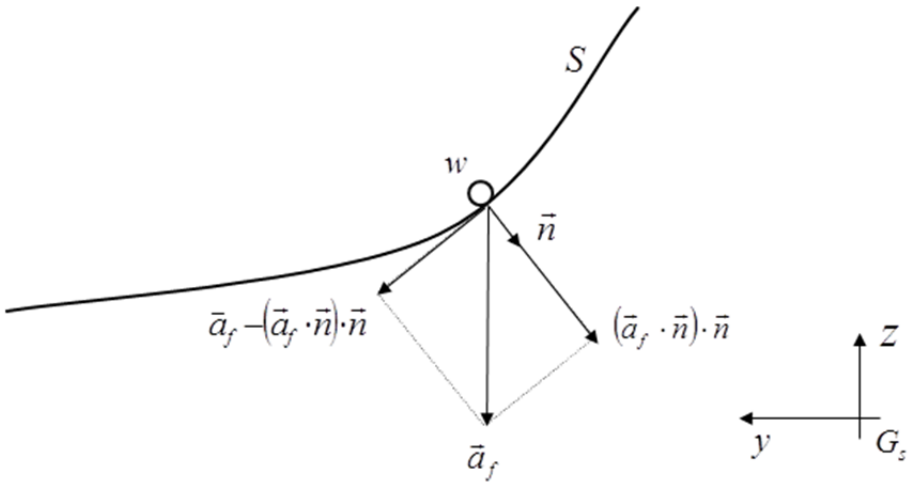

Figure 3-3: Sloshing model simplification

Fluid particle "w" (centre of buoyancy) in acceleration field $\vec{a}_f$ moving on the potential surface S; all vectors are resolved in the $G_S xyz$ system of reference.

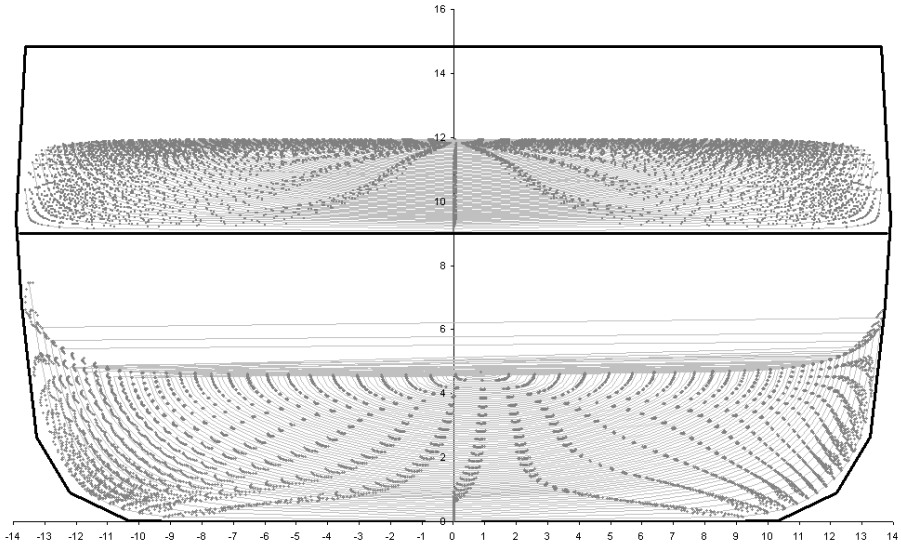

Figure 3-4: Geometric constraints for motion of centre of buoyancy of floodwater

Applies to symmetrical and asymmetrical compartments.

The total forcing acceleration vector is shown in equation 3-3 where $\vec{a}_s$ is a ship motion-related acceleration vector expressed in a body-fixed system of reference (see eq. 3-4).

$$\vec{a}'_f = \vec{g}' - \vec{a}'_s - 2 \cdot \vec{\omega}' \times \vec{v}'_w - \mu^* \cdot \vec{v}'_w \tag{3-3}$$

$$\vec{a}'_s = \frac{d}{dt}\vec{v}'_{Gs} + \frac{d}{dt}\vec{\omega}' \times \vec{r}'_w + \vec{\omega}' \times (\vec{v}'_{Gs} + \vec{\omega}' \times \vec{r}'_w) \tag{3-4}$$

$\vec{n}$ is the instantaneous normal vector to the potential surface of floodwater motion, determined from a damage compartment geometry database. Note that the vector is a function of $\vec{r}_w$ and volume of the fluid. Finally, μ^* is an artificial coefficient introduced to represent the damping of floodwater motion. This coefficient is assigned an ad hoc value derived from experimental data using a simple box-shaped compartment. With the geometric information concerning the tank stored in a database, such as shown in figure **3**-4, the model is complete. Equation (3-2) is set up for each flooded compartment within the ship and solved simultaneously with the equations for ship motion.

Having determined fluid motion, the forces and moments due to its displacement can be calculated. For demonstration purposes, the moment vector extracted from equation (3-1) is used and presented in the form of equation (3-5), where three components are distinguished, representing inertial, gravity and non-linear effects and presented in equations (3-6), (3-7) and (3-8), respectively. Note here that the fluid inertia matrix I'_w contains only the inertia of a single point-mass located at a position r'_w in the ship-

fixed system of reference at the centre of gravity, G_s. Since the mass is constant, the terms containing the time derivative of the mass disappear.

$$\vec{M}'_{wat} = \vec{M}'_I + \vec{M}'_g + \vec{M}'_N \tag{3-5}$$

Where:

$$\vec{M}'_I = \vec{I}'_w \cdot \frac{d}{dt}\vec{\omega}' \tag{3-6}$$

$$\vec{M}'_g = \vec{M}'_w \cdot \vec{r}'_w \times \vec{g}' \tag{3-7}$$

$$\begin{aligned} &\vec{M}'_N = M_w \cdot [(\vec{\omega}' \times \vec{r}'_w) \times \vec{v}'_w] + \\ &+M_w \cdot \left[\vec{r}'_w \times \left[\frac{d}{dt}\vec{v}'_w + \vec{\omega}' \times (\vec{v}'_w)\right]\right] + \\ &+\frac{d}{dt}\vec{I}'_w \cdot \vec{\omega}' + \vec{\omega}' \times [(I'_w) \cdot \vec{\omega}'] \end{aligned} \tag{3-8}$$

3.1.3 Floodwater ingress/egress

Water ingress/egress affects the dynamics of a damaged ship in two distinct ways: firstly, the influence on ship hydrodynamics and through coupling of floodwater dynamics with ship dynamics the overall dynamic behaviour; secondly, and the most considerable consequence of flooding in a typical Ro-Ro scenario, is vessel capsize or sinking as a result of water accumulation, as shown in figure **3**-5.

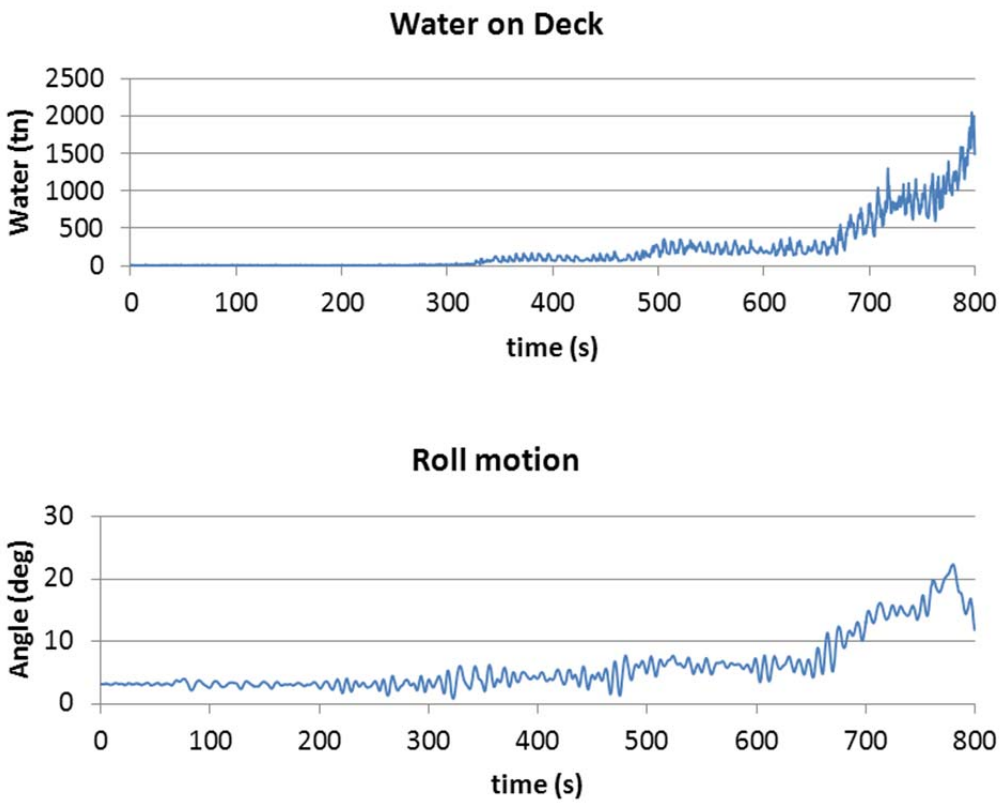

Figure 3-5: Impact of water on deck on capsize of Ro-Ro

It is clearly visible that once the vessel starts taking water in the car deck, heel increases gradually in the beginning and rapidly later until it capsizes.

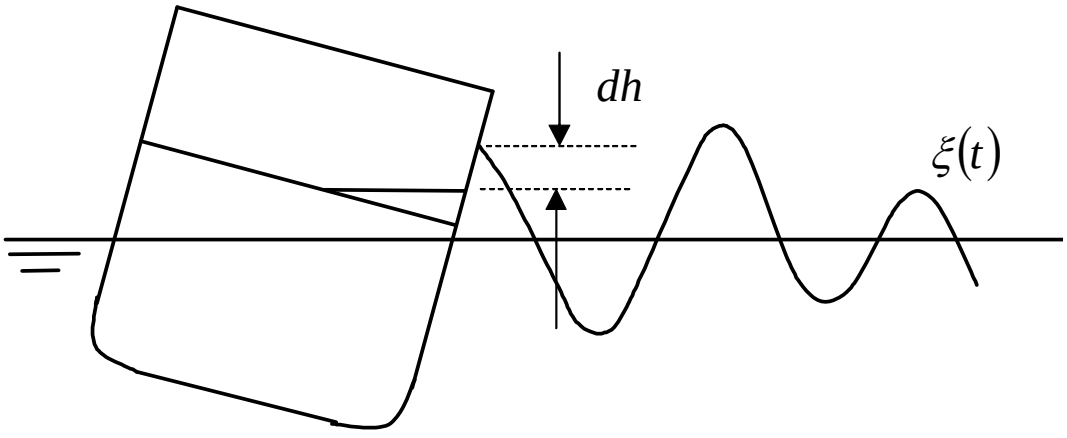

Figure 3-6: Water ingress model

This is a simplified depiction of the model used for water ingress in a Ro-Ro vehicle deck.

Modelling of ingress/egress should be performed to the highest accuracy attainable. However, knowledge on the mechanics of water flow through the damage opening of a moving ship in the presence of incident, diffracted and radiated waves, is limited. Therefore, the fundamental Bernoulli fluid momentum equation is used most commonly, as depicted in figure **3**-6, with all the unknown flow physics encapsulated in a single averaged flow loss coefficient K derived from experiments. The mathematical expression is shown in equation 3-9.

$$Q = K \cdot A \cdot \int_{t} \sqrt{2 \cdot g \cdot dh} \cdot dt \tag{3-9}$$

Where:

K: Flow loss coefficient

A: Submerged area of damage opening

Although this model can prove accurate in many cases, it does not resolve the problem of not knowing the instantaneous water ingress/egress in case of marginal survivability. This directly affects the accuracy of estimations of how long it takes a vessel to sustain the action of waves whilst undergoing progressive flooding that leads to eventual capsize (time to capsize). Considering the subtlety of new regulations for SRtP, the accuracy of predictions of ship survivability including the time it takes for a vessel to capsize from the instant the hull is breached, is of paramount importance.

3.2 Current developments

First-principles tools are still struggling to deliver the necessary accuracy and level of detail within a time frame that can be routinely utilised by industry. Thus contemporary regulatory developments are a step ahead for the first time in Naval Architecture history. This means that concentrated effort is necessary at global level to ensure the safe transition from deterministic to performance-based safety. IMO have expressed their concern whether SOLAS requirements, several of which were drafted before some of the large ships recently built, duly address all the safety aspects of their operation particularly in hazardous situations, calling for a critical review of the safety of large passenger ships. This led the IMO Maritime Safety Committee (MSC) to adopt a new philosophy and working approach for developing safety standards for passenger ships. In this approach, illustrated in figure **3**-7 (SLF 47/48), modern safety expectations are expressed as a set of specific safety goals and objectives, addressing design (prevention), operation (mitigation) and decision making in emergency situations with a principal safety goal: no loss of human life due to ship related accidents. The term "Safe Return to Port (SRtP)" has been widely adopted in discussing this framework, which addresses all the basic elements pre-requisite to quantifying the safety level of a ship at sea.

The following elements are specifically addressed:

Prevention/Protection: Emphasis must be placed on preventing the casualty from happening in the first place as well as on in-built safety to limit consequences. Attention must also be paid to the many international regulations addressing prevention of accidents.

Timeline Development: The new focus here is on the timeline development of different events. For the first time in the history of rule-making, it is not only important to know whether a vessel will survive a given casualty in a given loading condition and operating environment but also the time the vessel will remain habitable and the time it takes for safe and orderly abandonment and for recovery of the people onboard.

Casualty Threshold: This advocates the fact that the ship should be designed for improved survivability so that, in the event of a casualty, persons can stay safely on board as the ship proceeds to port. In this respect and for design purposes only, a casualty threshold needs to be defined whereby a ship suffering a casualty below the defined threshold is expected to stay upright and afloat and be habitable for as long as necessary in order to return to port under its own power or wait for assistance. Currently it constitutes part of the design work to determine this value rationally, as it greatly influences the design arrangements.

Emergency Systems Availability / Evacuation and Rescue: Should the casualty threshold be exceeded the ship must remain stable and afloat for sufficiently long time [3 hours recommended] to allow safe and orderly evacuation (assembly, disembarkation and abandoning) of passengers and crew. Emergency systems availability to perform all requisite functions in any of the scenarios considered is, therefore, implicit in the framework. In addition, the ship should be crewed, equipped and have arrangements in place to ensure the health, safety, medical care and security of persons onboard in the area of operation, taking into account climatic conditions and the availability of SAR functions until more specialised assistance is available.

Considering the above, it is worth emphasising that none of the questions arising (survival time; functional availability post-casualty; time needed for abandonment) can be addressed in terms of rule compliance. Nonetheless, achievement of these goals in the proposed holistic, goal-based and proactive approach would ensure safety of human life commensurate with the safety expectations of today, by implicitly addressing all key elements of risk, for total risk (Safety Level) estimation and for direct use in Risk-Based Design, as explained be Vassalos et al. in [44].

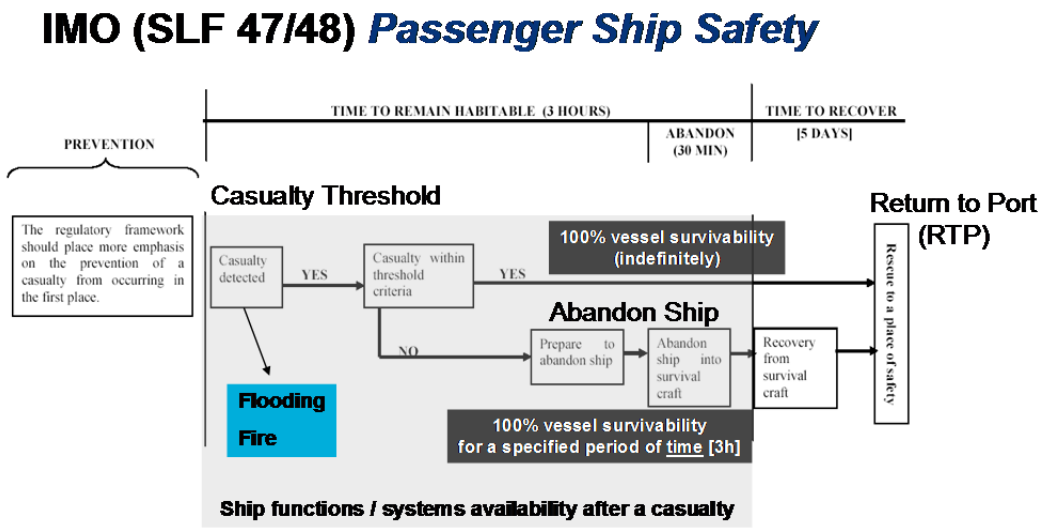

Figure 3-7: The framework of IMO for passenger ship safety

A set of specific safety goals and objectives are expressed with the ultimate goal of safe return to port.

Chapter 4 – Approach adopted

4 Approach adopted

4.1 Preparation and utilisation of results

The main parts of this thesis are shown in figure **4**-1. Firstly, a comparison of the performance-based assessment methods for damage survivability took place. This was done so that it could be decided how each method could be used and if the SOLAS 2009 Index A is an adequate measure of survivability due to the relatively simple way to use. Once this was done the Index A was benchmarked against other regulatory frameworks so as to demonstrate its advantages over deterministic methods of the past and also to identify any drawbacks in need of reconsideration. These first two processes were utilised to carry out the third objective, namely to identify and quantify the vulnerability of modern passenger vessels. Following these two preparatory steps and knowing the flaws of Index A thoroughly it is the time for the s-factor to be revised. The process is described in the following paragraph in detail. Finally when survivability was finalised the results were used to conduct parametric studies in search of ways to limit the vulnerability of passenger vessels.

4.2 Survivability Re-modelling

Survivability re-modelling is separated in two main phases, the experiment and post processing one. Figure 4-2 shows a flowchart of the way work progressed. Due to the tedious nature of the physical and numerical experiments, special attention was given to the previously acquired data to avoid repetitions and most crucially to avoid making the same mistakes. The

dataset had been accused of lack of variety [45] so the collection of vessels for experimentation had to be enhanced as well.

Having obtained the sample vessels and more or less concluded in a methodology for experimentation phase 1 started with numerical experiments. Various parameters that are known to affect ship stability in damage condition were altered so as to attained an as detailed as possible result. With these results at hand a preliminary analysis led to a re-definition of the critical significant wave height as can be seen in chapter 8. The prevailing parameters were also identified so as to avoid confusion and focus the experiments on only the important ones.

Once the important parameters had been identified and critical significant wave height defined the resolution of the experiments was increased so as to get more accurate results and the dataset was enriched with more vessels. Experiments in the towing tank were also carried out so as to verify the results obtained from the numerical experiments.

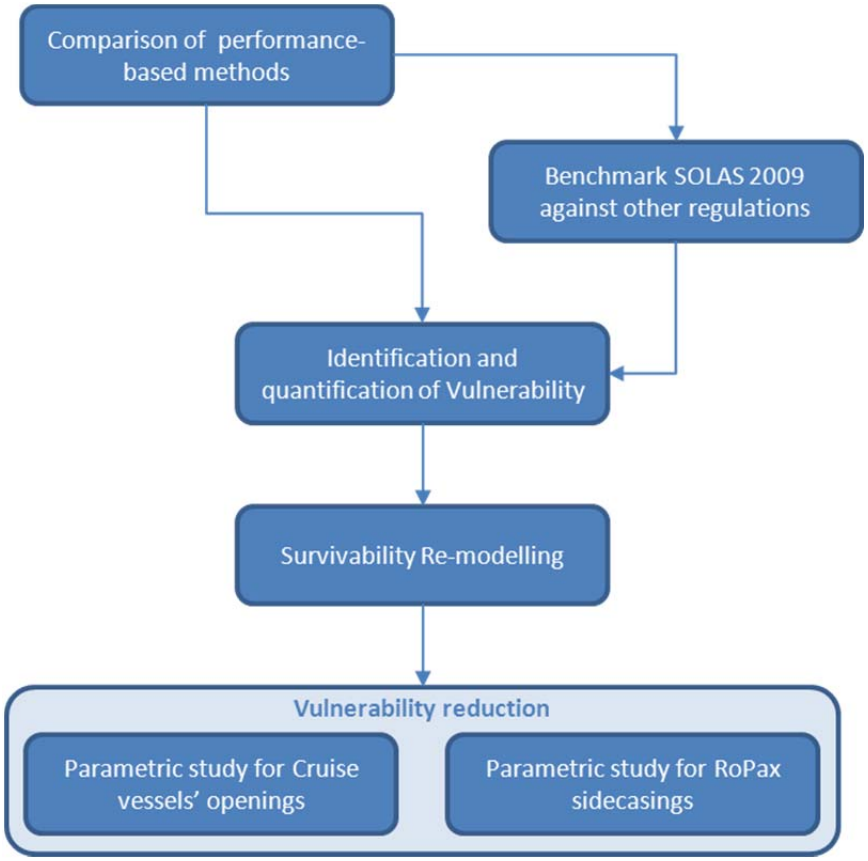

Figure 4-1: Approach adopted

This flowchart shows the steps that were followed in order to accomplish the thesis objectives. The "Survivability Re-modelling" part can be found in detail in the following figure.

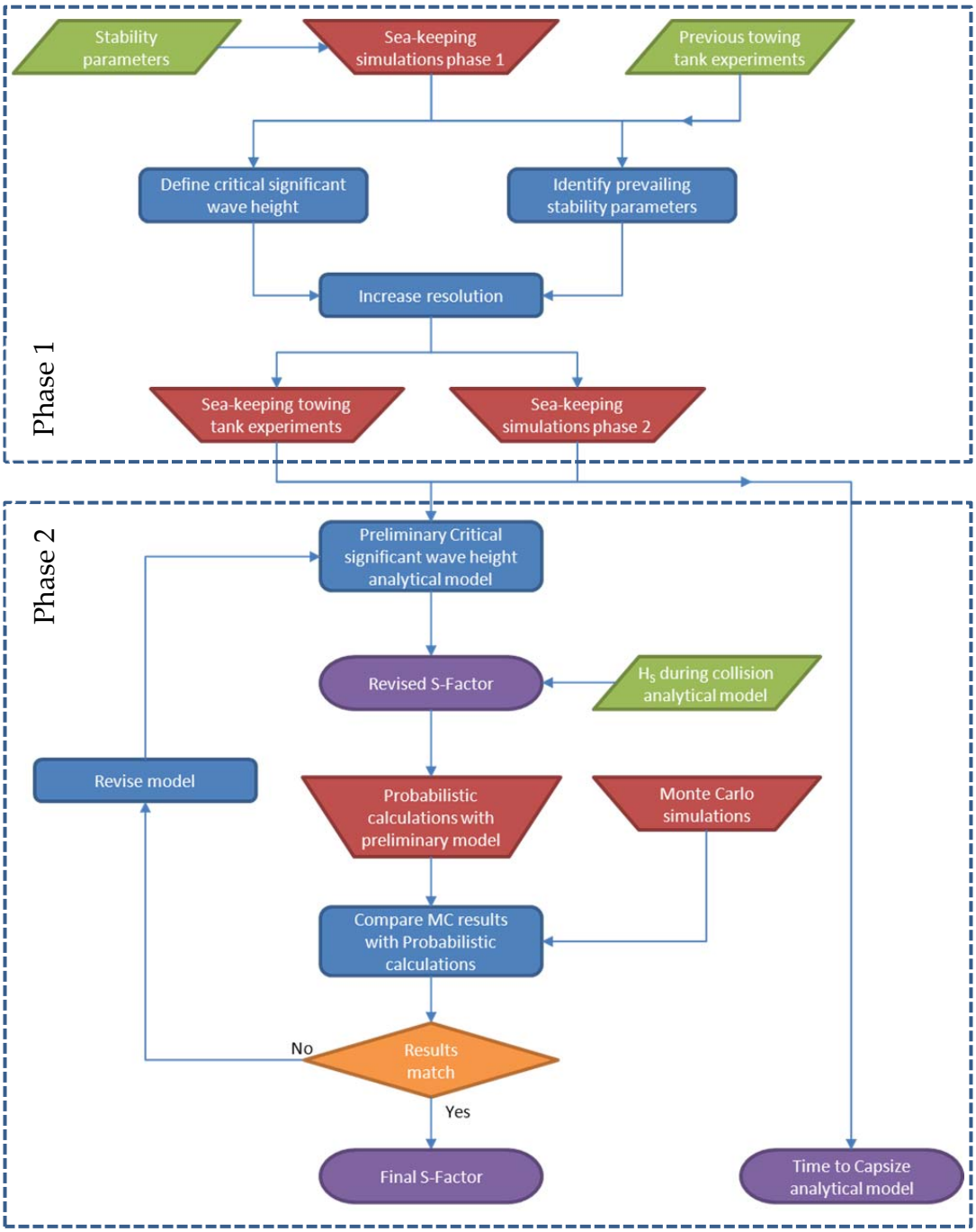

Figure 4-2: Schematic representation of survivability re-modelling

This flowchart shows the basic steps followed and components used in order to amend the SOLAS 2009 s-factor and derive the formulation for time to capsize.

The finalisation of the physical and numerical experiments meant the end of phase 1 and the beginning of post processing – phase 2. The results were used to create preliminary analytical models for critical significant wave height and an analytical model for time to capsize. The critical wave height analytical models were checked for quality of fit to the obtained points and the best ones were converted to s-factor by use of the analytical model for significant wave height during collision [4]. The resulting s-factor was inserted in the methodology for probabilistic calculations of Index A [29] and the result benchmarked against Monte Carlo simulations runs [14] for all the vessels to check consistency with the most accurate method of assessing ship vulnerability to date. After some repetitions and revisions of the critical wave height model the final s-factor occurred.

Chapter 5 – Performance-Based Assessment

5 Performance-Based Assessment

5.1 Introduction to performance – based assessment

Whether the task is design or regulation, there are two roads to follow; deterministic approaches and Performance-Based approaches. Unlike deterministic approaches when design is usually governed by some constraints, a performance-based assessment method allows for an increased level of freedom by means of goal-setting. The added value of Performance-Based methods compared to deterministic ones lies in the fact that instead of only providing information on whether the vessel in question complies with a set of requirements, there is also the potential to provide quantitative results about the performance with respect to specified elements like survivability (i.e. what is the maximum wave height a damaged vessel can withstand) and "evacuability" (i.e. how long does it take to muster and evacuate all passengers on-board) [34]. A motoring world equivalent, speed related, could be a unit from our daily lives like "miles per hour". Without this unit we could state weather a vehicle is fast or not but not how fast or if it is faster than another one in comparison. The difficulty lies at inventing the proper tools that will enable to measure the performance. Once the tools exist, the next challenge is to determine the correct use so the results will make sense. Additionally, Performance-Based Assessment can provide an objective tool for the estimation of the survivability of any vessel, irrespective of which – deterministic or not – regulatory instrument has been used for the vessel's design, build and operation [33].

There are two principal ways of carrying out a performance-based assessment; knowledge intensive methods based on analytical formulations

and first principles. The latest regulatory instrument for damage stability, namely SOLAS 2009, has been developed in this scope and as such can be used as an analytical method for survivability assessment for example [29]. What SOLAS 2009 cannot provide is information regarding the time to capsize. This can be obtained by either another analytical method, namely UGD, developed during the course of European Commission funded project SAFEDOR [25] or numerical simulations. Numerical simulation tools have been in use for decades, ever since the development of modern computers enabled the handling of more complex problems of ship stability in the presence of wind and waves. Following the early work of pioneers like Newton, Euler, Froude, Stokes, Green, Rayleigh and other advances of mostly fundamental sciences, modern approaches to dynamic ship response in random seas were initiated with the advent of spectral analysis. This was followed by the first ship motion theories suitable for numerical computations, introduced in the 50s. Notable advances contributing to developments of intact ship motion prediction tools include: 2D free surface ship hydrodynamics; pioneering calculations of 3D hydrodynamics of a semi-submerged heaving sphere; first successful applications of integral equation techniques in 3D; application of that method for arbitrary 3D bodies oscillating at the free surface; linear motion dynamics using strip theory in 5 DOF with forward speed; other endless variants of strip theory giving way to 3D panel methods at 1st, 2nd and higher orders. The many techniques developed facilitated almost routine analyses for many fluid flow and dynamic phenomena pertinent to ship performance and safety, all focusing on ships in intact condition [43].

It was not until the 1980s and 90s that eventually one of the most difficult problems of dynamic stability pertaining to ship in a damaged condition,

was addressed initially by simplified numerical modelling techniques, dealing with water on deck and the numerical model of damaged Ro-Ro vessel dynamic stability and survivability, Vassalos and Turan, [38], Jasionowski, [15], the latter's development being the code used primarily by the SSRC, namely PROTEUS3 (figure 5-2). The numerical, time domain simulations can provide a more accurate estimation of the survivability in damaged condition but are more costly in terms of both time and effort to perform than analytical calculations. The most widely trusted first-principles method is that of physical tests in the towing tank which is the most demanding one to carry out given the complexity of the models involved and the uncertainty of physical experimentation.

The following sections will provide an overview of the methods mentioned above and all the tools that have been used within this thesis.

5.2 First Principles PBS Assessment methods

5.2.1 Numerical – PROTEUS3

5.2.1.1 PROTEUS3 overview

PROTEUS3 [15] is a state-of-the-art time-domain numerical simulation tool capable of handling complex geometries. Ship hydrodynamics, derived from properties of the intact hull, are based either on asymmetrical strip theory formulation with Rankine source distribution or a 3D source code, both accounting for non-linearities arising from instantaneous variation of the mean ship attitude and large amplitude motions. The effects of floodwater dynamics are described by a full set of non-linear equations derived from rigid-body theory. Floodwater motions are modelled as a Free-Mass-on-Potential-Surface (FMPS) de-coupled system in an acceleration field. Water ingress/egress is based on Bernoulli's equation.

Forces are predicted with conventional for Naval Architecture methods. The Froude-Krylov and restoring forces and moments can be integrated up-to the instantaneous wave elevation or conventional linear approach can be used, the radiation and diffraction forces and moments are derived from linear potential flow theory and expressed in time domain based on convolution and spectral techniques, respectively. The correction for viscous effects on roll and yaw modes of motion is applied based on the well-established empirical methods and the second order drift and current effects are catered for, at present, based on parametric formulations. Naturally the gravity force and moment vectors correspond to ship and floodwater weights. The model includes a non-linear treatment of the hydrodynamic coefficients varying with the vessel mean attitude (heave, heel and trim) using a database

approach. It encompasses the generation of the hydrodynamic coefficients beforehand and uses interpolation between these forces during simulation.

The motion equations are solved for position in space of the centre of gravity of the intact ship and rotations vector through a 4th order Runge-Kutta-Feldberg integration scheme with variable step size.

Since the database generation usually requires extensive computational effort, particular attention has been paid towards enabling easy variation of the centre of gravity of the ship (particularly KG), without the requirement of regenerating the whole database. This has been achieved by formulating the equations of motions in a reference system located at an arbitrary location "A" and not, as is common practice, at the centre of gravity "G" of the ship.

The floodwater motion is modelled as a mass point moving due to the acceleration field and is geometrically restrained by predetermined potential surfaces of centre of buoyancy for given amount of floodwater (FMPS).

5.2.1.2 Utilisation of PROTEUS3 – critical sea-state

Possibly the most important way PROTEUS3 has been used in this study, the search for the critical sea-state has very important information to provide towards understanding the behaviour of a damaged ship in waves. The model comprises of the intact hull, the damaged compartments and the openings. The latter consist of both the damage opening, allowing for water ingress from the sea to the damaged compartments, and the internal openings enabling water transfer from one compartment to others. A sample arrangement can be seen in figure 5-1. The model is subjected to a number of simulations for each sea-state. The ratio of lost runs over the total number of runs for a specific sea-state is the probability of the specific model to capsize

in the specified loading condition in that sea-state for the time of simulation. This probability is extremely important since, if carried out for several consequent sea-states and loading conditions, it gives information on the transition band from safe to unsafe region as shown by Jasionowski et al. in [16] (see figure 5-3). A series of simulations for a specific loading can be found in figure 5-4. A more elaborate description of the capsize band and its properties will be given in chapter “Capsize Band”.

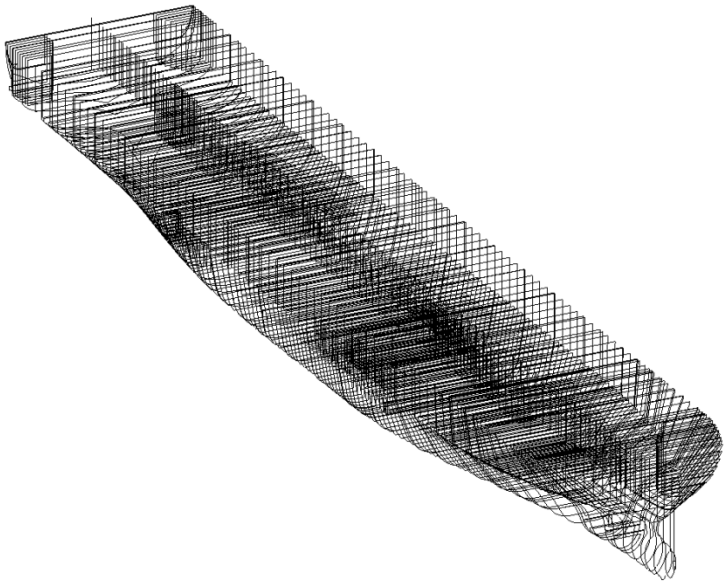

Figure 5-1: RoPax model prepared for simulation in PolyCAD
Software tools like PolyCAD enable the making of high complexity models for testing

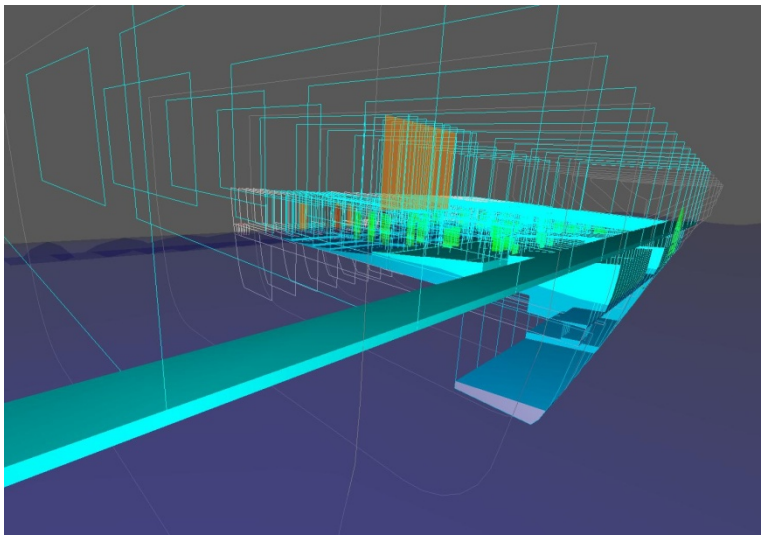

Figure 5-2: Visualization of simulation with PROTEUS3
This picture is taken from a visualisation in Monolax[1] of a simulation of a RoPax vessel. The accumulated water on deck is visible as well as the multiple free surfaces of water in the flooded compartments.

[1] Monolax is an in-house developed visualization software for PROTEUS.

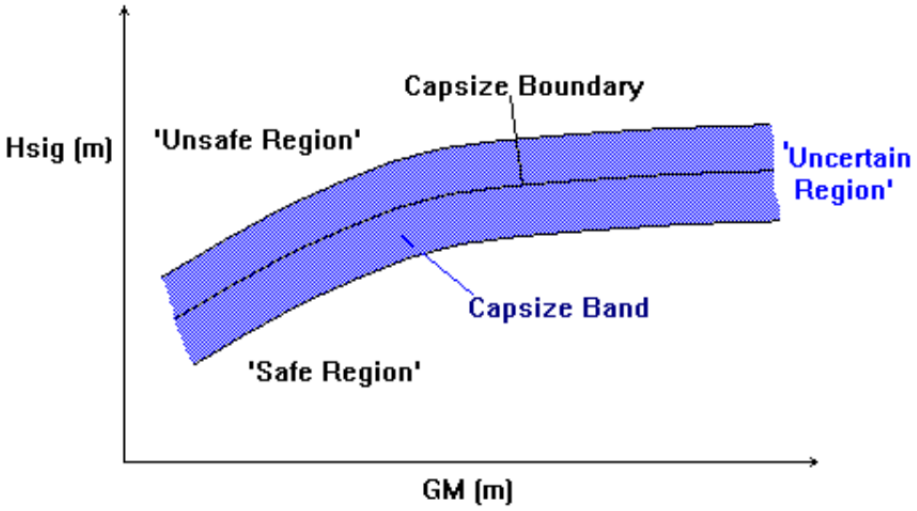

Figure 5-3: Uncertain Region

A schematic definition of the uncertainty band lying between safe and unsafe regions of operation

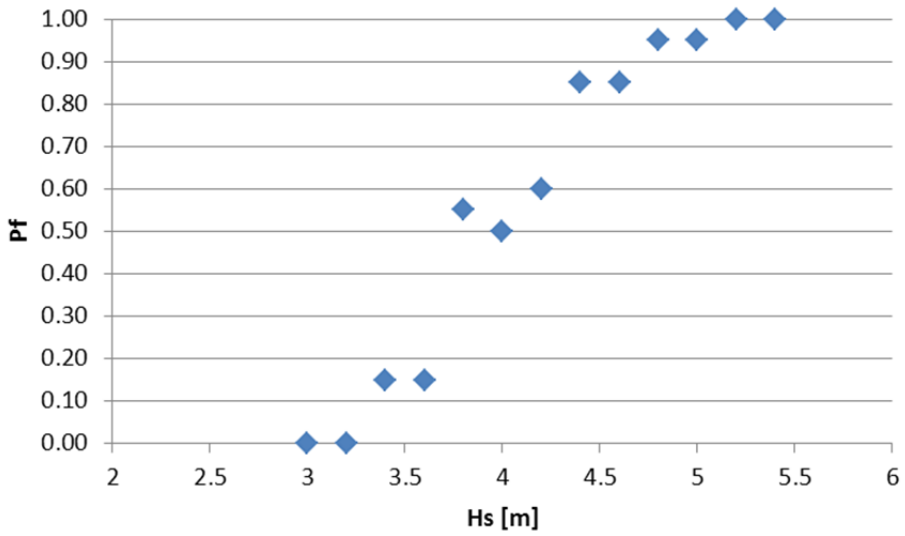

Figure 5-4: Capsize Band

The capsize band shown here is the transition band from safe sea-state (<3.2m significant wave height) to unsafe (>5.2m H_S). Significant wave height is on the horizontal axis while the vertical axis is the probability to capsize (P_f) given sea-state, loading condition and 30 minutes simulation in this case.

5.2.1.3 Utilisation of PROTEUS3 – Monte Carlo simulations

PROTEUS3 can also be used for the estimation of the overall level of survivability from flooding of a ship design. This can be accomplished by running a series of simulations for the study ship in a number of randomly generated damage scenarios. Damage opening size and location as well as environmental conditions are specified for each scenario. A typical value for the number of scenarios is 500, although the higher the number the lesser the uncertainty of the output (figure 5-6). Scenarios are automatically generated using a Monte Carlo sampling scheme. The probability distributions used for this purpose are the same that were used for the development of the P-factor currently in SOLAS 2009 standard (figure 5-5), derived from EU-funded project HARDER [4], although they can be updated, if necessary, to match the latest developments.

The result of a series of Monte Carlo simulations can be seen in figure 5-7. Both the probability density and the cumulative distribution functions for time to capsize are visible. The information acquired from the marginal value of the cumulative distribution function (CDF) is the probability of the vessel to capsize in the time of simulation given a specific loading condition, or the vessel's vulnerability to flooding [14]. The compliment of this value represents the vessel's global survivability.

The results of this method can be used in a multitude of ways, from directly getting a vessel's survivability to validating analytical approaches like those presented in the following paragraphs. The downside is the immense time and resources needed for calculation, albeit not quite as much as physical tests.

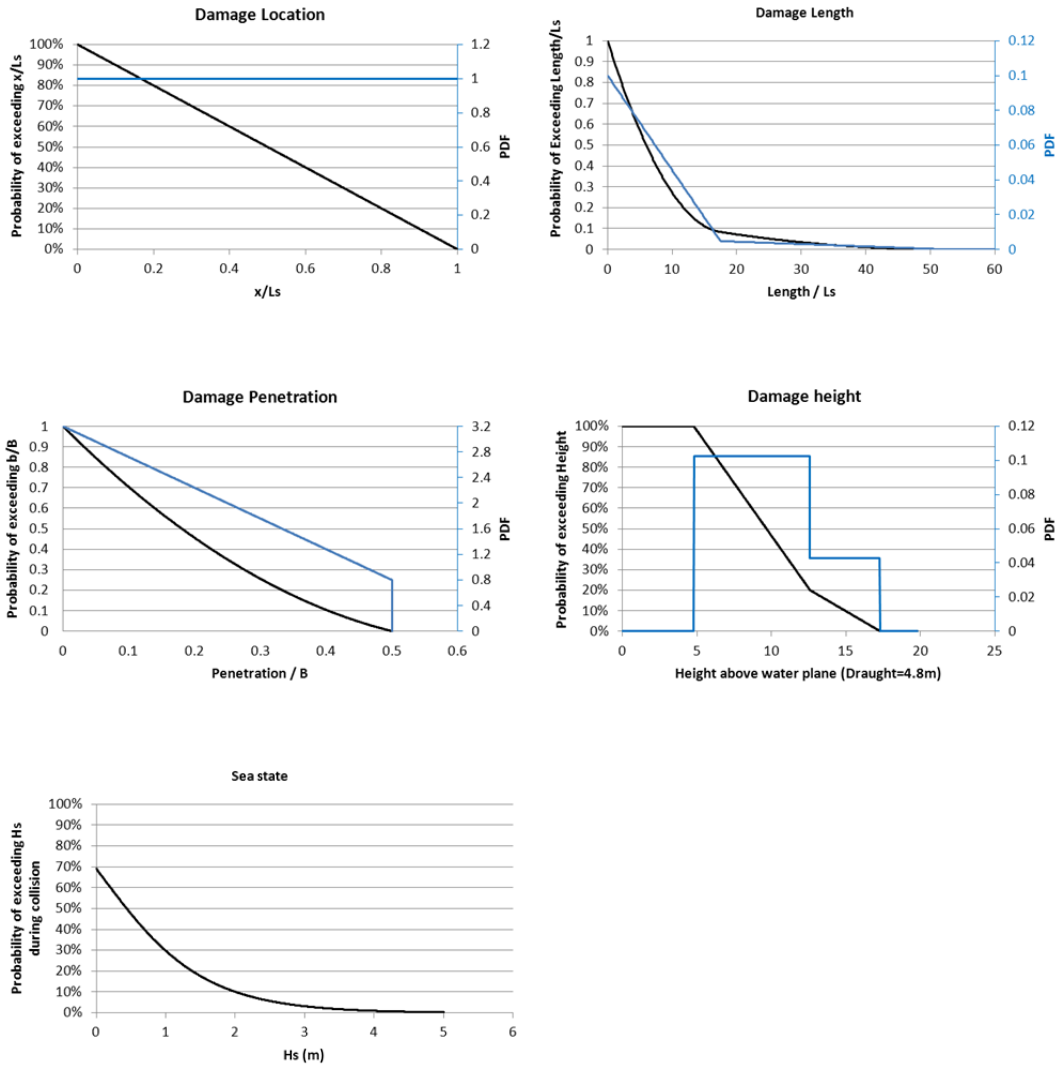

Figure 5-5: Damage characteristics

The above shown statistical distributions have been obtained through project HARDER and were used for the derivation of the current P-factor in SOLAS 2009. They are used by PROTEUS3 for the automatic generation of equal probability of occurrence damage scenarios by Monte Carlo sampling.

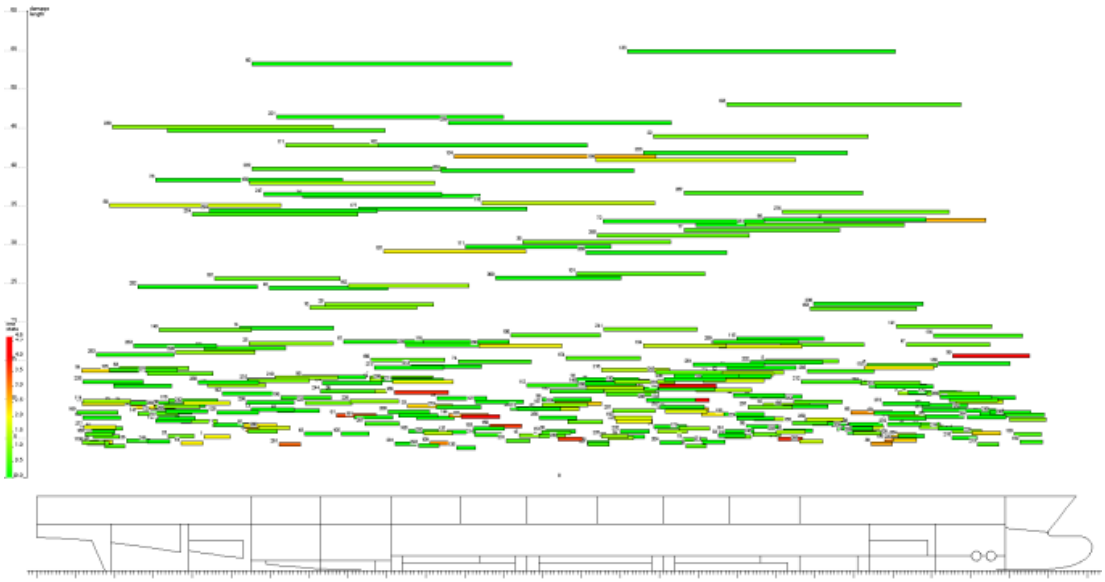

Figure 5-6: Damage scenarios.

In this example of a simulation setup for a 200m RoPax vessel, 300 scenarios have been generated by means of Monte Carlo sampling. The scenarios are located according to damage length and location and colour coded according to sea state

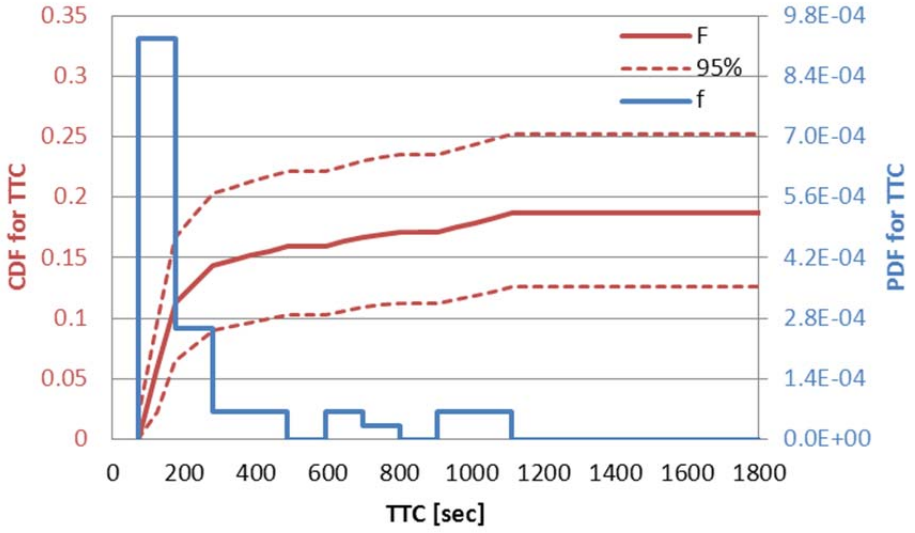

Figure 5-7: Result of a series of Monte Carlo simulations.

The bar chart shows the probability density function (PDF) for time to capsize. The curves show the cumulative distribution function for time to capsize and the confidence intervals. The result is given a specific loading condition and 30 minutes simulation time.

5.2.2 Physical – Towing tank testing

The most "ancient" of the testing techniques, towing tank testing, is still regarded by the community as the most trustworthy. Towing tank tests have been used over the centuries for many reasons, from stability tests to ship response in waves, resistance and propulsion and manoeuvring. Some of the most remarkable breakthroughs have been made in towing tanks and tanks today have extended their activities to include more modern problems. It was not until relatively recently though that damage stability problems were tackled in the towing tank.

Nowadays physical testing is mostly used in damage stability to validate numerical results due to the prohibiting costs involved with it. As such, the same experiments can be reproduced in the tank, like capsize transition band, transient flooding in complex geometries and progressive flooding. The models range from simple parallel section bodies for experimentation on properties of the damaged ship, like roll damping [2] to exact miniatures of the largest cruise ships in operation today. This inevitably involves not only a high level of skill and precision but also flexibility to a degree that not many tanks in the world have the capability to accomplish (figures 5-8 and 5-9).

A typical testing schedule for the determination of the capsize band, for example, involves a number of realisations – usually 10 – for a sequence of wave height values, with as high resolution as possible by time or other constraints. Tests are usually performed in irregular waves according to the JONSWAP or Pierson-Moskowitz spectra.

Figure 5-8: Waves in Vienna Model Basin

Vienna Model Basin GmBH is pioneering in the field of damage stability of cruise vessels with continuous involvement in all major research and commercial projects.

Figure 5-9: Damaged cruise vessel in waves

The largest of the contemporary vessels can suffer incredibly large damages without compromising their stability in waves.

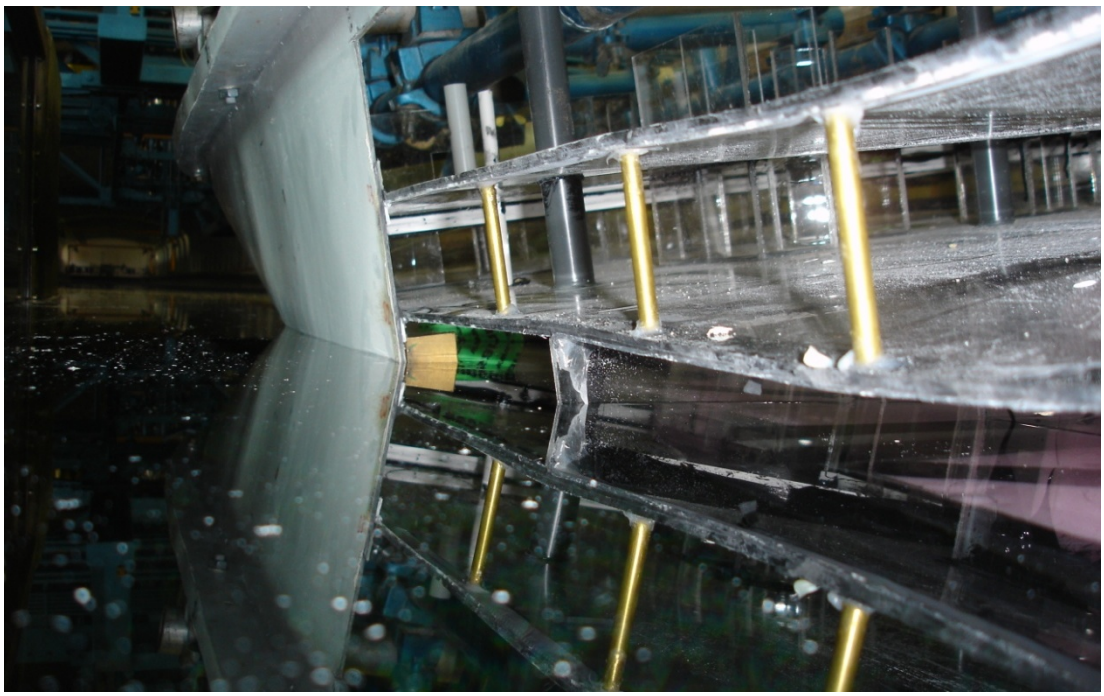

Figure 5-10: Cruise vessel in damaged condition.
The complexity of the model is visible in this picture as well as a watertight door (green) holding progressive flooding, thus saving the vessel from capsize.

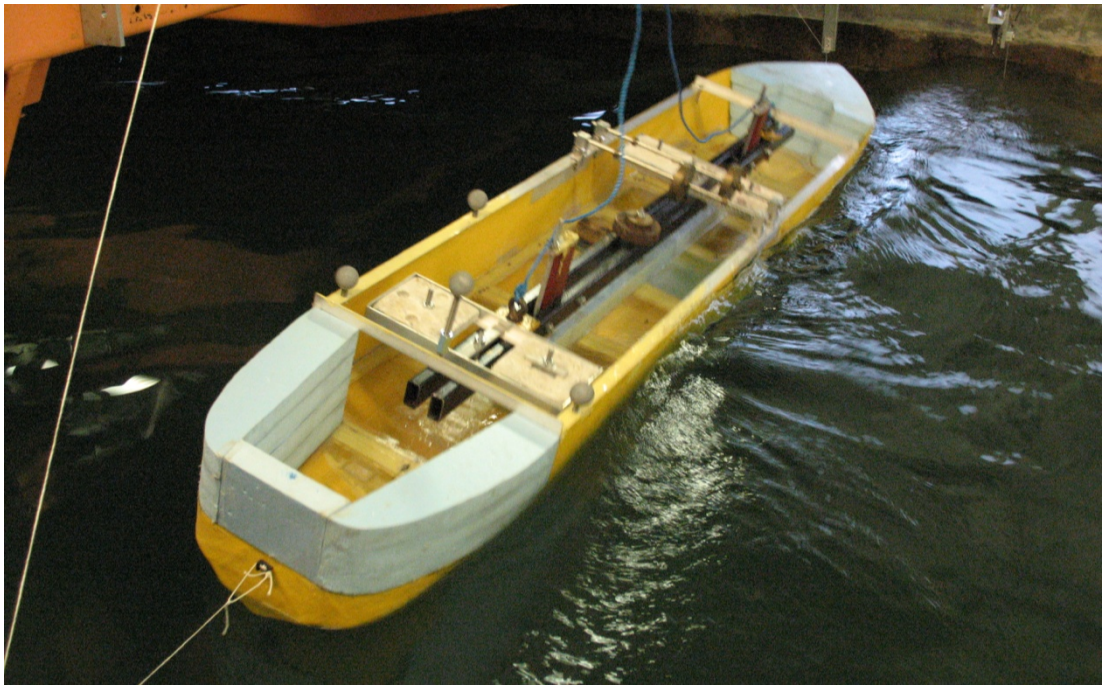

Figure 5-11: RoPax experimental setup.
The model is held with the damage opening facing the waves.

There are two principle ways to conduct a test in waves. The first is subjecting the ship to waves while it's in damage equilibrium position thus doing away with any transient phenomena. The second is opening the damage while the ship is encountering waves in intact condition. This way, transient phenomena are allowed. Each method has its advantages and drawbacks inevitably but both are necessary as each one gives unique information. Major criticism regarding the transient method is that there is no practical way of a real damage opening to happen in a few seconds, while for the other method there is no way of knowing if the equilibrium tested is the equilibrium, a very complicated geometry, is going to end up with or if there's going to be an equilibrium at all. A more realistic approach that has been followed in some experiments, with good results, is conduct a transient test in calm water and continue with waves from that, naturally occurring, equilibrium.

5.3 Analytical PBS assessment methods

Analytical assessment methods can provide an alternative to costly first principles ones for a slight reduction in accuracy and certainty. The huge gains in terms of time and effort though, cast them a very attractive solution when an extensive number of tests is necessary. Those that have been used in the course of this study are explained in the following.

5.3.1 Index A

The first probabilistic regulations were introduced in the late sixties as an alternative to the deterministic regulations of the time (SOLAS 1960). These were offering an assessment of the ship's watertight subdivision within a probabilistic framework, without initial considerations to stability post damage. SOLAS 2009 has been based on that first attempt with the added functionality of stability information. This is exactly where problems begun. While, although determining whether a vessel, post damage, has sufficient buoyancy to stay afloat in a static situation is relatively easy, doing so in a dynamic situation with waves, water ingress, transient phenomena etc. is not so. Nevertheless, Index-A has been developed as a tool that would measure the performance of a vessel to damage survivability. As such it is an excellent tool for Performance-Based Survivability Assessment, in principle at least. In the core of Index-A lies Risk. By definition: *"Risk is a chance of a loss"* [34], that is Probability × Consequences or P × S as it's more commonly seen. This applies for each probable damage scenario, which will have its own probability of occurrence and probability of survival. To this end the P and S factors have been developed. An overview of the basic concept of SOLAS 2009 is shown in the following.

$$A = \sum_{j=1}^{J} \sum_{i=1}^{I} w_j \cdot p_i \cdot s_{i,j} \;\; ; \; A \geq R \tag{5-1}$$

Where:

A	attained index of subdivision
R	required index of subdivision
j	loading condition
J	number of considered loading conditions (3 currently in SOLAS 2009)
i	one or a group of damaged compartments
I	the total number of feasible damage scenarios
w_j	probability mass function of the loading conditions
p_i	probability mass function of the extent of flooding
$s_{i,j}$	probability of surviving the flooding of the group of compartments under consideration (i) given loading conditions (j)

The probability of survival is given by equation 5-2

$$s = k \cdot \left(\frac{GZ_{MAX}}{0.12} \cdot \frac{Range}{16} \right)^{\frac{1}{4}} \tag{5-2}$$

Where GZ_{MAX} and Range are properties of the residual (post flooding of compartments of group i) GZ curve, 0.12 and 16 are limits occurring form the study of stability of ships in damaged condition during project HARDER [4] and k relates to heel at equilibrium, which is little related to survivability as such but more to do with safe deployment of LSAs and ship abandonment.

Even before SOLAS 2009 came to force, certain problems with its formulation came to light [45], leading industry into confusion but most importantly, and wrongly, with lost confidence towards the probabilistic framework altogether. This was hardly the message the scientific community was trying

to get through at the time but it took a number of projects to restore the framework's reputation. What has now become clear is that while for individual damage cases Index-A might not always be correct, the result of the summation of all the damages is close to the actual survivability of the vessel, as it has been measured by more reliable means, like numerical simulations by Monte Carlo sampling (figure 5-12). In this figure it can be seen that the measurement of survivability with Index-A is within 10% of MC simulations. Although this is far from perfect when measuring survivability in absolute terms, it is more than adequate for comparison purposes, casting Index-A a very attractive means of PBS assessment for optimisation studies by use of, e.g. parametric models. This can be simply explained by decomposition of the sample of damages according to survivability. A percentage of damages will be 100% survivable, another percentage 100% non-survivable and the remaining of ambiguous survivability. The latest studies have shown that for RoPax ships this split is 80%, 15% and 5% roughly (figure 5-13). Thus, even if the error of measurement for any s-factor is large, the contribution to the Index will be small. What is more worrying than the 5-10% uncertainty is that a large proportion of the feasible damages a vessel can suffer will result in no stability, whatsoever. This result is, questionably, allowed by the current R-factor. Previous regulations like SOLAS '90 [28] postulated that ALL 2-compartment damages result in no submergence of the margin line. In line with this, current regulations should request that ALL feasible damage cases remain afloat and upright [11], [12]. It is believed as well that not only regulations should be stricter but they could afford to be as well without major inconvenience to the industry, as will be shown in following chapter.

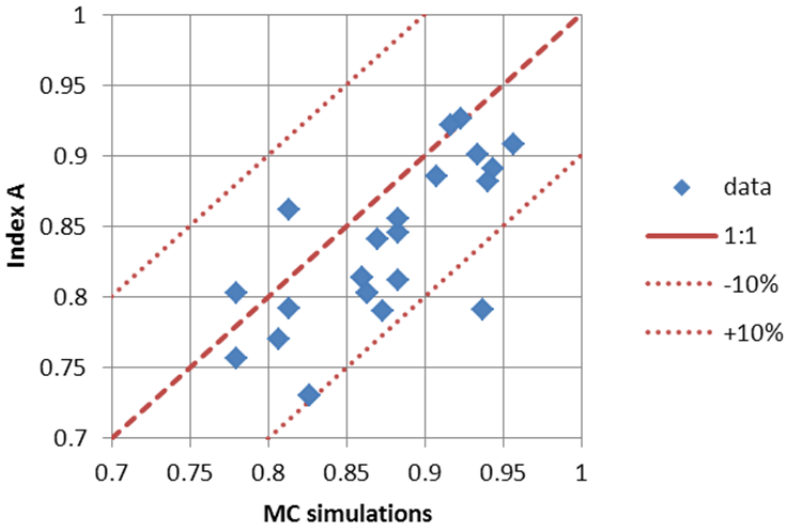

Figure 5-12: Comparison of Numerical Simulation with Index-A.

In this comparison between Index-A results for a selection of various sizes RoPax ships and the corresponding numerical simulations with Monte Carlo sampling it is obvious that Index-A is a very accurate (within 10%) representation of the vessel's actual survivability for current RoPax vessels.

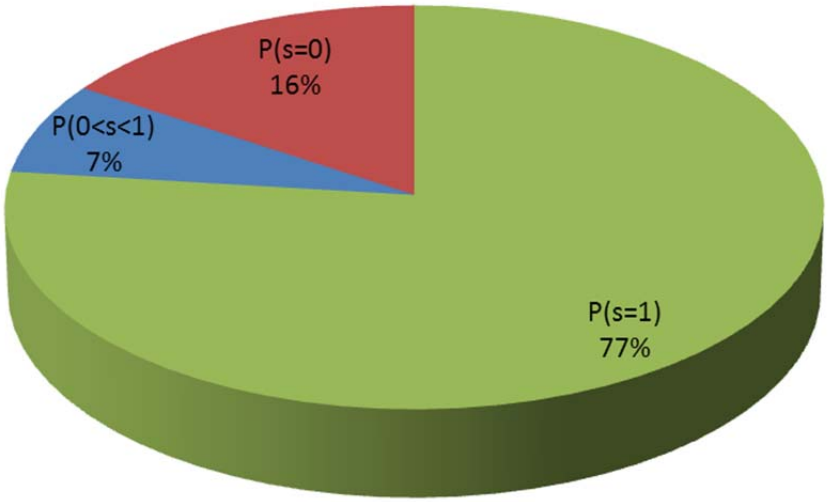

Figure 5-13: Probability of s_i

Separation of s_i according to survivability; It shows the potential outcome of a collision accident for a RoPax ship.

5.3.2 Univariate Geometric Distribution

Developed within the EC funded project SAFEDOR, UGD is an analytical method, based on SOLAS 2009 s-factor, for the calculation of the ship vulnerability to flooding. The basic principle can be seen in equations 5-3 and 5-4. For a more detailed description of the method refer to [14].

$$F_T(t) = \int_0^1 dt \cdot f_T(\tau) = \sum_i^3 \sum_j^{n_{flood}} \sum_k^{n_{Hs}} w_i \cdot p_j \cdot e_k \cdot \left(1 - \varepsilon_{i,j,k}^{\frac{t}{t_0}}\right) \tag{5-3}$$

When:

$$\varepsilon_{i,j,k} = 1 - p_f = 1 - \Phi\left(\frac{Hs_k - Hs_{crit}(s_{ij})}{\sigma_\gamma\left(Hs_{crit}(s_{ij})\right)}\right) \tag{5-4}$$

The basic principle of UGD is that with just the use of one parameter (s_{ij}) it gives the vulnerability to flooding in the form of the cumulative probability distribution function for time to capsize (figure 5-14). UGD has been validated in numerous projects and has been observed that its results (and subsequently Index-A) lie consistently within the confidence intervals of the numerical simulations for RoPax ships (figure 5-14).

Another important contribution from UGD is the conditional probability for time to capsize given loading condition and damage extent occurred, for each one of the feasible damages, tested during Index-A calculation according to SOLAS 2009. A typical outcome of this probability is shown – conveniently set-up for ease of visualisation – in figure 5-15.

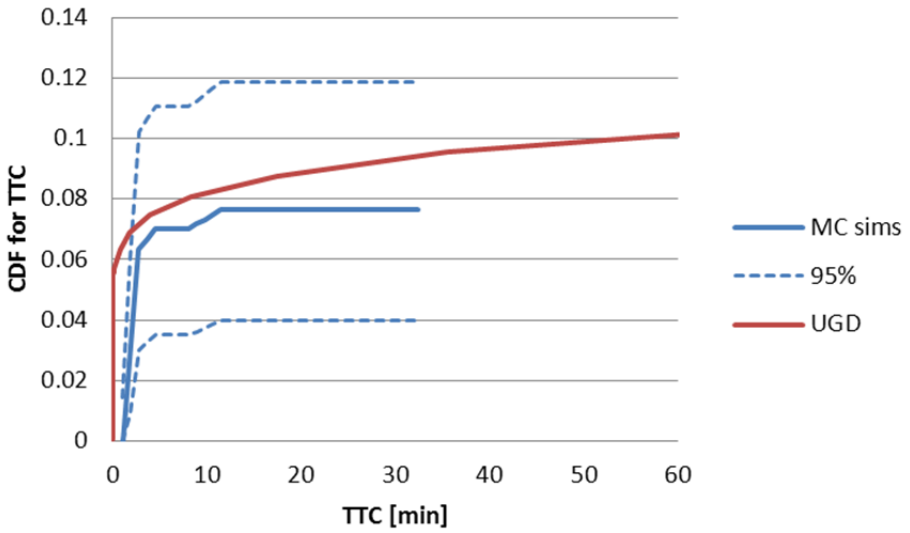

Figure 5-14: UGD vs. MC simulations

Both methods result in ship vulnerability to flooding so can be directly compared. In this sample for a 105m RoPax ship fitted with a LLH the two methods give remarkably similar results.

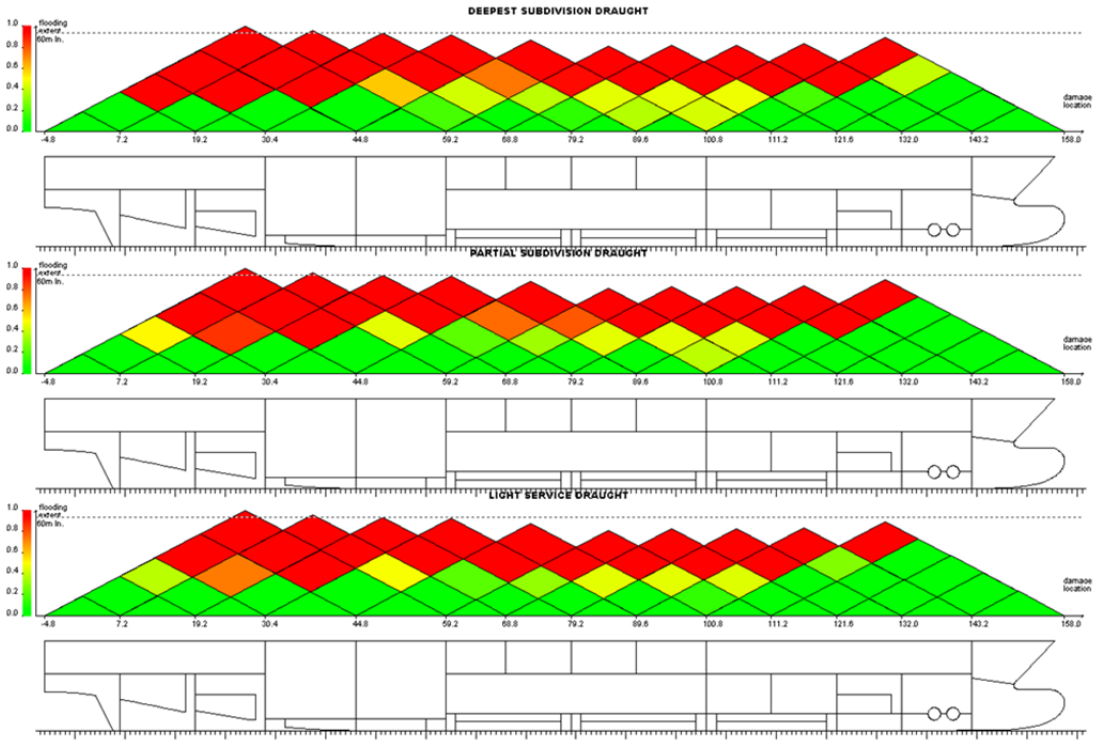

Figure 5-15: Distribution of conditional probability

Probability to capsize (colour coded - green is 0, red is 1) given loading condition and damage extend occurred for an 150m RoPax with LLH.

Chapter 6 – Vulnerability of modern passenger vessels

6 Vulnerability of modern passenger vessels

Shipping is a life-critical industry as the potential for life threatening events to happen exists. Even though looking at statistics leads to an impression that serious accidents are really rare in the shipping industry, history is dotted with catastrophic accidents leading to hundreds or even thousands of people dead. The 1500 fatalities of the Titanic [1912], 193 fatalities of the Herald of Free Enterprise [1987], 4000 fatalities of Dona Paz [1987], 852 of Estonia [1994] and 1018 fatalities of Al Salam Boccaccio 96 [2006] are just a small example according to LMIU database. Such is the nature of naval accidents that either most people on-board will be lost or none. The vast majority, those that lead to few or none casualties mostly happen in sheltered waters or close to shore where traffic is heavier but also help is close. Those very few that will happen in open water and will lead to losses are very probable to result in many fatalities. And given the all increasing size of modern passenger vessels, "many" can easily mean thousands. This is why it is of grave importance that vessels are designed and operated to the highest standard possible. This chapter will attempt to measure the safety level of modern passenger vessels so as to summarise current attempts at setting the standard of future regulations of damage stability.

6.1 Known issues

There are a few known issues with modern passenger vessels, each with their own contribution to the overall risk level. In the next paragraphs the most provoking ones will be outlined, from water on deck to evacuation procedures for the two dominant categories of passenger vessels, the Roll on – Roll off passenger vessels (RoPax) and the cruise vessels. These two categories of ships are specifically designed to address not only transport needs but also passenger entertainment and well-being. In the past decade they have grown to extreme sizes, the largest of which are built to accommodate up to 8000 people on-board. The cross-breed of ro-ro cruise vessels has also appeared, narrowing the gap between the two. Each type has their own, distinct problems, generally associated with individual geometry features but also common ones, associated with accommodating a large number of persons on-board as well as water accumulation. Another common hazard, evacuation, has only recently begun to be required for evaluation at the design stage. That is because only recently has it been identified as a potential hazard to people aboard. Finally, the framework for ship safety could not be complete without consideration of grounding.

Grounding has been identified as a principal hazard to passenger vessels with almost 4x higher frequency than collision. The estimates for the annual frequencies of occurrence for flooding and fire-related hazards have been derived based on statistics, [32] and are shown in figure 6-1. In addition, previous efforts in projects like SAFEDOR and on-going research in current projects aim to derive these from first principles. Particularly in passenger ships, flooding and fire-related scenarios comprise over 90% of the risk (regarding loss of life) and almost 100% of all the events leading to ship

abandonment. Therefore, it is possible to estimate the total risk (safety level) of a passenger vessel by addressing these two principal hazards in a consistent manner and framework, allowing for their contribution to risk to be formally combined as indicated schematically in Figure 6-2 derived from [44].

With developments in probabilistic regulations for the control of collision damages this is a serious issue in need of immediate attention. Fortuitously, the same tools used to determine probability of survival for collision damages can be utilised to provide the information needed for the development of a probabilistic framework for grounding damages, if deemed appropriate. By doing so, the designer would be able to assess the contribution of grounding to the overall ship safety, thus addressing the relevant part in the framework presented in figure 6-2.

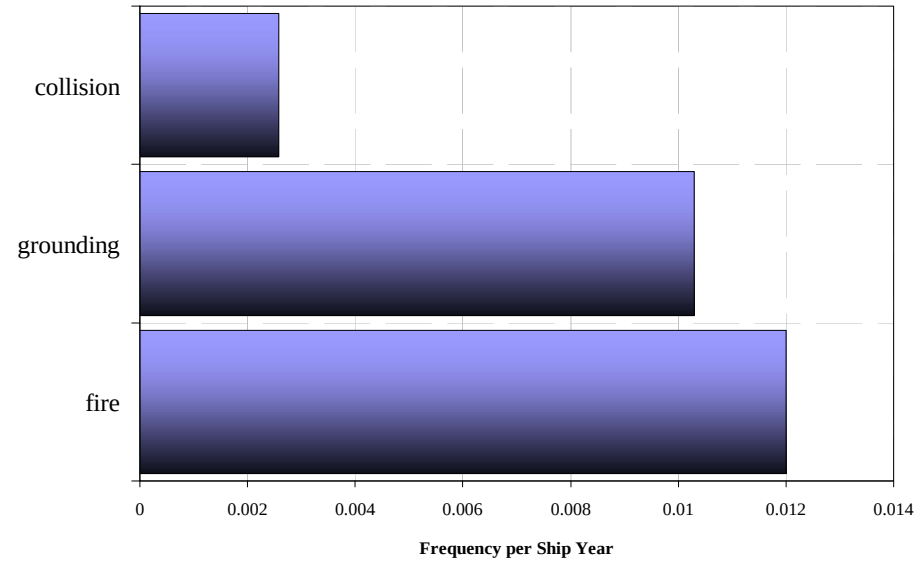

Figure 6-1: Principal hazards – Frequency of event occurring

Flooding and fire related event count for 90% of risk to human life and almost 100% of events leading to evacuation of ships. Grounding has 4x higher frequency than collision

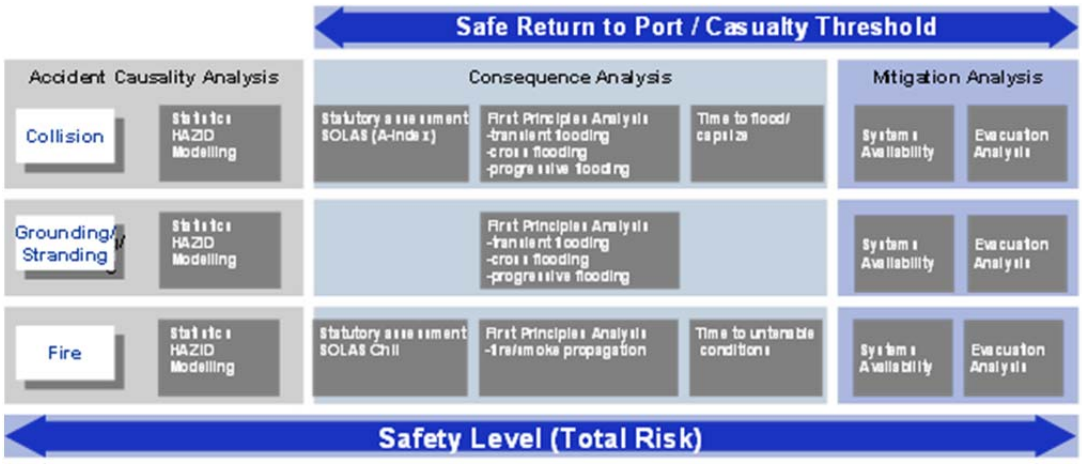

Figure 6-2: Risk-Based Design Implementation (Safety Level)

6.2 Vulnerability to collision

6.2.1 RoPax

RoPax vessels feature a ro-ro deck (figure 6-7) which, as a large unsubdivided space close to the waterline, can severely deteriorate the vessel's stability if it gets flooded in case of an accident. The major problem associated with flooding of the ro-ro deck is the so-called water-on-deck (WoD). Being unsubdivided, the ro-ro deck allows for a big area to be covered by shallow water (figure 6-8), thus creating a substantial free surface effect, on its own capable of capsizing the vessel, as was the case of the M/V Estonia, among others, that capsized with her hull intact, when water flooded in the car deck from a detached bow loading door.

Water on deck is pumped into the car deck by wave action if the vessel's freeboard in damaged condition is low. It has been and used in regional Northern European Stockholm Agreement [6],[7] that no water is capable of entering the car deck if the vessel's freeboard is higher than 2 metres, even in the worst sea-states statistically possible to be encountered during collision, that is 4m (figure 6-4) [4]. Water pumping on the car deck is of a stochastic nature, related to the probability of a wave group to be high enough for water to access the car deck and the probability of time between consecutive high wave groups to be small enough so water on deck can be sustained [16].

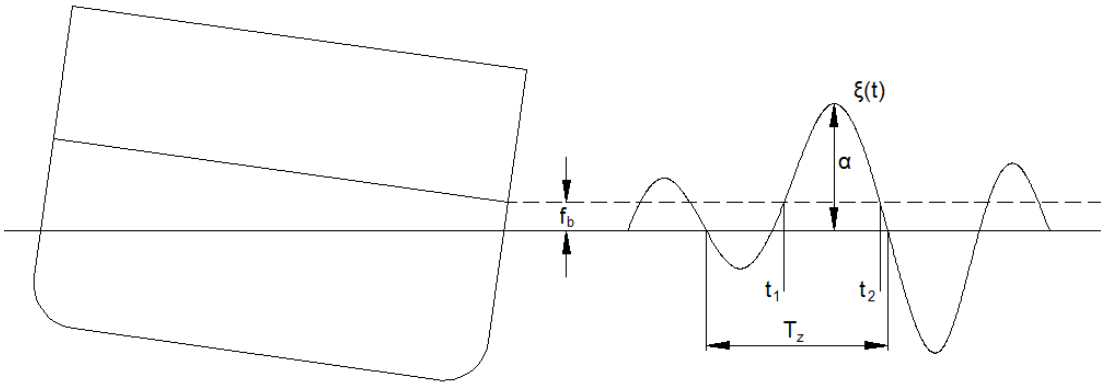

Figure 6-3: Simplified model of water ingress according to [16]

f_b is freeboard, ξ(t) is time history of wave, α is wave height, T_z is zero crossing period and t_1 and t_2 time that ingress starts and ends respectively.

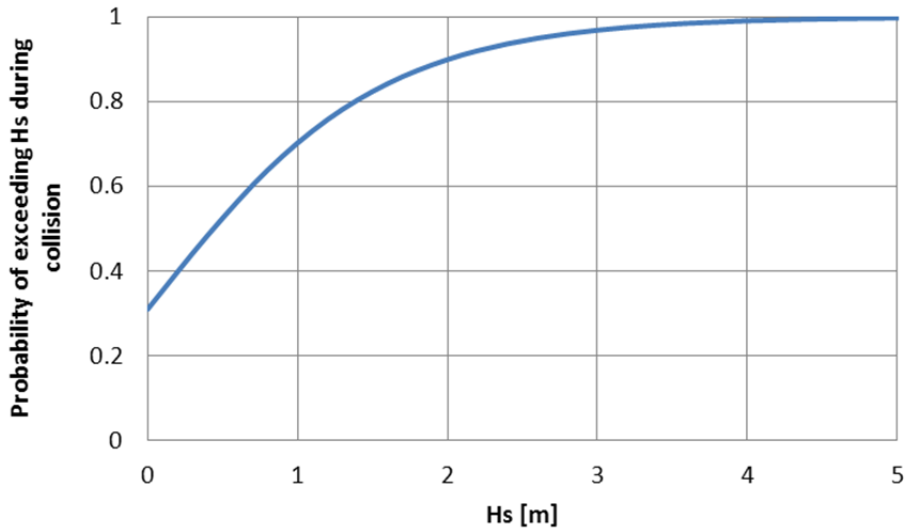

Figure 6-4: Probability of exceeding Hs during collision

This probability has been obtained from collision statistics collected during project HARDER and used in SOLAS 2009 for the derivation of s-factor.

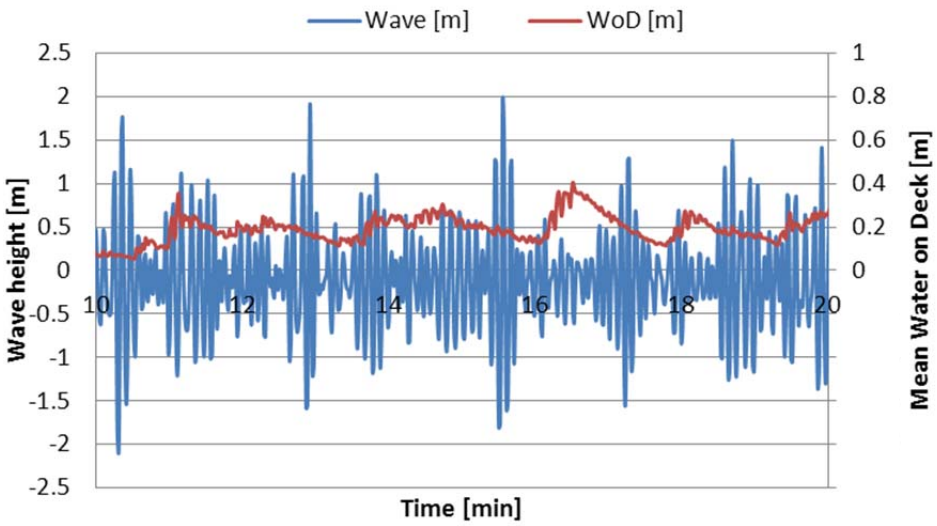

Figure 6-5: Water on Deck – Model experiment (1)

In this time frame from a model experiment on a small RoPax vessel the pumping of water on deck by wave action is visible. Note that water is not accumulated always in phase with waves because of the motions of the vessel.

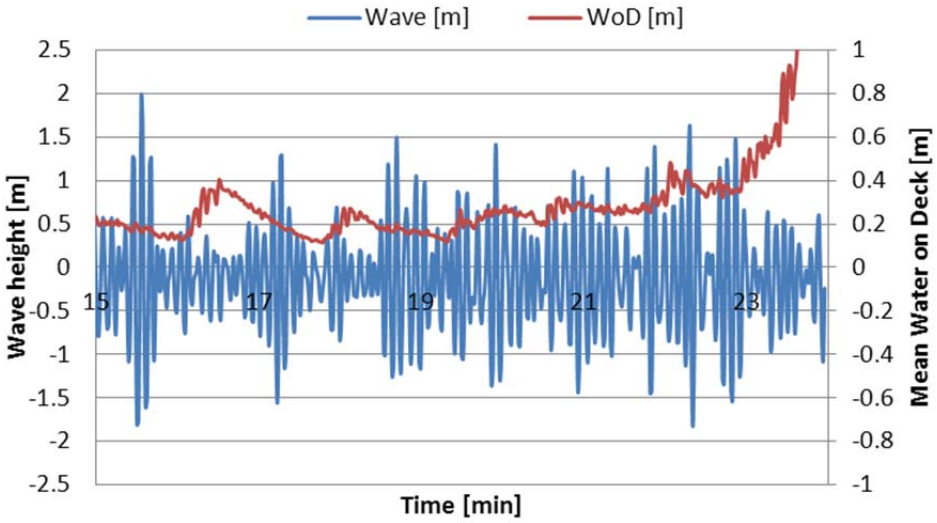

Figure 6-6: Water on Deck – Model Experiment (2)

This time frame demonstrates the instance of capsize for this experiment. Note how water on deck continued to accumulate when high wave groups became more frequent.

Figure 6-7: Car Deck
The car deck of vessel “Spirit of Britain”; courtesy of P&O ferries

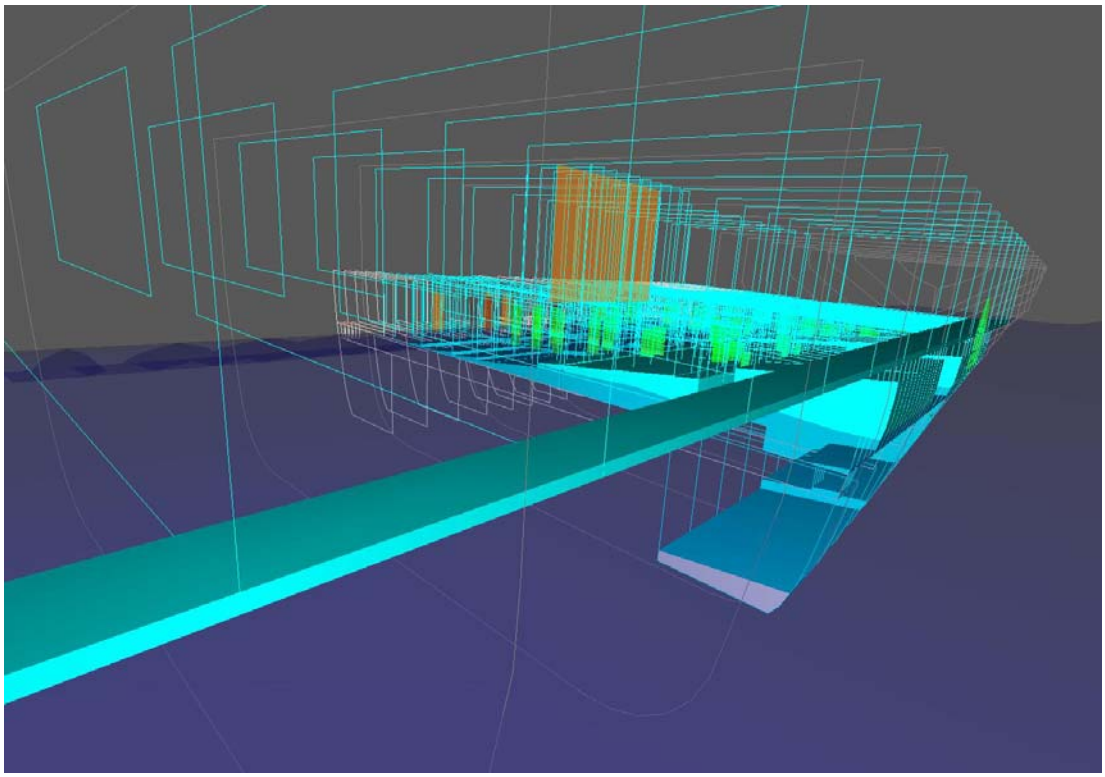

Figure 6-8: Water on deck
Snapshot of WoD from a numerical simulation with PROTEUS3

Another major contributor to risk of RoPax vessels is the lower hold, referred to in the industry as the Long Lower Hold or LLH for short. A highly viable commercial feature, the LLH utilises spaces in the vessel's lower compartments that would otherwise remain empty. The problem is that because it needs to be loaded with vehicles, a certain length is required, necessitating the need for the hold to extend to several watertight compartments (figure 6-9). Even worse than the normal ro-ro deck, due to it being situated below the waterline, it instantly gets flooded in case of breach. If the vessel is not properly designed to sustain flooding of the LLH, compensating by watertight volumes elsewhere (figure 6-10), it can lead to rapid sinking. The original SOLAS 1990 (Ch.II-1, Reg. 4-12) would not allow for a LLH unless its flooding would not submerge the margin line. However, it was decided that penetration beyond a fifth of the vessel's beam was not probable, thus allowing transverse subdivision to be limited to that virtual limit of B/5. This decision rendered SOLAS 1990 "blind" to lower holds on RoPax vessels, while had SOLAS persisted in the floodable lengths regulation, designers would have been forced to "find" additional buoyancy elsewhere. On the positive side, since the LLH is located low in the vessel, its flooding leads to significant reduction of the KG, meaning that, provided the ship remains afloat, it will have somewhat increased stability. Throughout this work it has been noticed that damage cases involving the lower hold that survive, have a remarkable capacity to resist capsize in waves.

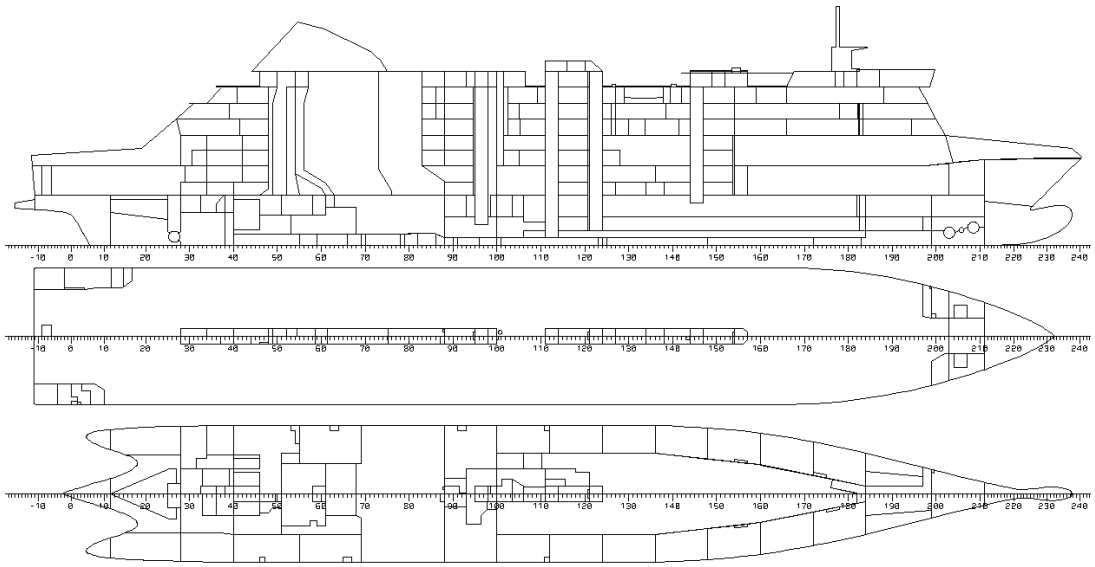

Figure 6-9: Plan of RoPax with LLH

A medium sized RoPax vessel used in several studies. The car deck and Long Lower Hold are visible in this figure

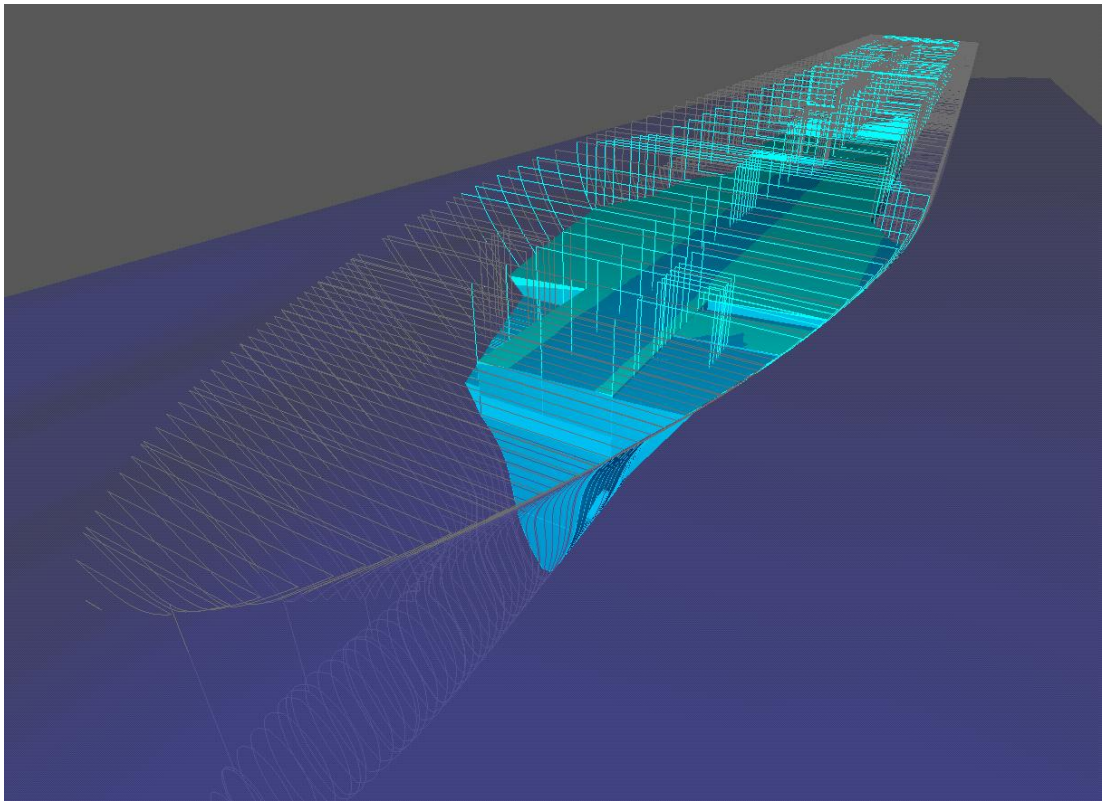

Figure 6-10: Damaged RoPax

In this, 3-compartment damage case including the LLH, the ship is kept afloat by the sidecasings – watertight, loadable, compartments on the sides of the car deck.

6.2.2 Cruise ships

Cruise vessels have somewhat different mechanisms of capsize to those of RoPax vessels, although the cause, WoD is the same. The stochastic behaviour of accumulation of water on deck is less pronounced here, since there is no large, unsubdivided space to create a large free surface effect. However, the complexity of their geometry, as can be seen in figure 6-11, although in general mostly responsible for the cruise vessels' increased survivability compared to RoPax vessels, it contains a potentially fatal threat. Caused by accumulation of water in higher decks, leading to the creation of multiple free surfaces, the so-called transient capsize is the situation when the vessel can capsize following breach and flooding before reaching the equilibrium condition, in time shorter than its natural roll period. The other major mechanism of loss for cruise vessels is progressive flooding. It is caused by insufficient protection of openings, leading to flooding of adjacent spaces, gradually deteriorating stability, until vessel capsizes. Cruisers are particularly vulnerable to progressive flooding in larger damages when higher decks can get submerged allowing flooding through openings in the vessel's central corridor. A time-lapse sequence of a visualisation of a PROTEUS simulation where progressive flooding took place can be seen in figure 6-13. In this particular case, water had spread to half the vessel in less than 7 minutes and then remained there resulting in a survival. Progressive flooding though can last for much longer and is as dependent on the damage case as is on the sea-state encountered during collision. On the positive side it does not last a few seconds like a transient loss, so crew can have the chance to block passage to the floodwater.

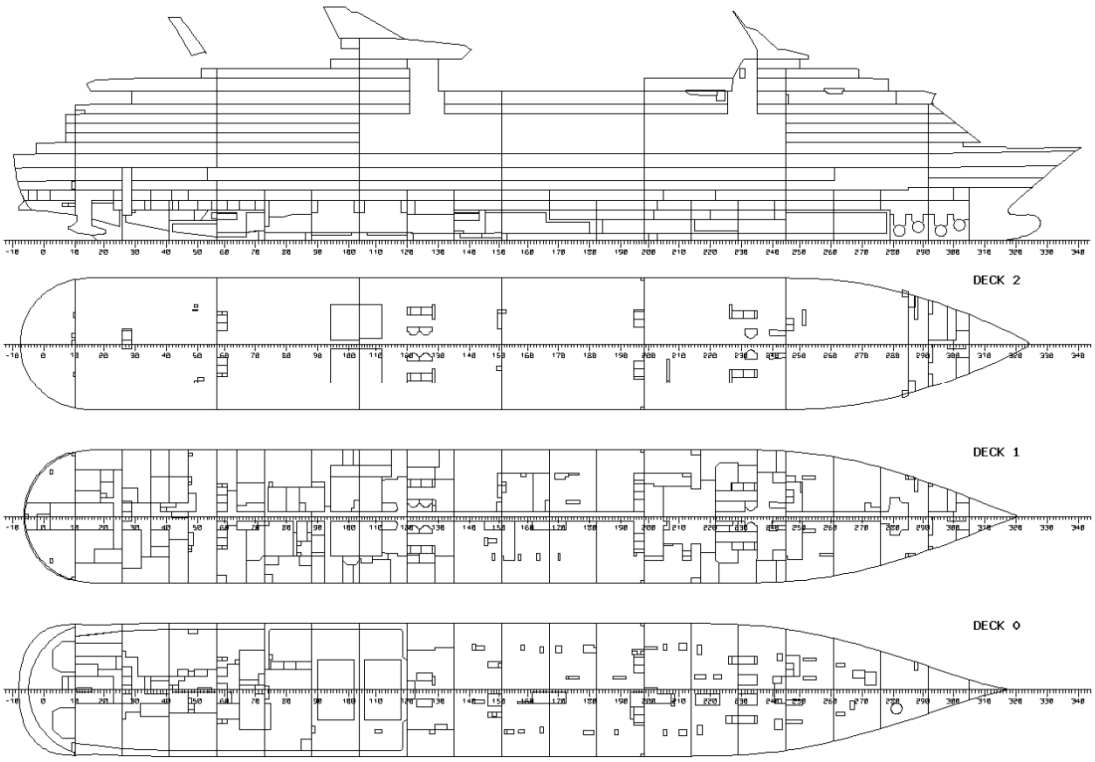

Figure 6-11: Cruise vessel plans

In this figure are visible the lower accommodation decks, the ones closer to the waterline. These are the decks that will create the multi free surface effect during transient stage. Note the increased complexity of the geometry.

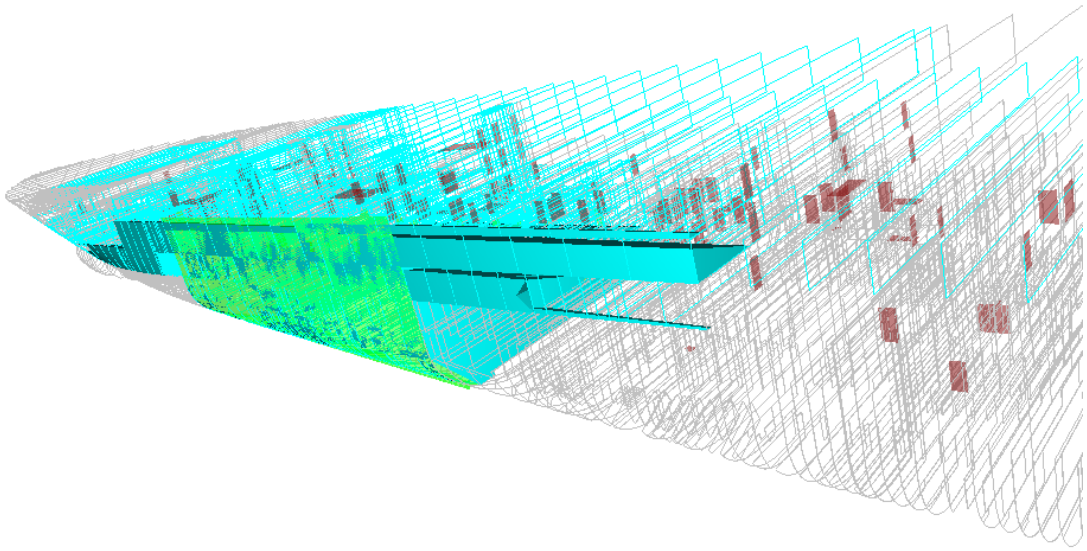

Figure 6-12: Multi free surfaces

An instant from a transient flooding simulation showing the multiple free surfaces created due to large heel angles.

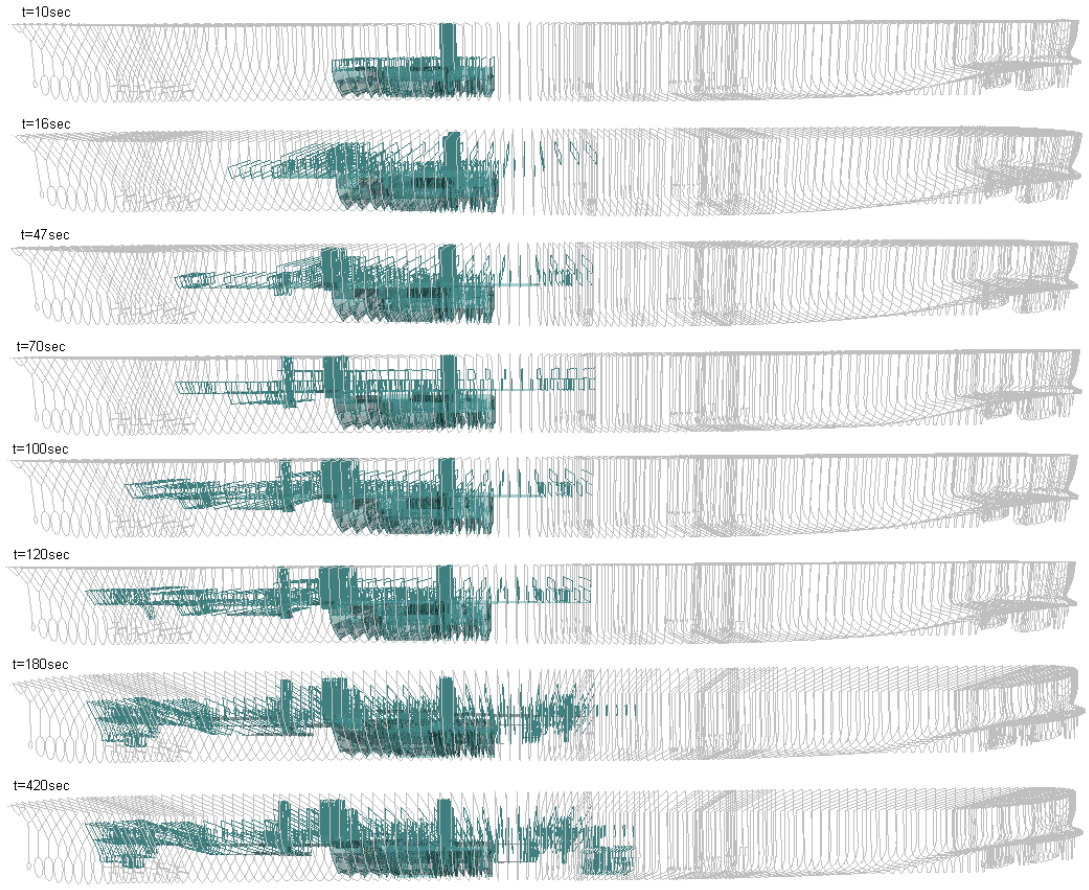

Figure 6-13: Progressive flooding

Damage case simulation in 4m significant wave height; water spread to half the ship length, in less than 7 minutes.

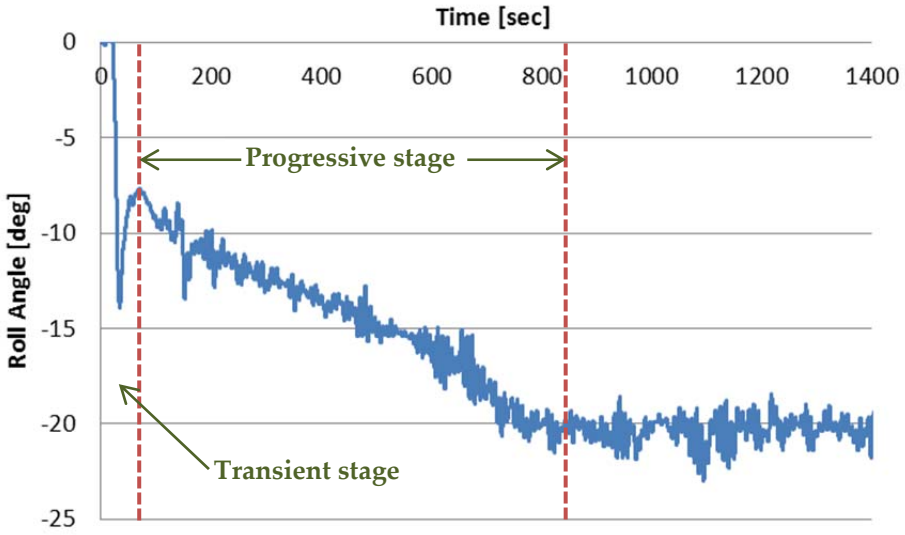

Figure 6-14: The 3 "stages" of the flooding process

Although the transient and progressive stages of flooding have been presented as two separate mechanisms, in fact they are both part of the flooding sequence. Transient is the first few seconds of flooding while progressive follows and can last for anything from minutes to hours. As can be seen in figure 6-14 showing the time history of roll motion during a simulation for vessel EUGD01-C2, the vessel reaches almost 15 degrees of heel in less than a minute post-damage and then recovers to 7.5 degrees at the end of the transient stage. Then water starts spreading to adjacent compartments slowly increasing heel to 20 degrees in little more than 15 minutes post damage. Once the progressive flooding stage is also over, the vessel remains in that condition until the end of the simulation.

The maximum value of roll angle during transient stage is affected by initial KG value as can be seen in figure 6-15. The tests resulting in this figure were carried out for 4 different KG values in the same sea-state of 1m significant wave height. Final equilibrium position is also affected by the variation in transient roll angle as various compartments submerge causing differences in accumulation of water. If initial GM is very low, like in the case of KG=20.0m, the vessel will not recover from the transient stage. From another experiment carried out for the same vessel, this time with constant KG for increasing sea-states, it seems that the transient stage is also affected by environmental conditions. As can be seen in figure 6-16, progressive flooding stage can be massively accelerated by severe weather conditions, leading to a situation similar to a transient loss. A common outcome from both of these experiments is that there is a sea-state up to which the vessel does not capsize and above which loss is a matter of time. As will be demonstrated in following, time is also dependent on this, critical, sea-state, which in turn is dependent on geometry like damage case and loading condition.

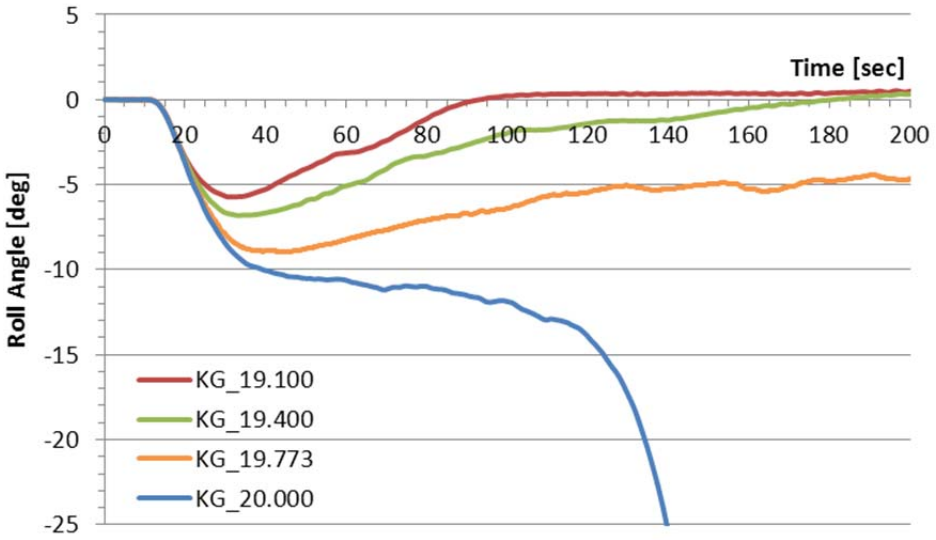

Figure 6-15: Transient flooding for different loading conditions

Maximum roll angle during transient stage is affected by KG. Equilibrium position is also affected, since angle during transient stage determines which compartments get flooded.

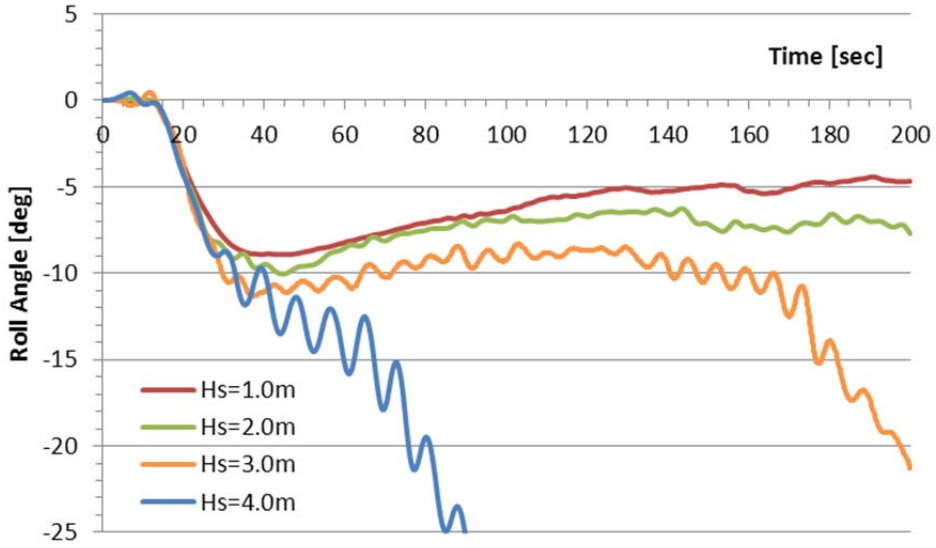

Figure 6-16: Transient flooding for different sea-states

Loading condition is the same in this series and the variable is the sea-state. Apparently, maximum roll angle of transient stage is less affected by environmental conditions than it is by loading condition. KG=19.773

In fact, cruise vessels are so vulnerable to transient and progressive stages of flooding, that a simple operational change like the opening of some semi watertight doors can have massive influence on a vessel's overall survivability. Current regulations demand that semi watertight doors can be open only during time at port. However due to operational requirements like passenger and crew movement, it is common practice that these doors can be opened at more times than those allowed. To make matters worse, SWD are placed on the decks mostly susceptible to multi free-surface effects and progressive flooding.

In order to measure the effect that these openings might have on the survivability level, a specific exercise was conducted. The smaller cruiser in the sample was run in two different conditions. The first was as designed to operate, that is with the SWD closed, and the second with them open. The arrangement of a section in her freeboard deck, where the doors in question are placed is shown in figure 6-17. The Monte Carlo simulation setup [see Chapter Performance-Based Assessment] was exactly the same for the two different arrangements; same loading conditions, same damage scenarios and same time (30 minutes simulations).

The results support the initial hypothesis that survivability is massively influenced by openings on the freeboard deck of such vessels as seen in figure 6-18. Openings allow water to spread into adjacent spaces and result in a transient or progressive capsize. One might argue that these openings can be operated and closed remotely in case of a damage but in many cases, when capsize occurs in less than 10 minutes, accompanied by large roll angle amplitudes in seconds post damage there's hardly any time for operation of SWD.

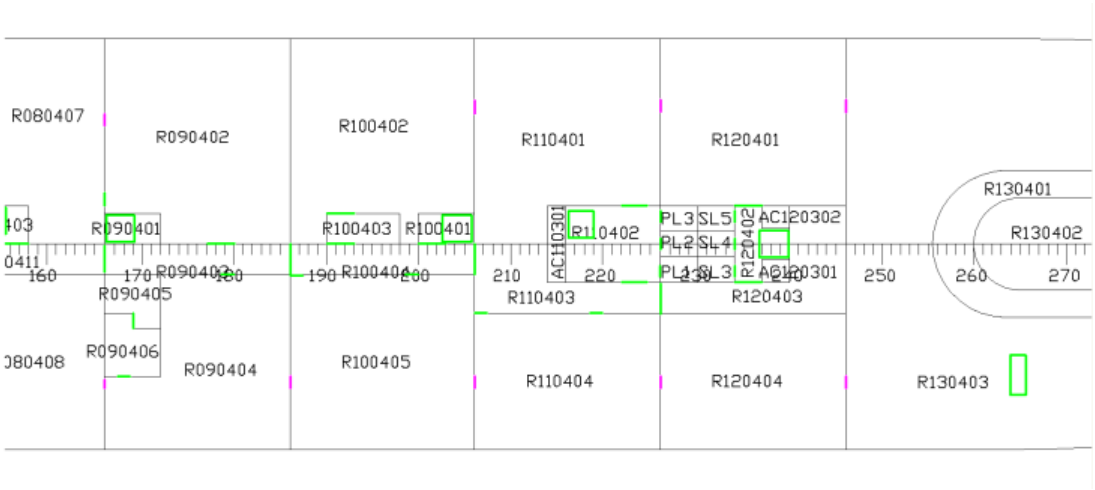

Figure 6-17: EUGD01-C2 freeboard deck and location of semi-watertight doors.

Normal openings and doors are shown in green, while the SWD are shown in red. 9 SWD in total are located on deck 4 of this ship since it is the embarkation and services deck and needs to facilitate the movement of passengers and crew.

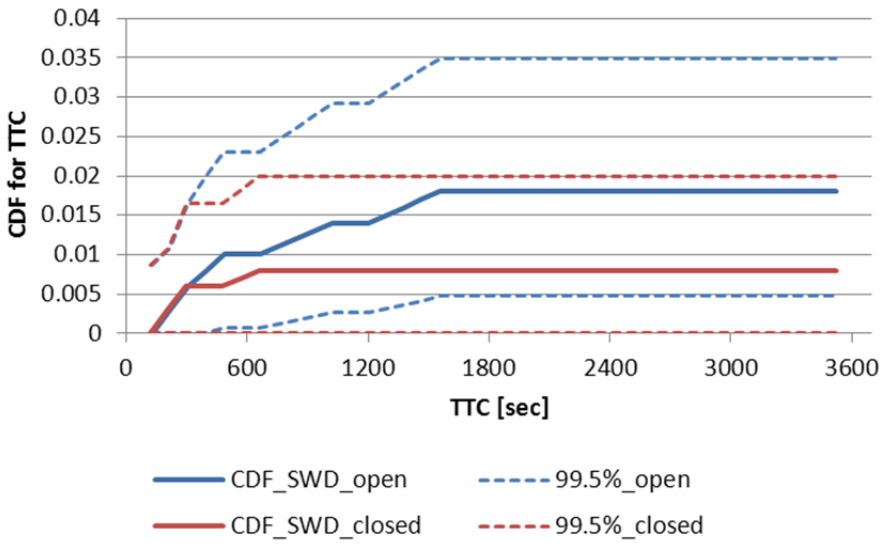

Figure 6-18: Contribution of SWD to survivability.

There is a vast deterioration of stability with SWD open, translating in 80% increase of the probability to capsize given the particular loading condition and 30 minutes.

6.3 Vulnerability to grounding

Grounding damages are almost 4 times more frequent than collisions, yet somehow, is presently only taken care of by the deterministic measures of double bottom provisions. This is partly justified by the statistics derived in task 3.2 of GOALDS [1], highlighting the dimensional nature of penetration in grounding damages. As can be seen in figure 3 almost 90% of grounding damages could be contained by a 2m double bottom. However, this is not feasible for smaller vessels and such an approach would return survivability assessment back to the time of deterministic measures that little have to provide to the design process but constraints. To this end, a study has been performed that aims at providing the information with regards to the contribution of grounding to risk. The aim is to integrate grounding to the probabilistic framework for damage stability as shown in figure 6-2.

The vessels used are those described subsequently in 6.5.2 and comprise of two cruise vessels and two RoPax, the subdivisions of which can be found in Appendix I.

The study was carried out on a global level with simulations using the Monte Carlo sampling technique described in chapter "PBS". The statistical distributions used this time are not those used for collision damages but the newly derived data from GOALDS project [1]. MATLAB is used for the sampling from the distributions to generate the damage scenarios. 300 damages were deemed adequate for the cruise vessels while 500 scenarios were simulated for the RoPax vessels. All were simulated for 60 minutes.

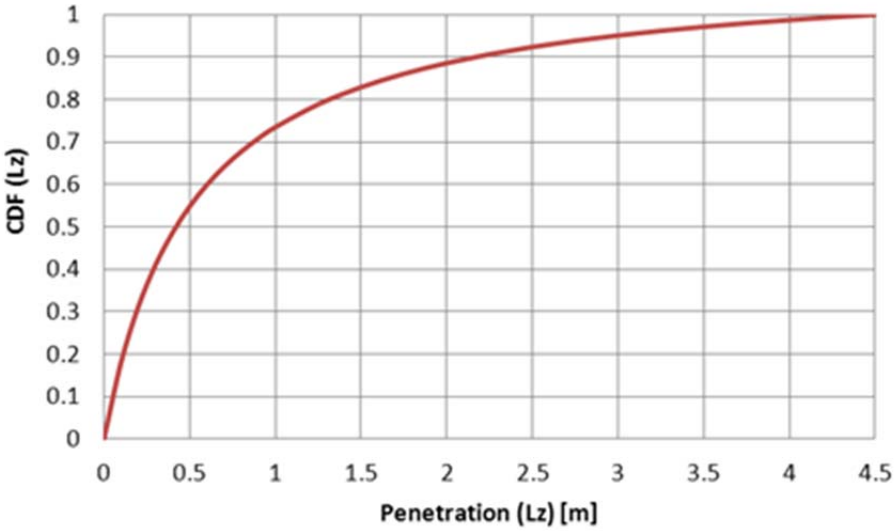

Figure 6-19: Probability distribution function for penetration of grounding damages

In this dimensional approach it is visible that all grounding damages will result in less than 4.5m penetrations. However, imposing a deterministic requirement for a 4.5m double bottom is not feasible and would provide nothing in terms of knowledge of the safety level pertinent to a design.

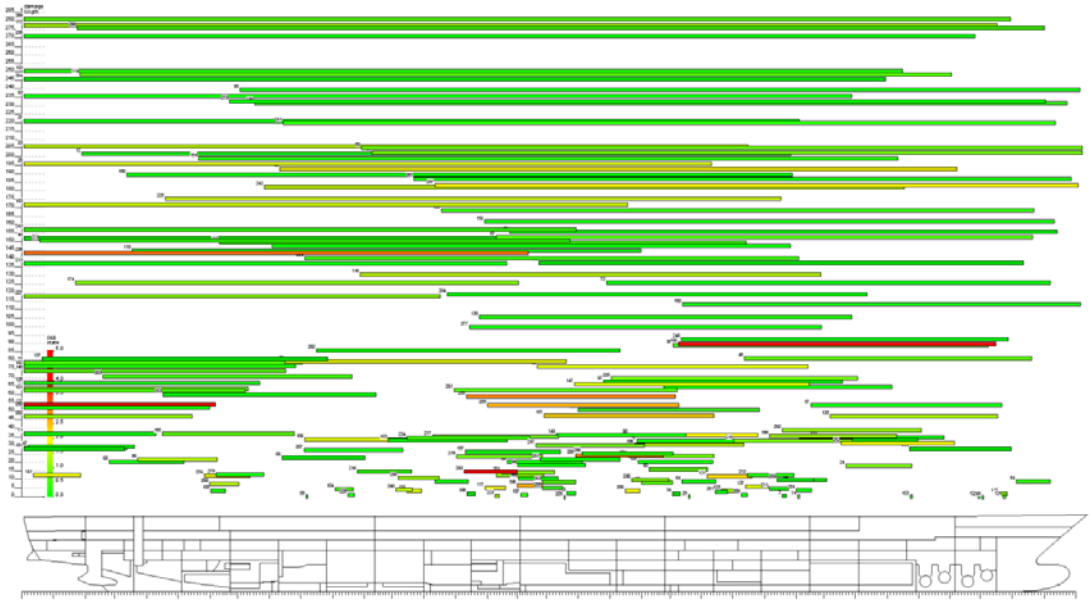

Figure 6-20: Setup for the simulated scenarios for EUGD01-C1

About half of the scenarios generated were simulated for the large cruise vessel

6.3.1 MC simulation results for grounding

The problem with this approach is that due to its simplistic approach of regarding the ship as a box-shaped object (pretty much like its LBT would suggest), many of the generated damages did not actually result in penetration of the hull. As can be seen in Appendix VII the statistics for the simulated damages are somewhat different to those generated but not much. The cases that were actually simulated for EUGD01-C1 are shown in figure 6-20. The rest of the grounding simulation setups can be found in Appendix VI. The results for those that were simulated are shown in figures 6-21 and 6-22.

Apparently there is no significant difference in probability to capsize due to flooding from grounding damages compared to flooding from collision. In the case of C1, four damage cases resulted in loss of the vessel while only two did so for C2. However, given that the frequency for grounding is much larger than collision (figure 6-1), the contribution to overall risk is probably higher. Note though that the time to observe any losses due to grounding is 15 minutes in the case of C1 and more than 30 minutes in the case of C2, which would provide with adequate time to evacuate.

Monte Carlo simulations for RoPax vessels did not result in any capsizes. No water reached the car deck at any of the simulations carried out, possibly due to the limited up-flooding routes and limited penetration to 4.5m according to statistics. Even though the long lower hold of the large RoPax vessel (EUGD01-R1) was damaged in a number of cases, the buoyancy of the decks above, including the car deck was sufficient to keep the vessel afloat in all grounding damage scenarios.

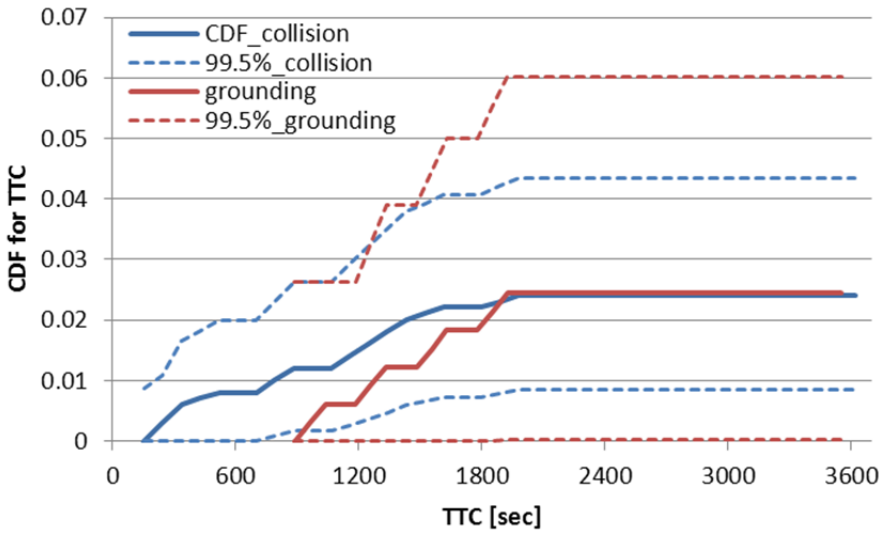

Figure 6-21: MC simulation results for EUGD01-C1

In comparison to the collision results both hazards result in almost the same probability to capsize within 60 minutes which means that given the higher frequency of occurrence of grounding, risk related to it is higher

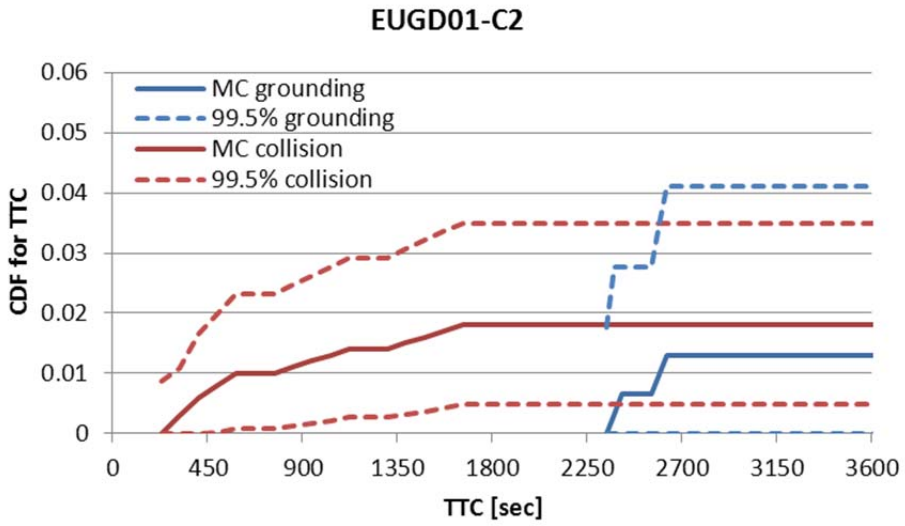

Figure 6-22: MC simulation results for EUGD01-C2

Probability to capsize within 60 minutes is slightly lower from grounding than collision in this case but overall risk related to grounding should also be higher.

6.3.2 Grounding loss mechanism

An observation made from the grounding simulations is that loss generally takes more time than in collision damages. It is noteworthy that no losses occurred in less than 15 minutes for C1 while it is over an hour for C2. A closer examination of the time histories of the motions of the lost cases revealed that the problem is of a (steady) progressive nature rather than a stochastic one. As shown in figure 6-23 the stability characteristics of the vessel gradually deteriorate due to progressive flooding until capsize occurs. This also happens with collision damages but on a smaller percentage. In the case of grounding all cases lost exhibit the same behaviour. That is because grounding affects lower compartment only (figure 6-24), which means that the stability of the vessel is actually improving following a grounding incident, given that there's no progressive up-flooding through stairwells and lifts.

Further analysis of individual damages demonstrated the above hypothesis. As can be seen in table 6-1 the GM values of the damaged vessel (highlighted) are actually higher than the corresponding intact ones as a direct result of the reduction of the KG due to floodwater in lower compartments. The comparison of the GZ curves in intact and damaged condition shown in figure 6-25 also suggest that the vessel in damaged condition indeed demonstrates at least equal survivability with intact condition. This was also observed in all ships. Even the damage cases that resulted in loss in the case of the cruise vessels, when progressive flooding was not allowed (after identification of the responsible routes and their blocking) resulted in high stability characteristics.

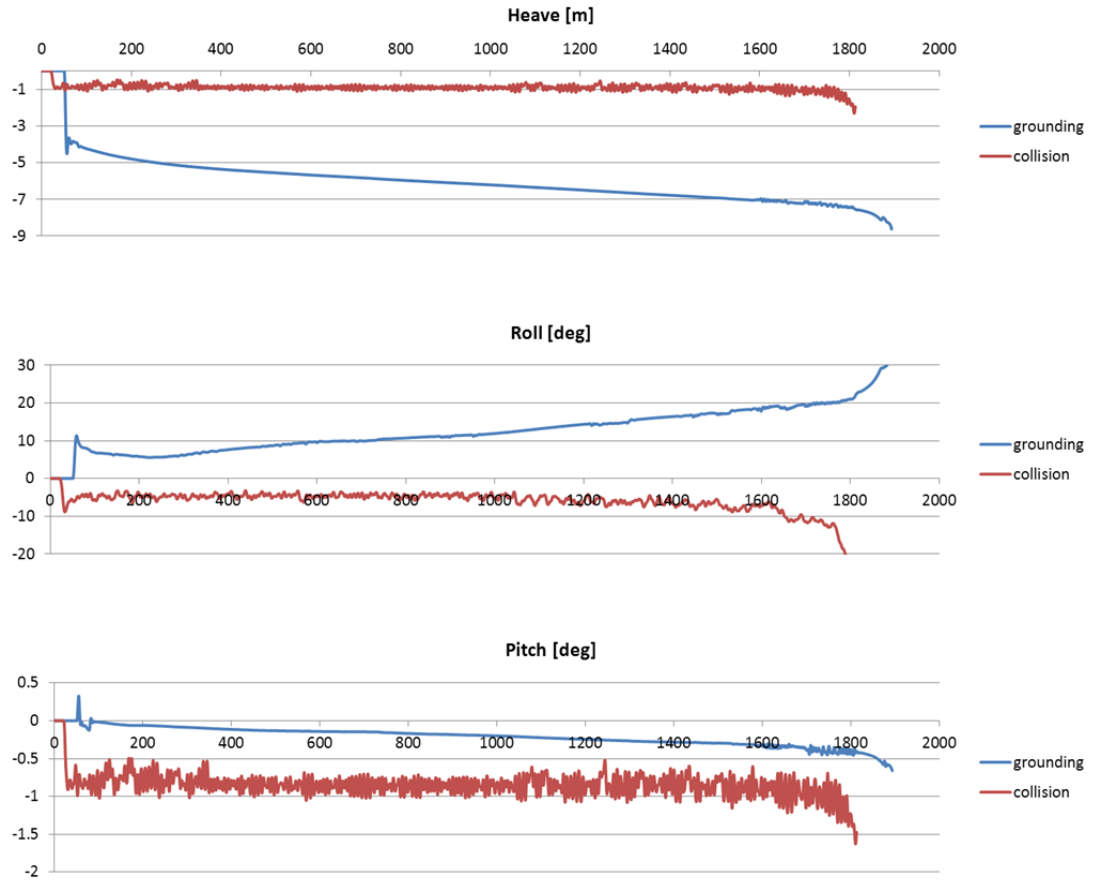

Figure 6-23: Motions' time history – grounding vs. collision lost case

Values of heave, roll and pitch gradually increase as stability deteriorates due to progressive flooding until vessel is lost.

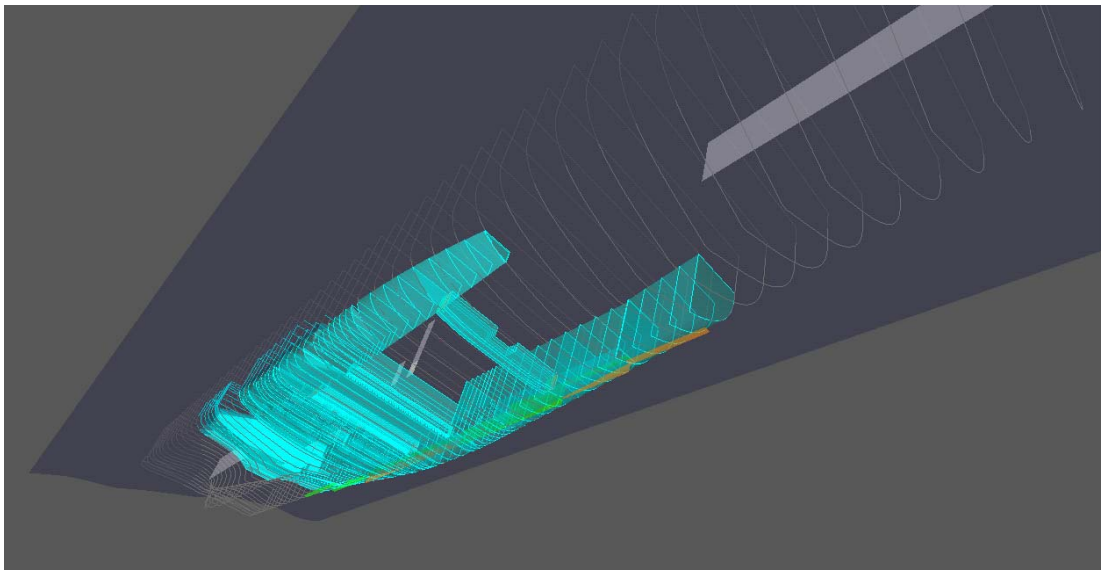

Figure 6-24: Large, side grounding case (EUGD01-R1 – DMG255)

Flooding of the lower compartments actually improves stability in waves

Table 6-1: Hydrostatics of two grounding damages for EUGD01-R1

In this table a comparison is presented of the hydrostatic values of two damage cases taken from the MC simulations for grounding with the intact values. Note the increase of GM value in damaged condition for both damages

		DMG062	DMG255	
Kxyz	Lpp	174.8	174.8	[m]
	Breadth	25	25	[m]
	Draught	6.4	6.4	[m]
	Mass	16717.32	16717.32	[t]
	CGs (X)	-5.265	-5.265	[m]
	CGs (Y)	0	0	[m]
	CGs (Z)	12.33	12.33	[m]
Oxyz	Intact			
	GMT	2.16	2.16	[m]
	GML	412.532	412.532	[m]
	WPA	3691.537	3691.537	[m^2]
	Displ	16717.2	16717.2	[t]
	CB (X)	-5.265	-5.265	[m]
	CB (Y)	0	0	[m]
	CB (Z)	-2.683	-2.683	[m]
	After Equilibrium Reached condition			
	GMT	2.233	3.352	[m]
	GML	389.725	502.63	[m]
	WPA	3484.748	3598.064	[m^2]

CB (X)	-5.265	-5.265	[m]
CB (Y)	0	0	[m]
CB (Z)	-2.991	-3.066	[m]

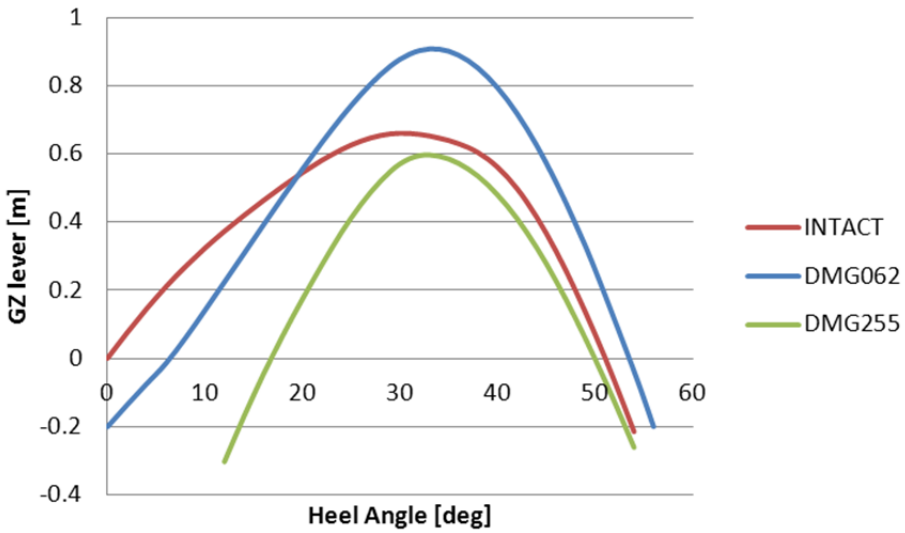

Figure 6-25: Comparison of GZ curves for intact and two damage cases for EUGD01-R1

Stability of the damaged vessel seems to be at least equal to that of the intact condition. High heel angles are caused by large asymmetrical flooding and are no threat to the survivability of the vessel.

6.3.3 Critical wave height simulations

Given that progressive flooding can potentially by sped up by severe weather conditions, an additional exercise was carried out in order to identify the contribution of the environment to the survivability of the damaged vessel. To this end, the damages that resulted in loss were individually simulated in various sea-states. Each damage case was tested at 4 wave heights, twice for each wave height.

The results of this study are presented in figures 6-26 and 6-27. Time to capsize demonstrates remarkable consistency against varying wave height, meaning that there is no ambiguity regarding the outcome of a grounding damage. That is, it will either be a survivable one or a non-survivable one. That can only be attributed to the hydrostatics of the damaged vessel.

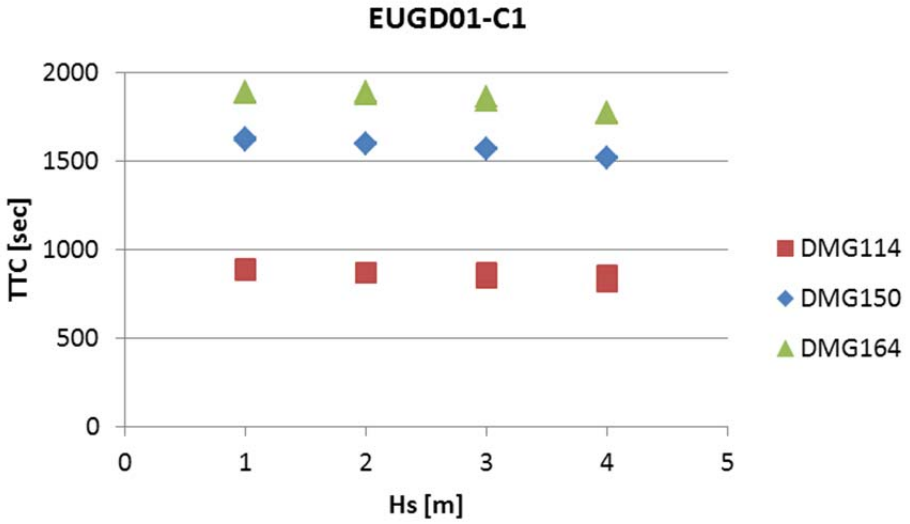

Figure 6-26: Time to capsize for the 3 damage scenarios tested for C1

Time to capsize seems to be unaffected by the increase in significant wave height.

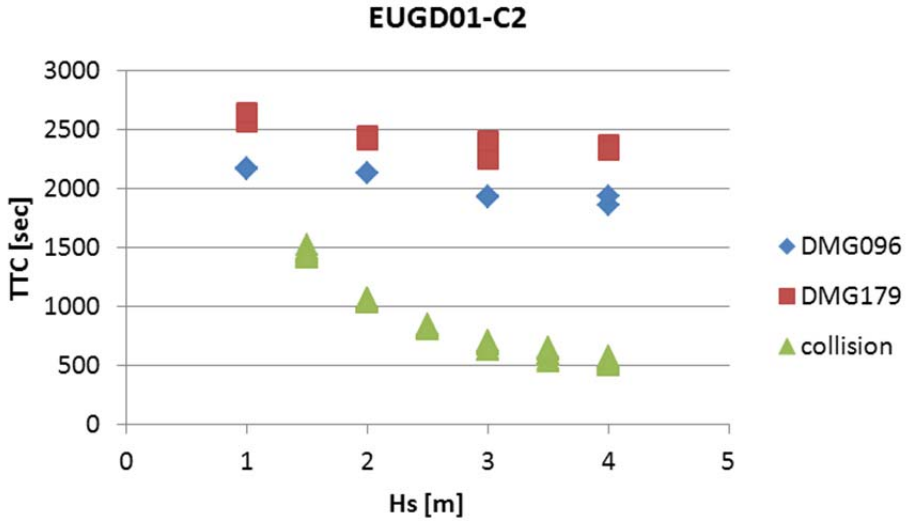

Figure 6-27: Time to capsize for the 3 damage scenarios tested for C2

The same observation made for C2, where TTC is not influenced by significant wave height as much as in the case of collision also pictured.

6.4 Risk from evacuation

The process of evacuating a large passenger vessel is a very complex situation. There are numerous reasons for that among which the complexity of the ship layout, of which the passengers have very little knowledge as they have probably only been there for the first time. Another contributor to the difficulty is the management of such huge numbers of people at the same time. Even when passenger vessels were limited to 2-3k passengers, designers and operators were discussing about the perils of evacuation, never mind now that it is common to have double that amount of guests in a modern cruise vessel. Add the unpredictability of humans when it comes to panic situations, the motions of the vessel that would probably make things even worse and the inaccessibility of some spaces due to flooding or fire. It becomes apparent that the moment evacuation is ordered we have already started to measure fatalities. This suggestion is backed up by the fact that fatalities have occurred even in drills.

For this reason it has been suggested in [41] that the ship itself is the best lifeboat available leading to the Safe-Return-to-Port regulations of the latest generation. However, the tools exist to measure the performance of a given design in evacuation in order to compare and identify any possible bottlenecks in the design that hinder the evacuation process.

6.5 Safety level

The major benefit of the change from the deterministic frameworks for damage stability of the past to the current performance-based state of the art is the ability to have a measurement of the level of survivability of any given design. The required level of survivability is probably the key parameter in any probabilistic framework, in essence answering the question "how safe is safe enough?" To this end, survivability analysis results on representative cruise and Ro-Pax ships can be related to design and operational parameters with a view to define and quantify the relationships between damage survivability characteristics following a collision and time available for evacuation with potential outcomes in terms of people potentially at risk.

To this end, a comprehensive performance-based survivability assessment of 4 passenger vessels has taken place within EU funded project GOALDS. The target is to provide an answer regarding the safety level offered by modern, state-of-the-art ships, firstly for the development of an analytical methodology for the estimation of risk from flooding but also for the development of a rational level for the required index of subdivision. Independent as well as in-house developed tools provided us with the capability to perform the survivability assessment in various ways and compare them against each other, thus securing a reliable result.

6.5.1 The R-Factor

The minimum level of survivability a vessel should offer is postulated by the R-factor. This applies either to new ship designs or existing ships and should reflect the societal acceptance of risk from loss of life. Currently, the R-factor as postulated by SOLAS 2009 is calculated based on the size of the vessel, the number of passengers and the available life-saving appliances [29]. The formulation can be seen below.

$$R = 1 - \frac{5000}{L_S + 2.5N + 15225} \tag{6-1}$$

Where: N = N1 + 2N2

N1 is the number of passengers for which lifeboats are provided

N2 is the number of passengers for which lifeboats are not provided

The SOLAS 2009 R-factor is currently being subjected to major investigations. Most of the important European projects at the moment have a task of estimating if the current formulation is reasonable and if not what needs to be changed.

A typical F-N diagram contains 3 zones according to severity as can be seen in figure 6-28. A common mistake between the people in the industry is the perception that if the F-N curve lies within the boundaries of the ALARP region the design is acceptable. Since risk is a product of probability (P) and consequences (C), it is relatively easy to prove that if we accept that C = 1 then it is reasonable to suggest that P has to be as small as possible. Or, in other words, the F-N curve should in fact be as noted by the acronym: As-Low-As-Reasonably-Practicable, thus not low enough in the example of the

figure. The ALARP region boundaries have been obtained by Skjong et al. [27] and could change.

Using the previously described methods for performance-based assessment, a series of experiments were conducted towards the estimation of the safety level of the vessels in question.

6.5.2 Sample vessels

The study vessels have been selected in such a way so as to ensure coverage of the design space for passenger vessels. The sample consists of two RoPax ships, a small one of 89m length for short daily voyages and a larger one of 174.8 m length for longer, night voyages, and two cruise ships. The cruisers are one vessel built to fit the Panama Canal, with approximately 2.5k passengers and a larger post-PANAMAX class with almost 4k passengers on-board. The latter belongs to a relatively new class of cruise vessels developed recently to accommodate for the entertainment needs of an increasing in popularity cruise holiday sector. The dramatic increase of size of cruise vessels also serves the purpose of cost reduction for the guests and company. With the new, wider Panama Canal almost complete at time of writing, such vessels are almost certainly going to be the dominant form of the cruise industry in the years to come. Their attributes can be seen in table 6-2. These are also the vessels used concurrently for the derivation of the model for the survivability of damaged passenger vessels in waves. The selection also ensures that any similarities or differences existing between these ship types will be well pronounced so as to be dealt with accordingly.

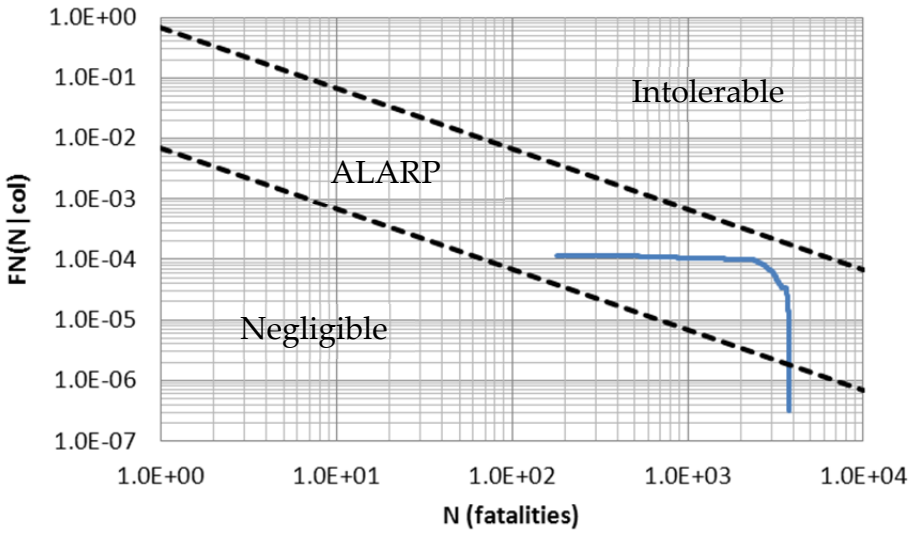

Figure 6-28: A typical F-N diagram.

The dashed bold lines separate the diagram in "Intolerable", "ALARP" and "negligible" areas according to difference of severity.

Table 6-2: Principal dimensions of study ships

The sample consists of two RoPax Vessels (R1 & R2) and two cruise vessels (C1 & C2)

	R1	R2	C1	C2
Number of passengers	1400	800	3840	2500
LOA [m]	194.3	97.9	311	295
LBP [m]	176.0	89.0	274.7	260.6
Breadth moulded [m]	25.0	16.4	38.6	32.2
Deepest subdivision load line [m]	6.55	4.0	8.6	8.0
Depth to bulkhead deck	9.1	6.3	11.7	10.6
Displacement [tn]	16,6	3,4	62,5	45.0
Service speed [kn]	27.5	19.5	22.6	22.0

6.5.3 Method

A selection of tools has been used for the calculation of the PLL for the sample vessels. The tools have been developed within the SSRC in pursue of performance-based assessment in every conceivable sector of ship safety. Only a brief description has been included in this chapter for reference and explanation of the method since they have been presented in detail in chapter "Performance-Based assessment".

6.5.3.1 Evacuability

EVI – short for Evacuability Index – is a software product developed to measure the performance of a vessel with respect to evacuability. It can provide information in a microscopic level regarding local vulnerabilities of the design vessel or, more relevant in this case, in a macroscopic level, provide with the cumulative distribution function for time to evacuate. The models for evacuation are extremely complicated to manufacture and take a very long time and skill to complete and make work properly. This is because, although the program is built to replicate passengers' movements and crew tasks to the highest degree of realism, it still has certain limitations so, in order to make the "agents", as passengers and crew are called, to behave as expected, certain tricks have to be followed. For these reasons, and given that it is generally accepted that accuracy in evacuation is of little significance to the overall result in risk to human life, given the mostly binary result of damage survivability no models for evacuation of the specified ships were developed. Instead, the results of similar models that were developed for other vessels were used, scaled to match the number of people on-board the sample ships used here. The results were, in any case,

compared to previous studies during SAFEDOR [26] to ensure their validity. The results used include day and night evacuation scenarios to reflect real life situations. A number of differences have been modelled between different times of day evacuation. For example, the passengers will mostly be in their cabins during the night, so evacuation should start from there. In addition the agents have some response delay time in night case evacuation to reflect the time it takes for people to become aware of the situation and start heading for the muster station. On the other hand, people will mostly be in public places during day time and their awareness time will be shorter. Thus the difference in evacuation time could be as much as double for a night case scenario compared to a day one. At this point, it would be reasonable to explain that by saying "evacuation", in this case what is actually implied is mustering. The processes of embarkation and abandonment, although very important and would most certainly add to the total time of ship abandonment have been knowingly omitted for a number of reasons, the main one being that the means have not yet been to developed to a reliable standard. Another reason is that these tasks would probably run in parallel with the task of mustering and would not be expected to alter the outcome more than a few minutes. Nevertheless, for the purpose of completeness, it is necessary for these tools to be developed for higher accuracy.

An example of an evacuation completion curve, as used, is shown in figure [6-29], where the difference between day and night evacuation is visible as well as the awareness delay during night time evacuation. Table [6-3] that follows shows the evacuation times for all the study vessels as these have been used in the study.

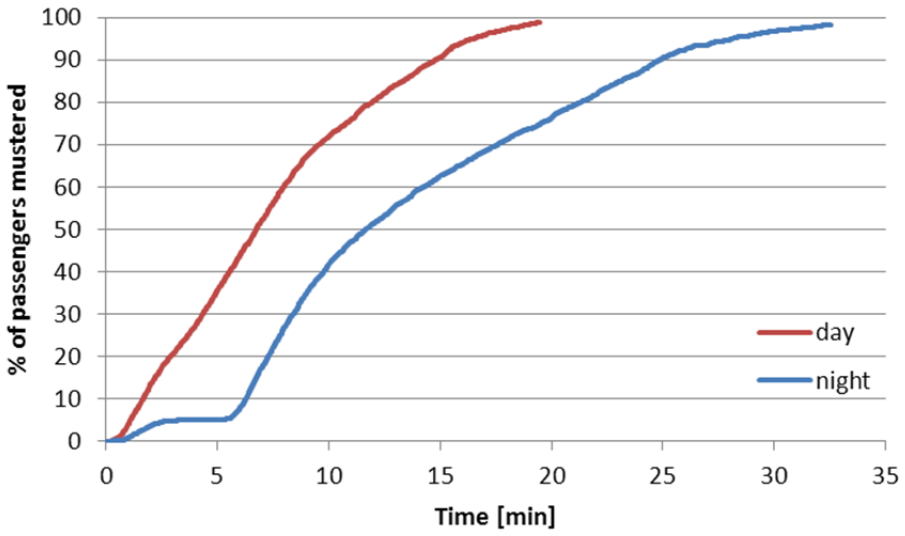

Figure 6-29: Evacuation Completion Curve

The evacuation completion curves are shown here for the PANAMAX vessel of 2500 passengers (EUGD01-C2) for the day and night evacuation cases. The stagnation point up to the first 5 minutes in the night scenario reflects the delay in awareness associated with night time evacuation procedure.

Table 6-3: Summary of the evacuation times for the study vessels

The complete evacuation completion curves for all the vessels can be found in appendix II.

	Complete	Day	Night
EUGD01-C1	50%	<10	<18
	100%	<30	<50
EUGD01-C2	50%	<7	<12
	100%	<20	<33
EUGD01-R1	50%	<2	<10
	100%	<7	<17
EUGD01-R2	50%	<4	<8
	100%	<14	<17

6.5.3.2 UGD

Univariate Geometrical Distribution utilises current SOLAS s-factor to predict a vessel's vulnerability to flooding. It does so by calculating the cumulative distribution function for time to capsize. At the same time it can use the predicted time to capsize to estimate the fatalities of each damage scenario, as per figure 6-31. In this way, and knowing the probability of occurrence of each damage scenario, the Frequency vs. Number of Fatalities (F-N) curve can be drawn. What is obvious in figure 6-31 is that in case the vessel is lost in less than 5 minutes, it can be assumed that all her passengers will be lost. It is a particularly big problem in RoPax vessels since, as it can be seen in figure 6-30, the CDF for Time to Capsize is very steep in the first few minutes meaning that most of the capsizes will have occurred within a very short time or indeed that the probability to capsize in a short period is very high. This is translated as either all passengers will be lost or none. This binary behaviour has led researchers to believe that a simplified method using none of the evacuation part and assuming that in every vessel loss all the passengers will be lost, an attractive alternative [9]. The model is presented in equation 6-2 below.

$$PLL = fr_{col} \cdot (1 - A) \cdot N_{PAX} \tag{6-2}$$

Where: PLL is Potential Loss of Life

fr_{col} is the frequency of collision as measured from statistics

A is the SOLAS 2009 Index-A and

N_{PAX} is the maximum number of passengers on-board

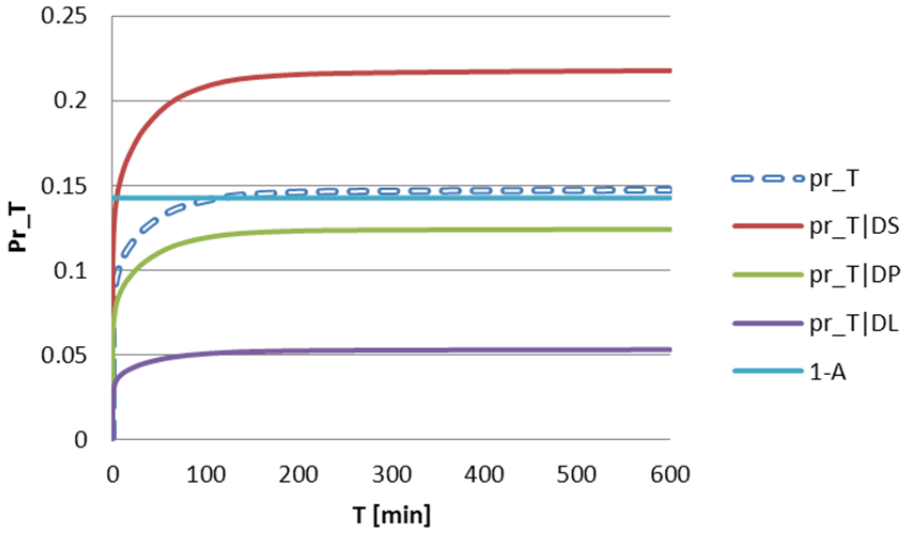

Figure 6-30: Probability of time to capsize

In this example of the outcome of UGD, the expected probability of time to capsize is visible; conditional, given the 3 individual loading conditions and unconditional as: $0.4 \cdot D_S + 0.4 \cdot D_P + 0.2 \cdot D_L$. The simplifying ***1-A*** is also shown. Probability of TTC for all the vessels can be found in Appendix III

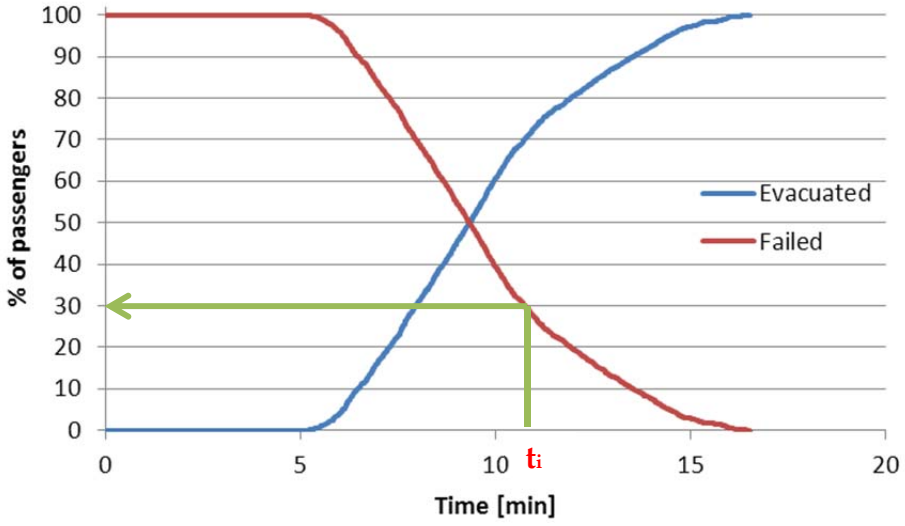

Figure 6-31: Model of fatalities in an event.

Knowing the time to capsize, t_i, the number of fatalities can be obtained.

6.5.3.3 MC simulations

A tool that is regarded as more accurate than analytical UGD, Monte Carlo simulations, has been used in order to validate its results. The setup is that each vessel is subjected to a series of simulations of damage scenarios that have been created by means of Monte Carlo sampling, drawing data from statistical distributions for damage characteristics as used in SOLAS 2009. More information regarding the code that has been used for the simulations, PROTEUS3, and the method of MC simulations can be found in chapter "Performance-Based Assessment".

500 damage scenarios were generated and simulated for 1 hour for the large cruise vessel (figure 6-33). The smaller cruiser was also simulated for 500 times for the same duration. The RoPax vessels were simulated for 300 times each, for duration of 30 minutes. Simulation setups for all vessels can be found in appendix VIII. Given the difficulties associated with numerical simulations, a realistic setup had to be devised. The more the simulations carried out the lesser the uncertainty of the outcome. Time of simulation has to be adequate so the stagnation point of the probability mass function for time to capsize will be found. Given that results for RoPax vessels are known to reach a stagnation point earlier than 30 minutes, this was regarded as an adequate time. 1 hour was chosen for cruise vessels. The uncertainty associated with 500 runs is estimated to be around 30% when this is about 50% for 300 simulations.

As can be seen in figure 6-32 below, UGD showed good agreement with simulation results, lying consistently within the simulations' uncertainty boundary. The complete results from the MC simulations and the validation of the UGD can be found in Appendix IV.

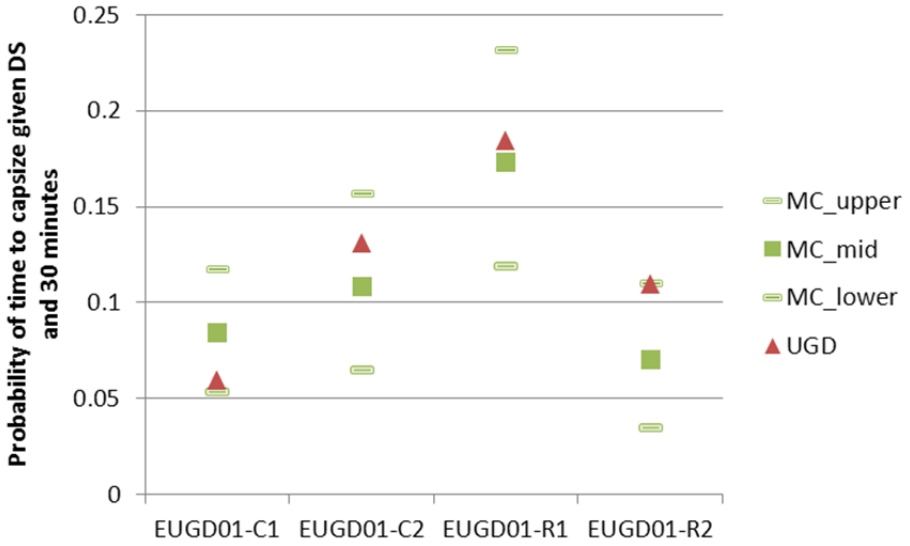

Figure 6-32: Results of the validation of UGD

A summary of the validation exercise is shown here. Results of the UGD fall consistently within the uncertainty boundary of the numerical simulations. Figures can be found in Appendix IV.

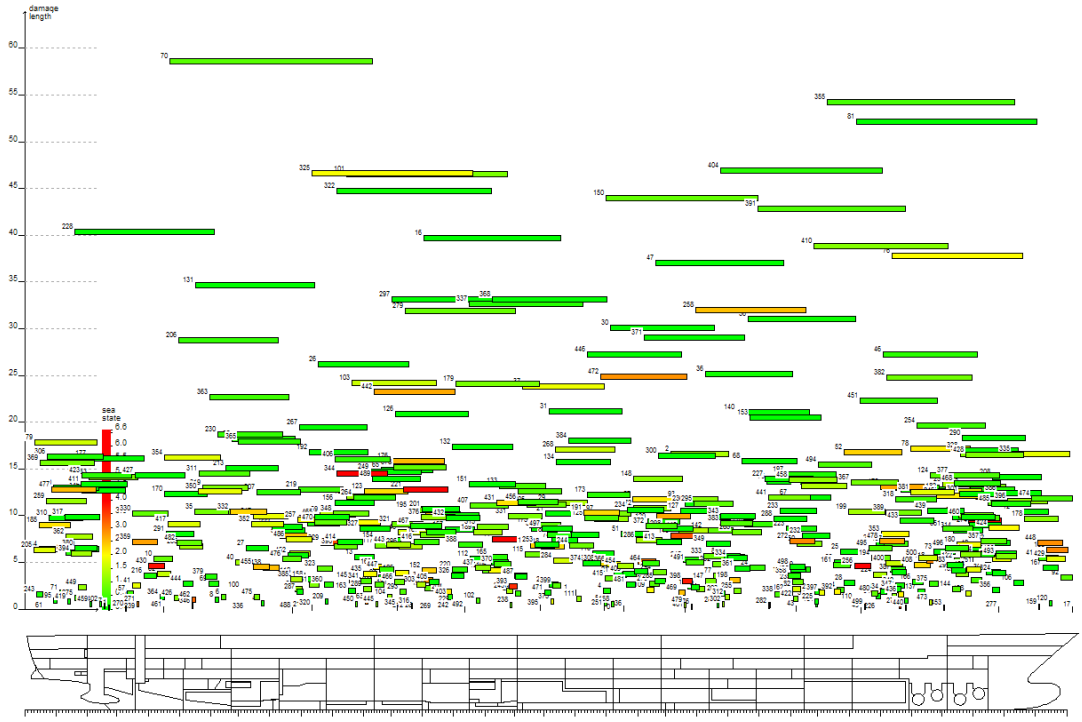

Figure 6-33: 500 damages simulation setup for EUGD01-C1

All simulation setups of the vessels can be found in Appendix VIII

6.5.4 Risk from flooding

There has been a lot of discussion regarding the frequency of the hazards of modern vessels. Numerous attempts have been made within projects in an attempt to establish reasonable values and all have been accepted with a lesser or larger degree of scepticism. In order to get a definitive answer regarding the influence of frequency, the study involved getting the F-N curves and PLL values for various collision frequencies for the study ships that range from 5.0E-04 to 1.0E-02. An extra value of 3.21E-04 according to an FSA for MSC85 [18] has been used for the small RoPax for benchmarking of the method against existing studies. It appears though that no matter the frequency, the potential loss of life is quite high, not only for the vessels carrying thousands of passengers, figure 6-34, but also for smaller vessels as pictured in figure 6-35.

From figures one could easily argue that both these cases definitely require risk control options irrespective of cost effectiveness. The resulting PLL for all the ships and frequencies is visible in table 6-4.

It can be generalised that PLL is increased according to the order of magnitude of passengers carried by the vessel. The linear relation between frequency and potential loss of life can be seen in figure 6-36 where the average PLL values for night and day cases have been plotted against frequency values considered.

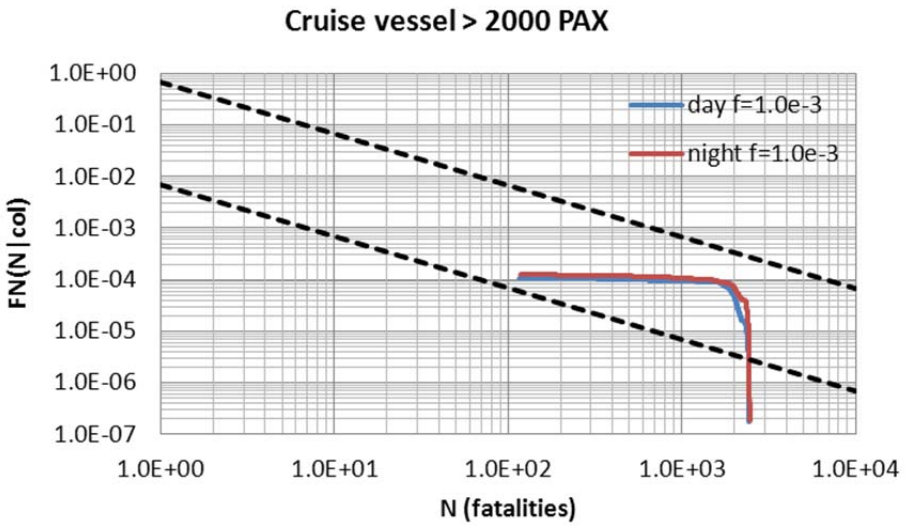

Figure 6-34: F-N diagram for one of the cruise vessels.
The frequency of collision is equal to 1.0E-03. The societal criteria have been placed according to [19] and [27].

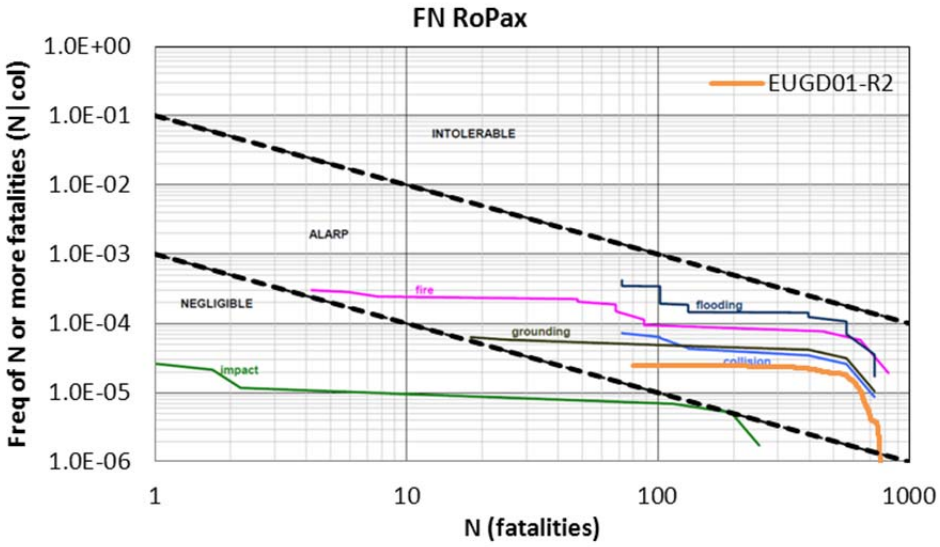

Figure 6-35: F-N diagram for EUGD01-R2 and comparison with FSA [18].
The frequency of collision is equal to 3.21E-04 [18]. The societal criteria have been placed according to [18] and [27].

Table 6-4: Summary of resulting PLL values

The frequencies tested can be seen in the first column while the corresponding vessels in the first line. The table is separated according to day and night evacuation analysis. The average is also shown. PLL values are in fatalities per shipyear.

day

f	C1 day	C2 day	R1 day	R2 day
1.00E-02	2.1301E+00	4.1819E+00	1.4342E+00	1.4862E+00
5.00E-03	1.0843E+00	2.1920E+00	7.2680E-01	7.2100E-01
1.00E-03	2.2125E-01	4.3239E-01	1.4224E-01	1.5331E-01
5.00E-04	1.0935E-01	2.0827E-01	7.1820E-02	7.9615E-02

night

f	C1 night	C2 night	R1 night	R2 night
1.00E-02	2.9909E+00	5.8213E+00	2.8226E+00	1.2854E+00
5.00E-03	1.4845E+00	2.8361E+00	1.4625E+00	6.9774E-01
1.00E-03	2.9085E-01	5.8016E-01	2.8990E-01	1.3640E-01
5.00E-04	1.5004E-01	2.9393E-01	1.5004E-01	6.7026E-02

average

f	C1	C2	R1	R2
1.00E-02	2.56E+00	5.00E+00	2.13E+00	1.39E+00
5.00E-03	1.28E+00	2.51E+00	1.09E+00	7.09E-01
1.00E-03	2.56E-01	5.06E-01	2.16E-01	1.45E-01
5.00E-04	1.30E-01	2.51E-01	1.11E-01	7.33E-02

Simplified model - $f*(1-A)*N_{MAX}$

	C1	C2	R1	R2
Index-A	0.9217	0.8507	0.85734	0.9021
N_{MAX}	3840	2500	1400	800
1.00E-02	3.01E+00	3.73E+00	2.00E+00	7.83E-01
5.00E-03	1.50E+00	1.87E+00	9.99E-01	3.92E-01
1.00E-03	3.01E-01	3.73E-01	2.00E-01	7.83E-02
5.00E-04	1.50E-01	1.87E-01	9.99E-02	3.92E-02

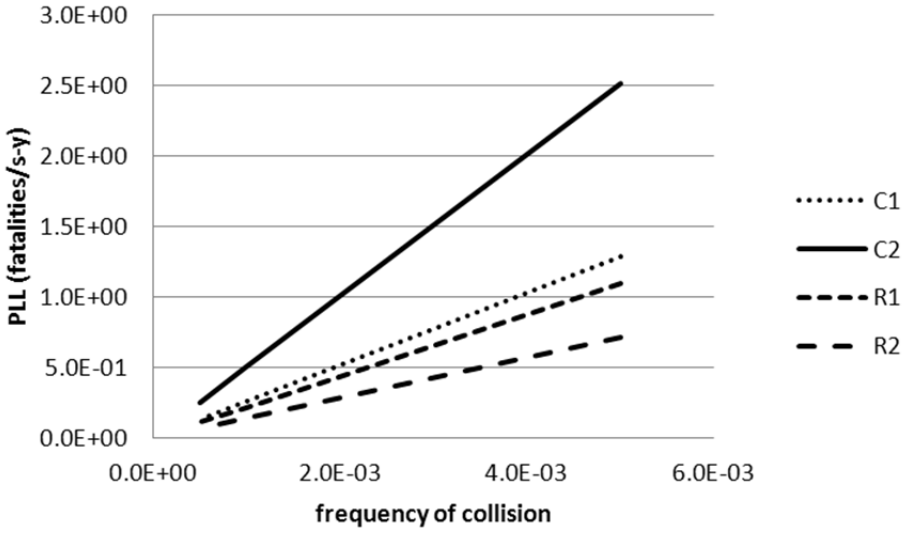

Figure6-36: Average PLL vs. frequency of collision.

Values are shown for the four sample ships and average is calculated from day and night evacuation scenarios

6.6 Discussion

Although there is still a great distance to be covered with respect to establishing a reasonable required level of survivability, this study has provided with a few insights to the right direction. Probably, the most important of those is that, no matter what the frequency of incidents compromising the ship safety, the large number of guests in modern ships suggests that if the potential exists the consequences will be catastrophic. As it has been stated in [46]: *"…for any probable but non-survivable scenario (i.e., with s=0), consequences are likely to be intolerable and hence the risk unacceptable. Therefore, the probability of a non-survivable damage scenario must be remote or in other words there cannot be feasible damage scenarios with s=0, irrespective of what the value of A and hence R is!"* Note in figure 6-36 that for ship C2, a frequency of collision of 2.0E-03 translates in 1 fatality per ship year or for a fleet of 100 vessels, 1000 fatalities every 10 years – a value that seems to be supported by accident statistics.

Adding the fact that there are experiments that suggest that modern ships could capsize within a few minutes thus leaving little time for evacuation only strengthens the suggestion that the required index should be revised. Furthermore, this study has supported the belief that, irrespective of how safe a ship is, risk will always increase as the number of passengers onboard increases.

Chapter 7 – Evolution of regulatory frameworks

7 Evolution of regulatory frameworks

Deterministic regulatory frameworks of the past could provide information of whether a vessel complied with a pre-determined set of criteria but failed to provide information on the level of safety pertinent to the specific design. Probabilistic frameworks by definition can provide such sort of information, necessary for comparison in an optimisation process. SOLAS 2009, as a probabilistic framework, entails this capability but failed to inspire confidence in the maritime industry due to a series of misconceptions and inherent drawbacks in its formulation and application. The latest developments in survivability assessment have provided the ability to measure the survivability of any design, irrespective of which standard it is developed to comply with. Both numerical and analytical performance-based assessment methods will be utilised, highlighting in the process any inherent inconsistencies in each framework, in an attempt to restore confidence in state-of-the-art on damage stability assessment. Specific attention is to be paid to the controversial design feature of the long lower hold as industry had good reason to believe the new regulations did not properly take care of this specific commercially viable feature. To this end, this section is aimed at conducting a direct comparison of probabilistic and deterministic regulatory frameworks for damage stability on a selection of Ro-Ro passenger vessels of various sizes with special focus on the level of safety implied by current and past regulations, overall as well as regarding such specific features, in an attempt to estimate their contribution to survivability and restore confidence in overall probabilistic frameworks.

7.1 Method of approach

The study is separated in two parts. The first part is the evaluation of the accuracy of Index-A as an analytical tool for performance-based assessment. To this end various RoPax and cruise vessels' vulnerability is measured by means of numerical simulations with the method of Monte Carlo, as described in chapter "PBS". Then the Index-A of the models is calculated and based on that, the marginal distribution for time-to-capsize by use of the UGD. The results of these two can be directly compared as they both calculate the same thing. During the second part, which is only done for RoPax vessels, the design alternatives developed would form the basis for a statistical evaluation of the regulatory instruments in question. 3 parametric models of 3 different sizes of RoPax vessels were automatically varied to generate a large number of design variants that would be checked with respect to their vulnerability and compliance with previous regulatory standards. Due to the increased time and effort required by the numerical simulations to evaluate the survivability of a design, it would have been impossible to repeat the procedure for each one of the hundreds of different designs developed for the second part, thus rendering the analytical model (i.e., Index-A), albeit not as accurate, the only choice.

7.2 Sample vessels

7.2.1 Parametric RoPax vessels

3 different parametric models of typical RoPax ships, of small, medium and large size form the basis of this study. Details of their principal dimensions can be found in table 7-1. Based on these initial designs, 15 models were generated for the first part of the study, 5 for each size, each one complying with a different set of regulations. The regulations taken into account are:

A. SOLAS 1990 (Chapter II-1 Regulations 4-12)
B. SOLAS 1990 (Chapter II-1 Regulations 8-12)
C. A.265 (Regulation 1-11)
D. SOLAS 2009 (Chapter II-1 Regulations 5-9)
E. SOLAS 1990 (Ch. II-1 Reg. 8-12) + MCA additional requirements

Sample arrangement of the RoPax ships can be seen in figure 7-1. The vessels were prepared with high accuracy and detail, although, as concept designs, their survivability performance might be slightly higher than that of a built ship, due to asymmetries and several other compromises that inevitably reach production.

The calculations were carried out for two loading conditions for each vessel, the first loading condition being the same for all vessels of the same size. The second corresponds to limiting conditions according to the regulation in question. The results were quite interesting as they highlighted the effect of operational conditions on the survivability of each vessel. Limiting KG value (maximum allowable) has been applied for deterministic regulations while A=R was sought for probabilistic ones.

Table 7-1: Properties of study RoPax ships

Parameter	Ship 1	Ship 2	Ship 3
Length (BP)	105 m	150 m	200 m
Breadth (moulded)	18.6 m	26.5 m	29.4 m
Depth (moulded)	12.8 m	14.3 m	15.3 m
Draught (design)	4.8 m	6.2 m	6.7 m
Displacement	5955.68 t	16653.4 t	26090.7 t
Passengers	600	1400	2000

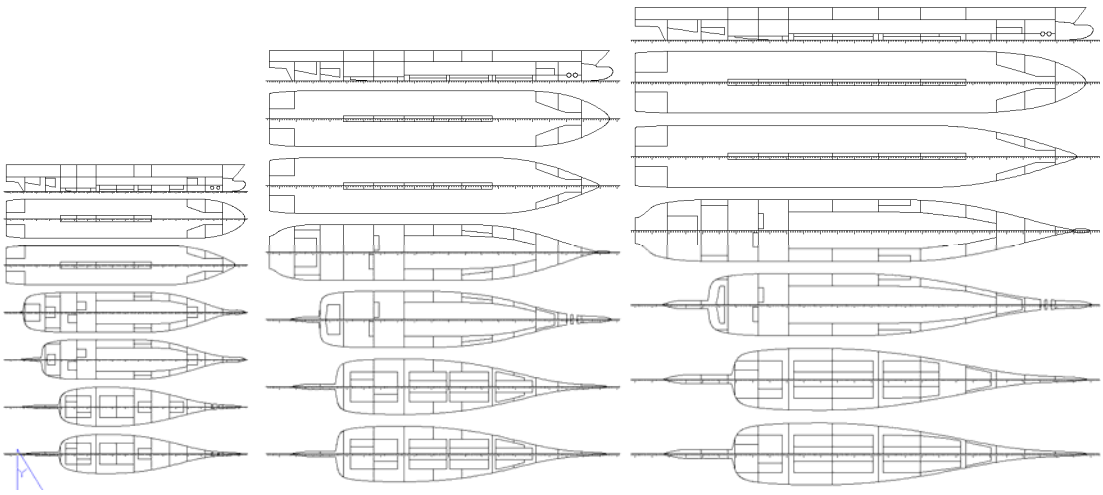

Figure 7-1: Sample subdivisions

A sample variant from each size is shown here in scale for comparison. All the designs had the ability to be subdivided in such way so as to comply with each one of the regulatory frameworks considered. Samples shown here are equipped with a lower hold but they could be subdivided without one as well.

7.2.2 Cruise ships

Regarding the cruise vessels, due to the difficulty involved in developing and running a parametric model, they were limited to only two different designs. These are the same two SOLAS '90 designs, the PANAMAX and the post-PANAMAX vessels, called EUGD01-C1 and C2, used in chapter "vulnerability". Their principal dimensions and other properties are shown in table 7-2 as a reminder and their subdivisions can be found in Appendix I.

Table 7-2: Attributes of the cruise ships

	C1	C2
Number of passengers	3840	2500
LOA [m]	311	295
LBP [m]	274.7	260.6
Breadth moulded [m]	38.6	32.2
Deepest subdivision load line [m]	8.6	8.0
Depth to bulkhead deck	11.7	10.6
Displacement [tn]	62,5	45.0
Service speed [kn]	22.6	22.0

7.3 Accuracy of Index A – a comparison with first principles

In order for Index-A to be used as a measure of survivability, its accuracy needed to be evaluated. This meant that it would need to be compared with the results from a method with accepted accuracy. The method at hand was no other than numerical simulations. The method described in chapter "Performance-Based Assessment" as Monte Carlo numerical simulations was used. As a reminder, this method uses probability distributions, obtained from statistics, for damage characteristics to generate a number of damage cases (300 for the RoPax vessels and 500 for the cruisers) which involve damage opening extent and location as well as environmental conditions. Each damage scenario is then simulated for 30 minutes for RoPax and 60 minutes for cruise vessels. The overall result is the marginal probability for time to capsize, given the particular loading condition and the time of simulation, or else ship vulnerability to flooding due to collision. The uncertainty of this method, for 300 simulations per ship is an estimated 10% approximately while for 500 cases is less at 4% roughly. Index-A was calculated for these vessels as well by use of naval architecture package NAPA. The results of this first part of the study are very encouraging regarding the validity of Index-A in the case of RoPax but no so in the case of cruise ships. For RoPax, the index presents a positive relation with the more accurate Monte Carlo simulations, increasing confidence in the use of the index as a means of performance-based survivability assessment. Figure 7-2 demonstrates how Index-A lies mostly within the confidence intervals of the Monte Carlo simulations. The correlation is strong enough for the data to be regressed in an attempt to reduce the error of prediction [23]. The error of the distribution can be seen in figure 7-3. The histogram is symmetrical around a mean value of 4.8 with a standard deviation of 4.6.

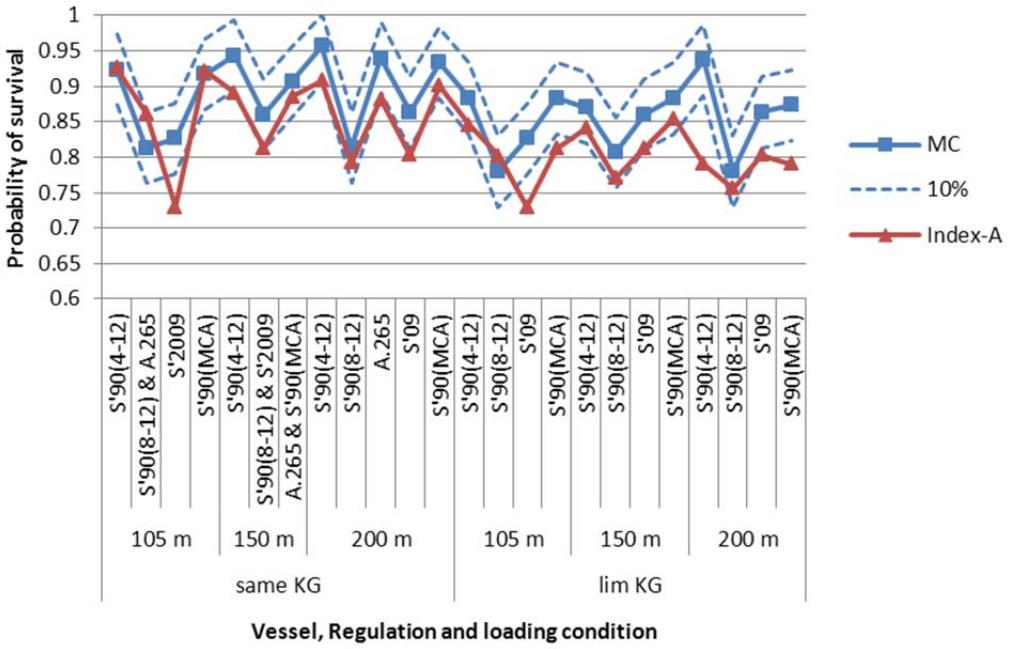

Figure 7-2: Index-A vs. MC simulations

A comparison of the results of MC simulations with Index-A; the index values lie mostly within the 5% confidence interval – shown in the figure – of the numerical simulations. Note that Index-A results are regularly lower (conservative) than numerical.

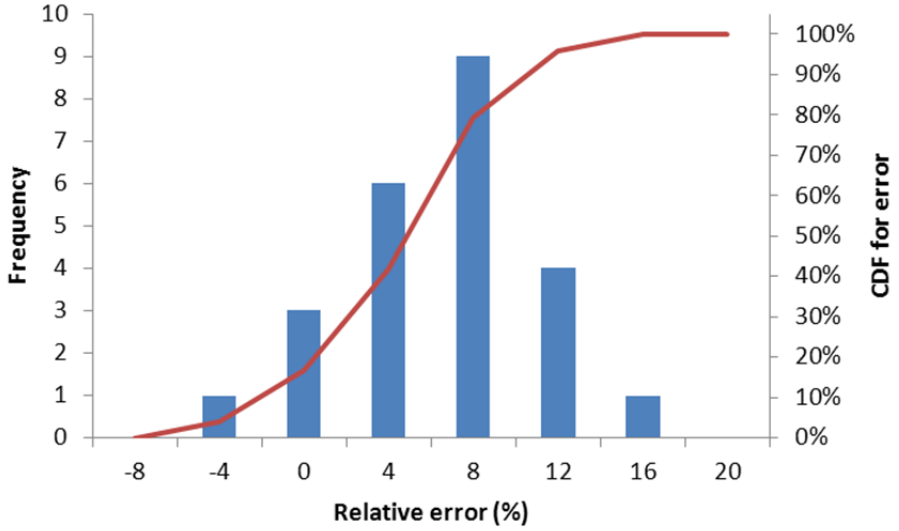

Figure 7-3: Approximation error

The error of Index-A is shown in this histogram. It is a symmetrical distribution around a mean value of 4.83. The results were further regressed with the method of design of experiments [23], reducing the prediction error to less than 6%.

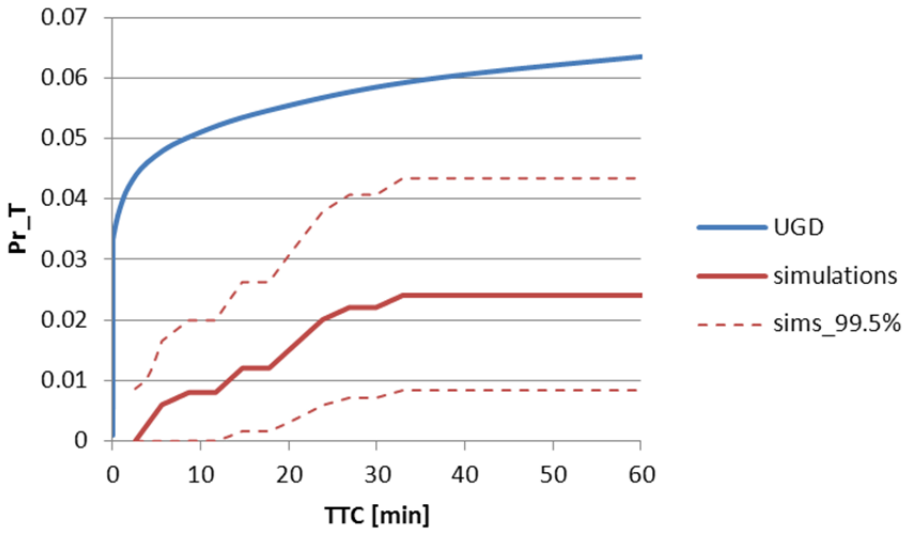

Figure 7-4: Simulations vs. UGD for EUGD01-C1

Index-A based UGD results in more than double the vulnerability to flooding suggested by MC simulations. Index-A in this case is 0.93263.

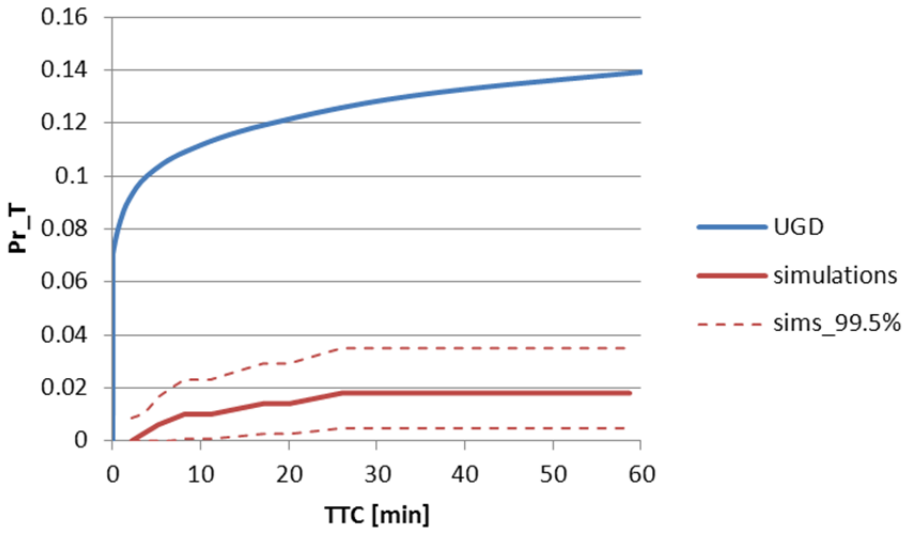

Figure 7-5: Simulations vs. UGD for EUGD01-C2

In the case of the smaller cruise vessel, the gap between the UGD and MC simulations is still greater with the former predicting that 14% of collisions will lead to capsize within 60 minutes as opposed to the simulations' 2% (4% max) prediction. C2's Index-A is 0.85070.

7.4 Inconsistency of previous regulatory frameworks

Since Index-A has proven to be an accurate measure of survivability, it can be safely used in the second part of the study as a PBA tool for the large number of variants needed for statistical investigation of the regulations [23]. Each variant was checked for its compliance with each regulation set thus resulting in compliant vessels that had the same PBS with non-compliant ones. In fact the level of overlap between compliant and non-compliant variants was, particularly in the case of the small vessel, alarming. A typical case of overlap is shown in figure 7-6, where medium ship variants are checked against their compliance with SOLAS '90. It appears that, while a ship that complies with any deterministic regulation does have a high level of survivability, the opposite is not guaranteed, meaning that if a ship is not compliant with a deterministic regulation doesn't necessarily have low survivability. Figure 7-7 depicts the percentage of overlap for all studied ship variants, separated by size and regulation. A 30% overlap as in the case of the medium and large designs is alarming enough but the close to 90% overlap in the case of the smaller vessel is simply unacceptable.

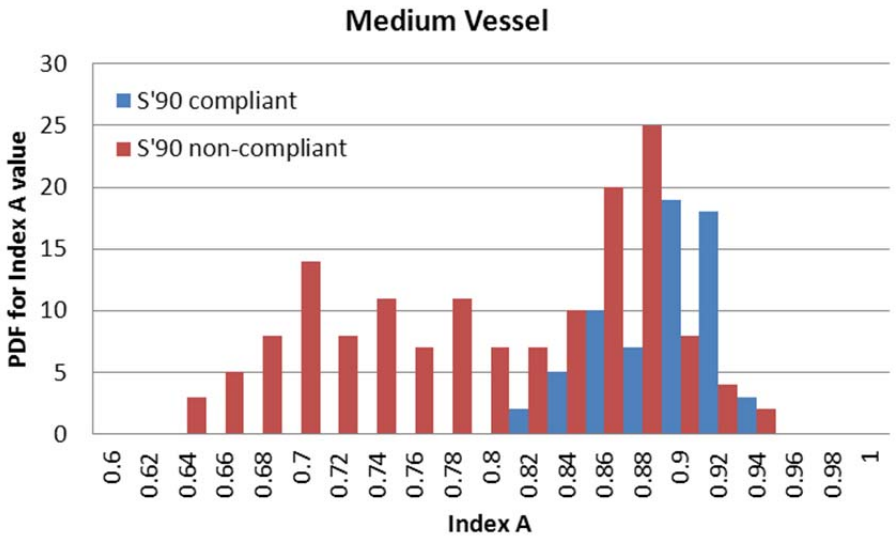

Figure 7-6: Overlap example [23]

In this example of superimposing of compliant and non-compliant variants of the medium sized vessel, it is made obvious that a region exists that complying and not complying to SOLAS '90 vessels have the same level of survivability.

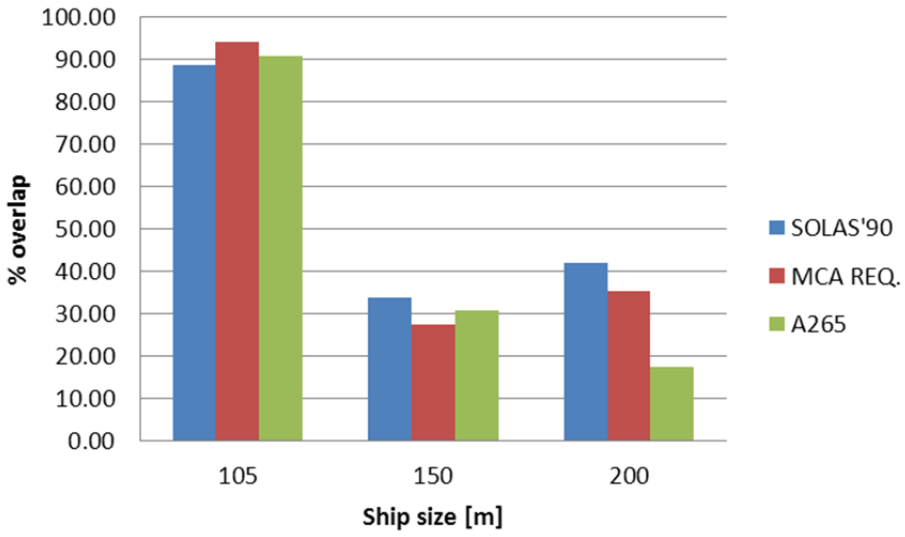

Figure 7-7: Percentage of overlap.

In this separation of compliant and non-compliant variants with respect to size and regulation [23] it can be seen that in the case of the smaller vessel the overlap is roughly an astonishing 90%.

7.5 Comparison of regulatory frameworks

Regarding the variants that comply with the regulations, the results seem to be rather consistent. Generally, when the additional MCA requirements are applied to SOLAS '90 ships these appear to have the highest survivability, followed closely by A.265 as can be seen in figure 7-8 that shows the expected mean Index-A given size and regulation. Another fact also apparent in the same figure is that in order to guaranty that compliance with SOLAS 2009 offers as high a level of survivability as the previous regulations, required index of subdivision, R, will need to be increased.

Regarding numerical simulations, the picture changed when limiting loading conditions were applied. Limiting conditions mean, in this case, that the KG of the vessel is the maximum allowable by each regulation and in case of SOLAS 2009 A is as close to R as possible. Due to the complications involved, limiting loading conditions were only applied for the initial 15 designs used for the evaluation of Index-A as a measure of survivability. The results are shown in figure 7-9 where the bars on the left correspond to the numerical simulations' results of ships without a long lower hold, complying with SOLAS '90 (Ch.II-1, Reg. 4-12). It can be said that vessels designed specifically to comply with SOLAS 2009 and MCA additional requirements, even if the ship is equipped with a lower hold, have comparable risk level to ships that don't. The reason for this seems to be that SOLAS '90 (Ch. II-1, Reg. 8-12) is virtually "blind" to the feature of the lower hold, while MCA requirements take it into consideration and the fact that a LLH would penalise Index-A massively, its size is indeed effectively kept under control.

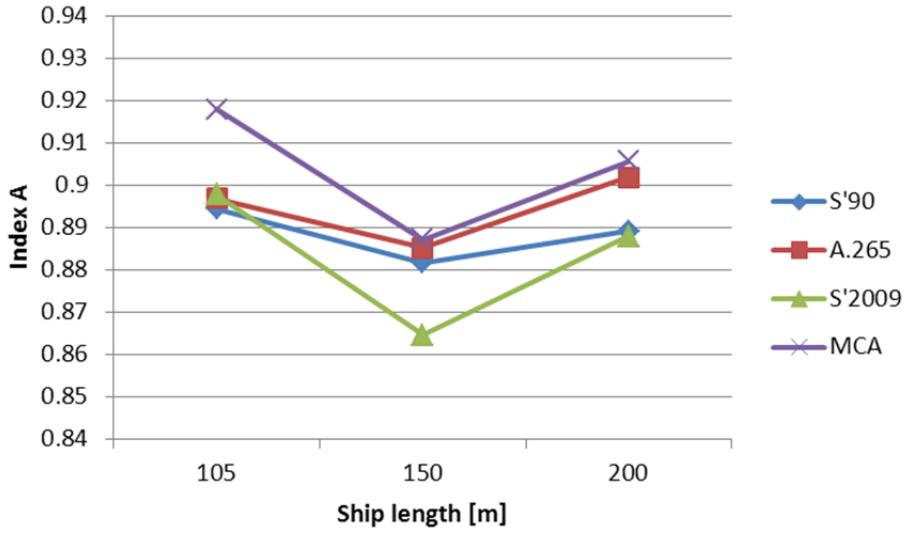

Figure 7-8: Expected mean Index-A [23]

Results here are split with respect to size and regulation. Medium vessel variants have somewhat lower survivability as do, on the average, ships complying with SOLAS 2009, although in this resolution the error of measurement is comparable.

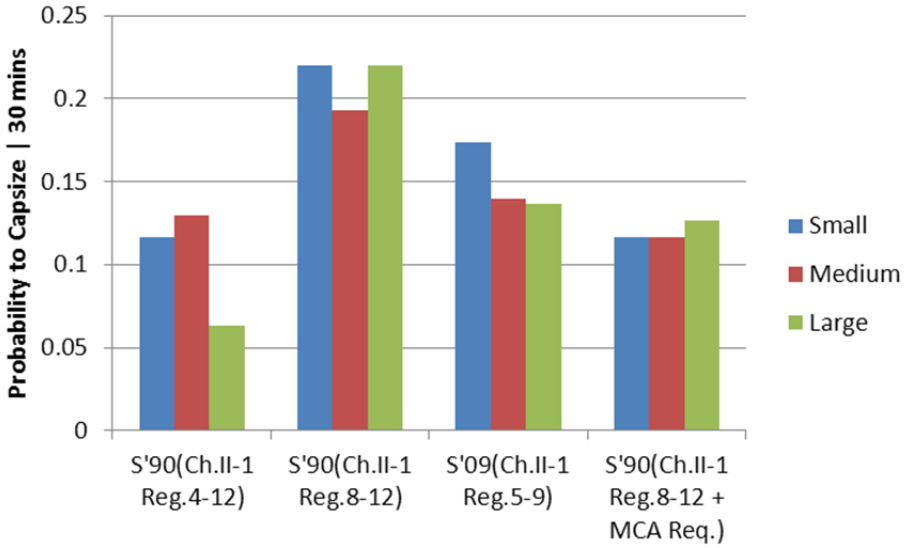

Figure 7-9: Numerical simulation results – limiting loading conditions

Maximum allowable KG and A close to R were applied to get limiting loading conditions. SOLAS '90 has the highest vulnerability – due to its "blindness" to LLH, while the other regulation seem to be better fitted to handle the lower hold as their performance matches ships without a LLH (bars on the left)

7.6 Contribution of LLH

The LLH is highly valued in the industry for commercially utilising spaces that would otherwise have no use. However, it is a large un-subdivided space low in the ship making it particularly vulnerable in case of flooding. Should the LLH be flooded it essentially means that there wouldn't be enough residual buoyancy to stay afloat. That said, if the residual buoyancy exists, the decreased centre of gravity that is the result of flooding of a lower space would mean that the ship would have no problem of stability. The probability of damaging the LLH is proportional to its size compared to the size of the vessel as visible in figure 7-10. The following figures show the distribution of probability of the s-factor with the contribution of the LLH.

The example of figure 7-11 demonstrates that the LLH is damaged in approximately 40% of the cases that have no stability whatsoever (s=0) but is also involved in roughly 25% of the cases that have GZ_{MAX} and Range of stability larger than 0.12 m and 16 deg. respectively. Overall, the number of cases resulting in no stability and involve the LLH decreases as ship size increases as can be seen in figure 7-12. This under no circumstances means that larger vessels have lower vulnerability than smaller ones when equipped with a lower hold (see figure 7-9). Put simply it means that the percentage of damages that result in no stability whatsoever and involve the LLH, over the total number of damages that result in no stability, is smaller the larger the vessel.

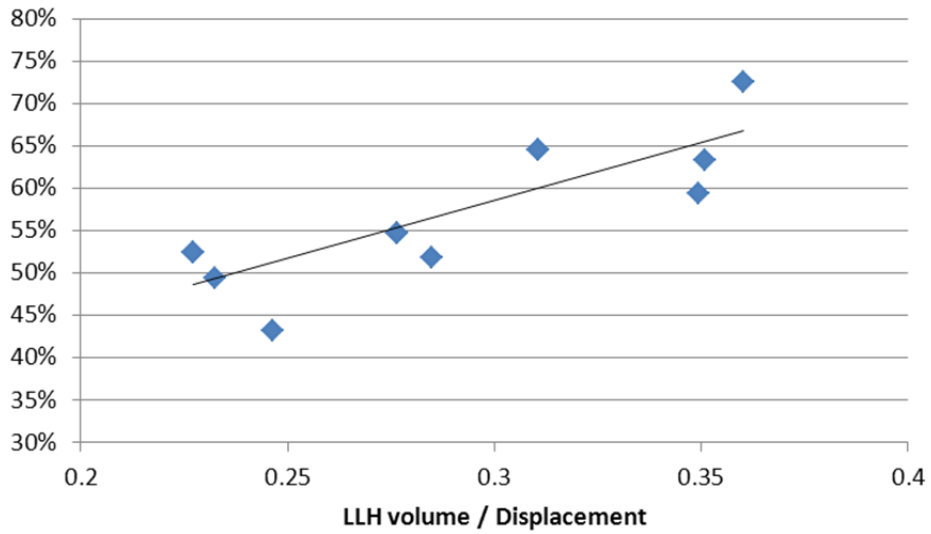

Figure 7-10: Percentage of damages involving LLH over total number of damages

Expectedly, involvement of LLH in damages increases as its size relative to the vessel's increases

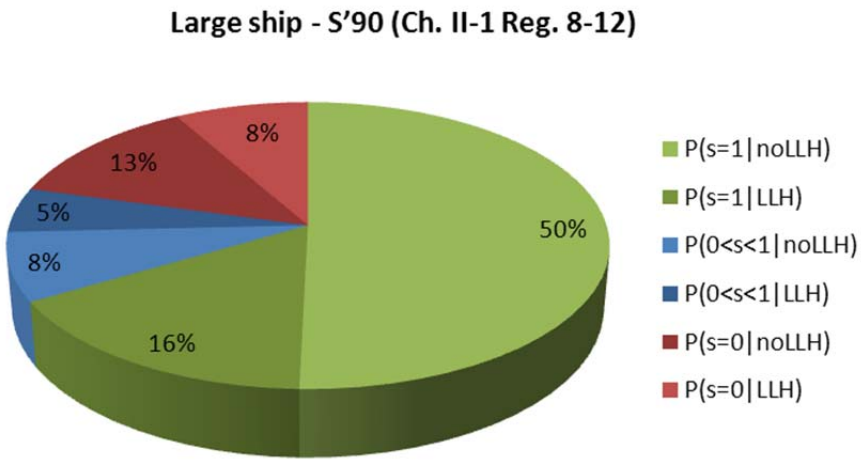

Figure 7-11: Distribution of probability of s_i additionally separated with respect to involvement of LLH

A quarter of the damages that survive include the LLH when it is present in 40% of the damages that result in s=0.

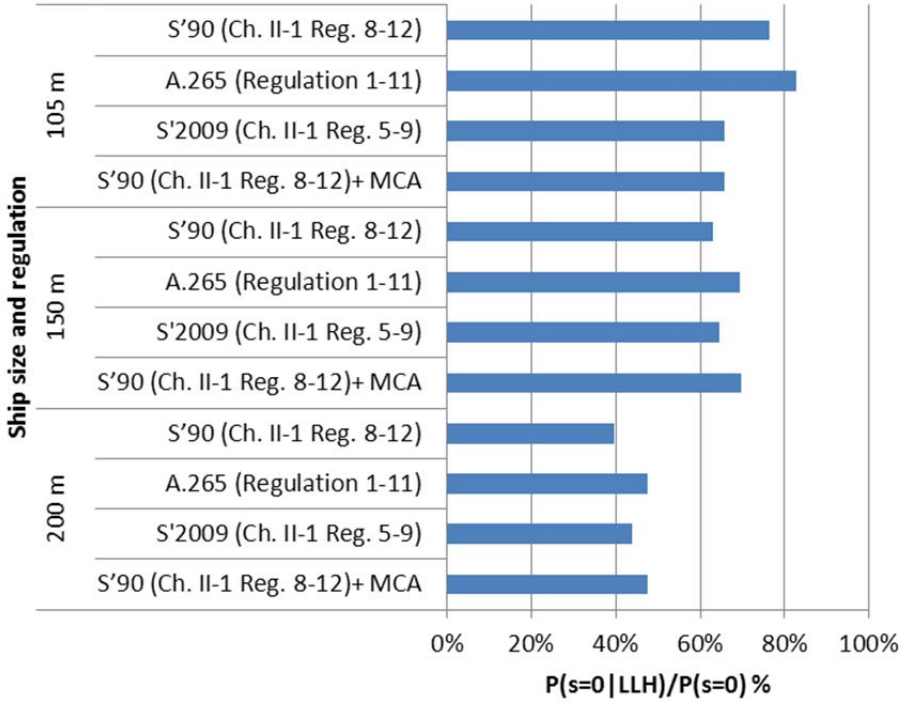

Figure 7-12: Involvement of LLH in non-survivable damages

The ratio of the probability of damages that result in s=0 that involve the LLH over the total probability of the damages that result in s=0 increases as ship size decreases. This means that a non-survivable damage is more likely to include the LLH in smaller vessels than larger ones. With respect to regulation, there is no significant trend to be observed.

Chapter 8 – Survival probability and time to capsize

8 Survival probability and time to capsize

8.1 The concept

A concept for analytical representation of the capsize rate, a measure directly related to damaged ship survivability, has attracted attention ever since the first attempts were made to explain the behaviour of a damaged ship in waves. Attempts in the late 1990s helped to enhance understanding and facilitate characterisation of phenomena pertaining to capsize probability and time to capsize in given environments and loading conditions, but a consistent verifiable formulation is still lacking. In this respect, pursuing an analytical approach to express the capsize rate offers many advantages, time efficiency being amongst the most important. In an era when stability/survivability calculations are required to be carried out in real time, there is a need for a model combining accuracy close to that of time-domain simulations whilst relying on hydrostatic models, catering for uncertainty and capsize boundaries in the process. This study is an attempt to establish a new methodology for survivability assessment by means of a multivariable analytical model based on numerical simulations, validated against the results of physical model tests. The concepts of capsize boundary and capsize band lie at the core of damage survivability assessment of ships. The s-factor used to derive the Attained Index of subdivision corresponds to the 50% probability of survival in damaged condition and in a sea state characterised by what is called *critical significant wave height*. Hs_{crit} is nothing else than a capsize boundary – a wave height at which the capsize rate (P_f) equals 0.5. The capsize band, in turn, reflects the marginal nature of the capsize phenomena and by analogy to statistics it can be interpreted as a confidence

interval about Hs_{crit}. In fact, the capsize band is not a confidence interval in a strict sense[2] – it is rather a measure of dispersion of capsizes, separating sea states in which the capsize rate (i.e. the conditional probability of capsize given H_S) is very low from those in which the rate is very high. In other words, the capsize band emphasizes a well-known fact that there is no distinct boundary separating safe from unsafe sea states; instead there is rather a transition zone within which capsize is possible. The presence of the band also implies that although there must be sea states at which the vessel will never capsize and that there must be sea states at which she would inevitably capsize, due to limited resolution of physical or numerical experiments the lower and upper boundaries can only be expressed by means of limits. Such asymptotic nature requires the use of some threshold values of P_f outside of which occurrence of capsize will either be impossible or practically certain. Making use of analogy to statistics again, such limiting sea states corresponding to threshold values of P_f can be interpreted as confidence limits. Although the capsize rate, P_f , is a function of many variables, such as sea state, loading condition and damage characteristics, it has been observed that in all cases it follows a clear and recurring trend. This has triggered the pursuit for an analytical representation that could be used in parametric studies on capsize phenomena in order to derive universal formulae for probability of capsize and corresponding time to capsize.

---

[2]With significant wave height at the instance of capsize being a random variable, the confidence interval would simply be a band of wave heights containing most of the area under the P(Hs|capsize) probability density function curve. Instead, boundaries of the capsize band are expressed with the use of the following equalities: $(H_S)_{low} = H_S|_{P_f(H_S)=\alpha}$ and,$(H_S)_{high} = H_S|_{P_f(H_S)=1-\alpha}$ where α is some (small) number.

Understandably, such studies require a vast number of experiments to be performed, which sets particular limits on the achievable resolution and accuracy of the results. In this paper, the authors present a brief account of the current state-of-the-art, discuss advantages and shortcomings and propose an alternative approach, which can offer significant reduction of effort (normally expended in numerical simulations and model experiments) whilst retaining comparable accuracy of the outcome.

8.2 Software Tools

Numerical experiments supporting this work have been carried out with PROTEUS3; an in-house developed software that has been successfully employed over many years in a number of research and commercial projects. It has been referenced a number of times, benchmarked against experimental data and other numerical codes successfully and has aided greatly in our understanding of capsize phenomena in damage conditions. OriginPro8 – a powerful statistical package – was used for processing of the results, parametric studies and development of the methodology.

8.3 Ship Models

Three Ro-Pax vessels have been used for the developments in this chapter; the 89m L_{PP}EUGD01-R2, the 170mL_{PP} PRR01 and the 176m L_{PP} EUGD01-R1. The ships are codenamed after the projects they are being used at the moment. One of the projects these have been used at is the current (at time of writing) EC FP7 funded project GOALDS that aims to re-engineer the probabilistic rules formulation for damage survivability of passenger ships. Physical model experiments have been carried out for these ships in the course of the project for the validation of the numerical results. PRR01 has

been used in previous research projects, including HARDER, the foundation of the current probabilistic regulatory framework for damage stability. Results of physical model experiments carried out on this vessel are being used for validation of the numerical code. The chosen ships cover different regions of the design space to ensure universal application of the results. The PRR01 was designed for transport of, primarily, vehicles across short routes such as the English Channel, actually converted to carry a number of passengers in addition to that during the building stage. The small ship was designed for transport of a small number of both passengers and vehicles within an island archipelago in short-crested, choppy seas. The R1 is a night ferry fitted with a lower hold, casting it an ideal candidate for this kind of experiments. Their General arrangements can be found in figures 8-1 through 8-3.

Table 8-1: Main Particulars of Models

Model	PRR01	EUGD01-R1	EUGD01-R2	
Passengers	1420	1400	622	
L_{OA}	178.25	194.3	97.9	m
L_{BP}	170.0	176.0	89.0	m
Breadth	27.8	25.0	16.4	m
Deepest subdivision loadline	6.25	6.55	4.0	m
Depth to bulkhead deck	9.0	9.1	6.3	m
Displacement	17,100	16,558	3,445	tn
Service speed	21.0	27.5	19.5	kn

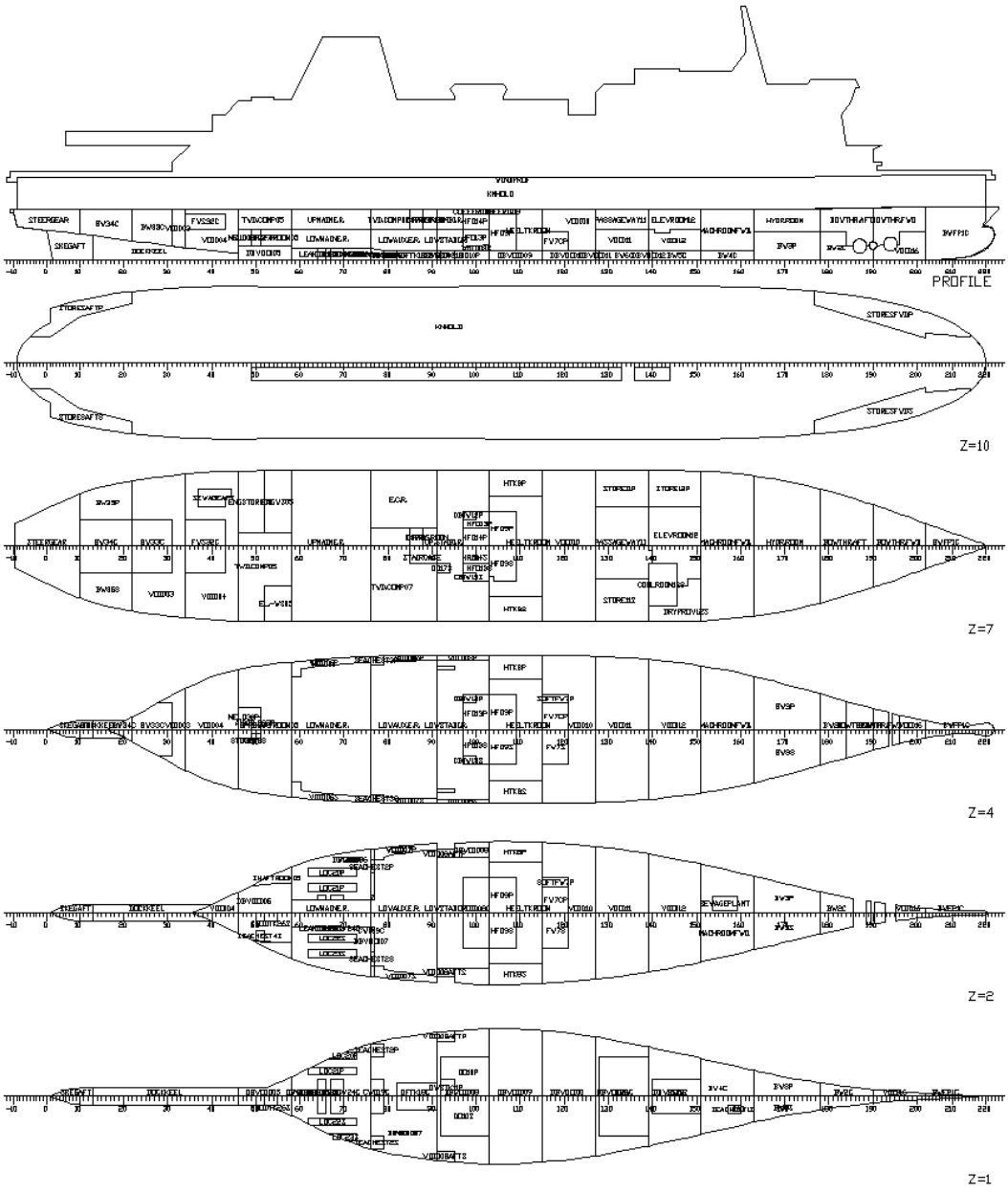

Figure 8-1: General arrangement of RoPax vessel PRR01.

This is the vessel's watertight subdivision as derived from NAPA

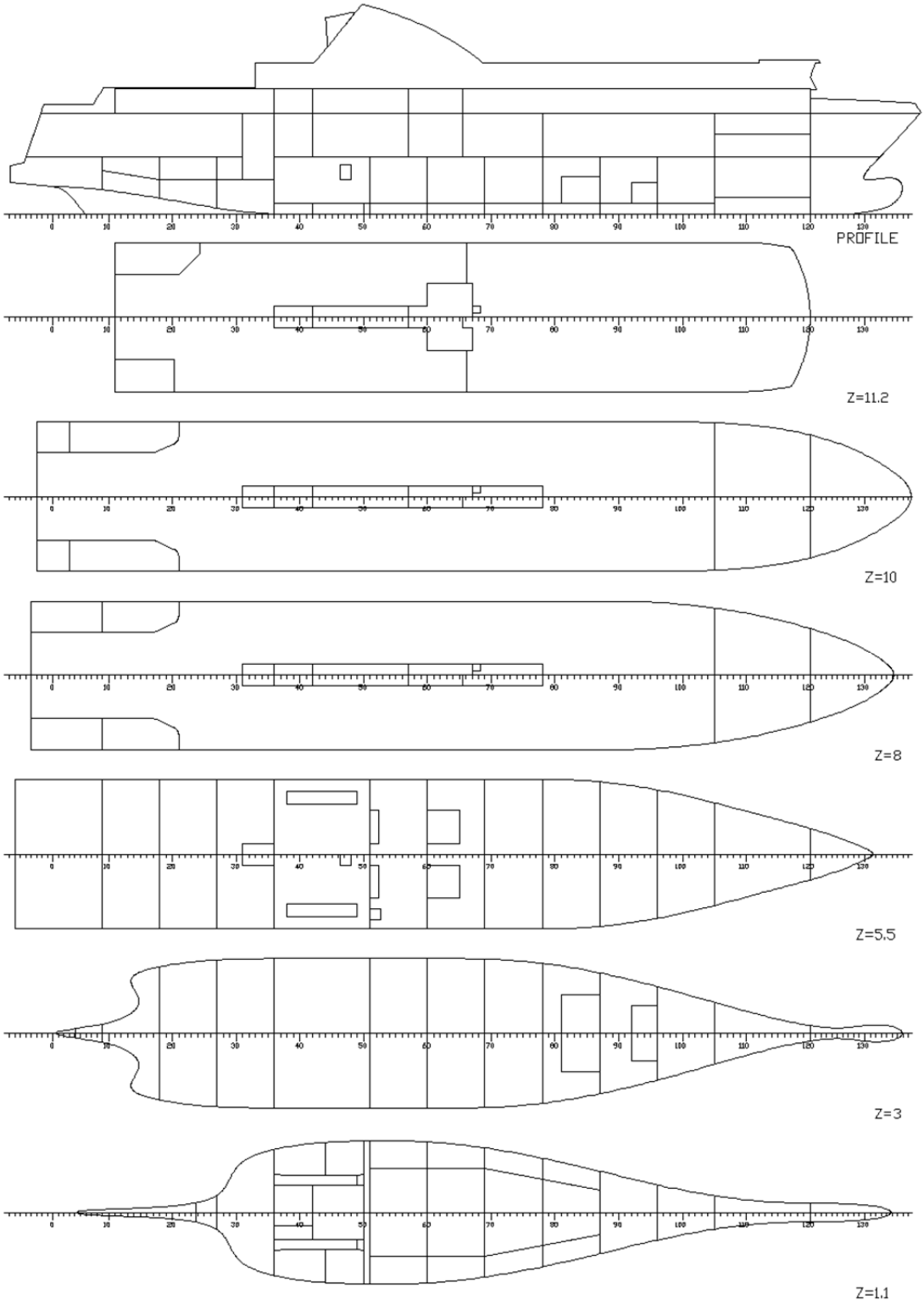

Figure 8-2: General arrangement of RoPax vessel EUGD01-R2.
Watertight subdivision as derived from NAPA

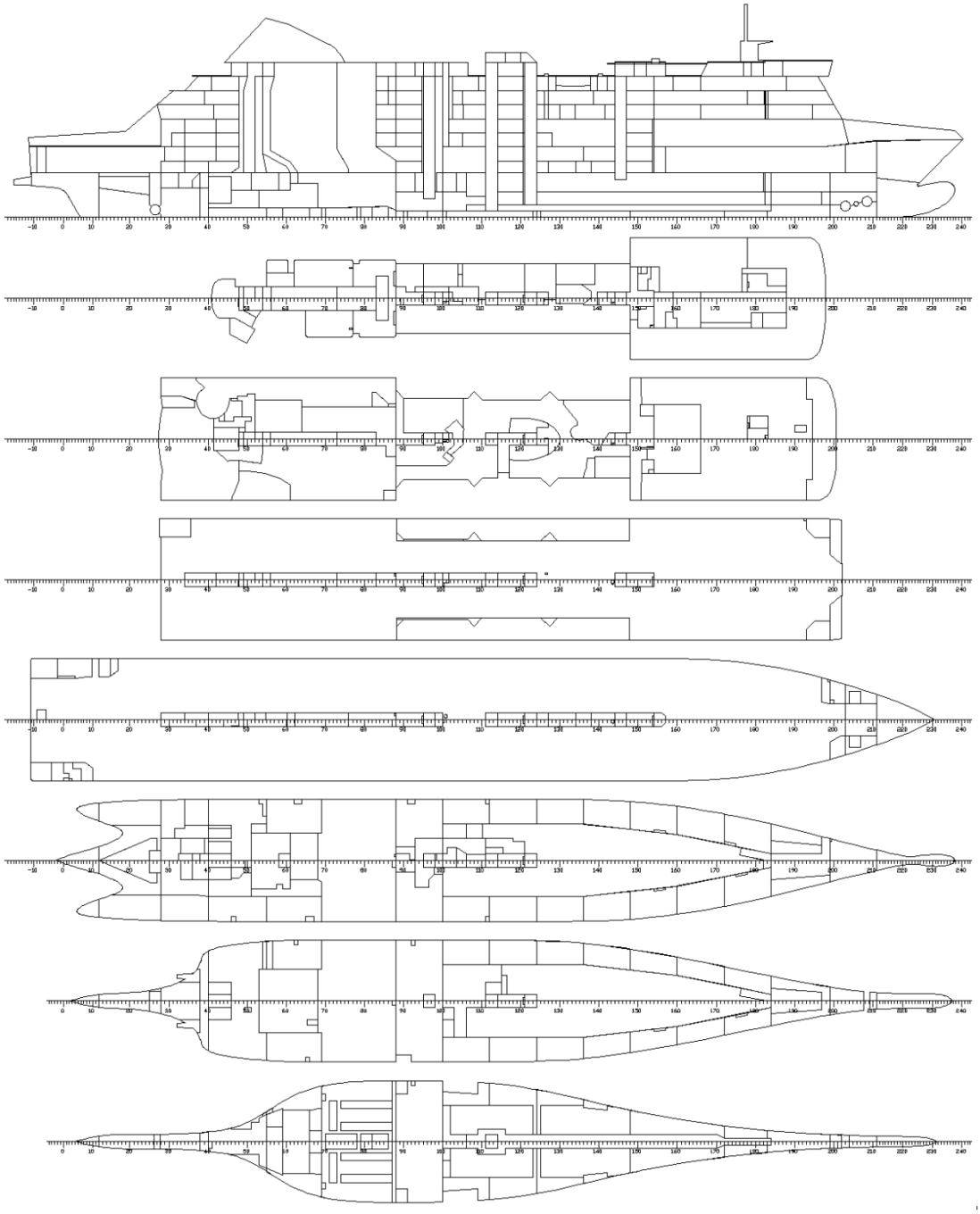

Figure 8-3: General arrangement of RoPax vessel EUGD01-R1.
Watertight subdivision as derived from NAPA. A night ferry, this vessel is equipped with a long lower hold.

8.4 Numerical Experiments

8.4.1 Setup

Accurate representation of the capsize rate characteristic across the entire capsize band, requires adequate resolution. Therefore, it was deemed necessary to use at least 10 measurements within the transition zone, performed by increasing H_S in small steps, varying from 0.1m to 0.25m depending on the width of the capsize band. For each wave height, Pf was determined on a basis of at least 20 wave realisations to maintain at least 5% resolution. The larger ship was tested in seven and the smaller in five different loading conditions, including variations of draught and KG. Additionally, the survivability of the smaller vessel was studied in two distinct damages and various wave spectra. Waves were modelled using JONSWAP spectrum of slope (height to length ratio) equal to 1/20 and 1/25, respectively. Each realisation was limited to 1,800 seconds, which is the maximum time currently required by regulations for evacuation of a vessel. Complete time history of the motions and water accumulation (including water on Ro-Ro deck) was measured and recorded. No wind effect was included in the experiments. All simulations started with the ship in the damage equilibrium position.

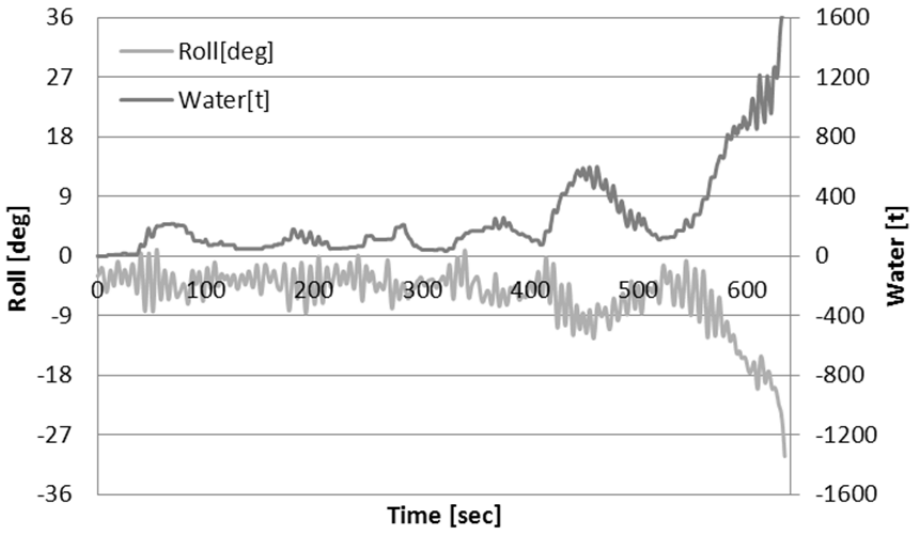

Figure 8-4: Roll motion and water accumulation.
Time histories as obtained from PROTEUS3 output; Capsize case.

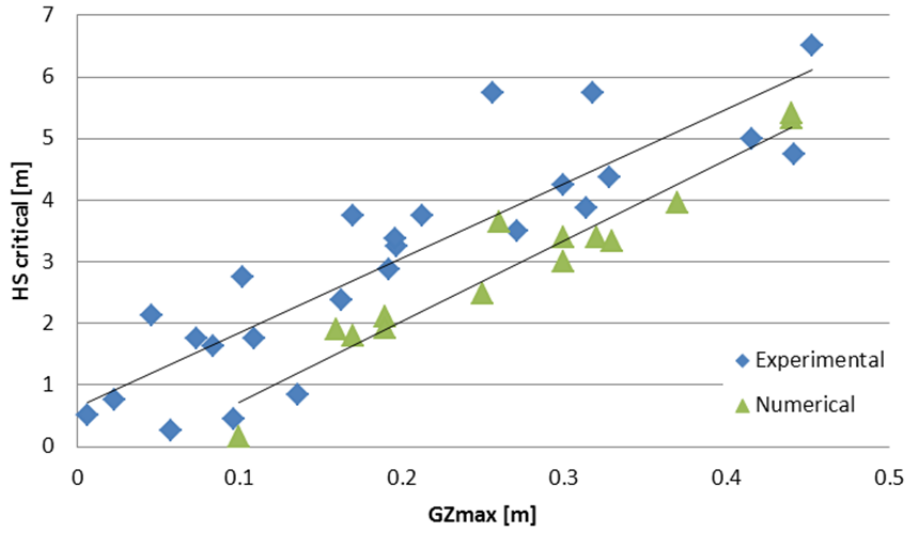

Figure 8-5: Validation of numerical code.
Shown here is a comparison of the experimental data against the numerical results for vessel PRR01.

8.4.2 Numerical code Validation

Given the relative ease of use of numerical tools it is possible to carry out hundreds of simulations in a short period of time, given that results can be verified. Within the present study, the outcome of numerical software was benchmarked against available experimental data from project HARDER (availability of data was one of the reasons for selecting PRR01 as sample ship). Comparison between numerical and experimental results shows satisfactory agreement (Figure 8-5).

It should be noted here that the quantitative agreement between the results was considered of minor importance with emphasis being put on the observed trends. However large any discrepancies might be regarded, it is obvious that both sets of data bear large uncertainties. Nevertheless, for the purpose of this work it was decided that as long as the differences are systematic an exact match is not required and no further numerical model calibration was performed, particularly as observations show that numerical results err on the side of safety.

8.4.3 Capsize rate

The term capsize rate (P_f) is used to denote the approximation[3] of the probability of capsize of a damaged ship, given loading conditions and sea state. Predictably, for a given number of realisations[4], capsize rate will vary from 0 for very small[5] to 1 for very large waves. Between minimum H_S for which $P_f = 0$ and maximum H_S for which $P_f = 1$, P_f can take any value ranging from 0 to 1. Following an adopted convention [39], critical wave height corresponds to the significant wave height for which capsize rate is 0.5. Disregarding the experimental errors, it is obvious from figure 5 is that data follow a specific pattern throughout the range. The evident trend common for all the observations made across the entire H_S range led previous attempts to approach this characteristic by making use of its similarity to the integral of a normal Gaussian distribution – Cumulative Density Function (CDF) [14]. A major advantage of such approach is that the normal distribution is a well-known function and statistical tools can be readily applied to the recorded data in order to find an interval around critical H_S, which could be interpreted as capsize band by use of standard deviation of the derivative of capsize rate. The biggest downside of this method is that it

---

[3] This follows the classical definition of probability, expressed as the ratio of favourable experiment outcomes over the total number of trials. It would become a probability of capsize (conditional on loading condition and wave parameters) if the number of trials approached infinity.

[4] A time series of seakeeping either by means of numerical simulations or physical model tests

[5] Relative to the critical significant wave height

requires numerical differentiation of recorded data, i.e. it involves computation of the derivative of the capsize rate, P_f. As differentiation of infrequent data unequally distributed along the H_S range may introduce large uncertainties, the approach is practically limited to large[6] data sets.

[6] Word *large* in this context refers rather to computational or experimental effort than actual, numerical size of the data.

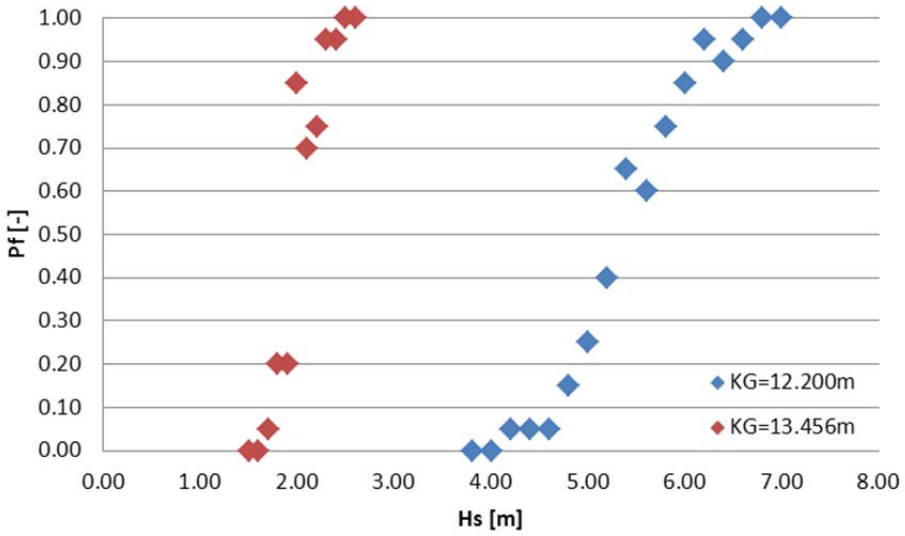

Figure 8-6: Capsize rate values.

The two distinct sets of data correspond to different loading conditions. The increase in spread is in line with Jasionowski et al. [14]

8.5 Non-Linear Regression

Exhaustive pursuit for a more convenient functional representation of the capsize rate resulted in a parametrically defined sigmoid function that turned out to be an attractive alternative to the Gaussian distribution. Bolzman's sigmoid allows direct regression of measured rates, without the need for prior numerical differentiation. The resulting function can be differentiated easily afterwards to derive the requisite information on the capsize band. In its most general form the function is given by means of four parameters: A_1, A_2, x_0 and d_x as in (8-1).

$$y(x) = A_2 + \frac{A_1 - A_2}{1 + e^{\frac{x - x_0}{dx}}} \tag{8-1}$$

Where: A_1 : asymptotic lower limit

A_2 : asymptotic upper limit

x_0: abscissa of the centre of symmetry

d_x : time constant[7]

By nature of the capsize rate observations, the first two parameters can be constrained to 0 and 1 respectively, which leaves just two parameters requiring estimation and allows for, after some basic manipulation, the expression of P_f as a function of H_S, x_0 and d_x (8-2). The derivative of P_f with respect to H_S is given as in (8-3)

---

[7] The parameter *dx* is referred to by analogy to dynamic system response to step input. In context of current application is a span parameter (related to slope at inclusion point).

$$P_f = \frac{e^{\frac{x-x_0}{dx}}}{1+e^{\frac{x-x_0}{dx}}} \tag{8-2}$$

$$\frac{dP_f}{dx} = \frac{e^{\frac{x-x_0}{dx}}}{dx\left(1+e^{\frac{x-x_0}{dx}}\right)^2} \tag{8-3}$$

Figures 8-7 and 8-8 depict an example of Bolzmann's sigmoid fitted to the experimental data as well as residuals of fitting. Statistical data describing goodness of fit are presented in tables 8-2 & 8-3.

Results of employing this technique to data deriving from numerical simulations performed at different KGs are presented in figure 8. It can be readily seen that increasing KG causes a shift of P_f characteristics towards lower sea states with a more rapid transition from low to high capsize rates (probability distribution becoming narrower as KG increases). This implies that as survivability decreases the transition from the region considered safe to that considered as unsafe is faster. The performance of this particular probability distribution's parameters against other ship characteristics can be established in the same manner, with the scope to detect any dependencies between survivability and specific design variables.

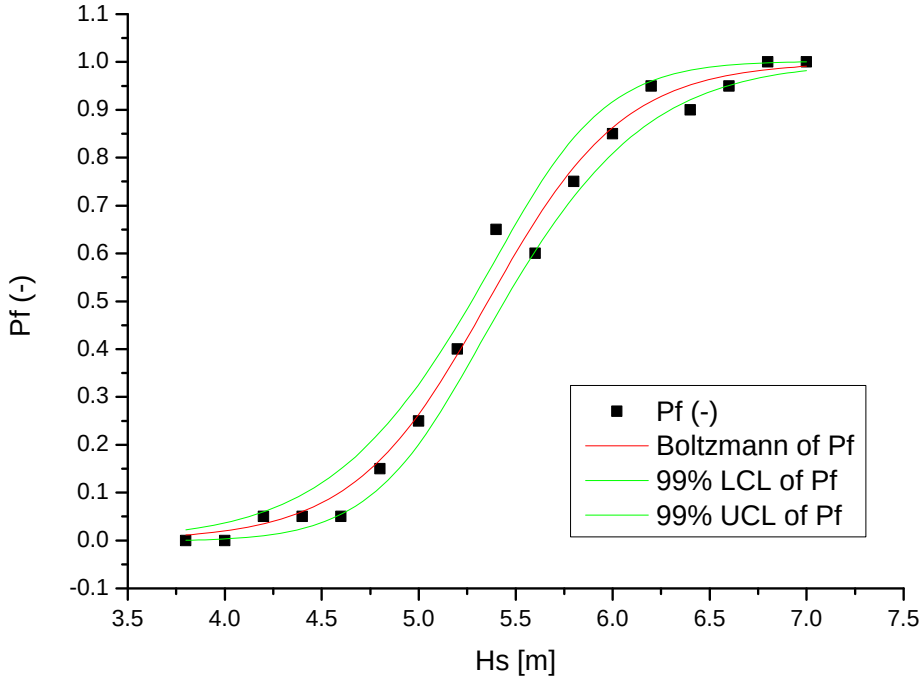

Figure 8-7: Fitted sigmoid.

Pictured here is the result of a regression by use of Bolzman's sigmoid on the experimental data. 99% confidence boundaries are also visible.

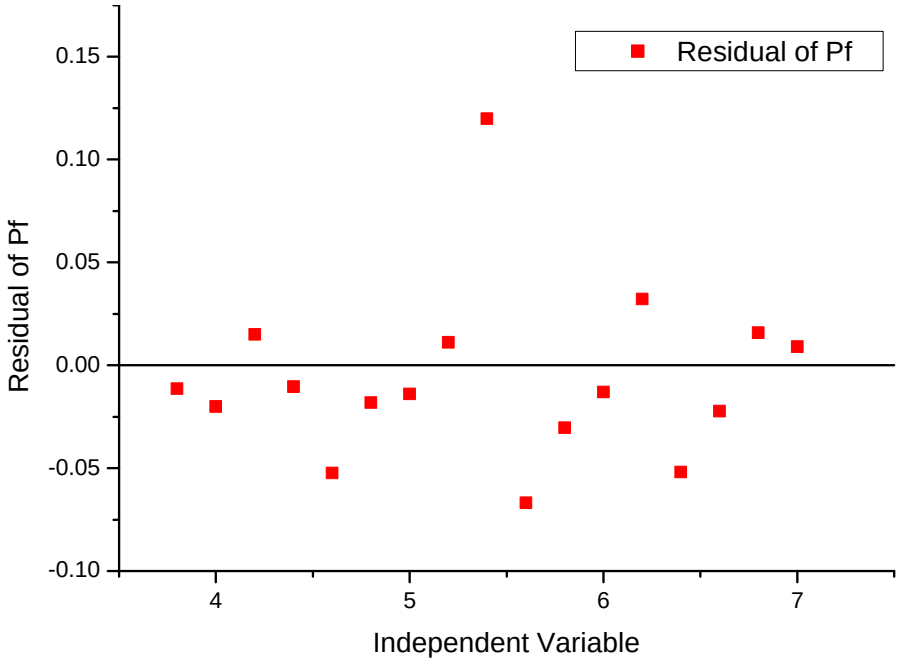

Figure 8-8: Residuals of fitting.

The scattering lies within engineering acceptable ±5%.

Table 8-2: Parameters of sigmoid regression

	Value	Standard Error
A1	0	0
A2	1	0
x0	5.35778	0.02832
dx	0.34893	0.02503

Table 8-3: Statistics of sigmoid regression

Number of Points	17
Degrees of Freedom	15
Reduced Chi-Sqr	0.00192
Residual Sum of Squares	0.02873
Adj. R-Square	0.98814

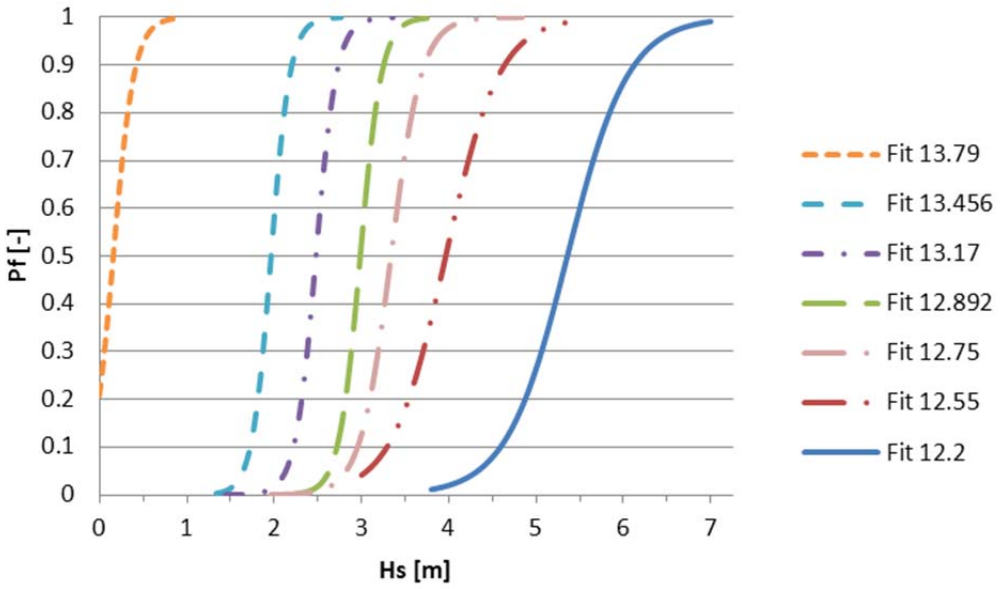

Figure 8-9: Capsize rate for various critical significant wave heights

For simplicity reasons the experimental data have been omitted from this graph. The functions shown are the fitted sigmoids for each set of experiments for various loading conditions tested.

8.6 Estimation of the capsize band

The previous observation can be quantitatively confirmed by use of critical significant wave height and capsize band parameters. The first quantity is associated with x_0 parameter of the regression's sigmoid function whereas the latter can be easily calculated using equation (8-1). By analogy to statistics the capsize band can be interpreted as the range of the probability distribution, spreading either side of the capsize boundary (P_f = 0.5), symmetrically. In a more straightforward interpretation limits of the capsize band simply determine boundaries outside which capsize rate is either so high or so low that capsize in given H_S is either certain or unlikely, beyond upper and below lower limits, respectively. In order to determine such limits, it is convenient to take some small number α, and find those values of H_S, which satisfy the following conditions:

$$\left(H_S\right)_{low} = H_S\big|_{P_f(H_S)=\alpha} \tag{8-4}$$

And

$$\left(H_S\right)_{high} = H_S\big|_{P_f(H_S)=1-\alpha} \tag{8-5}$$

The boundaries $(Hs)_{low}$ and $(Hs)_{high}$ can be calculated using the inverse P_f function, given as:

$$H_S\left(P_f\right) = x_0 + dx \cdot \ln\left(\frac{P_f}{1-P_f}\right) \tag{8-6}$$

Lower and higher limits of the capsize band, given as $Hs(P_f = a)$ and $Hs(P_f = 1 - a)$ respectively, are shown in equations 8-7 and 8-8.

$$H_S\left(P_f = \alpha\right) = x_0 + dx \cdot \ln\left(\frac{\alpha}{1-\alpha}\right) \tag{8-7}$$

And

$$H_S\left(P_f = 1-\alpha\right) = x_0 + dx \cdot \ln\left(\frac{1-\alpha}{\alpha}\right) \tag{8-8}$$

Figure8-10 demonstrates these limits, calculated with the parameter α = 0.05. In this figure it is apparent that not only does the survival wave height decrease with increasing KG but also the band contracts. The contraction of the band is a direct consequence of the time to capsize, which also decreases as KG increases. As the vessel's survivability decreases, i.e. the critical wave height decreases, it is more likely that a potential capsize will have occurred within the simulations time, thus the band contracts in the same manner as when simulation time increases, as will be demonstrated in following section.

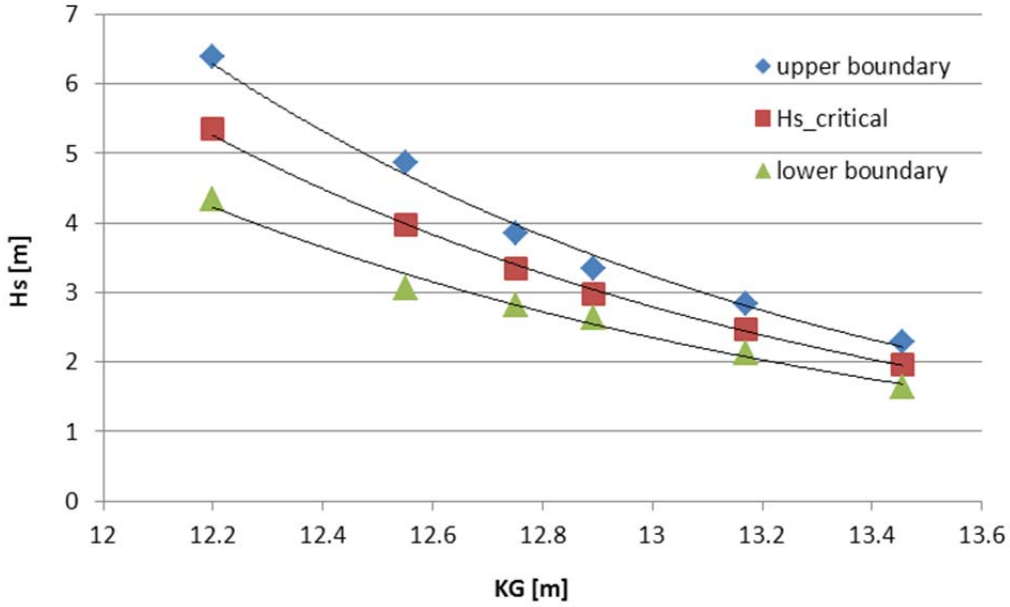

Figure 8-10: Capsize band vs. KG

Plotting only the boundaries and the x_0 of the bands, resulting from KG variance, of figure 8-9 one of the most important attributes of the band becomes apparent. That is that the band contracts as survivability decreases.

8 7 Parameterisation

Attempts to derive a simple analytical function to represent capsize boundaries and capsize band revealed new possibilities for parameterisation of the formula to populate a family of functions, which could be used as a universal tool for survivability assessment in both design and operational stages. In case of the sigmoid, the two defining parameters, i.e. x_0 and d_x can be expressed by means of wave characteristics (other than H_S, which is explicitly present in the P_f formulae) or parameters related to loading condition, damage extent etc. Understandably, parametric studies require extensive and systematic simulation (testing) effort but some rough examples may be presented here. They may also shed some light on sensitivity problems associated with these studies. A single-variable parameterisation of the sigmoid's x_0 and dx using KG as a parameter is presented in figures 8-11 and 8-12.

In fact, parameterisation of dx with respect to x_0 can lead to a single parameter representation of the capsize band. This relation is shown in figure 8-13. The model fit to the experimental data for dx is shown in equation 8-9.

$$dx = 0.062 \cdot e^{0.32 \cdot x_0} \tag{8-9}$$

Where x_0 is, as a reminder, the abscissa of P_f=0.5. This changes 8-2 into 8-10 which can be directly used for the derivation of the capsize rate function by the knowledge of only x_0.

$$P_f = \frac{e^{\frac{x - x_0}{0.062 \cdot e^{0.32 \cdot x_0}}}}{1 + e^{\frac{x - x_0}{0.062 \cdot e^{0.32 \cdot x_0}}}} \tag{8-10}$$

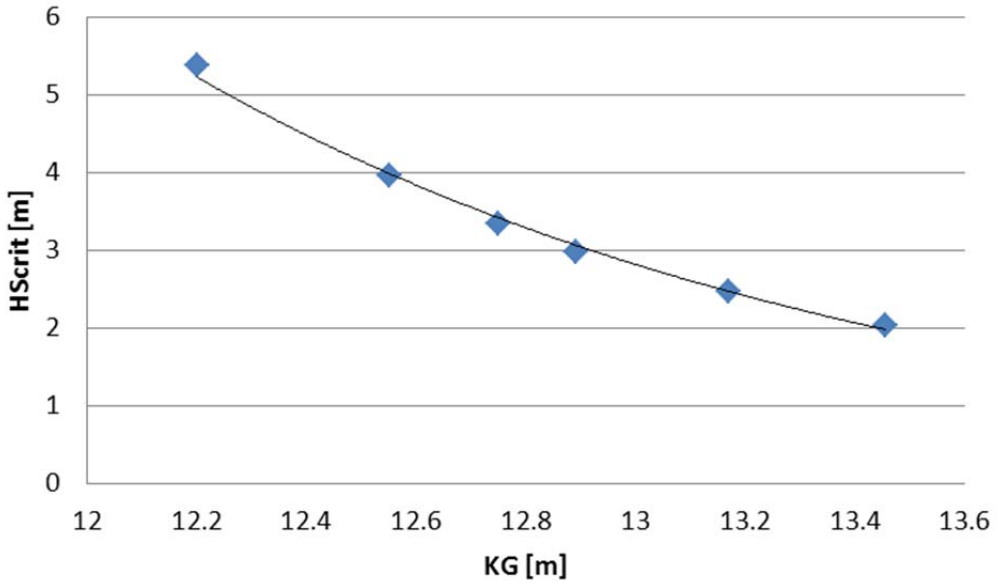

Figure 8-11: x_0 vs. KG

The reduction of x_0 with the increase of (intact) KG is visible in this picture.

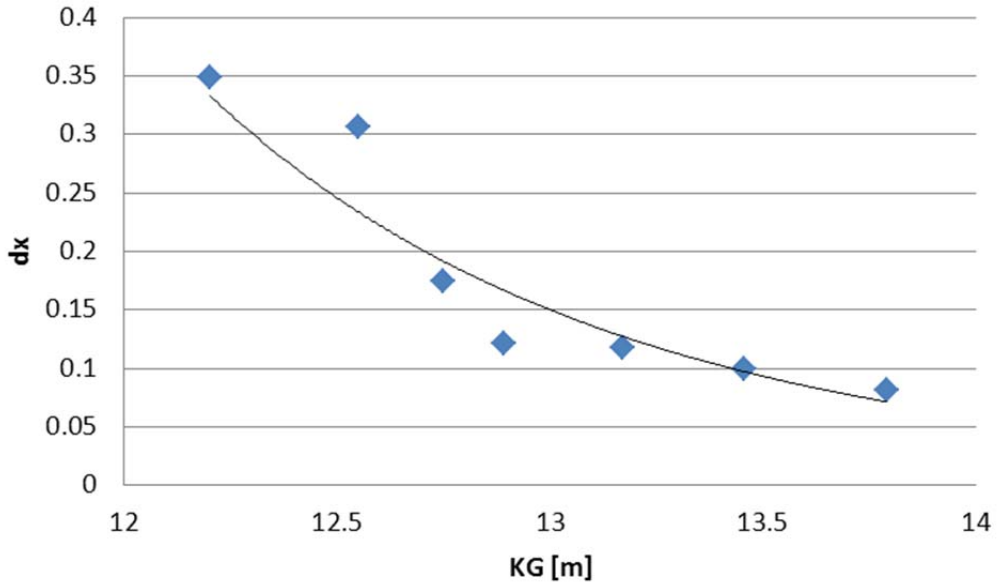

Figure 8-12: d_x vs. KG

Visible here is the reduction of the bandwidth (d_x) with the increase of (intact) KG. The scattering is related to error of experiment. Note that the scattering is not evident in figure 8-11.

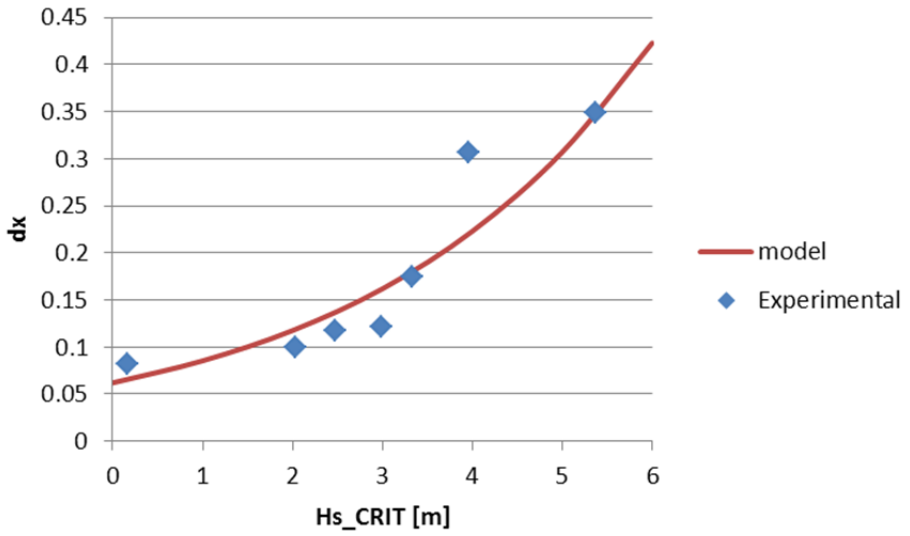

Figure 8-13: Parameterisation of dx with respect to Hs_{CRIT}

By expressing dx in terms of Hs_{CRIT} we can have a single parameter function for P_f given in equation 8-2. In this case an exponential function of the form $y=a \cdot e^{b \cdot x}$ has been fit to the experimental data that can be used as a model for dx. The parameters a and b are 0.062 and 0.32 respectively.

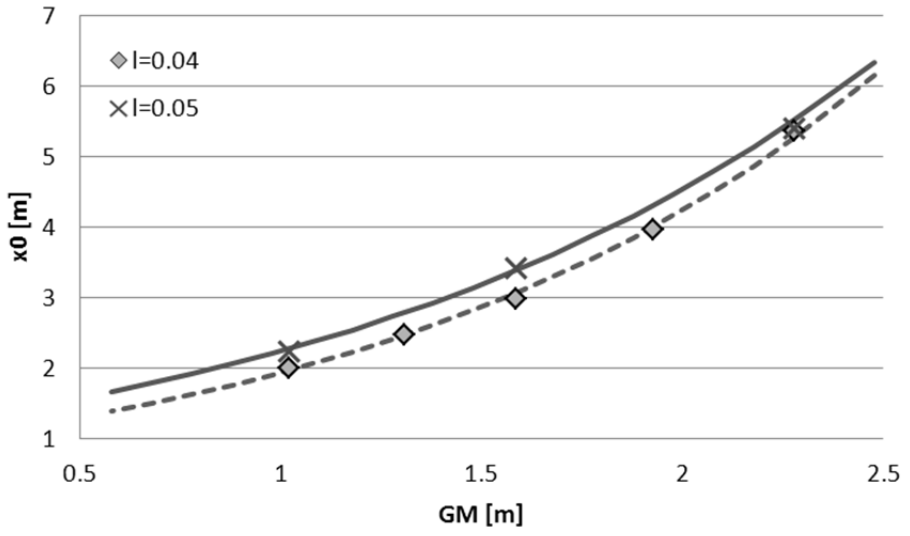

Figure 8-14: Effect of wave slope, λ.

Shown here is a bi-variate parameterisation of x_0 vs. (intact) GM for the demonstration of the effect of wave slope to the x_0.

Obviously, the family of sigmoids describing the capsize rate should be populated with as many parameters as necessary to enhance its functionality. Parameters include those specific to the damaged ship, e.g. residual freeboard, water head on a car deck etc. or those specific to the damage case, e.g. volume of damaged compartments, possibly in relation to the volume of the total watertight volume, permeability of the damaged compartments, centre of buoyancy of damaged compartments etc. At this stage, the parameters investigated are associated with the intact ship characteristics, and environmental parameters, leaving aside quantities related to the damage case, until more research output is available. Figure 8-14 shows an example of decomposition of critical significant wave height with respect to (intact) GM and wave slope λ.

8.8 Linear approximation

However convenient the sigmoid regression is to use, it also comprises some significant drawbacks. To start with, something that is particularly evident in cases of very narrow capsize band is that the goodness of fit depends strongly on the quality of data in the proximity of tail asymptotes. Unfortunately, due to limited resolution of experimental data, these regions bear the highest uncertainty.

Assuming that the data in proximity of the critical value, lying in the middle of the range of P_f should be the most reliable, an attempt has been made to simplify the approach and to use linear regression instead of non-linear, with encouraging results. It can be noticed that some cases demonstrate higher goodness of fit for linear regression than for a sigmoid. In order to achieve this, though, the tails of the series needed to be omitted as that is where the non-linear behaviour is dominant. However, it was observed that removing "tails" from the data set has no major impact on the result.

This, as demonstrated in table 8-4 by comparison of the residual sum of squares for one sample dataset, makes this approach really attractive. A major concern whilst using linear regression is related to the capsize band and its analogy to the confidence interval.

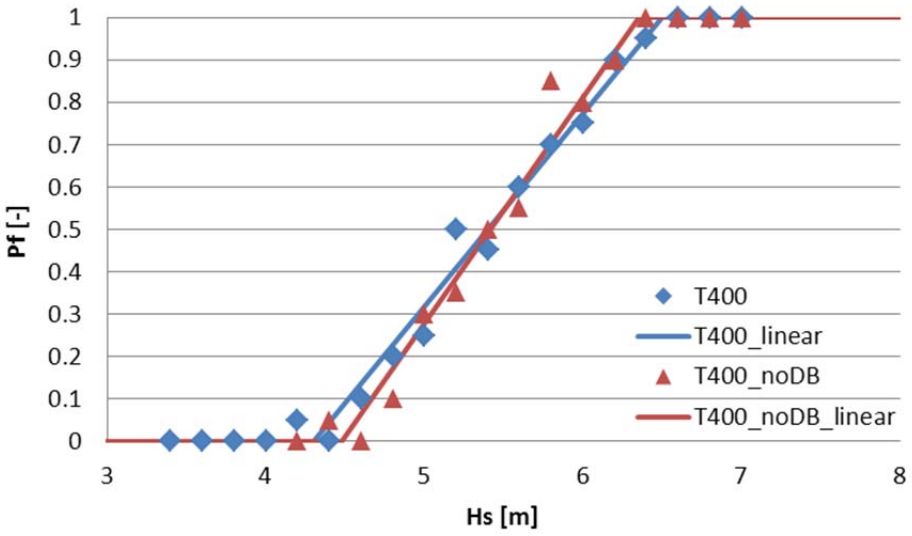

Figure 8-15: Linear regression for different damage cases

The experiments shown here, carried out with the smaller RoPax ship (EUGD01-R2), correspond to two variations of a damage case with respect to the involvement of the double bottom.

Table 8-4: Sigmoidal vs. linear regression

In this case, the linear fit is actually more accurate than the sigmoidal one, although it has not always been the case.

	Sigmoid	Linear
Number of Points	19	13
Degrees of Freedom	17	11
Reduced Chi-Squares	0.00211	
Residual Sum of Squares	0.03595	0.03247
Adj. R-Square	0.98703	0.97626

It is obvious that relying on statistical measures of goodness of fit may overshadow the fact that linear regression does not bring any information about the "tails" of the capsize rate distribution and therefore any prediction of capsize band based on this method should be approached carefully. However, closer examination of the linear regression and its affiliation with the sigmoid reveals some important virtues. Linear regression of the data close to x_0 will actually result to the tangent of the sigmoid at the inclusion point (x_0, 0.5). Therefore, for the linear regression parameters α (slope) and β (intercept) the following relation holds:

$$\alpha = \left.\frac{dP_f}{dH_S}\right|_{H_S=x_0} = \frac{e^{\frac{H_S-x_0}{dx}}}{dx\left(1+e^{\frac{H_S-x_0}{dx}}\right)^2} = \frac{1}{4dx} \tag{8-11}$$

$$y(x_0) = \alpha x_0 + \beta = \frac{1}{2} \tag{8-12}$$

The parameters for the bandwidth and centre of symmetry of the sigmoid function can be derived directly from the linear regression formula:

$$dx = \frac{1}{4\alpha} \tag{8-13}$$

$$x_0 = \frac{0.5-\beta}{\alpha} \tag{8-14}$$

Finally, since all the parameters required for the sigmoid representation can be evaluated on the basis of a linear fit, it is sufficient to apply linear regression to the observations and once x_0 and d_x are estimated, the capsize band limits can be calculated with the use of equations 7 and 8, respectively.

Table 8-5: Impact of slope estimate on the capsize band and x_0

As the estimate of the slope of the linear approximation becomes more accurate, the resulting sigmoid function will better represent the experimental data. Contents of the table are also visible graphically in figure 8-16

	Fitted	Estimate 1	Estimate 2
0.05	1.28691	0.99266	1.16301
0.5 (x_0)	1.68031	1.70087	1.68481
0.95	2.07372	2.40909	2.20661
band	0.78681	1.41643	1.0436

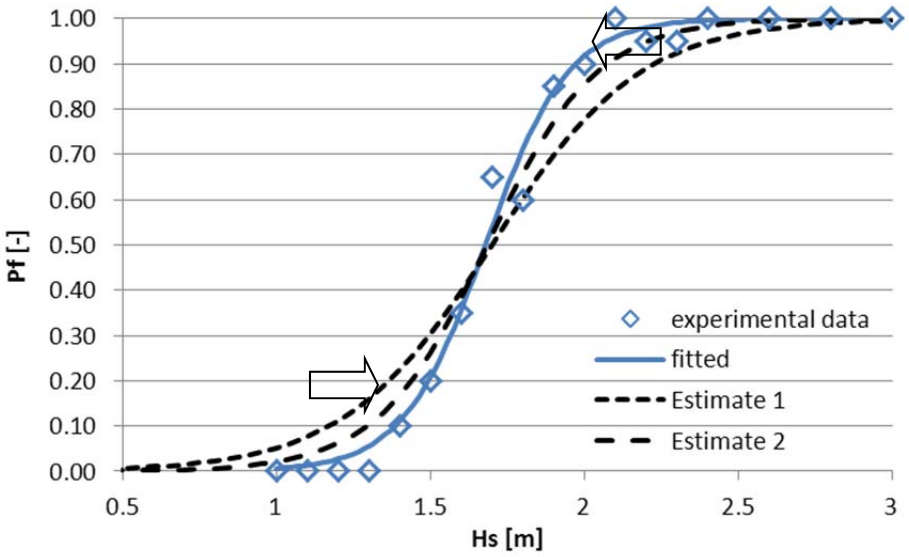

Figure 8-16: Fit convergence

A more accurate estimate of slope at x_0 results in a closer match.

An approach based on linear regression has some welcomed advantages. First of all, it allows use of formulae derived for the sigmoid curve, well representing observed phenomena, but without the necessity of non-linear (least-squares) regression. Furthermore, as discussed earlier, experimental results in close proximity to 0 and 1 asymptotes are expected to suffer due to large uncertainties and in general, they require higher resolution. On the contrary, points corresponding to moderate capsize rates are usually following the trend better. An approach based on linear regression makes it possible to disregard those regions entirely or just the parts that might be ambiguous. In the latter case (partial reduction) it is important that the remaining data preserve the basic characteristics of the distribution, such as symmetry around x_0. Given that sufficient resolution is available around the x_0 region, the resulting sigmoid function should be very accurate. The benefit of this approach is that one could derive an approximate capsize band, having nothing more than 2 measurements of the capsize rate, as long as they are different than 1 and 0 – ideally – and the smaller measurement corresponds to lower H_S. Of course, this should only be treated as an indication and a more accurate calculation of the slope of the probability distribution at its centre would have to be available for reliable results.

8.9 Effect of time of experiment

All the previous have been carried out with time of experiment being a constant 30 minutes. Based on the fact that time of observation is an important parameter, an additional study has been carried out that treated time of experiment as an additional variable. The expected survivability in a seaway is given by equation 8-15.

$$s = \int_0^\infty dH_S \cdot f_{H_S|col}(H_S) \cdot F_{surv}(H_S) \tag{8-15}$$

Where: $f_{H_S|col}(H_S)$ is the probability mass function of the seastates expected to be encountered during collision and

$F_{surv}(H_S)$ is the probability of survival of a specific damage extent, in a specific seastate, in a specific loading condition and for specific time, t.

Thus, by treating time of experiment as a variable its contribution to survivability can be identified and measured. The two larger RoPax vessels were studied for this purpose. The damage cases and loading conditions selected for the experiments were chosen so that the band fall within the probable wave heights at time of collision, that is less than 4m H_S. The results seem to suggest that the critical wave height is not where it was previously believed to be. That is, the value of 50% probability of capsize, which was until now regarded as the critical wave height seems to shift with the increase of time of experiment. On the other hand, the lower boundary of the capsize band, the 5% probability of capsize remained unaffected by the variance of experiment time (figures 8-17, 8-18 and 8-19), casting it a undisputable candidate for critical wave height.

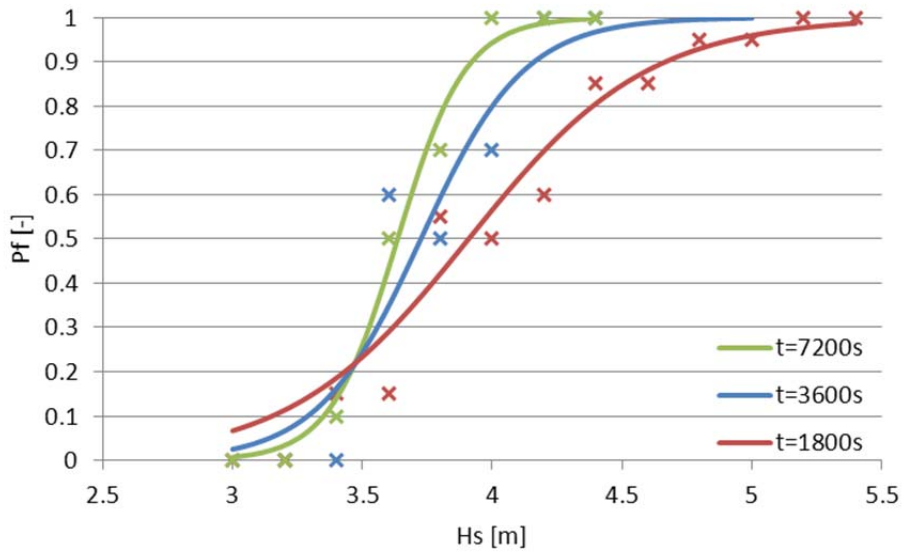

Figure 8-17: Contraction of the capsize band – PRR01

The experimental data and the fitted sigmoids are shown here for 176m long RoPax vessel PRR01; the bandwidth of the capsize band for this damage case contracted towards its lower end when time of experiment was doubled.

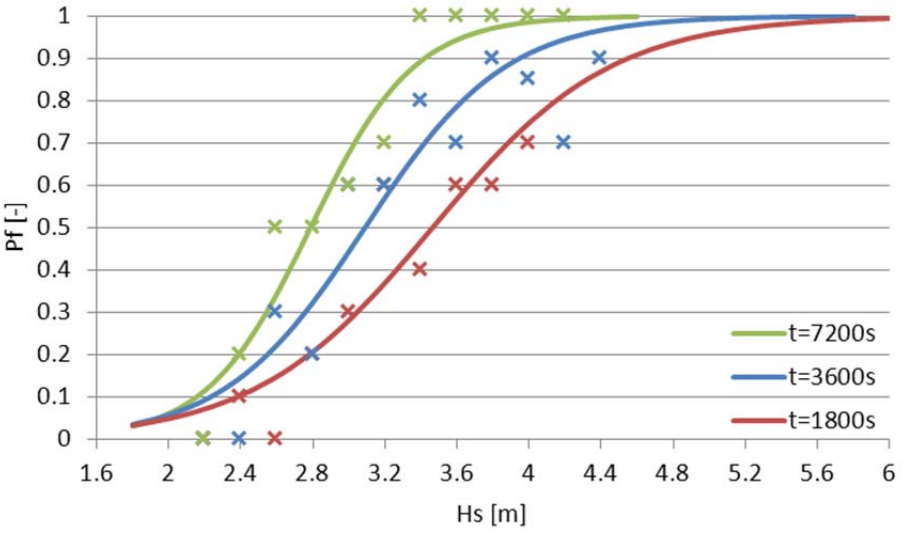

Figure 8-18: Contraction of the capsize band – EUGD01-R1

Same as previous figure for 174.8m long RoPax vessel EUGD01-R1; the capsize band contracts towards the lower boundary as experiment time increases.

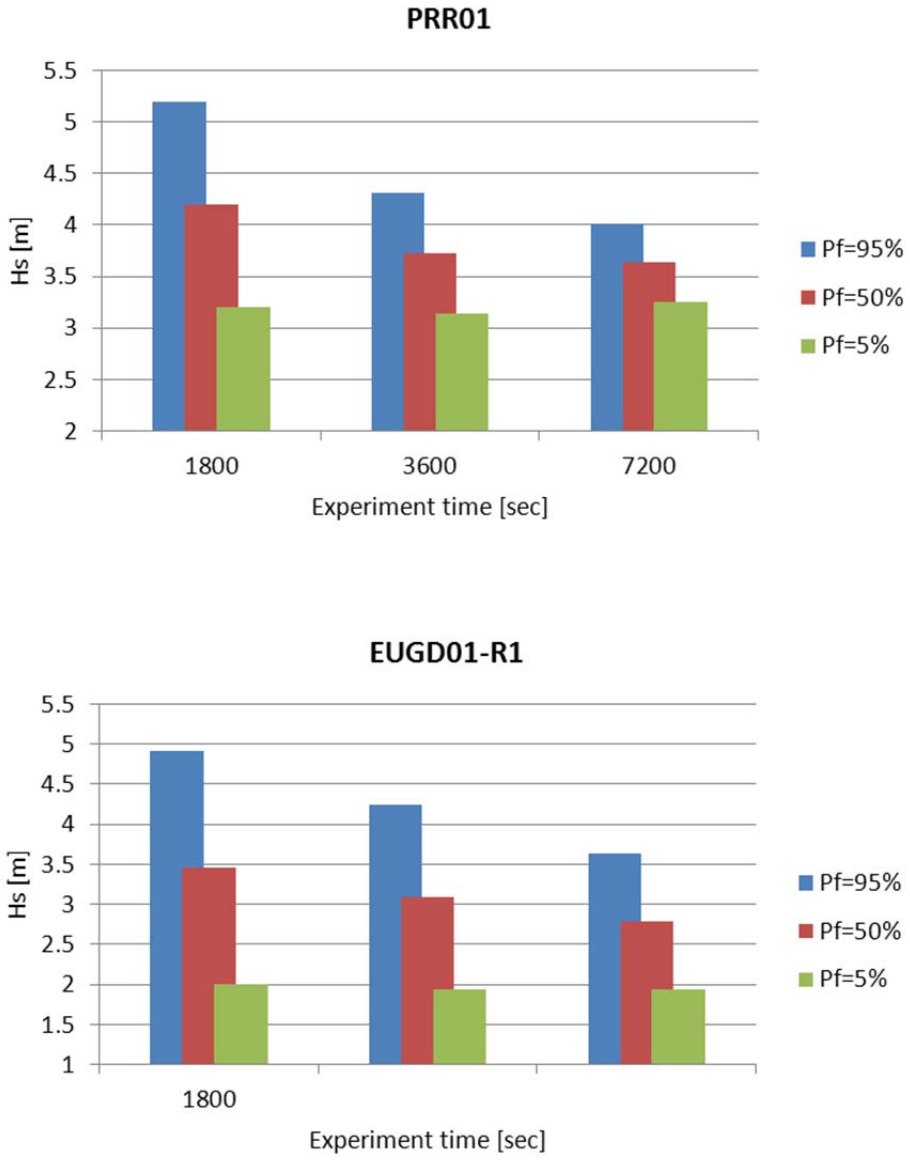

Figure 8-19: Pf with respect to observation time

The 3 values of Probability to capsize studied are plotted in this figure against observation time. Notice how for both vessels wave heights at which 95% and 50% occur change over time while the lower boundary, 5%, remains remarkably constant.

8.10 Discussion

This research focuses in an alternative approach to the representation of the behaviour of a damaged ship in waves. The approach adopted for analytical approximation of the capsize band has both benefits (speed) and drawbacks (uncertainty) but some compromise is not only inevitable but also necessary in most engineering applications – particularly those that are exceptionally labour intensive and costly.

The characteristics of the probability distribution that describes the behaviour of Ro-Ro ships in boundary conditions have been identified and an analytical model describing the capsize band has been developed.

Furthermore, the way to utilise the outcome to predict the critical wave height has been demonstrated. In addition, the capability to facilitate these characteristics in the design process as constrains and/or objectives, has been discussed.

Lastly, the merits of having an analytical approach to describe such a complex phenomenon are indisputable. The amount of realisation performed numerically for this work is counted in thousands, so the amount of work saved by such an approach is massive. The presented analytical approach offers the necessary flexibility to integrate this with more complex models for prediction of time to capsize, which in turn can be associated with number of people to successfully evacuate and finally risk from flooding etc.

With respect to critical wave height, based on the observations made when time of experiment was increased, it is more than reasonable to suggest that the most appropriate value would be the wave height at which the probability to capsize, as this has been defined in the previous, is 5%. The

correct value would be 0 but given the uncertainties involved, 5% is an acceptable approximation. Given that 50% probability to capsize has been used in the past for the derivation of the s-factor of SOLAS 2009 [4], a shift of this nature would inevitably decrease the expected survivability of a damage scenario, something that some would argue is unnecessarily conservative. However, as it has been demonstrated in chapter "Performance-Based Assessment" and in [11] and [12], it will only affect a minor number of the total damages involved in Index-A calculation, thus only slightly altering the result. At the same time, shifting H_{Scrit} to the lower boundary means that if the critical wave height – which will need to be calculated based on stability characteristics of each damage case, just as in SOLAS 2009 currently – is not exceeded, there will be no capsizes. That is, survival time is infinite (within reason) which is very convenient for the latest developments at IMO regarding performance-based regulations like Safe-Return-to-Port [41].

Chapter 9 – Performance-Based Damage Survivability

9 Performance-Based Damage Survivability

The first international system of subdivision was agreed following the Titanic accident, in the form of the first Convention for Safety Of Life At Sea in just 1929. This was only addressing floatability of the damaged vessel and it wasn't until SOLAS 1960 that the first requirements for residual stability post damage were introduced. A minimum GM value of 5cm became mandatory as a margin to compensate for the input of the environment. In the late 60s, the first probabilistic framework of subdivision was proposed by Kurt Wendel [48] as an alternative to deterministic regulations, giving way to the steepest learning curve in the history of naval architecture [43]. A series of deterministic regulatory frameworks followed, with special interest in stability in waves that culminated in SOLAS 2009. With the introduction of the probabilistic framework for damage stability in 2009, every one of the thousands of possible damage scenarios' stability in waves had to be measured Arguably the most accurate way to measure a vessel's performance when it comes to survivability in waves is by use of first principles methods. That is either physical, towing tank testing or numerical simulations. Albeit accurate, they both come with their drawbacks and limitations, the greatest of which, the cost and time to carry out. Given the sheer number of damages considered, first principles are rendered, for the time being, unrealistic to say the least. To this end, alternative knowledge intensive methods' development was finalised during project HARDER, as an analytical way for the estimation of the survival wave height. These methods are SEM [30] [4] and the current SOLAS' 2009 s-factor.

The SEM has been developed over many years of experiments and although it demonstrates high correlation with experimental data for RoPax vessels

[22], it has been largely dismissed by the international community basically because it's too complicated to calculate. As its name – Static Equivalent Method – suggests, it involves calculation of the amount of water that the vessel could take on-board in damaged condition, statically and then compares this with the height of water that accumulates in the car deck (figure 9-1) to estimate the survival wave height according to equation 9-1

$$Hs_{critical} = 2.221 \cdot \log(h) - 0.635 \cdot f + 4.676 \quad (9\text{-}1)$$

However, in spite of the fact that the mean error of the fit is quite low and that the coefficient of multiple determination (R^2) is relatively high as shown in table 9-1, the uncertainty of estimation of the critical sea-state, as denoted by the highest overestimate and lowest underestimate is almost 2 metres. This is hardly negligible but it is almost insignificant compared to the misconceptions and approximations of the s-factor that was finally postulated by SOLAS 2009.

The final outcome of HARDER, a project that was mainly an IMO vehicle for the development of the probabilistic framework for damage stability that would form the SOLAS 2009, suggested that SEM should be used for the estimation of survivability of waves while the conventional s-factor should be used for the estimation of survivability of cargo ships. A distinction was made at the time between the low freeboard Ro-Ro vessels and the non-RoRo vessels, because of the observed differences in their mechanisms of capsize.

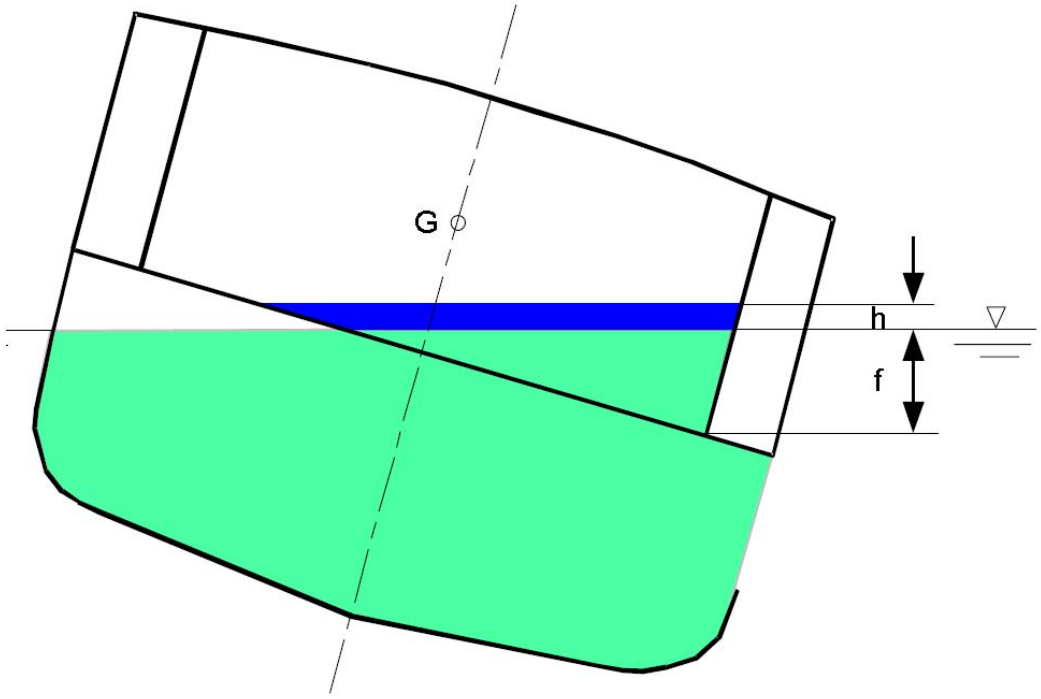

Figure 9-1: The parameters f and h of SEM

Pictured here is the basic principle behind the SEM. The parameters f and h are used in the estimation of the critical wave height.

Table 9-1: SEM statistical data

The statistical data for the goodness of fit as obtained from [30] are shown in the following table

Residual Sum of Squares	12.27	
Standard Error of the Estimate	0.476	
Coefficient of Multiple Determination (R^2)	0.8245	
Highest Overestimate	0.904	m
Lowest Underestimate	-1.064	m
Mean Error	0.378	m

9.1 The SOLAS 2009 s-factor

The conventional methodology for the estimation of the critical wave height was finally adopted at SOLAS 2009, apparently with harmonisation in mind. In doing so, it was assumed that the parameters and regression formulated in the s-factor applied to all ship types. That is hardly the case as was pointed out in [45]. The formulation of the s-factor is shown in equation 9-2.

$$s = k \cdot \left(\frac{GZ_{MAX}}{0.12} \cdot \frac{Range}{16} \right)^{\frac{1}{4}} \tag{9-2}$$

$GZ_{MAX} \leq 0.12m$

$Range \leq 16\ degrees$

$$k = \begin{cases} 1, & \theta_e < \theta_{min} \\ 0, & \theta_e \geq \theta_{max} \\ \sqrt{\dfrac{\theta_{max} - \theta_e}{\theta_{max} - \theta_{min}}}, & otherwise \end{cases} \tag{9-3}$$

Where:

"GZ_{MAX}": Maximum positive righting lever up to θ_v (meters).

"Range": Range of positive righting lever, measured from θ_e. Positive range is to be taken up to θ_v (degrees).

"θ_e": Equilibrium heel angle in any stage of flooding (degrees).

"θ_v": Angle where GZ becomes negative or the angle at which an opening that is not watertight becomes submerged (degrees).

"θ_{min}": 7^o for passenger ships and 25^o for cargo

"θ_{max}": 15^o for passenger ships and 30^o for cargo

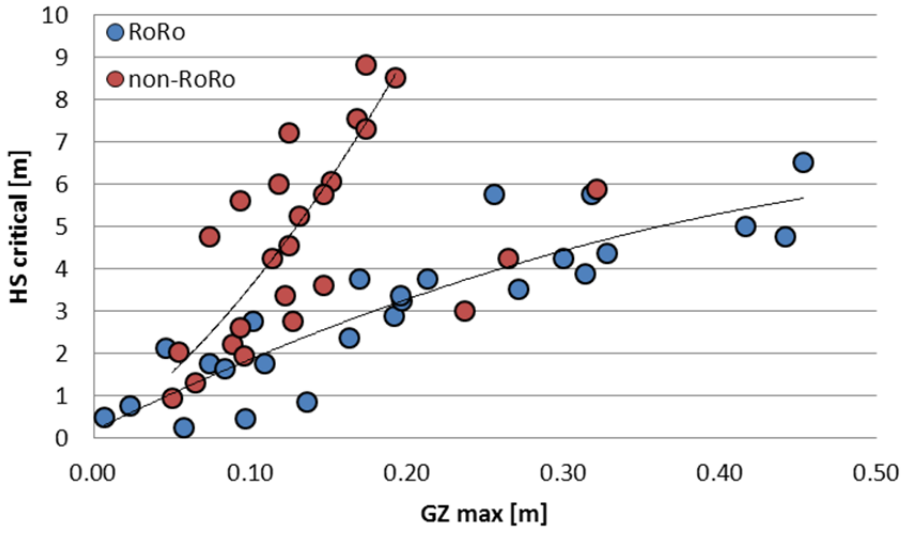

Figure 9-2: Critical significant wave height vs. GZ_{MAX} for RoRo and non-RoRo vessels

A distinction exists between the results for survival wave height of RoRo vessels and conventional vessels.

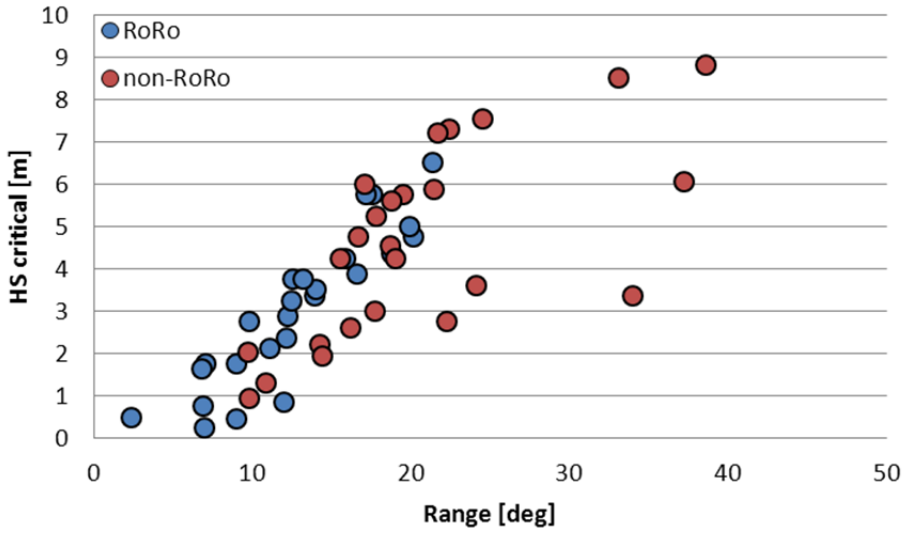

Figure 9-3: Critical significant wave height vs. Range for RoRo and non-RoRo vessels

Results are much closer than in the case of GZ_{MAX}

What is assumed in equation 9-2 is that if GZ_{MAX} and Range in damaged condition are equal or greater than 0.12m and 16deg respectively, s=1. This is because we have, from statistics, the probability density distribution of sea-state during collision, which is given by equation 9-4 and shown graphically in figure 9-4.

$$P_{H_s|col} = exp\left(-exp(0.16 - 1.2 \cdot H_S)\right) \tag{9-4}$$

Essentially it means that there is a 30% probability that a collision will happen in calm water, 90% of all collisions have happened in 2m or lower wave height, while 99.9% of collisions have happened in lower than 4m significant wave height. If a vessel can withstand 4m wave height in damaged condition, it can survive 99.9% of collisions, thus probability of survival is 99.9%. The formulation of the s-factor is made so that it reflects exactly that and as such there is nothing wrong with it. The problem is that the assumption that if GZ_{MAX} is equal or larger than 0.12m then the vessel can survive 4m wave height is only true in the case of non-RoRo vessels. The sample acquired during HARDER, shown in figure 9-2, demonstrates that. In the same figure one can understand that for a RoRo vessel to be able to survive 4m significant wave height, its GZ_{MAX} has to be greater than 0.25m approximately (the value where the fitted line crosses the horizontal line of 4m). Another shortcoming of the SOLAS s-factor is that it's based on essentially only one vessel. When other vessels were added to the sample, the model did not fit anymore. Experiments of other RoPax vessels were added to the sample during newer project GOALDS and others. The results were looking strange at first glance, with some vessels regarded as "outliers" (figure 9-5). Especially Range values looked as if experiments were wrong.

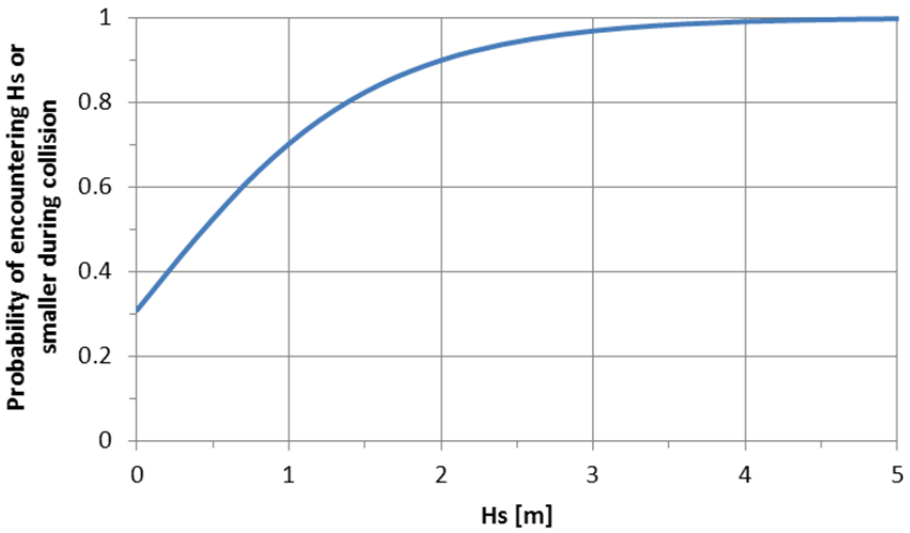

Figure 9-4: Probability mass function of significant wave height during collision.

There is a 30% probability that collision will occur in calm water, while almost 99.9% of collisions have happened in wave height smaller than 4m.

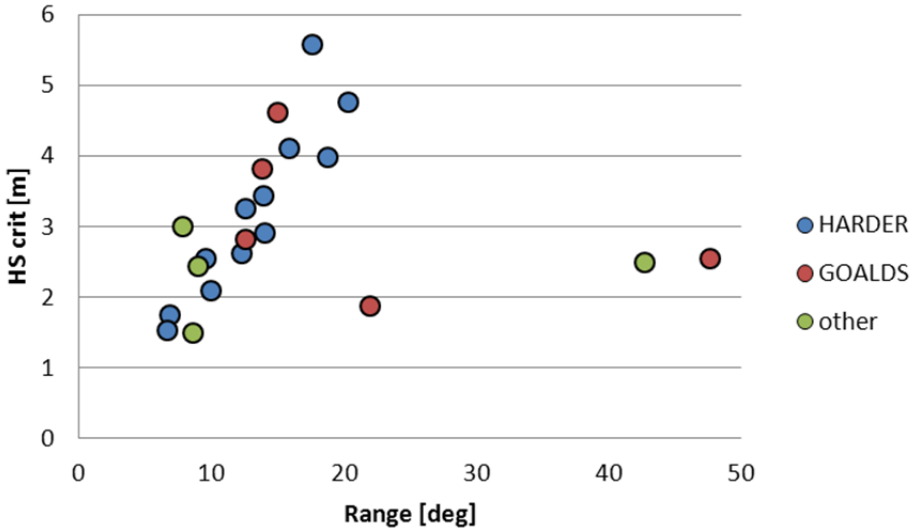

Figure 9-5: Experimental results from 7 different RoPax vessels

These experiments were carried out during projects HARDER, GOALDS, EMSA and FloodSTAND. Critical significant wave height is shown here against Range of the GZ curve.

A closer examination showed that the apparent outliers were all smaller vessels and later studies made it clear that they were no outliers at all as will be explained in the following. It was another indication though that the current s-factor was completely unable to be used generally for all vessels. SOLAS 2009 s-factor could not predict the survival wave height accurately either. In [45] it is explained that the s-factor would potentially over-predict the survivability in waves of RoPax vessels but this is not accurate either. In the same paper, cases were presented that resulted in s=1 and capsized in numerical simulations, when other cases that resulted in s=0 survived. The latest experiments have shown that it can also under-predict (figure 9-6). In general it is inaccurate.

Apart from the inaccuracy, the biggest problem of the current s-factor is hidden in its fundamental meaning. The s-factor was modelled by regression of the critical wave height as derived from the experimental data. The definition of the critical wave height though is where the real problem lies. At the time, the critical wave height was perceived as the wave height at which there is 50% probability of survival in 30 minutes. As described in detail in chapter "capsize band", this is where the probability mass function of the capsize rate shown in figure 9-7 takes the value 0.5. Building on that, the s-factor essentially also gives the wave height value up to which the vessel has 50% probability to survive for 30 minutes at least and little else. This is not adequate for the latest performance-based, zero tolerance regulations like Safe Return to Port, according to which the vessel needs to remain afloat and habitable for safe return to port or for a minimum time like 3 hours to allow for assistance or orderly evacuation [41]. The fact that the s-factor can tell us nothing about the vessel's capacity to return to port renders it unusable for such applications where it matters the most, the design stage.

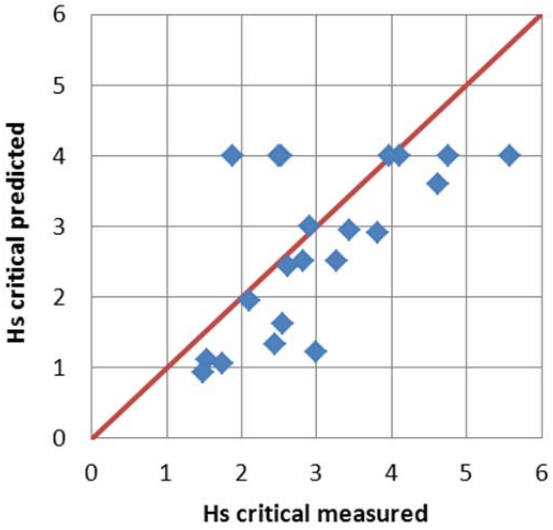

Figure 9-6: SOLAS 2009 s-factor predicted Hs_{CRIT} against measured values

These values have been obtained by solving equation 9-4 for *Hs*, using s-factor as $P_{Hs|col}$. In fact SOLAS s-factor cannot return values greater than 4m due to the "caps" of GZ_{MAX} and Range in its formulation.

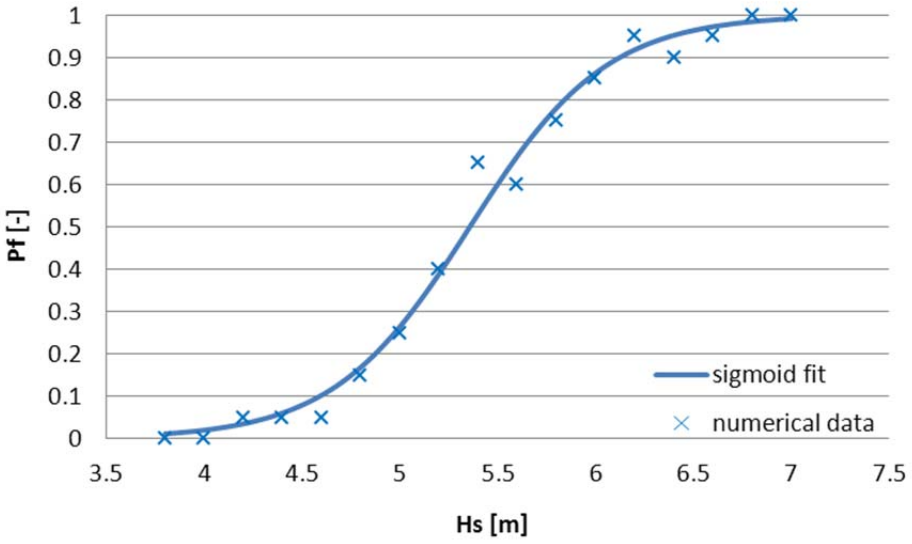

Figure 9-7: Probability to capsize with respect to Hs given 30 minutes simulation and a specific damage case and loading condition

The otherwise known as the capsize band, the probability mass function of the capsize rate with increasing H_S, as derived from numerical experiments and validated through physical tests. Its properties are described in detail in chapter "Capsize band".

Another drawback of the SOLAS 2009 s-factor, deriving from the fact that it is a regression formula, is that it is very sensitive to the regression sample. As previously mentioned, the sample upon which the s-factor was modelled consisted primarily of one vessel, tested in various loading conditions and different damages (figure 9-8). Although this is a representative model of medium-sized RoPax vessels, it cannot possibly represent other sizes or configurations, for example side casings or long lower holds exiting in other vessels. For this reason the sample has been extended in order to capture the influence of these features. Numerical experiments carried out for the other models resulted in figure 9-9. It can be seen that the dispersion has increased significantly, especially in case of range, suggesting that the parameter set is incomplete.

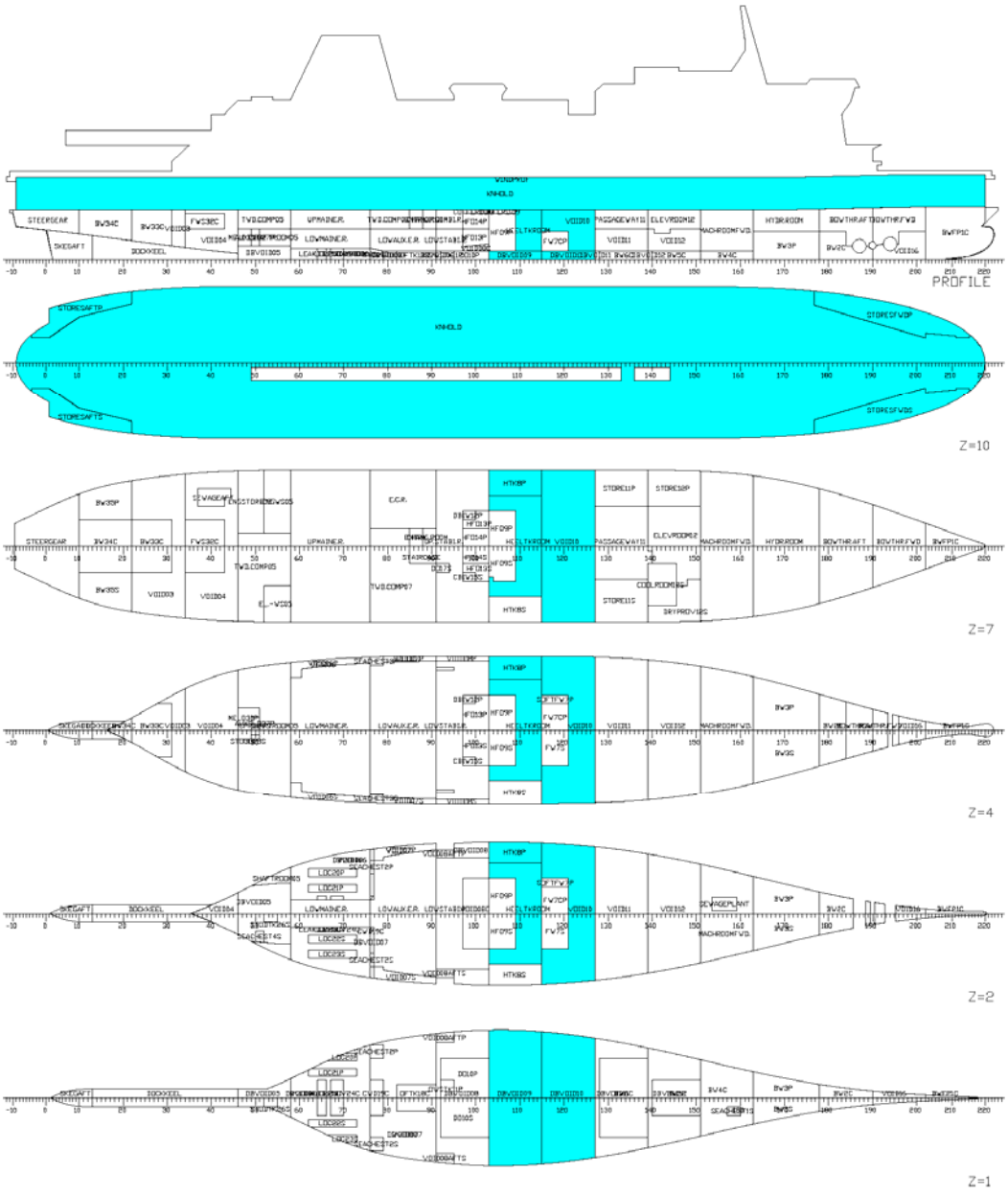

Figure 9-8: General arrangement and damage case of PRR01

This model has been used in a multitude of projects and was also tested during project HARDER for the derivation of the s-factor. The damage case is a 2-compartment, asymmetric damage to port.

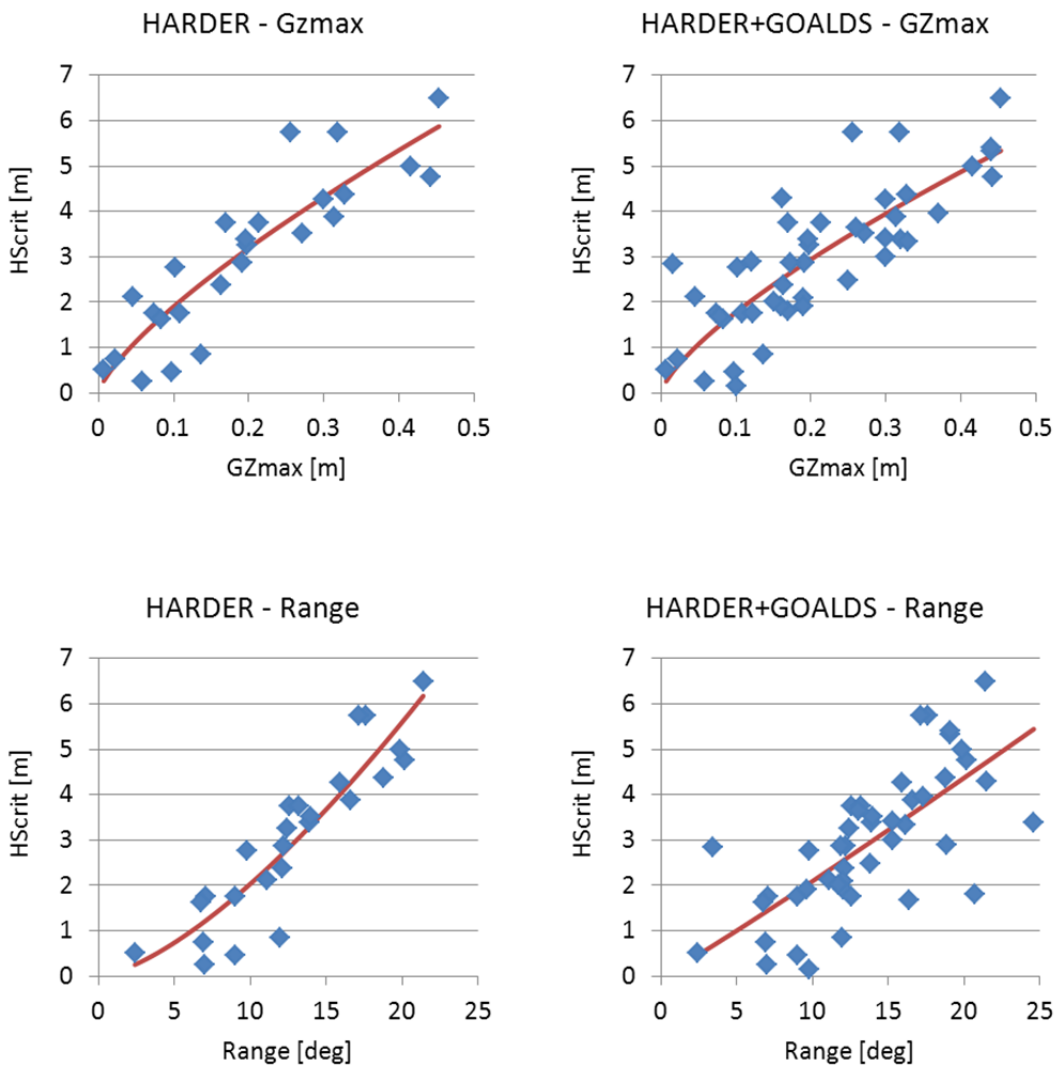

Figure 9-9: Enhancement of the sample

The regression of the sample points has been included in these graphs to demonstrate the sensitivity to the enhancement of the sample. Particularly in the case of Range the scatter has increased significantly suggesting that there might be missing parameters.

9.2 The critical sea-state

9.2.1 Defining the Hs_{CRIT}

Engineering the new s-factor to meet the latest standards required revision of some basic definitions like the critical wave height. Specific groups or categories of vessels also required to be treated separately. For this reason, project GOALDS that started in 2009 targeted passenger vessels including RoPax and cruise ships. Numerical simulations alongside towing tank tests were done for 4 passenger vessels. One of the most significant findings is that the capsize band depends strongly on the time of experiment. It has been explained in detail in chapter "Capsize band" that the band contracts towards its lower boundary when the time of simulation is increased. Based on this observation, the decision was made to shift the critical wave height from 50% probability of capsize to 5% (figure 9-10). This way it is insured that, regardless of experiment time, the critical wave height is fixed, within an engineering acceptable 5%, in essence removing the necessity for long and resource-expensive experiments.

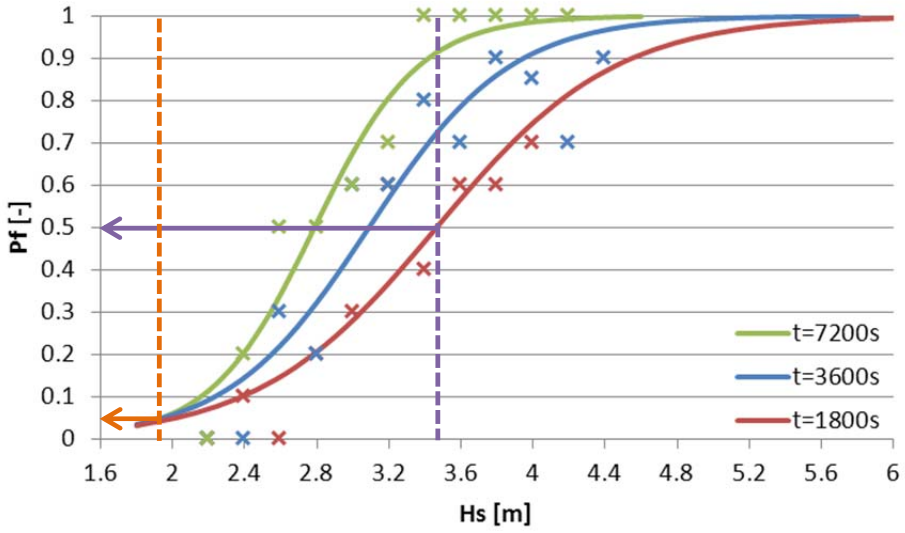

Figure 9-10: Contraction of the capsize band

As simulation time increases the capsize band contracts towards its lower boundary.

9.2.2 Impact on Index-A

This shift results in some reduction of the predicted survivability and could be characterised as conservative compared to the definition used during previous research. However, unlike the one in figure 9-10, the capsize band gets narrower in lower sea-states which means that the shift will not affect the s-factor much. In addition, anything above 4m significant wave height will not be influenced at all. Furthermore, the percentage of cases with s-factor between 0 and 1, those that will be affected by this shift that is, are but a small fraction of the total number of cases examined within the probabilistic framework of stability. In order to prove this statement, the following study has been performed for one of the RoPax vessels used at GOALDS. The dataset that was used during HARDER to formulate the SOLAS 2009 s-factor was modified according to the previous so that the shift of the critical sea-state can be translated in a new s-factor. To enhance the study, an additional modification to the s-factor was made as per [12]. That is, the value at which the function $Hs_{CRIT}(GZ_{MAX})$ meets Hs_{CRIT}=4m is taken as 0.25 to better reflect the data for RoPax vessels (see figure 9-2) to create a 3rd dataset for comparison of the results. All the damaged hydrostatic properties needed have been calculated with NAPA® so the 3 s-factors can be calculated. The result is 3 different A indices, one as SOLAS 2009 postulates, a second one for the change of GZ_{MAX} to 0.25 (eq. 9-5) and a third for the shift of the critical value of the significant wave height. The reduction of the Hs_{CRIT} to the lower boundary of the capsize band has been made according to the model notated by equation 9-6 and shown graphically in figure 9-11, which predicts the width of the capsize band at each wave height.

$$s_i = k \cdot \left(\frac{GZ_{max}}{0.25} \cdot \frac{Range}{16} \right)^{\frac{1}{4}} \quad (9\text{-}5)$$

$$Bandwidth = 0.0346 \cdot Hs^2 + 0.218 \cdot Hs \quad (9\text{-}6)$$

A simple 2nd order polynomial regression model has been used at this point displaying a good fit with R^2=0.8718. The calculation of Index-A has been carried as per SOLAS 2009. However, for simplicity reasons, only final stage has been assumed for all damages since it is a comparison and the outcome is not affected by this. The reduction of the Hs_{CRIT} according to the shift is shown in figures 9-12 and 9-13.

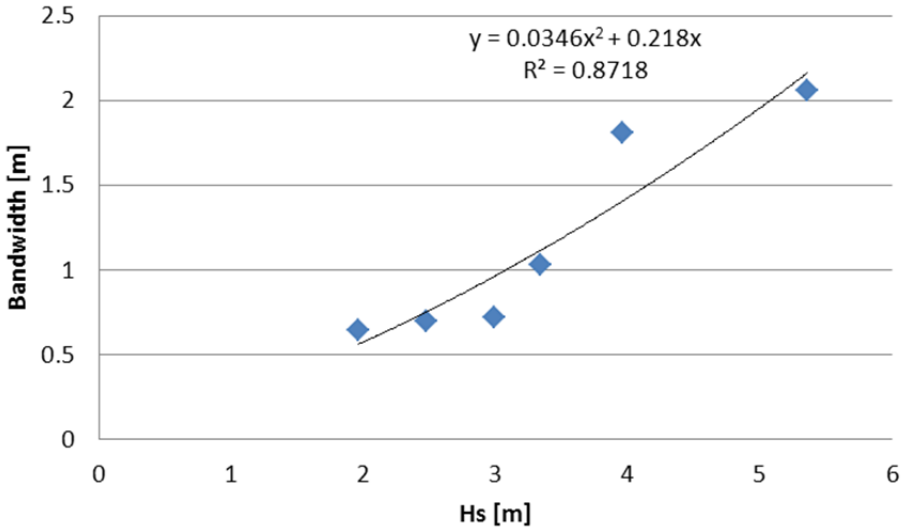

Figure 9-11: Bandwidth of the capsize band relative to wave height

This is an experimentally derived model for the change of the bandwidth of the capsize band for different wave heights for the same vessel (PRR01) used during the derivation of the current s-factor.

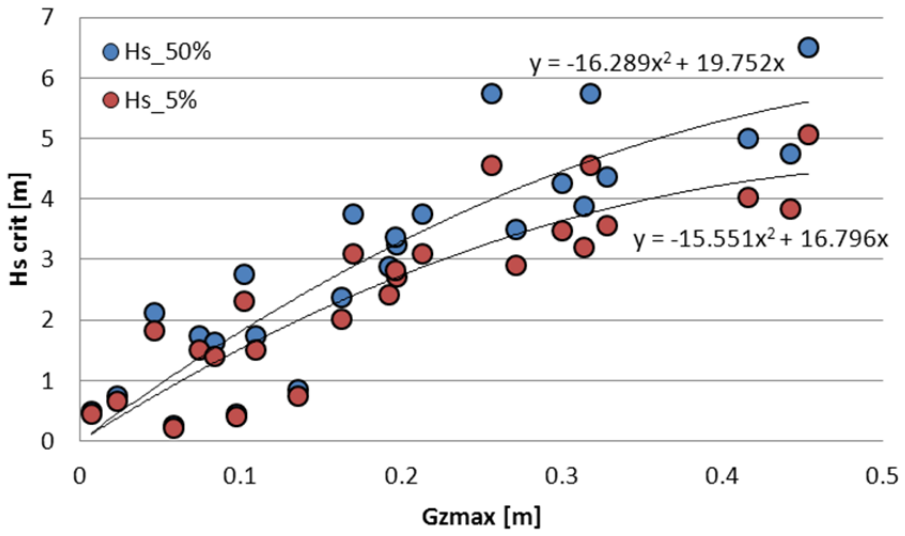

Figure 9-12: Shift of the Hs_{CRIT} with respect to GZ_{MAX}

The original dataset (blue) postulates that GZ_{MAX} has to be 0.25m to be able to survive 4m wave height while the modified dataset requires 0.35m approximately.

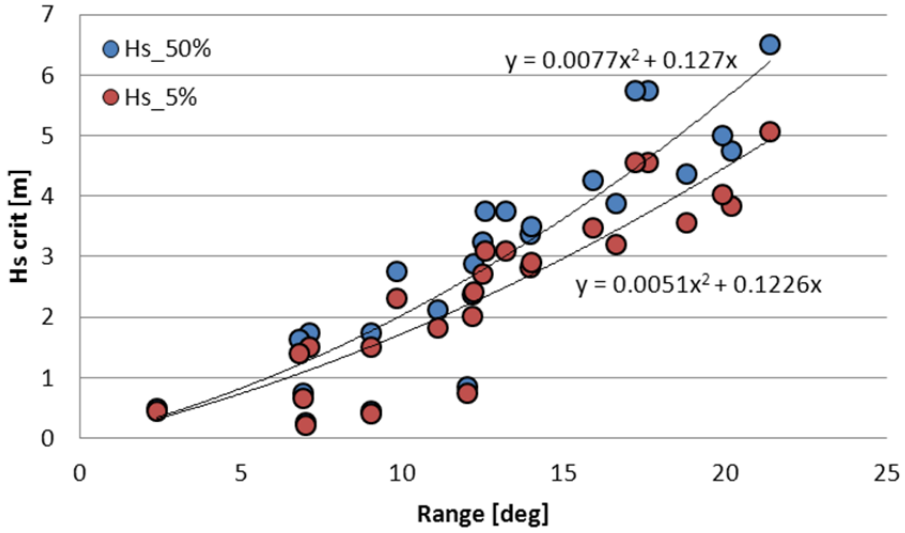

Figure 9-13: Shift of the Hs_{CRIT} with respect to Range

The original dataset (blue) postulates that Range has to be 16 degrees to be able to survive 4m wave height while the modified dataset requires 18.5 degrees approximately.

According to figures 9-12 and 9-13, the third s-factor will take the form shown in equation 9-7.

$$s_i = k \cdot \left(\frac{GZ_{max}}{0.35} \cdot \frac{Range}{18.5} \right)^{\frac{1}{4}} \tag{9-7}$$

Table 9-2: Results of the case study

Results shown here demonstrate the difference each considered formulation of s-factor makes to Index-A.

	Index A	Reduction (Abs.)	Reduction (%)
SOLAS 2009	0.882922	[-]	[-]
New 1	0.868765	0.014157	1.603465
New 2	0.850241	0.032681	3.701445

The results shown in table 9-2 demonstrate how small the difference is. The explanation behind how such a big difference in s-factor results in such benign change to the overall measured safety level lies in the distribution of the damage cases themselves. In any distribution of damage cases, some will have adequate stability to overcome severe sea-states; others will only be able to survive milder conditions, while a portion will not even have sufficient buoyance to stay afloat. Their distribution depends on the required standard – this is what makes the R-factor so important. Although the damage cases that result in no buoyance typically outnumber the other two categories, the probability of each damage scenario to occur is what makes all the difference.

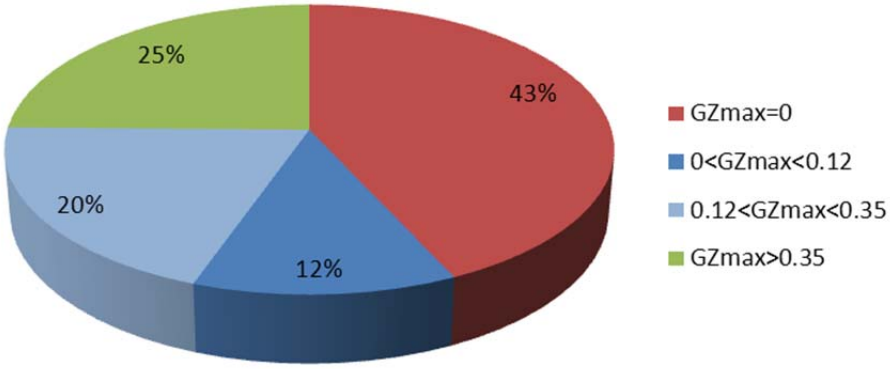

Figure 9-14: Distribution of damages according to GZ_{MAX}

Shown here is a pie chart demonstrating the sections of damages according to GZ_{MAX}. Note that damages that result in no stability (red) are more than those that result in more than adequate stability (green).

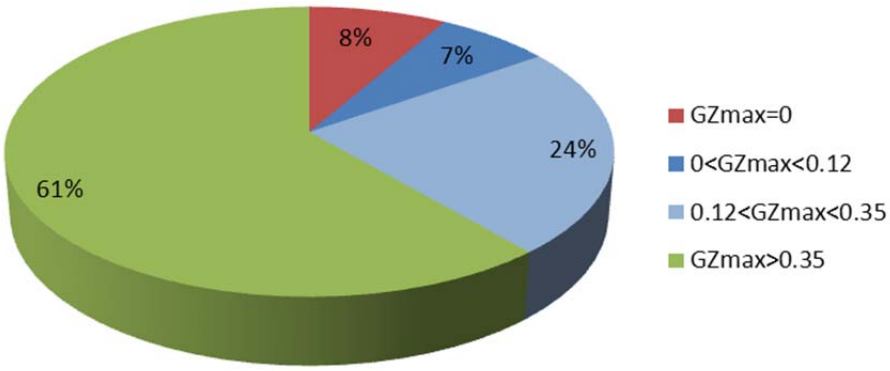

Figure 9-15: Probability distribution of damages according to GZ_{MAX}

The same chart as above but with the portions having been replaced by probabilities. Essentially, it means that although the number of damages that result in no stability (red) is greater than the rest, the low probability of these damages to occur limits their contribution.

As can be seen in figure 9-14, the quantity of damages that result in no stability – the red portion of the pie – are physically more than those that result in high stability. However alarming this might seem, one needs to consider that these are typically larger damages of 4 or more compartments that have quite low probability of occurrence. A more relevant distribution is shown in figure 9-15, where the quantity of damages has been replaced by their probabilities. Now it is visible that the particular vessel has a 61% chance of not encountering any problems of stability, while there's an 8% chance that a damage case will lead to rapid sinking due to lack of buoyancy. Considering that this vessel can carry up to 1400 persons on-board, the prospect of losing every one of them in almost one every ten collision accidents is a rather disturbing one. This is a product of the standard required by the regulation and it demonstrates how low it is. In previous regulatory frameworks like SOLAS 1990 it was required that every 2-compartment damage case should be able to remain afloat without submerging the margin line. At the time little was known about the probability of damage extents and was probably believed that such damage is the worst that could happen. This has been revised now but the current standard allows for probable damages to have no sufficient buoyancy which is not in line to previous generation's regulations mentality and seems to be a step backwards. The remaining part of the pie (blue), in this instance covering about one third of all probable damage cases, is separated from the green part as a means of demonstrating what part of the probable damage cases is likely to have some difficulty in maintaining stability in waves. Given the probability of sea-state occurrence shown in figure 9-4, the bigger variation in s-factor occurs between the cases that have the lowest survivability. Essentially, a damage case that can survive 1m wave height

will have a probability of survival of 70%, thus resulting in s=0.7 while a damage case that can withstand 1.5m wave height results in s=0.82 – some 15% difference. On the other hand, a case that can survive 3.5m wave height will have s=0.98, only 0.8% smaller than a case that can survive 4m with s=0.99. Therefore, the impact of damages with higher survivability on the total Index-A is minor, leading to the results seen in table 9-2.

9.3 Remodelling of the s-factor

The necessity for a thorough makeover of the current s-factor is made apparent by the previous sections. Observations made in the aforementioned studies have given evidence for several enhancements in order to improve the effectiveness of the formula.

9.3.1 Regression-based Hs_{CRIT} prediction

To start with, there was the observation that large positive range of the GZ curve would not lead to high survival wave heights for smaller vessels. As seen in figure 9-16, when a non-dimensional parameter, related to the size of the damage was applied to the sample, the dispersion was slightly reduced, strengthening the belief that it is size related dispersion. Dispersion was eradicated when purely dimensional parameters were applied, like the one in figure 9-17, where Range is multiplied by the vessel's intact KG value and the height of the car deck (D1) with the subtraction of the draught in damaged condition (T_d) – effectively a measure of the vessel's freeboard in damaged condition. A multitude of parameters was considered, beyond the two mentioned above, among which:

$$displacement \cdot {}^{T}/_{T_d} \tag{9-8}$$

$$displacement \cdot {}^{(D_1 - T_d)}/_{T} \tag{9-9}$$

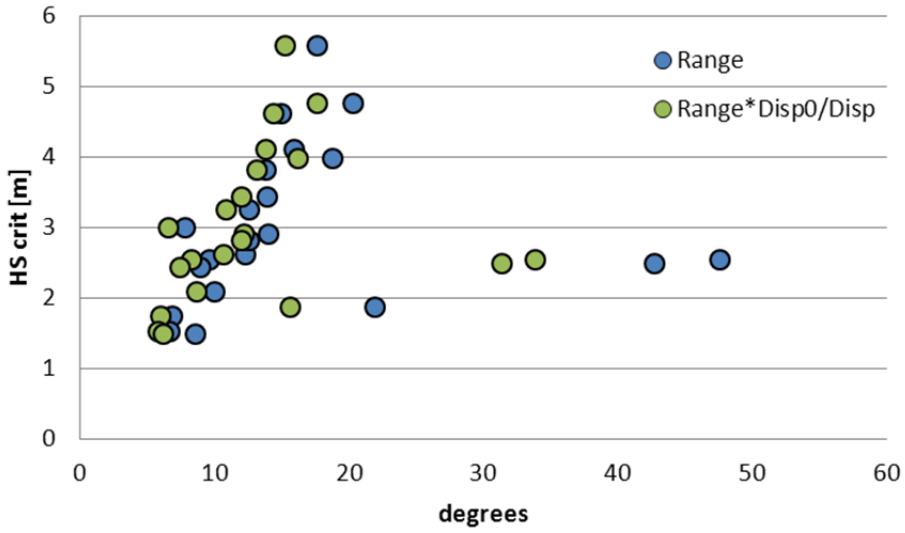

Figure 9-16: Effect of the application of a non-dimensional approach

The data dispersion is slightly reduced when a non-dimensional parameter, related to the size of the damage is applied. In this case Range values are multiplied by the ratio of displacement over displacement plus the volume of the damage.

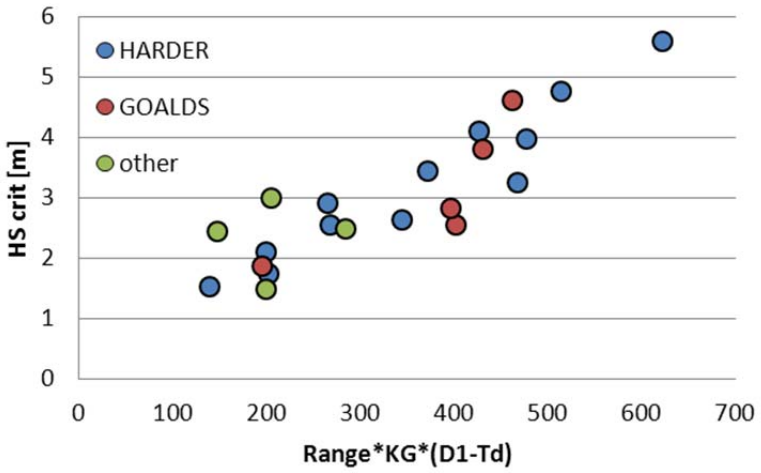

Figure 9-17: Effect of the application of a dimensional approach

The dispersion reduces dramatically when a dimensional parameter is applied. Range is multiplied here with the vessel's KG in intact condition and what is effectively a measure of the vessel's freeboard in damaged condition, the height of the deck minus the draught in damaged condition.

The coefficients tried involve size related parameters, like displacement and the vessel's main particulars as well as damage related parameters like draft in damaged condition and volume of the damage, on its own as well as a ratio with the vessel's volume. Other parameters tried are stability and response related parameters like GM, both in intact and damaged condition. The combination that finally resulted in the best fit, when GZ_{MAX} and Range are considered, has been named Z_V and is shown in equation [9-10]. A graphical representation can be seen in figure 9-18.

$$Z_V = \left(\frac{Z_{CB}(V_T) - Z_{CB}(V_d)}{T} \right)^2 \tag{9-10}$$

Where:

$Z_{CB}(V_T)$ is the vertical height from the base line to the centre of buoyancy of the considered hull

$Z_{CB}(V_d)$ is the vertical height from the base line to the centre buoyancy of the combined volume of all the damaged compartments

T is the intact draft

Z_V is effectively a lever related to the size and vertical position of the damage case. It results in quite good fit with the experimental data, which can be seen in figures 9-19 and 9-20. Regression on this dataset results in equations 9-11 and 9-12 that combine to give the Hs_{CRIT} as per equation 9-13.

$$f_1(GZ_{MAX}, Z_V) = 18.4 \cdot (GZ_{MAX} \cdot Z_V)^{0.5} \tag{9-11}$$

$$f_2(Range, Z_V) = 1.1 \cdot (Range \cdot Z_V)^{0.9} \tag{9-12}$$

$$Hs_{CRIT} = \sqrt{f_1 \cdot f_2} \tag{9-13}$$

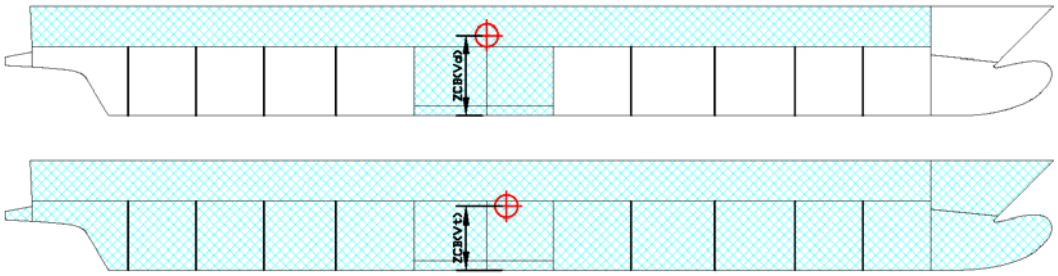

Figure 9-18: Graphical explanation of Z_V.

Z_V is the lever that results from the subtraction of the vertical height of the centre of buoyancy of the combined volume of the damaged compartments from that of the intact hull, non-dimensionalised with respect to draft (T).

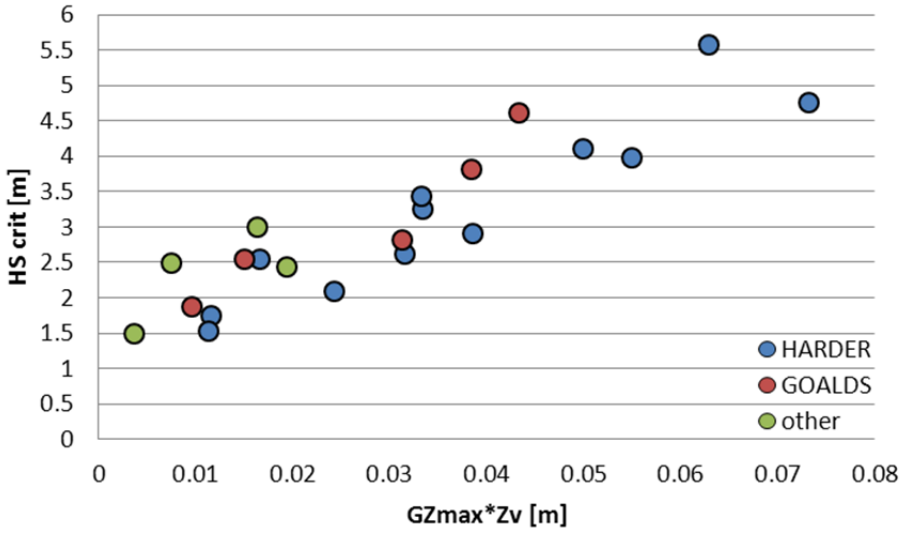

Figure 9-19: GZ_{MAX} corrected with Z_V

Z_V eradicates size related dispersion and reduces the uncertainty to less than 1.5 m Hs.

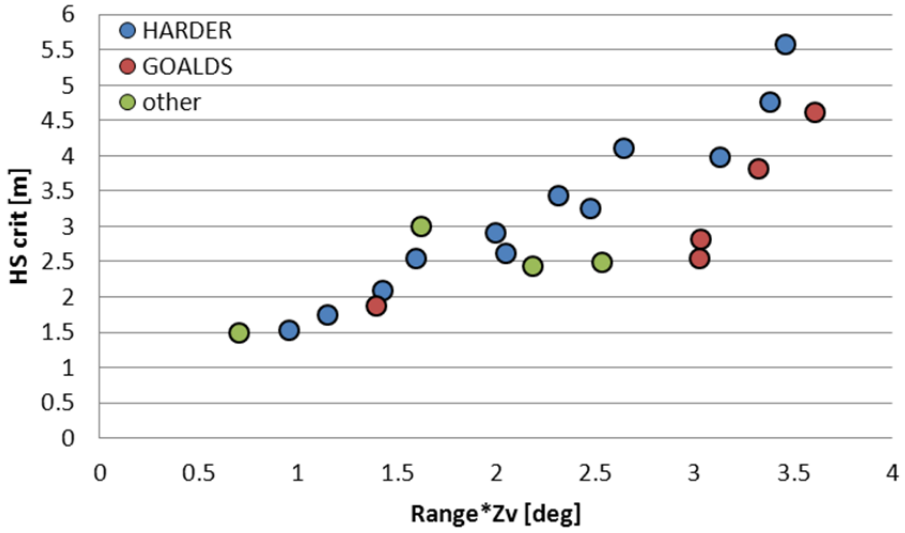

Figure 9-20: Range corrected with Z_V

The same apply to Range, which is the value that demonstrated the lowest degree of correlation.

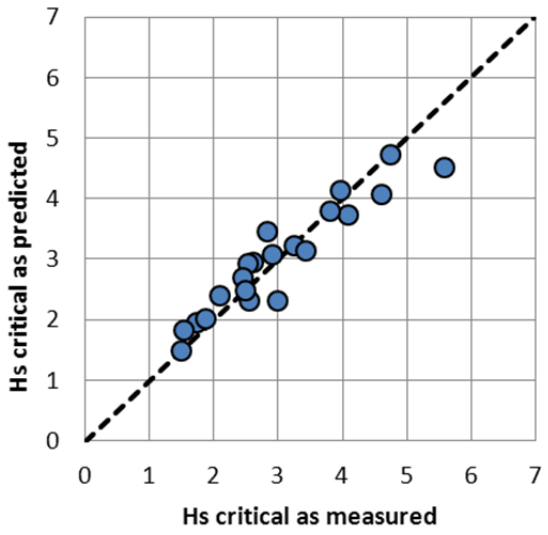

Figure 9-21: $Hs_{predicted}$ vs. $Hs_{measured}$ produced with the regression method

In this comparison between predicted and measured values for Hs_{CRIT} it can be seen how good the results are; correlation is quite high at ~94%.

However good the results of the regression based approaches might be their main disadvantage is regression itself. Just like previous regression attempts it depends heavily on the dataset used for the regression and although the dataset includes samples from the entire design space it cannot be ruled out that any new additions won't alter the coefficients or the equation itself.

In addition, the previous regression formula cannot be used for the prediction of the survivability in waves of cruise vessels. The main reason is that no cruise vessels have been included in the dataset since their behaviour appeared completely different to that of RoPax vessels probably due to Z_V which only works when the V_{CB} of the damaged compartments is higher than the V_{CB} of the intact hull, which is rarely the case for cruise vessel damages due to the lack of ro-ro deck.

9.3.2 Direct Hs_{CRIT} prediction

Due to the shortcomings of the regression type techniques an alternative method was sought. This had to be based on all the parts that were successful during the regression modelling but also include other parameters in order to be able to predict the critical wave height directly. As aforementioned, response in waves had been identified as an important agent from early on. As a measure of response in waves, GM in damaged condition (GM_F) was decided to be used. The limiting Z_V was substituted by the residual volume (V_R) which is the volume that remains if the volume of the damaged compartments is subtracted from the volume of the intact hull. Given the accuracy in prediction offered by GZ_{MAX} and Range, as explained in the previous, they were kept leading to a formula of the form shown in 9-14.

$$Hs_{CRIT} = f(GZ_{MAX}, Range, GM_F, V_R) \tag{9-14}$$

From a dimensional analysis it was discovered that:

$$\left(\frac{Hs_{CRIT}}{{V_R}^{1/3}}\right) = \left(\frac{GZ_{MAX}}{GM_F}\right) \rightarrow Hs_{CRIT} = \left(\frac{GZ_{MAX}}{GM_F}\right) \cdot {V_R}^{1/3} \tag{9-15}$$

Multiplying both numerator and denominator with 0.5·Range we get:

$$Hs_{CRIT} = \frac{\frac{1}{2} \cdot GZ_{MAX} \cdot Range}{\frac{1}{2} \cdot GM_F \cdot Range} \cdot {V_R}^{1/3} \tag{9-16}$$

Since ½ GZ_{MAX}·Range is an approximation of the area under the GZ curve it was substituted with the exact value to lead to the final equation, which was derived as described in detail in [3] and is shown in 9-17.

$$Hs_{CRIT} = \frac{2 \cdot A_{GZe}}{GM_F \cdot Range} \cdot {V_R}^{\frac{1}{3}} \tag{9-17}$$

There are a number of amendments already made following feedback from the industry but the basic idea is still the same. It has been verified in a number of ways and shows good correlation of approximately 90% with experimental data as seen in figure 9-22. It gives Hs_{CRIT} directly in meters, which means no regression coefficients dependent on the data set is needed. Although it is less than the one of the regression method described earlier, it has none of its problems and when a regression model is applied it leads to 99% correlation meaning that the dataset is fully described by the parameters used.

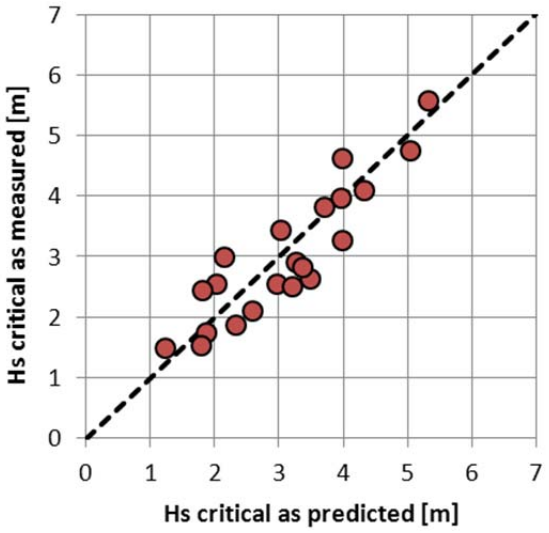

Figure 9-22: $Hs_{predicted}$ vs. $Hs_{measured}$ as derived from 9-17

The method resulted in very high correlation coefficient of 90%. Although it is less than the one of the regression method described earlier, it has none of its problems and when a regression model is applied it leads to 99% correlation meaning that the dataset is fully described by the parameters used.

9.3.3 Calculation of the s-factor

Whatever method is used for the derivation of the critical wave height, the calculation of the s-factor is the same. The s-factor represents the probability of survival and therefore wrongly named a "factor". The definition of survivability in waves can be summarised in equation 9-18.

$$s = \int_0^\infty f_{Hs|collision}(H_S) \cdot F_{survival}(H_S) \cdot dH_S \tag{9-18}$$

Where: $f_{Hs|collision}(H_S)$ is the probability density function of sea states expected to be encountered during collision

$F_{survival}(H_S)$ is the probability of survival given sea state, damage case, loading condition and time.

$F_{survival}(H_S)$ can be obtained analytically by equation 9-13 or 9-17 or any other formulation for that matter that provides with the critical wave height or even first-principles methods like numerical simulations or physical tests. The probability of encountering a sea-state during collision can be obtained by statistics. To the industry's best knowledge, the model that describes best this probability at the time has been shown in the previous in equation 9-4. Thus, the probability to survive a collision damage can be provided by 9-19

$$s = \begin{cases} e^{-e^{(0.16-1.2\cdot Hs_{crit})}}, & \forall\left(GZ_{MAX}, GM_f, Range, A_{GZe}, V_R > 0\right) \\ 0, & otherwise \end{cases} \tag{9-19}$$

9.4 Time to capsize

In sea-states exceeding the critical significant wave height, both the probability of survival and time to capsize decrease; the former following a sigmoid pattern described first in [8] as the probability mass function of the normal distribution and later described by Bolzman's sigmoid in chapter "the Capsize Band" in this thesis. The latter is expected to decrease in a hyperbolic manner as graphically explained in figure 9-23 according to [8] again. The properties of this hyperbola remained to this point unknown although the model can be described by equation 9-20

$$TTC = \frac{a}{Hs - Hs_{crit}} \tag{9-20}$$

Following a systematic investigation of the acquired data, the observation was made that parameter "a" appearing in formulation 9-20 can also be linked with Hs_{CRIT} as shown in figure 9-24, where curves for various ships and damages have been plotted together. Each point in figure 9-24 corresponds to the average TTC of at least 10 realisations for each sea-state. Figure 9-25 depicts this relation for various experimental data, derived by means of numerical simulations. The continuous line is the regression model which can be found in equation 9-21. The fit was successful with R^2=0.993 and correlation with experimental data 99.7%. Thus the final formula for TTC is given by equation 9-22.

$$a = 2.6 \cdot {Hs_{CRIT}}^{1.5} \tag{9-21}$$

$$TTC = 2.6 \cdot \frac{{Hs_{CRIT}}^{1.5}}{Hs - Hs_{CRIT}}\ [min] \tag{9-22}$$

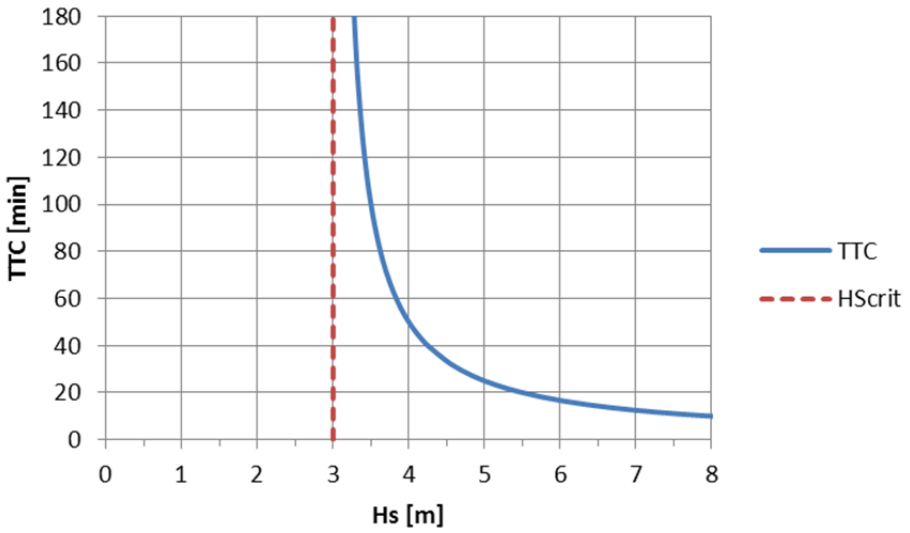

Figure 9-23: The concept of Time to Capsize

It is expected that the damaged vessel can survive indefinitely in sea-states up to the critical and that the time to capsize will decrease hyperbolically thereafter

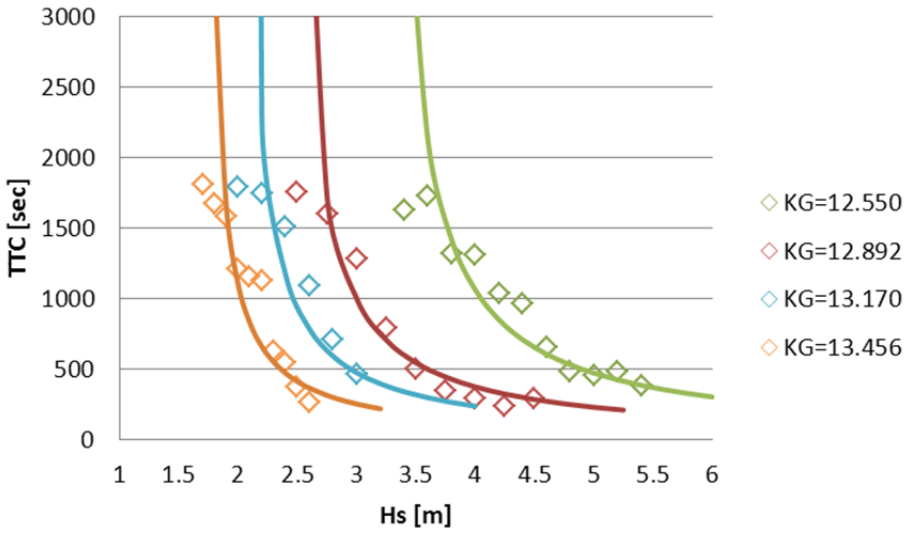

Figure 9-24: Model of Time to Capsize for different loading conditions

As a hyperbola, the model for time to capsize is governed by only two parameters, H_{SCRIT} and "α" which interestingly is also related to H_{SCRIT}.

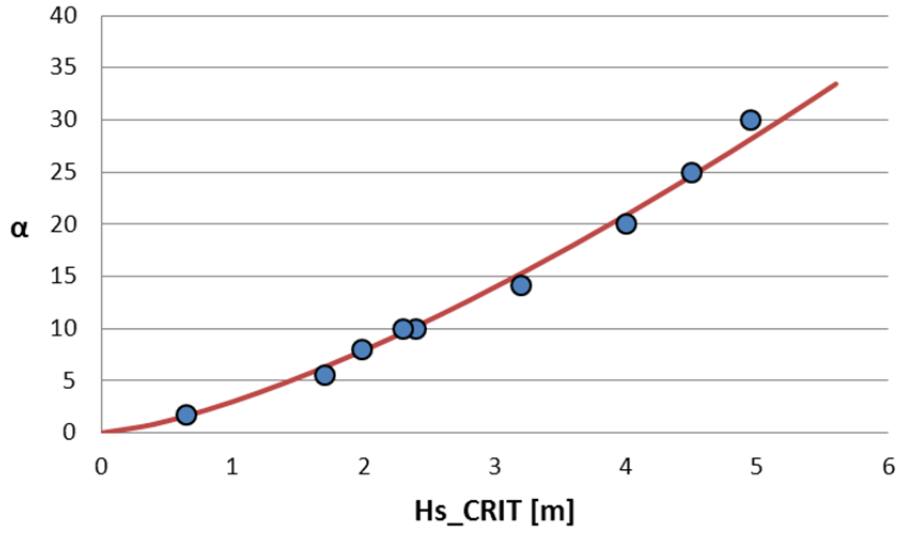

Figure 9-25: Parameter "α" for all vessels tested and model

An allometric power function was fit to the experimentally derived data as shown here. The regression resulted in R^2 of 0.993 and 99.75 correlation with experimental data.

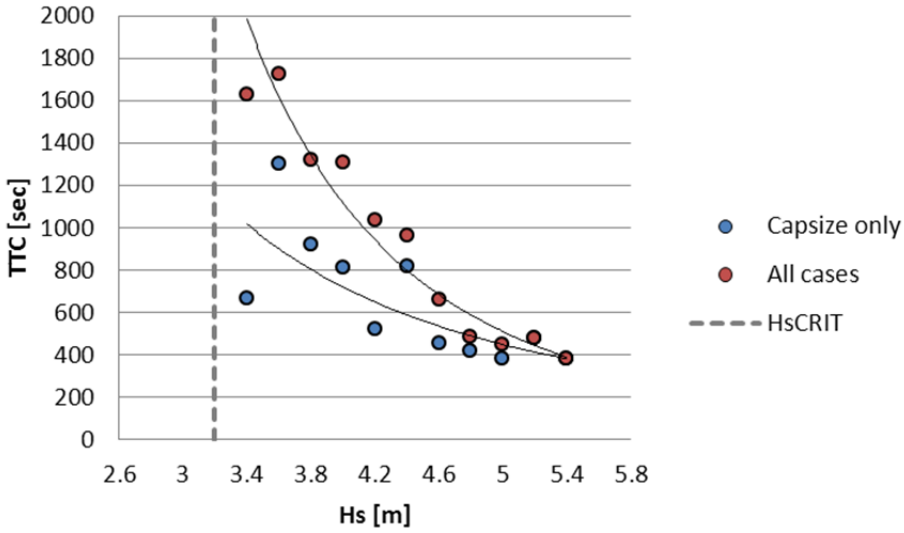

Figure 9-26: Comparison of average time to capsize for all and only capsize cases

If only capsize cases are used for modelling of the TTC the prediction will be too conservative and possibly misleading.

As with experiments for the estimation of the critical wave height, time of experiment plays a crucial role in the experiments for time to capsize. When experiment time is limited to a certain value, say 30 minutes, some cases will apparently survive for H_S values greater than the critical even though these cases would almost certainly capsize in longer runs. This is the same reason we observe a sigmoid transition from safe wave height to unsafe and not a step function. One solution for this that has been used in the past is to use for the modelling only the capsize cases only and discard those that survived to the end of the simulation. Such an approach though would lead to an over-conservative estimation of the TTC (figure 9-26) and is not the intention to do so as it could be misleading for the designer. The cases that survived to the end of the simulation "pull" the mean values upwards for a more realistic dataset. The result is still conservative as those "survival" cases are capped by the end of the experiment. In order to get more reliable results the simulation time was increased to 2 hours. The results demonstrate remarkable consistency with the model as shown in figure 9-28.

The apparent drawback of this approach is the uncertainty related to the dispersion of the experimental data. Although the mean TTC value is very consistent and correlates well with the model, the uncertainty is quite large. As can be seen in figures 9-29 and 9-30 the uncertainty is of the 100% magnitude. It can be approximated with a normal distribution with standard deviation of 0.5 around a zero mean value as shown again in figure 9-30. Admittedly this is quite a large uncertainty and special care has to be paid on how the method is used. In any case the benefits of even qualitative knowledge of the time to capsize are far greater than its uncertainty band.

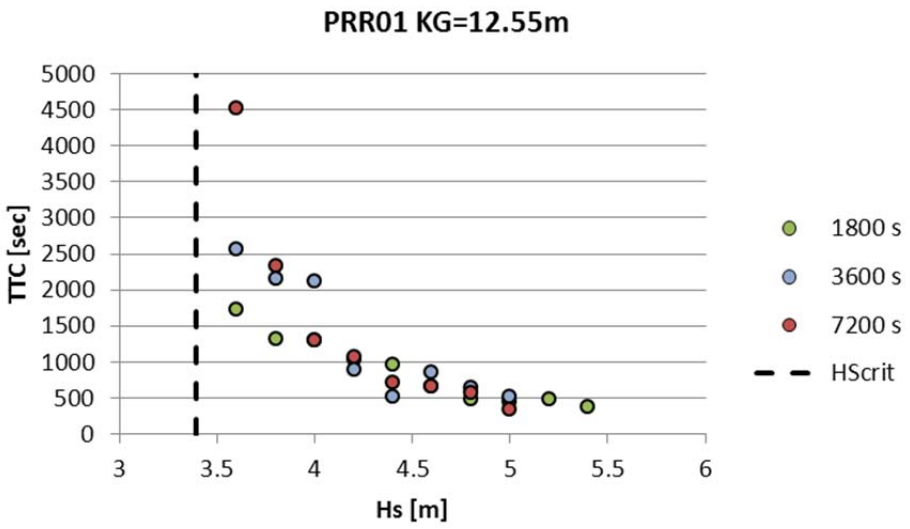

Figure 9-27: Effect of experiment time on TTC model

Dispersion is smaller for higher wave heights since fewer experiments are terminated by the end of the simulation.

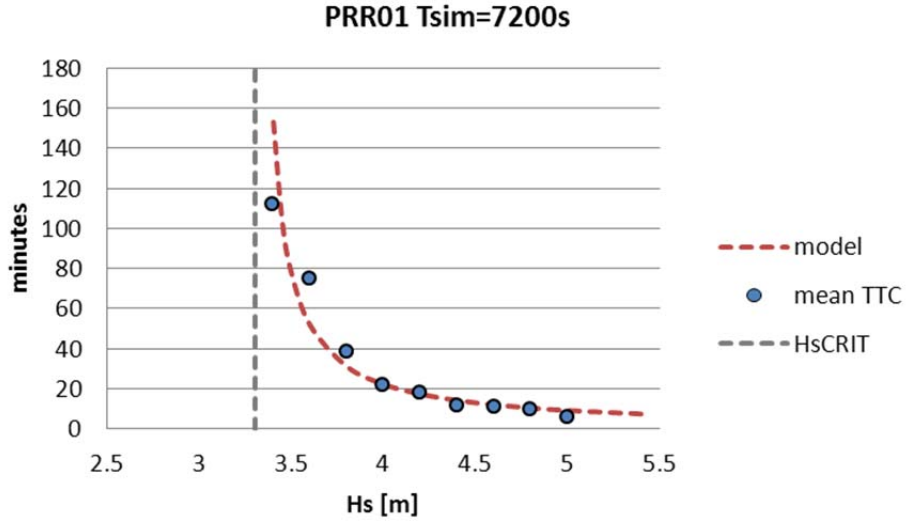

Figure 9-28: Fit of experimental data with analytical model.

The fit of the analytical model to the experimental data (mean TTC) for the longer simulation time is exceptional.

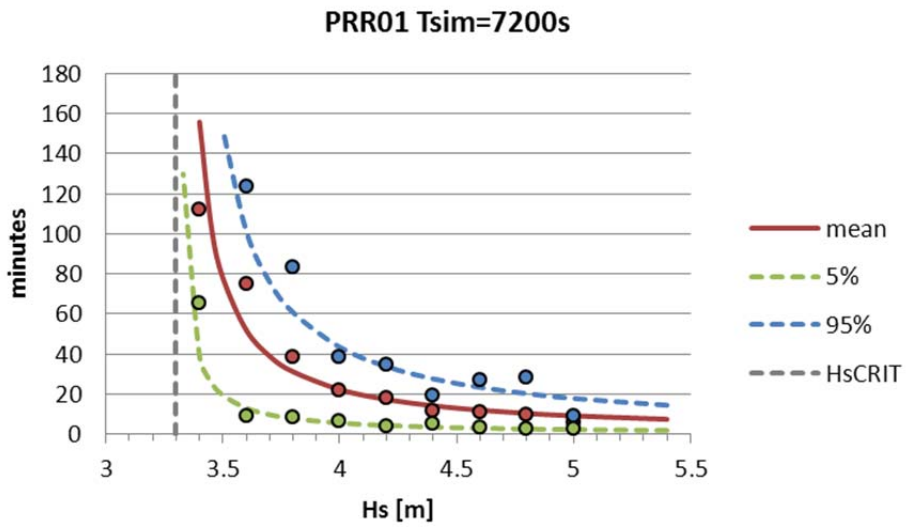

Figure 9-29: Mean value, 95th percentile and 5th percentile

The uncertainty band is visible in this figure, shown as the 5th and 95th percentiles of the experimental data (dots) and model (lines) either side of the mean value.

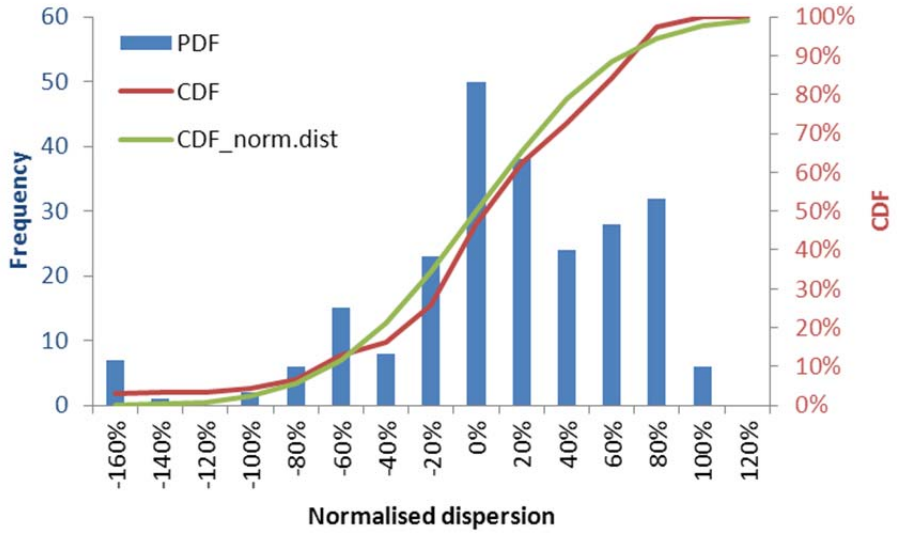

Figure 9-30: Normalised dispersion of the experimental data

The dispersion of the experimental data shown here has been derived by means of normalising the difference from the mean value with respect to the mean value. Apparently the 5th and 95th percentiles lie around the ±100% error – a quite broad band. The CDF of a normal distribution with mean=0 and STD=0.5 also shown.

Chapter 10 – Vulnerability Robust Design

10 Vulnerability Robust Design

Design for safety has never in the history of shipping been more prevalent. The last few decades have seen the struggle of the industry for ever more robust solutions that would eradicate the perils associated with passenger transport by sea. This struggle has been fuelled partly by the society's decreased tolerance to risk and partly by multi-fatality accidents, at a time that has seen the biggest boom in the shipping industry as its role has changed from merely transporting to recreational. It is this shift that has spawned a massive increase in ship size that has led to vessels capable of carrying thousands of guests in its turn increasing the risk of shipping. Adding to the above, the economic recession of the late '00s has made it even more difficult for the application of Risk Control Options by a cost-cautious industry. Subsequently the need for efficient design solutions is now more compelling than ever. To this end, this chapter aims to provide ways to utilise the tools presented in the previous chapters and demonstrate some possible solutions to identified problems.

10.1 State of the art

Recent studies in large cruise vessels have shown that they run a significantly lower risk than RoPax vessels. Numerical performance-based survivability assessment in cruise ships typically results in only a fraction of the vulnerability of RoPax vessels (figure 10-1) which probably is the product of their higher degree of subdivision. Water is pumping in at a far slower rate through a maze of compartments on the contrary to water being pumped unobstructed inside the car deck by wave action. Figure 10-2 shows the subdivision of the main deck for these two vessels.

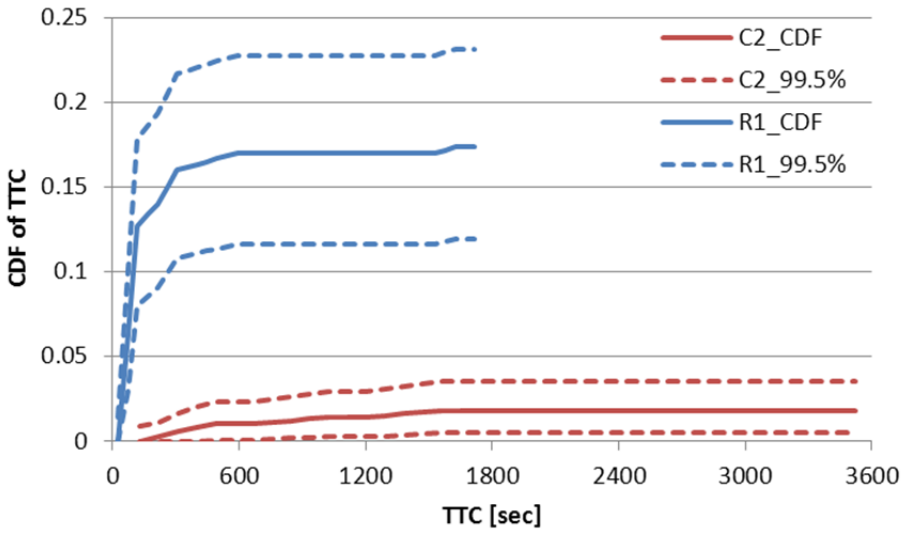

Figure 10-1: Comparison of probability to capsize between a RoPax and a cruise vessel

The assessment has been carried out by means of numerical simulations based on a Monte Carlo sampling scheme as described in chapter "Performance-Based Assessment". 500 simulations for the cruise vessel for 1 hour resulted in an order of magnitude less probability to capsize than the 300 simulations of the RoPax for 30 minutes. Both ships were tested at DS.

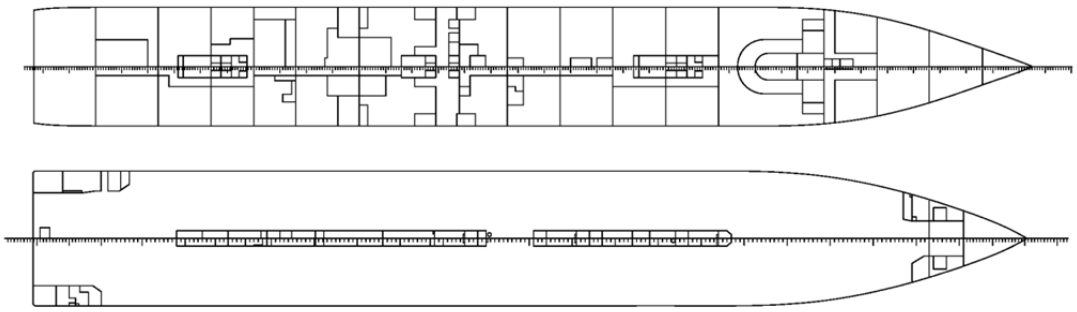

Figure 10-2: Comparison of main decks of a RoPax and cruise vessel

The higher degree of subdivision of the cruise vessel (upper) is apparent. Water in case of flooding has to find its way through openings to spread while it is unobstructed once in the ro-ro deck. Ships have been scaled for comparison.

Each of these ship types have their own peculiarities as well as their unique design difficulties to overcome. Cruise vessels for example need easy access for the thousands of guests and crew on-board to the various spaces around the vessel whether it is cabins or communal spaces. Although many of those spaces will be located on higher decks, some service related spaces still remain on decks in close proximity to the waterline. When openings leading to these spaces are left open the vessel is becoming extremely vulnerable to transient and progressive flooding as this has been presented in chapter "Vulnerability". A typical layout of the openings located on the main deck of a cruise vessel can be seen in figure 10-3. Openings in green are unprotected while the red ones are semi-watertight, to be kept closed at sea. Another vulnerability issue visible in figure 10-3 is the central corridor. Water can easily spread through there during transient stage of flooding when the vessel heels to large angles, deteriorating stability. Although the SWD should be kept closed at sea, operators readily admit that there are times when these doors can be left open, provisionally even en-route. In any case the vessel is at its most vulnerable at berth, when increased traffic conditions could lead to hull breach and flooding. When looked from a risk perspective, these openings have the potential to double the ship's vulnerability to flooding (figure 10-4). A rather simple solution that has appeared recently is to position the service deck one deck higher and make everything watertight below that. This increases the vessel's freeboard and capacity to heel without unprotected openings to submerge. While making already existent subdivision watertight is relatively straightforward, protecting a ro-ro deck from excessive flooding is not so. The solution so far is to ensure that the vessel in damaged condition can sustain an amount of water in the car deck in severe weather conditions, namely Stockholm Agreement (SA).

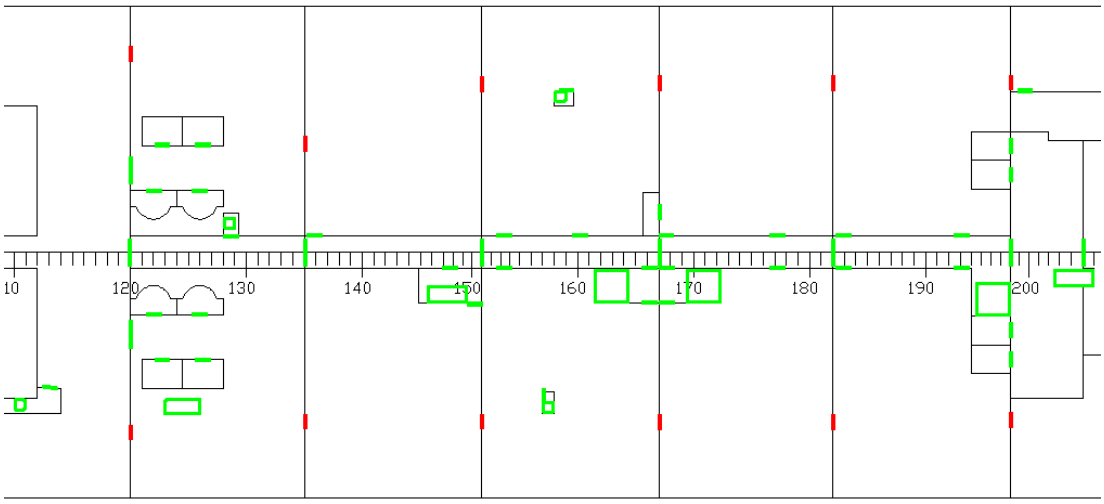

Figure 10-3: Section of the main deck of a large cruise vessel.
Note the high degree of subdivision as well as the openings. In green the unprotected openings while in red are the semi-watertight ones. The service corridor at the centre of the deck can lead to spread of floodwater due to wave motions for larger heel angles, common during transient stage of flooding.

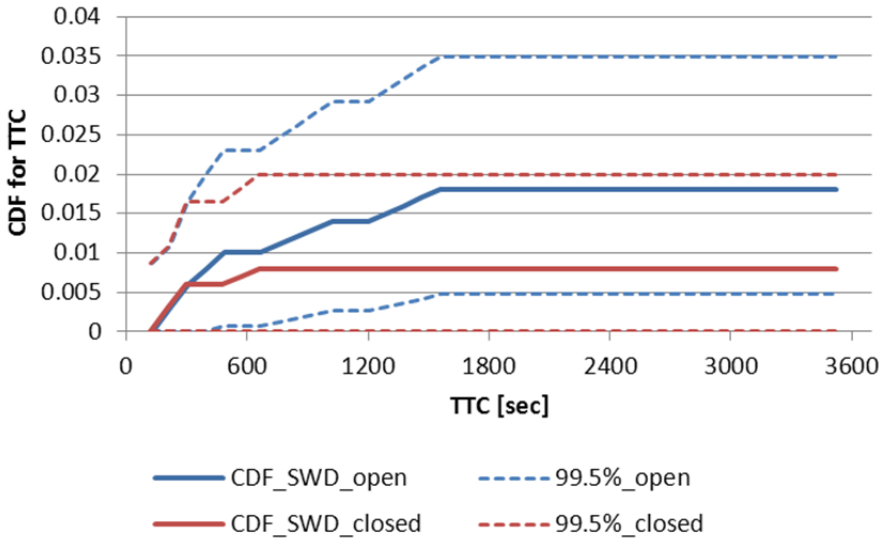

Figure 10-4: Increase of vulnerability due to SWD doors
Vulnerability to flooding can double due to SWD left open during operation or at berth.

In order to comply with the very stringent indeed – according to [12] – SA, RoPax vessels have to demonstrate very low KG values with implications not only in design but also in operation. Low KG values can either be achieved with the reduction of the height of the ro-ro deck, risking more water coming in because of low freeboard height or with the reduction of the payload, a solution that no operator is happy with. Strangely subdivision of the ro-ro deck has not been applied yet, although it has been demonstrated many times in the past that such a solution could be viable and most importantly, as it will be demonstrated in the following, very beneficiary to the survivability in waves and not only.

10.2 A study on side casings for RoPax vessels

The "safety belt" is an idea introduced a few years ago in an attempt to reduce cruise vessel vulnerability to flooding under the principle that in damaged condition the vessel is in need of stability high and wide (figure 10-5). Given that this is commercially valuable space, special thought needs to be put so that it is not made redundant by the side casings. Instead, either spaces that don't get frequently accessed can be placed there or spaces that would render it possible to be accessed through openings from above.

Following the same principle, side casings in a Ro-Pax vessel could potentially lead to very high survivability. Watertight subdivision in the car deck would firstly reduce the amount of water that can enter and secondly provide the high and wide buoyancy needed to support large, unsubdivided space in the lower decks that can be used for loading vehicles, namely the LLH. For this reason a specific exercise was done in order to quantify the contribution of the side casings to normal RoPax vessels. The study included vessels from various research projects like GOALDS [www.goalds.org] funded by the EC and RP592 [12] and RP625 [31] funded by the MCA which range from experimental concept designs to existing vessels.

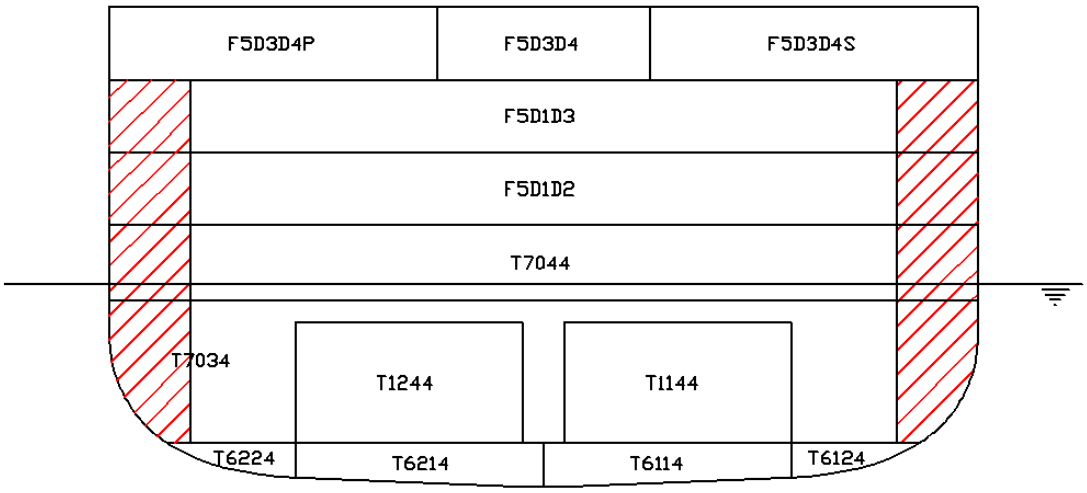

Figure 10-5: The concept of the "safety belt"

Applied here on a medium sized cruise vessel the safety belt can potentially provide the ship with the needed buoyancy high and wide to aid survivability in waves by enhancing stability in damaged condition.

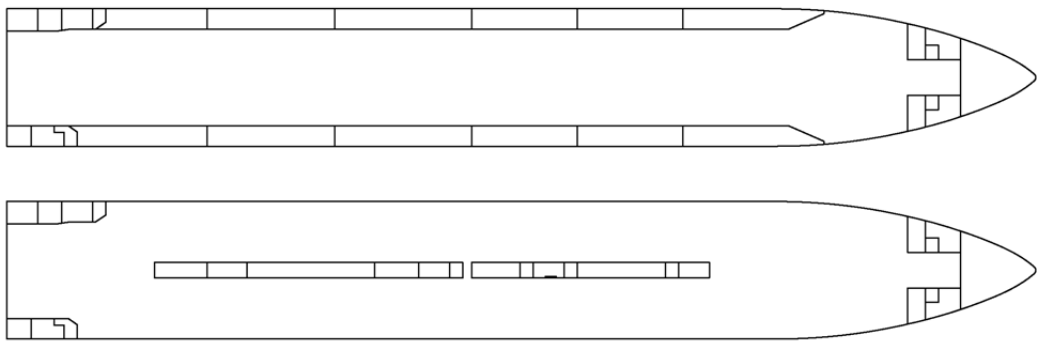

Figure 10-6: Subdivision of the vehicle deck of a RoPax vessel

This is an example of the subdivision of the car deck as realised on EUGD01-R1. The central casing has been removed since machinery and passages go through the side casings, which can also be loaded with vehicles. This way the capacity of the vessel remains in the worst case equal.

10.3 The vessels

Three medium-sized were chosen to be optimised with respect to their vulnerability. All of them were tested in original form and optimised one. One particular vessel was tested with various subdivisions on the vehicle deck. The vessels' vehicle decks have been subdivided as shown in the example of figure 10-6. Special attention was paid to the subdivision so the lane-meters are not reduced and different loading configurations were tried for this reason. Since the side casings are supposed to get loaded with vehicles, they would need to have doors. Understanding how expensive watertight doors are it was decided, since the program used enables doing so, to test if the benefits of the side casings would be any different if semi-watertight doors are used. The general arrangements of all the vessels, in original and modified form can be found in appendix IX.

Table 10-1: Study vessels main particulars

Model	EUGD01-R1	MCRP05-2A	MCRP08-2B	
Passengers	1400	1000	1400	
L_{OA}	194.3	182.6	164.13	m
L_{BP}	176.0	166.0	150.0	m
Breadth	25.0	27.2	26.5	m
Draught (Design)	6.55	6.2	6.2	m
Depth	9.1	8.7	9.1	m
Displacement	16,558	19,230.4	16,653.4	tn

Table 10-1 shows the vessels' main attributes. They are all very similar apart from the fact that the MCRP08-2B is a concept design and as such it contains none of the asymmetries and compromises inevitably reaching production within the other two. Apart from that, all three comprise a long lower hold which is thought to decrease survivability of such vessels. Subdivision-wise, transverse dividers do not have to be placed directly over bulkheads, enabling their optimisation with respect to loading. The scope of the changes made to the ships is to demonstrate the benefits in term of survivability that such a solution can offer to the vulnerable RoPax vessels so further analysis of their impact in operation and cost was not deemed necessary. The main consideration given to such aspects is to maintain or increase the capacity of the loading spaces. As can be seen in table 10-2 this has been achieved in all the models. Of course this is for comparison purpose only as the actual capacity as measured in lane-meters might differ. In any case, these vessels were modified to include the side casings, thus the benefit might not be maximised. The potential might be much higher if the vessel is designed from the beginning with the side casings. Apart from that, their size can be fine-tuned to optimise capacity.

Table 10-2: Vehicle deck of the vessels prior and post modification

Model	Car Deck Area		
	Original (m^2)	Modified (m^2)	Difference (%)
EUGD01-R1	3638	3735	+2.7
MCRP05-2A	3654	3654	-
MCRP08-2B	3133	3031	-3.3

10.4 PBS assessment of RoPax vessels fitted with side casings

The vessels were subjected to numerical performance-based survivability approach using the Monte Carlo simulation method with PROTEUS3 as described in chapter "performance-Based Survivability Assessment". An analytical assessment was also carried out by use of the Index-A of SOLAS 2009 and UGD, also described in the aforementioned chapter.

10.4.1 Numerical PBS

500, 300 and 300 damage cases were simulated for EUGD01-R1, MCRP05-2A and MCRP08-2B respectively. The random variables, chosen from the statistical distributions from collision statistics obtained from HARDER, are location, length, penetration and width of the damage opening as well as sea-state. An example of the experimental setup for EUGD01-R1 can be seen in figure 10-7. Similar setups were generated for the rest of the vessels and simulated for 30 minutes each.

The results of the numerical PBS can be found in figures 10-8, 10-9 and 10-10. Even though each vessel has its own configuration it seems that the application of the side casings can have a massive influence on survivability. Compared to the vulnerability of the original designs also shown in the figures it is apparent that the reduction in vulnerability is 60% in the worst case and ~75% in the best. Very consistently, the fitting of the casings always results in approximately 5% vulnerability to flooding. Compared to the almost 20% typically occurring in RoPax vessels, this is a vast difference. Probably equally important is the 31% reduction of vulnerability of the first modified version of MCRP08-2B where central casing has been replaced with narrow side casings. A summary of the results is presented in table 10-3.

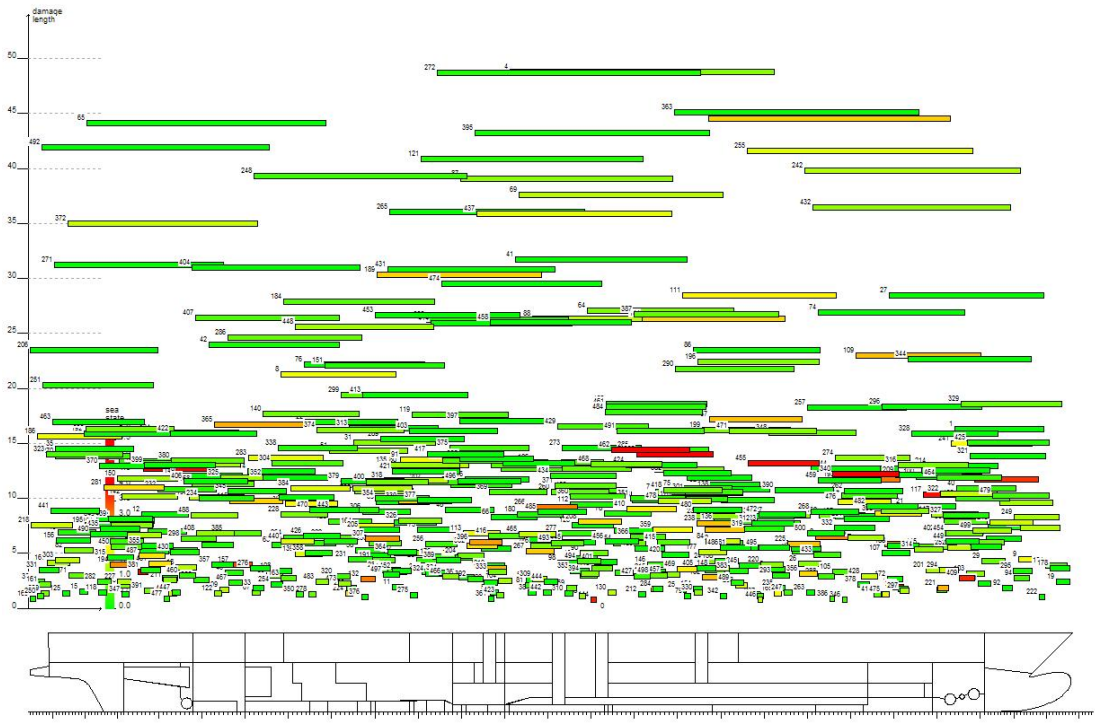

Figure 10-7: Experimental setup for 500 damage cases

Shown here is the setup of the Monte Carlo simulations for the EUGD01-R1. Sea-state is colour coded.

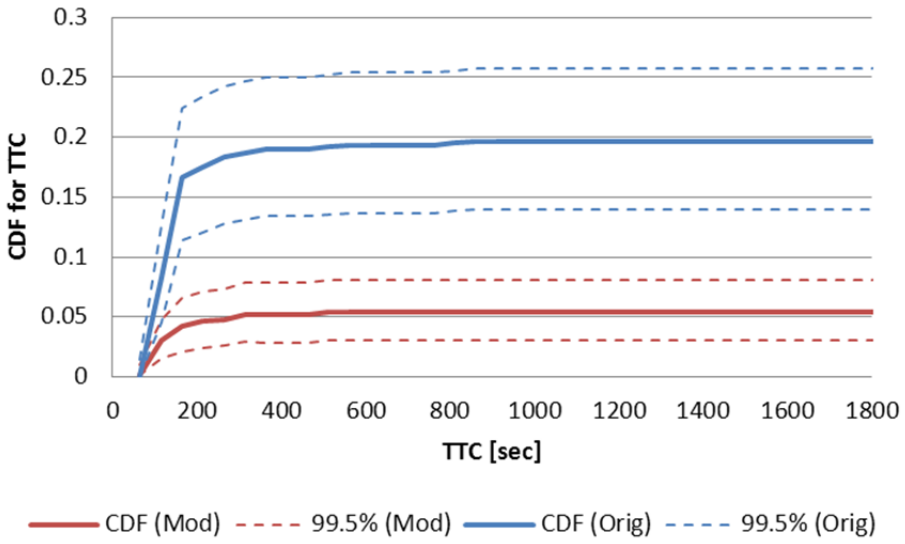

Figure 10-8: Result of Monte Carlo simulations for EUGD01-R1

Shown here are the results of the vulnerability assessment for the original R1 and its modified version. Subdivision of the car deck resulted in ~75% reduction of vulnerability to flooding.

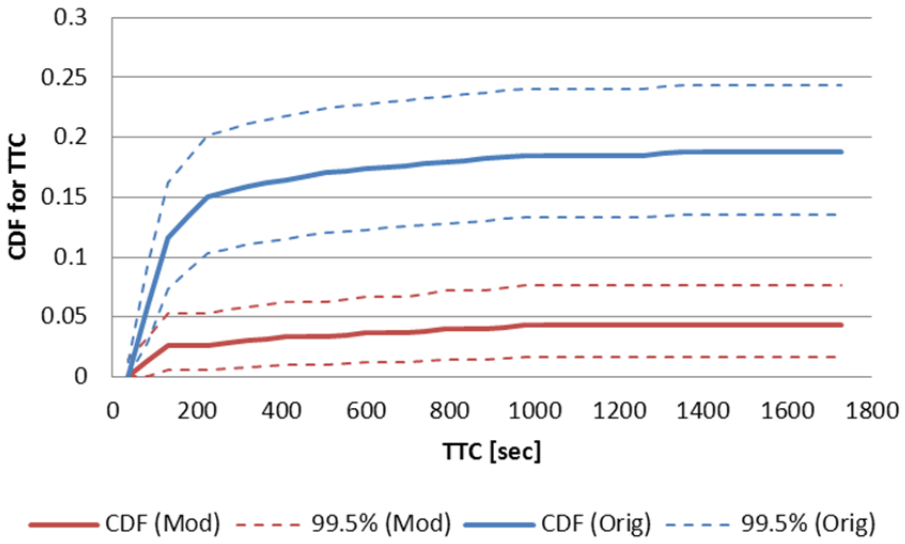

Figure 10-9: Result of Monte Carlo simulations for the MCRP05-2a

Vulnerability reduction with the application of car deck subdivision is the same as previous for the second actual vessel.

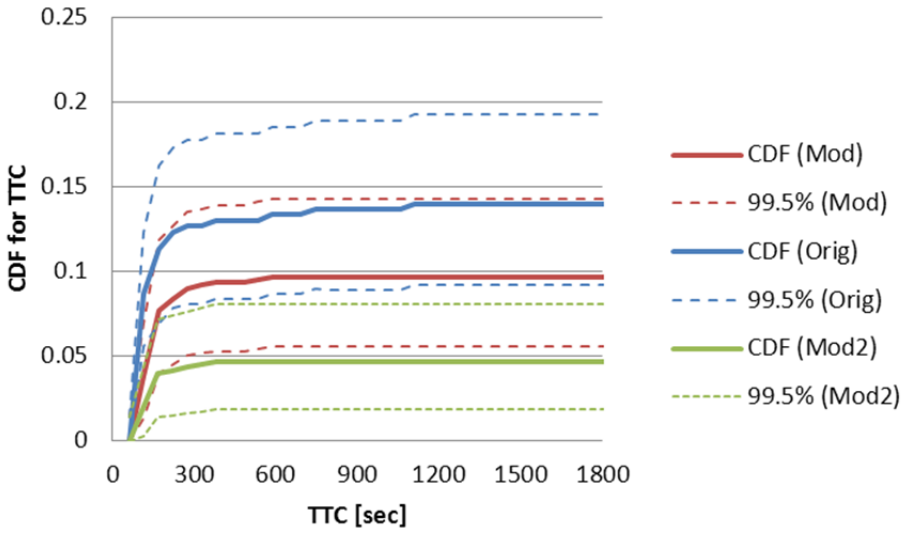

Figure 10-10: Result of Monte Carlo simulations for the MCRP08-2b

Results for 3 variants of this vessel are presented here. As this is a conceptual vessel, its vulnerability is approximately 20% less than the other two. The subdivision of the car deck results in similarly dramatic reduction of vulnerability.

Table 10-3: Summary of the results of the numerical PBS assessment

Irrespective of configuration, side casings always result in around 5% vulnerability, some 60% at least lesser than the original design's

	Original	modified	difference	reduction
EUGD01-R1	0.1967	0.0540	0.1427	72.54%
MCRP05-2A	0.1879	0.0433	0.1445	76.93%
MCRP08-2B	0.1400	0.0467	0.0933	66.67%

Clearly the side casings are a very attractive solution that can bring RoPax vessels' vulnerability down to the levels of cruise ships. If they are designed into the ship and not just fitted, their impact on cost and operation can be minimised. In fact it is my strong belief that a vessel can be designed as safe as needed, so long as the designer knows how much is actually needed.

10.4.2 Analytical PBS

The two available methods for the assessment of survivability analytically have also been utilised for obtaining a little more information regarding these vessels' vulnerability. These are the SOLAS 2009 [29] and UGD [14] also described in chapter "PBS" earlier in this thesis. The information sought concern the distribution of probability of the consequences of the damages. That is the probability distribution of damages to result to s=0, s=1 and those in between. To get this, the result tables for all the damages, obtained during the Index-A calculation are needed and have been obtained for the vessels EUGD01-R1 and MCRP08-2B using NAPA by doing complete Index-A calculations. The pie-charts in figures 10-11 and 10-12 show how the probability distribution of s_i has changed with the modification of the vessels.

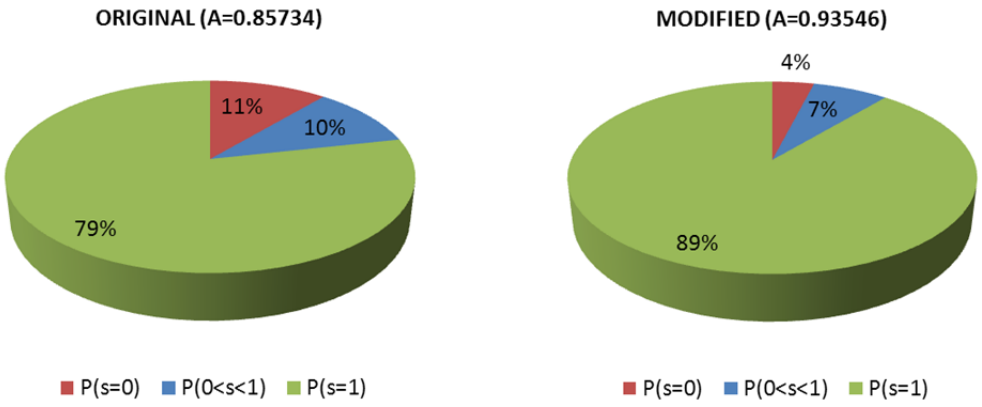

Figure 10-11: Distribution of probability of si – EUGD01-R1

Probability of s=0 (i.e. cases without any residual stability) has reduced to almost 1/3 while the probability of s=1 has increased by 13.3%.

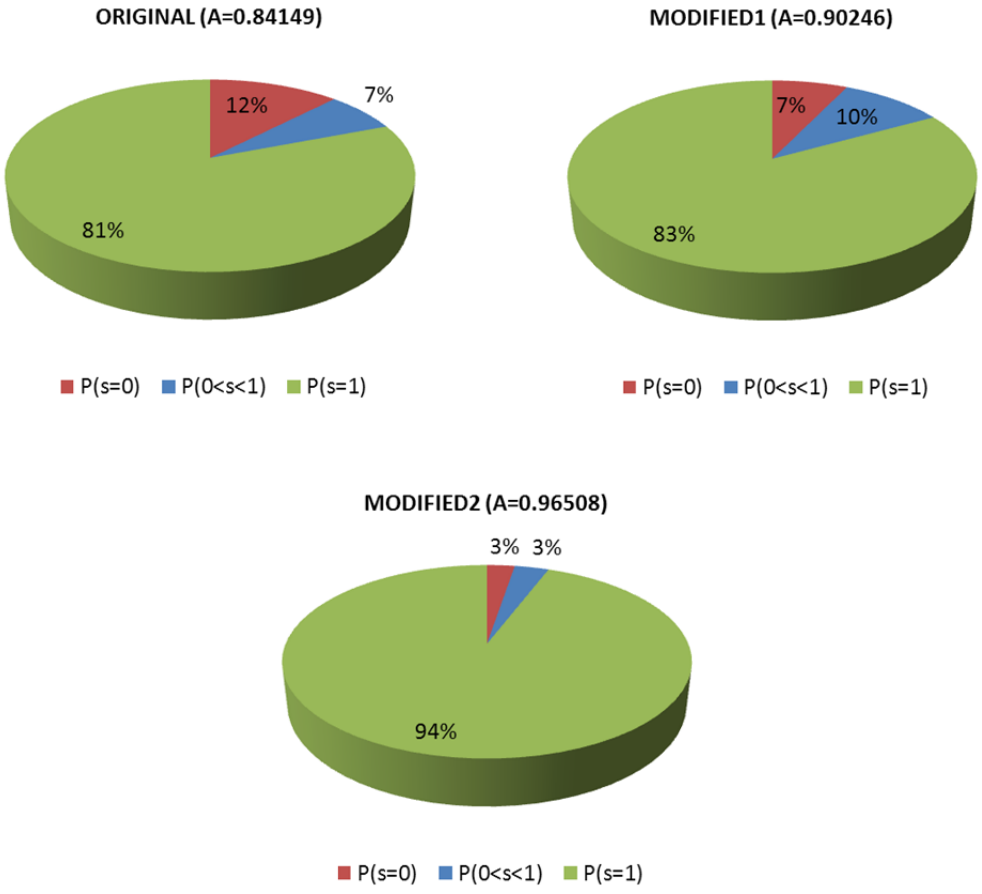

Figure 10-12: Distribution of probability of s_i – MCRP08-2B

In this case, probability of s=0 has decreased by 78.6% to an insignificant 3%, while probability of s=1 has increased to 94%

As demonstrated in figures 10-11 and 10-12 the contribution of the side casings towards increased survivability is unquestionable. The probability of no residual stability has decreased dramatically to 4% in the case of EUGD01-R1 and to an almost insignificant 3% for MCRP08-2B. The Index-A has subsequently increased from 0.85734 and 0.84149 to 0.93546 and 0.96508 for EUGD01-R1 and MCRP08-2B respectively. The contribution of side casings, even in their smallest possible for which is the first modified version of MCRP08-2B, can be seen in the relevant chart in figure 10-12. Although the probability of s=1 is very lightly changed by just 2%, the probability of s=0 has decreased to almost half, given the minor impact of such a configuration on a RoPax vessel.

Another important contribution of the side casings is the additional buoyancy that they provide, that helps to alleviate the massive loss of buoyancy caused by the flooding of the LLH, thus limiting its negative impact on survivability. As displayed in figure 10-13, the contribution of the LLH to no residual stability cases reduces to 2% or less. This way their commercial benefit can be fully exploited to increase the ro-ro lanes, way more than with any conventional design.

Finally, figures 10-14 through to 10-18 demonstrate graphically the distribution for conditional probability to capsize within 30 minutes given loading condition and damage extend. The improvement is apparent in the modified vessels where no damages result in s=0 up to 3-compartments and even most 4-compartment and 5-compartment damages have s>0, compared to the original designs when even some 2-compartment damages result in s<1.

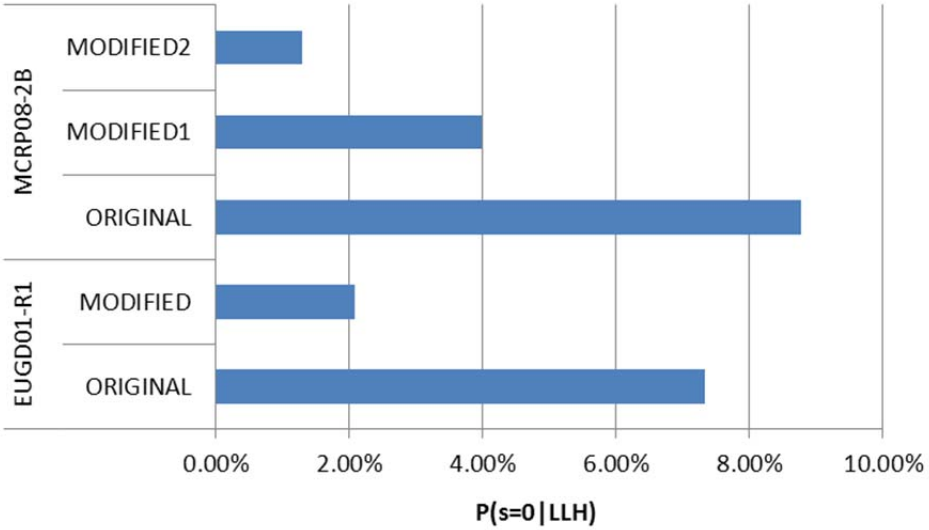

Figure 10-13: Probability of s=0 given the LLH is flooded

The probability of zero residual stability in case the LLH is flooded is massively reduced following the installation of the side casings. This is because the side casings' additional buoyancy compensate for the floodwater in the long lower hold

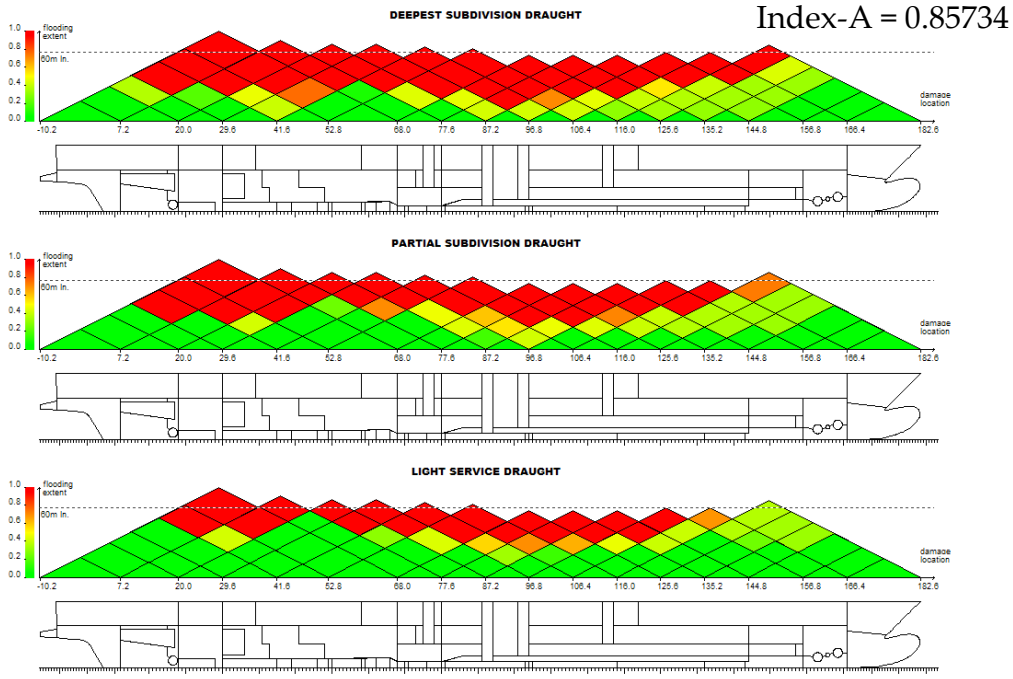

Figure 10-14: EUGD01-R1 (Original) – Distribution of conditional probability for time to capsize

Even some 2-compartment damages result in s<1 in deepest draught.

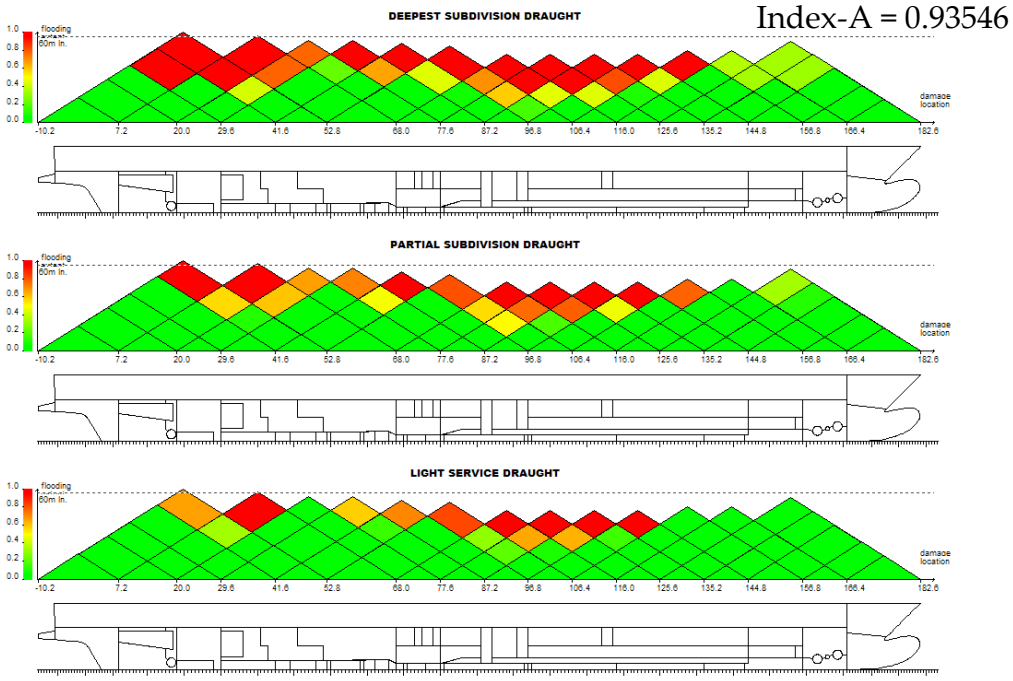

Figure 10-15: EUGD01-R1 (Modified) – Distribution of conditional probability for time to capsize

In its modified alternative, all 2-compartment damages result in s=1, while even most 4-compartment damages result in s>0

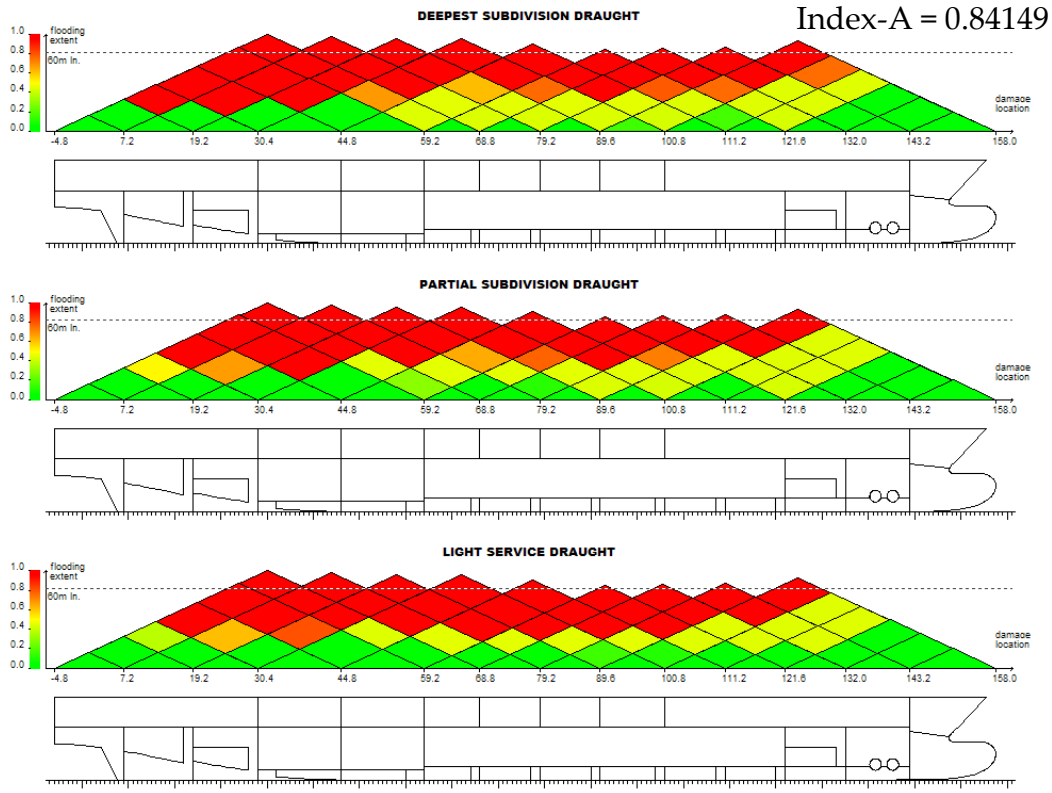

Figure 10-16: MCRP08-2B (Original)

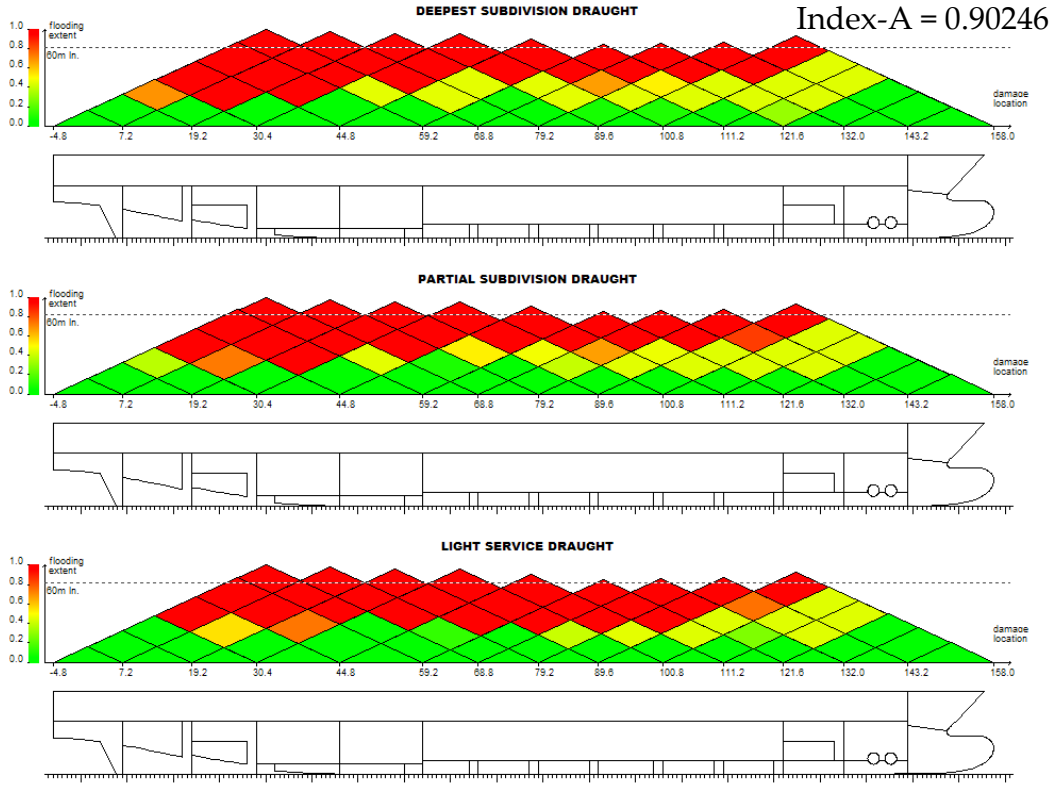

Figure 10-17: MCRP08-2B (Modified 1)

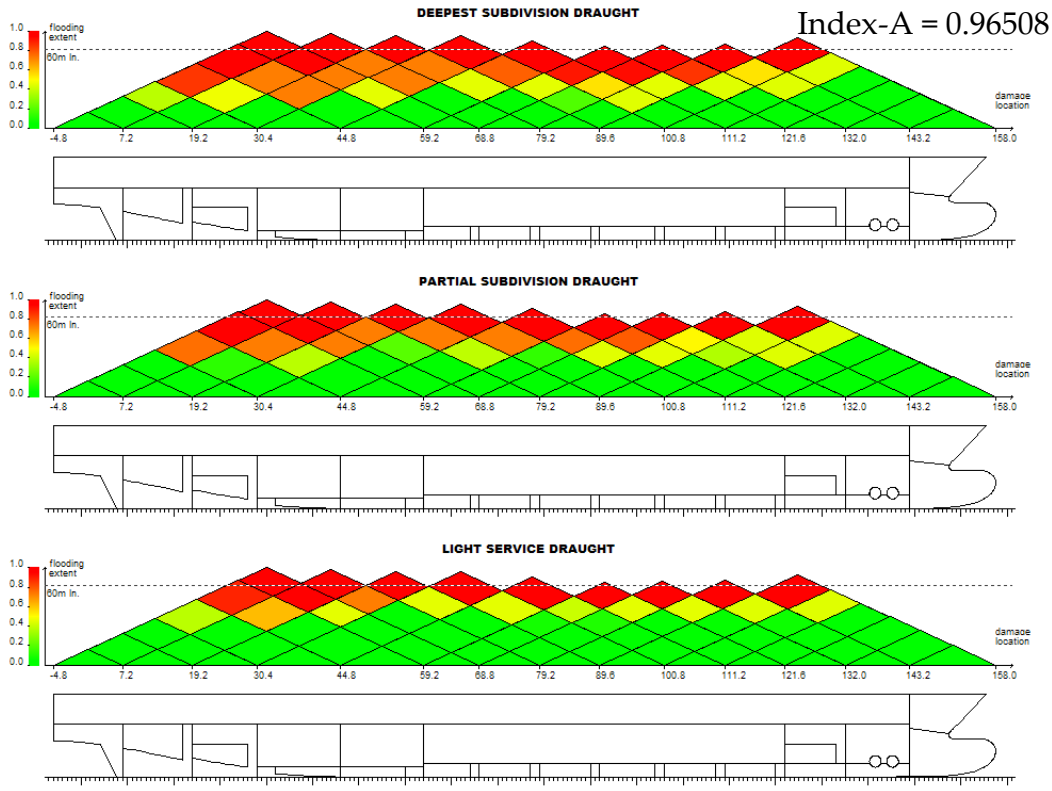

Figure 10-18: MCRP08-2B (Modified 2) – distribution of conditional probability for time to capsize

The probability to capsize reduces dramatically with the application of both the external and internal side casings in Version 3 of this vessel in all loading conditions. The vessel demonstrates enough stability to withstand all 3-compartment damages and even 4 and some 5-compartment damages.

10.4.3 Individual cases

The effect of the side casings has also been studied on an individual damage basis in order to show how exactly they benefit stability of specific damages. To this end, some damages have been generated identically for the original and the modified version and their hydrostatic properties were obtained.

EUGD01-R1 P5-6

2D Hydrostatic Calculations (Geometry file 'r1_l5.sus').

P5-6 without side casings:

```
 Ship's name      EUGD01-R1

Kxyz
 Lpp..............   174.800 [m]
 Breadth...........    25.000 [m]
 Draught...........     6.600 [m]
 Mass.............. 17488.324 [t]
 CGs..............    -5.541   0.000000     12.330 [m]

 Ship Damaged (Damage file 'r1_p5-6.dam')
 Flooding compartments:  R332 R333 R411 R453 R462 R502 R504 R506 R507 R508 R603 R604
R605 R607 R608 R609 R610
 No free surface effects considered

Oxyz
 Up-right/No-sinkage condition:
 GMT..............     2.206 [m]
 GML..............   420.886 [m]
 WPA..............  3803.305 [m2]
 Displ.............. 17488.324 [t]
 CB..............    -5.541   0.000000     -2.760 [m]

 After Equilibrium Reached condition:
 GMT..............     1.852 [m]
 GML..............   516.831 [m]
 WPA..............  3432.562 [m2]
 CB..............    -5.541  -0.000000     -2.994 [m]


  Sinkage[m]   Trim[deg]   Heel[deg]  GZ-Port[m]       TA[m]       TF[m]    Displ[t]
      -0.891      -0.426      -6.193   -0.000000       8.027       6.728   17488.324
```

P5-6 with side casings:

```
Ship's name      EUGD01-R1

Kxyz
 Lpp..............   174.800 [m]
 Breadth...........    25.000 [m]
 Draught...........     6.600 [m]
 Mass.............. 17488.324 [t]
 CGs...............    -5.541   0.000000     12.330 [m]

 Ship Damaged (Damage file 'r1_sc_p5-6.dam')
 Flooding compartments:
 No free surface effects considered

Oxyz
 Up-right/No-sinkage condition:
 GMT...............     2.206 [m]
 GML...............   420.886 [m]
 WPA...............  3803.305 [m2]
 Displ.............. 17488.324 [t]
 CB................    -5.541   0.000000     -2.760 [m]

 After Equilibrium Reached condition:
 GMT...............     1.988 [m]
 GML...............   517.082 [m]
 WPA...............  3457.951 [m2]
 CB................    -5.541  -0.000000     -3.000 [m]


  Sinkage[m]   Trim[deg]   Heel[deg]  GZ-Port[m]       TA[m]       TF[m]    Displ[t]
      -0.874      -0.419      -6.182   -0.000000       8.000       6.723   17488.324
```

Note the higher GM value in flooded condition (denoted as *GMT* in "after equilibrium Reached" section) for the side casing version

The GZ curves of the two versions can be seen in figure 10-19. The side casings increase the GZ lever values in damaged condition, offering far greater values of GZ_{MAX} and Range than the original vessel's values. In this case the side casings were not getting submerged in damage equilibrium which means that the vessel would also have an equilibrium without them but its survivability in waves would be lower thus resulting in lower s-factor value for this damage case. This is not always the case as the side casings could also make the difference for a case that would sink soon after breach due to lack of sufficient buoyancy as happens in the following case examined.

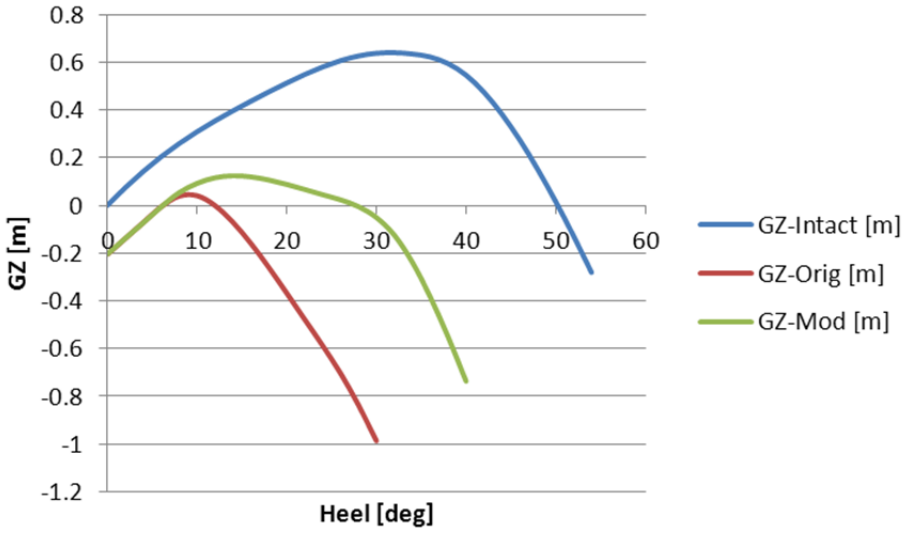

Figure 10-19: Comparison of GZ curves for R1 original and modified (SC) version for damage case P5-6

This is shown as an example of how the side casings can enhance the stability of a damage case so the vessel can survive more severe sea-states

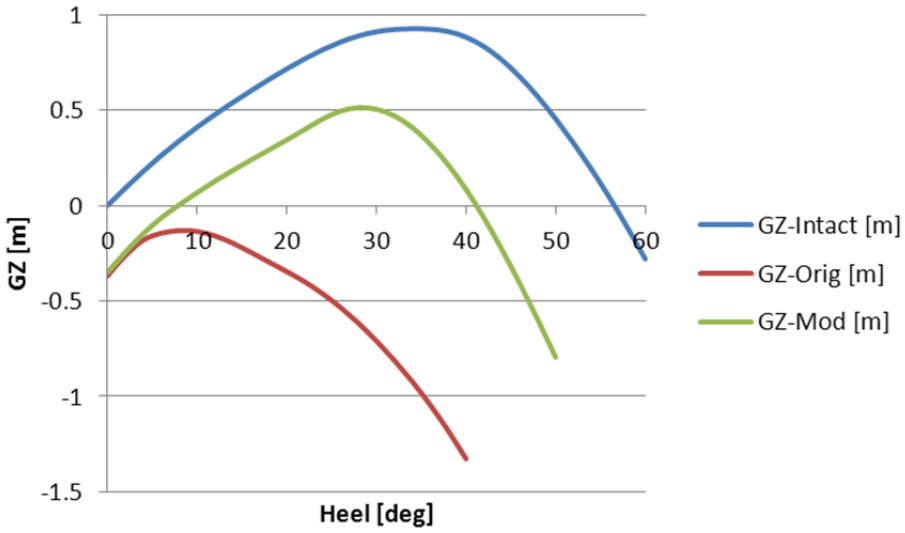

Figure 10-20: Comparison of GZ curves for R1 original and modified (SC) version for damage case P8-9

This damage case is shown as an example of the side casings rendering an otherwise lost scenario to a survivable one

EUGD01-R1 P8-9

In this damage case the LLH is flooded which results in loss for the original vessel, simply due to lack of buoyancy. With the application of the side casings the vessel reaches equilibrium, albeit with a large heel angle, and in addition the resulting stability characteristics suggest that the vessel can easily sustain even severe sea-states without problem. The resulting hydrostatic values from the modified vessel are shown below. Note the resulting very high GM value of 2.252m which is similar to the one in intact condition of 2.660m. A comparison of the GZ curves for the original and modified vessel can be found in figure 10-20.

2D Hydrostatic Calculations (Geometry file 'r1_l2.sus').

```
 Ship's name      EUGD01-R1

Kxyz
 Lpp..............   174.800 [m]
 Breadth..........    25.000 [m]
 Draught..........     6.400 [m]
 Mass.............. 16717.320 [t]
 CGs..............    -5.265   0.000000     11.830 [m]

 Ship Damaged (Damage file 'r1_sc[2].dam')
 Flooding compartments:
 No free surface effects considered

Oxyz
 Up-right/No-sinkage condition:
 GMT..............     2.660 [m]
 GML..............   413.030 [m]
 WPA..............  3691.537 [m2]
 Displ............. 16717.200 [t]
 CB...............    -5.265   0.000000     -2.683 [m]

 After Equilibrium Reached condition:
 GMT..............     2.252 [m]
 GML..............   389.918 [m]
 WPA..............  2856.851 [m2]
 CB...............    -5.265   0.000000     -3.334 [m]


  Sinkage[m]   Trim[deg]   Heel[deg]  GZ-Port[m]       TA[m]       TF[m]    Displ[t]
      -1.406       1.025      -7.883    0.000000       6.223       9.350   16717.320
```

10.5 Conclusion

Given the apparently quite high survivability of cruise vessels, RoPax vessels cannot possibly be left with such a high deficiency. The most important step is to locate and quantify a problem in order to solve it. Now that the methods exist to measure objectively the level of risk from flooding built into each and every design individually, the designers can produce as safe a vessel as they will. Undeniably, thinking out of the norm would have someone wondering which is the big difference between cruise and RoPax vessels that leads to such great difference to survivability. The answer is obviously subdivision. Thus the next step is to try to incorporate additional subdivision into the RoPax vessels. In the previous it was demonstrated how vulnerability is indeed massively decreased by additionally subdividing the car deck. The side casings, as this form of subdivision has been named, have the potential to not only enhance the safety of damage cases to withstand more severe sea-states but also to provide with the necessary buoyancy to withstand much bigger damages and the flooding of large spaces inside the vessel that would otherwise lead to rapid sinking. The overall vulnerability of the studied vessels was massively reduced by even 75% in some cases to levels as low as 3% in 30 minutes – a level directly comparable to that of cruise vessels. This would reduce the frequency of a major accident from once every 10 years which is now to once every 100 years. They provide with the added flexibility to increase the loading space inside the ship and be able to compensate for the lost subdivision with buoyancy elsewhere. They can be designed to be loaded with either small or large vehicles according to the owner's specifications and if done so correctly would not increase the cost of building or operating the vessel.

Chapter 11 – Discussion

11 Discussion

11.1 General

The shift from deterministic to probabilistic regulations and performance-based frameworks for addressing damage stability is arguably a step change in rule making history. The tools possessed by the naval architects are considered for the first time inadequate to address vulnerability. Therefore, it can been stated that for the first time rule making is ahead of technology and even that rule making is what is currently promoting technical advances. SOLAS 2009 is aimed at the right direction but lack of understanding of basic principles and maybe just a little bit of eagerness for harmonisation and urgency, mixed with pressure from an overwhelmed industry led to flawed results. These were identified and revealed even before it came into force and a wave of rethinking was started, leading to major projects for reformulation of the regulation.

Of course, those not in favour of the probabilistic framework for damage stability, found the opportunity to attack the probabilistic concept altogether so the first thing that had to be done was to demonstrate (or even make sure) that the probabilistic framework was indeed the way forward. Work done and presented in chapter 7 "Evolution of Regulation" is aimed at demonstrating exactly this. Specifically it has been shown how deterministic frameworks can, under certain conditions, appear more stringent but they provide no clear measure of a vessel's survivability and can lead to situations where a compliant vessel might have lower survivability than a non-compliant one. In addition they allow for little – if any – innovation since they are experience-based, leaving the industry incapable of handling

modern projects that have no resemblance to the past. For example the innovative designs that were presented in chapter 10, where side casings were introduced to the car deck allowing for a longer lower hold thus increasing the ro-ro lanes while at the same time decreasing vulnerability by 75%, would not be possible under SOLAS '90 due to the 2-compartment standard (albeit the relaxation of the B/5).

Having shown that the future is indeed probabilistic, the probabilistic regulations themselves had to be addressed. The aim of this project was the consequence part of the risk equation which has been defined as probability multiplied by consequence. This is no other than the s-factor in SOLAS 2009 terms. The s-factor was accused of under-predicting the survivability of cruisers while over-predicting the survivability of RoPax vessels. During this study it was actually observed that it is actually neither over-predicting nor under-predicting anything. It was merely inconsistent. Results in chapter 9 suggest that estimation can be under or over predicting according to damage case. Nonetheless, s=1 meant nothing more than that the vessel under the current damage could survive sea-states of at least 4 meters significant wave height for at least 30 minutes which is not very helpful when somebody has to make the decision to abandon ship or not. Towards addressing this deficiency, the physical and numerical tests carried out for the estimation of the capsize rate showed that the time of experiment (or the time of exposure in real life) could alter the critical significant wave height. In simple words, a damage case that leads to s=1 in 30 minutes exposure would have less than that in the long term! By carrying out longer tests it was established that the property of the capsize band, as this was defined in chapter 8, that remains unaffected by time of exposure is its lower boundary. Since this is an asymptote – thus impossible to determine – the wave height at which the

capsize rate is 5% was picked as an adequate engineering approximation for the critical significant wave height. This shift of the critical H_S from the 50% capsize rate to the lower boundary means that when a damage case leads to s=1 the vessel is (with 95% confidence) not going to capsize in waves, given the statistics provided by past research and presented here again in chapter 9, p150. For higher accuracy needed in on-board decision support and time to capsize estimation as presented in chapter 9, p175, the critical H_S can be estimated explicitly. This outcome is considered the missing link between the s-factor (and consequently the SOLAS 2009) and the latest Safe-Return-to-Port requirements suggested by IMO. What was also studied and presented in chapter 9 is the minor, potentially, effect that the shift of the critical wave height would have on Index A, in an attempt to address the industry's concerns that a re-formulation might make the requirement more difficult to attain.

That said, the requirement itself, namely the SOLAS 2009 R-factor, has proved to be inadequate, leading to very high frequency of accidents if it is to be accepted as is. Work done in chapter 6 and seems to be in accordance to research from other major projects running in parallel [9], suggests that the current R-factor is advocating a 10 year standard, which essentially means that a ship will be lost every 10 years, a rather unacceptable prospect by modern standards. What is worse is that this seems to be the reality as well with so many accidents of the recent past to confirm it. Therefore it is suggested that the required index is reconsidered so as to advocate safety rather than hinder it. Research carried out in chapter 6 even suggests that cruise vessels would present no challenge in meeting a higher standard so long as their vulnerability can be measured accurately and is not underestimated since the major factor that is hindering cruisers' safety seems

to be progression of water through unprotected or deliberately left exposed openings through common operational practise as shown in chapter 6. RoPax vessels on the other hand can also meet a high standard with minor modifications as shown in chapter 10.

11.2 Further work

Further research on the critical wave height estimation and time to capsize is deemed necessary. More experiments both physical and numerical would be recommended in order to solidify these results. The ship sample should be increased to include other vessel sub-categories as well as more cruisers which were used scantly during this research. This is not because of lack of material or experiments but solely due to the resistance of those vessels to capsize which made it almost impossible to make an accurate estimation of a full capsize band for the study vessels.

The SOLAS 2009 factors should be studied further in order to limit and if possible eliminate the fact that, due to the very nature of Index A as a summation of products, there can be vessels that meet the standard although they can suffer loss by damaging only 1 compartment. This should be taken care by an increase of the standard.

There is a great deal to be done with respect to optimisation of the subdivision of passenger vessels, like openings in cruisers and watertight arrangement of RoPax vessels. Correct positioning of openings could limit the need for them being closed and subdivision of the car deck of RoPax could create even more ro-ro lanes.

In a technical level, it could be beneficial if the codes used for simulation would be updated to match modern standards. In addition, the technique

used for sampling when the CDFs for time to capsize are sought by means of numerical simulations, namely Monte Carlo sampling, is a generic technique. As such it is not necessarily producing correct results since it can produce a damage with a huge penetration and a huge extent, something that experience has shown is impossible. There is a limited amount of energy in any collision. A technique that would take into account the relation between the various dimensions of the damage opening would produce more reasonable scenarios.

Chapter 12 – Conclusions

12 Conclusions

With respect to the objectives set in the beginning of the project, the observations made within this project have led to the following conclusions:

To evaluate the available first principles and analytical performance-based assessment methods towards identifying the most appropriate for use in this study.

With respect to the first objective, the results are vague. No assessment method is enough to give concrete answers when it comes to ship vulnerability on its own. Each one has its own advantages and disadvantages which makes it prohibitive for solitary use. The most appropriate way forward is a combination of all. Analytical methods such as SOLAS 2009 (Index A) even enhanced with the newer, more accurate, s-factor presented earlier and UGD lack the necessary accuracy but are fast enough for use in large number vulnerability estimations. More accurate methods such as numerical simulations and physical experiments are necessary to make sure that the results are true. Selective testing of some hazard scenarios should provide the required accuracy.

To estimate the level of safety imposed by previous and current regulatory instruments and specifically the adequacy of the required index –R– of SOLAS 2009.

As far as rules and regulations are concerned the observations are clearer. Prescriptive regulations of the past might appear to be more stringent in selective scenarios but are far more inconsistent than goal-based probabilistic approaches like SOLAS 2009. Specifically it was a revelation of some sort that when measured with a performance-based method, the survivability of compliant and non-compliant with SOLAS 90 vessels overlaps. That is a vessel that fulfils the SOLAS 90 requirements could have higher vulnerability than one that does not do so. At the same time the SOLAS 2009 R-factor has been proven insufficient for application to not only the latest mega cruisers carrying thousands of guests but also the smaller Ro-Pax vessels due to their greater numbers and should be revised.

> *To develop and validate a generalised and consistent analytical formulation for evaluating explicitly the vulnerability of passenger ships (Ro-Pax and cruise ships) to collision and grounding and collision damage and to WOD-problem by adopting a Unified Approach that accounts for key design and operational parameters within a probabilistic framework.*

Research towards the reformulation of the SOLAS 2009 s-factor has revealed a number of inconsistencies and misconceptions that prohibited an in-depth understanding of the Index A. Exactly how the index could fit with the latest developments and objectives of the industry like safe return to port was unclear since the current s-factor only implied that a damage scenario that led to s-factor equal to 1 could only survive up to 30 minutes. The shift of the critical significant wave height as presented in chapter 9 has led to a situation where s=1 implies infinite survivability and the s-factor can be linked directly to time to capsize, thus making it the backbone of any probabilistic framework for damage stability that can be used within a performance-based

regulatory instrument. The water on deck problem proved to be a common one to all passenger vessels whether cruisers or Ro-Pax. Although so far it was believed that water on deck is affecting only Ro-Pax vessels, the simulations and physical experiments showed that cruisers can too accumulate water above the water line through unprotected openings and central corridors leading to dramatic reduction of residual stability. The reduction of stability is proportionate to the volume that is flooded in equilibrium position and this has been incorporated in the proposed s-factor explicitly. Vulnerability of passenger vessels to grounding damages has also been proven to be of a similar order to collision damages because of the higher frequency of occurrence and needs to be addressed within a performance-based framework. Unlike survivability of collision damages, that of grounding damages is unaffected by sea-state. That said, the proposed s-factor can be used to measure the survivability of those since it encompasses the intact volume which is the only important parameter in a grounding event.

To elucidate this vulnerability in the design and operation of typical ship designs and operational profiles.

Extensive parametric studies carried out and presented in chapter 6 have demonstrated the vulnerability of modern passenger vessels. As mentioned previously, watertight doors that remain open during operation can present a serious threat to the vessel's survivability, particularly in transient flooding during the first few seconds of flooding. Overall risk from flooding doubles when ship is operated with open doors. Risk from grounding has also proven to be of a similar magnitude to risk from collision although loss

during the initial, transient stage is absent. Loss from grounding seems to be a solely progressive flooding problem.

To undertake parametric studies to develop passive (design) and active means (operational practice) to risk-manage damage vulnerability.

Previous studies as well as studies made during this project have suggested that the vulnerability of RoPax vessels is substantially greater to that of cruisers, mostly due to subdivision – or rather lack of – of space close to the water line. To this end a parametric study has been conducted with the scope to prove that subdivision of the car deck – in the form of side casings – can have a massive impact on the survivability of this type of ship. Studies have suggested that the overall vulnerability of the studied vessels was reduced by even 75% in some cases to levels as low as 3% in 30 minutes – a level directly comparable to that of cruise vessels which would reduce the frequency of a major accident from once every 10 years currently, to once every 100 years. At the same time, ro-ro lanes can be increased by fully exploiting the benefits of a lower hold since side casings can provide with the additional buoyancy needed that a long lower hold would deprive a vessel of.

To make suitable recommendations for the design, operation and regulation of passenger ships.

Mostly as a summary of the previous, it can be said that RoPax vessels can achieve high survivability if their ro-ro deck is subdivided and cruisers' survivability is at peril when operated with watertight and semi-watertight

doors open. This might sound like no news but it is commonly admitted and allowed in the industry to do so mostly due to the lack of understanding of what a high risk an operator is taking by such practise. The proposed s-factor can provide a better tool for legislation and regulation. Finally the need to increase the current R-factor of SOLAS 2009 has been revealed.

References

[1] Bulian, G., Francescutto, A.: "Probabilistic modelling of grounding damage characteristics", GOALDS Deliverable, GOALDS_D3 2_DINMA_grounding_final, September 2010

[2] Cichowicz, J., Vassalos, D., Jasionowski, A.: "Experiments on a floating body subjected to forced oscillation in calm water at the presence of an open-to-sea compartment", Proceedings, 12th International Ship Stability Workshop, Washington DC 2011

[3] Cichowicz, J., Tsakalakis, N., Vassalos, D., Jasionowski, A.: "Survivability of passenger vessels – re-engineering of the s-factor", Proceedings, 12th International Ship Stability Workshop, Washington DC 2011

[4] HARDER (1999-2003): "Harmonization of Rules and Design Rationale". Project funded by the European Commission, DG XII-BRITE, 2000-2003

[5] Himeno, Y: "Prediction of ship roll damping – state of the art", Report No 239, University of Michigan, College of Engineering, September 1981.

[6] IMO Resolution 14, "Regional Agreements on Specific Stability Requirements for Ro-Ro Passenger Ships" (Annex: Stability Requirements Pertaining to the Agreement), adopted on November 29, 1995.

[7] IMO Resolution 14, "Regional Agreements on Specific Stability Requirements for Ro-Ro Passenger Ships" (Appendix: Model test method), adopted on November 29, 1995.

[8] Jasionowski, A., Dodworth, K., Vassalos, D.: "Proposal for Passenger Survival-Based Criteria for Ro-Ro Vessels", International Shipbuilding Progress, Vol. 46, No 448, 1999

[9] Jasionowski, A.: "Study of the Specific Damage Stability Parameters of Ro-Ro Passenger Vessels According to SOLAS 2009 Including Water on Deck

Calculations", Final Report, Project No EMSA/OP/08/2009, University of Strathclyde

[10] Jasionowski, A.: "Survival Criteria for Large Passenger Ships", SAFENVSHIP Project, September 2005, Final Report, Safety at Sea Ltd

[11] Jasionowski et al: "Investigation Into The Safety Of Ro-Ro Passenger Ships Fitted With Long Lower Hold Phase 1", UK MCA RP564, 10 July 2007, Draft Report MCRP04-RE-001-AJ, Safety at Sea Ltd.

[12] Jasionowski et al: "Investigation Into The Safety Of Ro-Ro Passenger Ships Fitted With Long Lower Hold Phase 2", UK MCA RP592, December 2008, Report MCRP05-RE-001-AJPB.16, Safety at Sea Ltd.

[13] Jasionowski, A, Vassalos, D.: "Benchmark Study on the Capsizing of a Damaged Ro-Ro Passenger Ship in Waves", Final Report to the ITTC Specialist Committee on the Prediction of Extreme Motions & Capsizing, December 2001.

[14] Jasionowski, A., Vassalos, D., Scott, A.: "Ship Vulnerability to flooding", 3rd international conference for maritime safety, Berkeley, California, 2007

[15] Jasionowski, A.: "An integrated approach to damage ship survivability assessment", University of Strathclyde, 1997-2001.

[16] Jasionowski, A., Vassalos, D., Guarin, L., "Time-Based Survival Criteria for Passenger Ro-Ro Vessels", 6th International Ship Stability Workshop, Webb Institute, 2002

[17] Kat, J de: "Dynamics of a ship with partially flooded compartment", 2nd Stability Workshop, Japan, 1996.

[18] MSC85/INF.2 – FSA – RoPax ships: Details of the formal safety assessment, Submitted by Denmark, 21 July 2008.

[19] MSC85/INF.3 – FSA – Cruise ships: Details of the formal safety assessment, Submitted by Denmark, 21 July 2008.

[20] NEREUS, “First-Principles Design for Damage Resistance against Capsize”: EC Project CONTRACT No. G3RD-CT 1999-00029, 1999-2002.

[21] Papanikolaou, A, Zaraphonitis, G, Spanos, D, Boulougouris, E, Eliopoulou, E.: ”Investigation into the capsizing of damaged Ro-Ro passenger ships in waves”, STAB 2000, Launceston, Tasmania, Australia.

[22] Pawlowski, M.: “Comparison of s-factors according to SOLAS and SEM for Ro-Pax vessels”, Proceedings of the 11th International Ship Stability Workshop, Wageningen, The Netherlands, 2010

[23] Puisa, R., Mohamed, K.: “A critical look At SOLAS Ch. II-1 with respect to floodable length of compartments in passenger ships”, Work Package 3 report, UK MCA Research Project 625, 2011

[24] ROROPROB, “Probabilistic Rules-Based Optimal Design for Ro-Ro Passenger Ships”: EU FP5 RTD Project G3RD-CT-2000-00030, 1999-2002.

[25] SAFEDOR 2007: “Risk Analysis for Ro-Pax”, SAFEDOR Deliverable D4.2.2.

[26] SAFEDOR: "Design, Operation and Regulation for Safety". Integrated Project, www.safedor.org, 2006

[27] Skjong, R., Vanem, E. and Endresen, Ø.: "Risk Evaluation Criteria", SAFEDOR Deliverable 4.5.2, 2007

[28] SOLAS 1990

[29] SOLAS 2009

[30] Tagg, R., Tuzcu, C.: “A Performance-based Assessment of the Survival of Damaged Ships – Final outcome of the EU research project HARDER”, Proceedings of the 6th International Ship Stability Workshop, Webb Institute, 2002

[31] Tsakalakis, N., Puisa, R., Chen, Q.: “A critical look At SOLAS Ch. II-1 with respect to floodable length of compartments in passenger ships”, Work Package 2 report, UK MCA Research Project 625, 2011

[32] Vanem, E, Skjong, R.: “Collision and Grounding of Passenger Ships – Risk Assessment and Emergency Evacuations”, Proc. the 3rd International Conference on Collision and Grounding of Ships, ICCGS 2004, Izu, Japan, Oct 25. – 27. 2004.

[33] Vassalos, D., Jasionowski, A., Tsakalakis, N., York, A.: “SOLAS ’90, Stockholm Agreement, SOLAS 2009 – The false theory of oranges and lemons”, Proceedings of the 10th International Ship Stability Workshop, 2008

[34] Vassalos, D., Jasionowski, A.: “Conceptualising Risk”, 2006, Proceedings of the 9th International Conference on Stability of Ships and Ocean Vehicles

[35] Vassalos, D., Kim, H., Christiansen, G. and Majumder, J.: “A mesoscopic model for passenger evacuation in a virtual ship-sea environment and performance-based evaluation”, Proceedings of the International Conference on Pedestrian and Evacuation Dynamics, 2001

[36] Vassalos, D., Letizia, L.: "Formulation of a non-linear mathematical model for a damaged ship subject to flooding", Sevastianov Symposium, Kaliningrad, 1995.

[37] Vassalos, D., Turan, O.: "A realistic approach to assessing the damage survivability of Passenger ships", Transactions SNAME 1994.

[38] Vassalos, D., Turan, O.: “Development of Survival Criteria for Ro-Ro Passenger Ships - A Theoretical Approach". Final Report on the S0T Ro-Ro Damage Stability Programme, University of Strathclyde, December 1992

[39] Vassalos, D., Turan, O. and Pawlowski, M.: “Dynamic Stability Assessment of Damaged Ships and Proposal of Rational Survival Criteria”, Journal of Marine Technology, Vol. 34, No. 4, pp. 241-269, October 1997

[40] Vassalos, D, York, A, Jasionowski, A, Kanerva, M and Scott, A.: “Design Implications of the New Harmonised Damage Stability Regulations”, STAB 2006, Rio de Janeiro, Brazil. September 2006.

[41] Vassalos, D.: “Safe Return to Port – A Framework for Passenger Ship Safety”, 10th International Symposium on Practical Design of Ships and Other Floating Structures, Houston, USA, 2007

[42] Vassalos, D.: “Shaping Ship Safety: The Face of the Future”, Journal of Marine Technology, Vol. 36, No. 4, 1999, pp. 1-20.

[43] Vassalos, D., Jasionowski, A., Guarin, L.: ”The Damaged Ship”, RINA International Conference, 2011

[44] Vassalos, D., Jasionowski, A., Guarin, L.: “Risk-Based Design: A Bridge Too Far?” Seakeeping and Stability, Osaka, Japan, March 2008.

[45] Vassalos, D., Jasionowski, A.: “SOLAS 2009 – Raising the Alarm”, Proceedings of the 10th International Ship Stability Workshop, 2008

[46] Vassalos, D.: “A Risk-Based Approach to Probabilistic Damage Stability”, Proceedings of the 7th International Stability Workshop, Shanghai 2004

[47] Vassalos, D., Papanikolaou, A.: “Stockholm Agreement – Past, Present, Future (Part 1 & 2)”, Marine Technology, Vol. 39, Part 1: No. 3, July 2002, pp. 137-158, Part 2: No. 4, October 2002, pp. 199-210.

[48] Wendel, K.: “Subdivision of Ships”, Proceedings, 1968 Diamond Jubilee International Meeting – 75th Anniversary, SNAME, New York 1968, paper No 12, 27pp.

[49] Zaraphonitis, G., Papanikolaou, A. and Spanos, D.: "On a 3D Mathematical Model of the Damage Stability of Ships in Waves", STAB 1997, Bulgaria.

Appendix I – Model Drawings

This appendix provides the drawings for the studied vessels

Body Plans

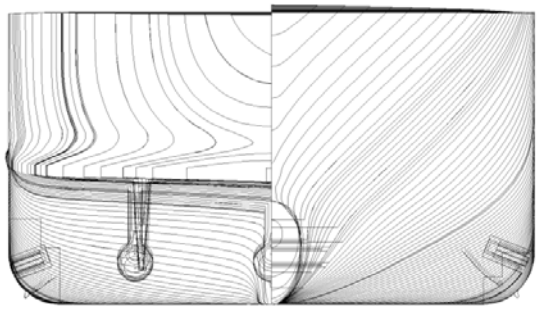

EUGD01-C1

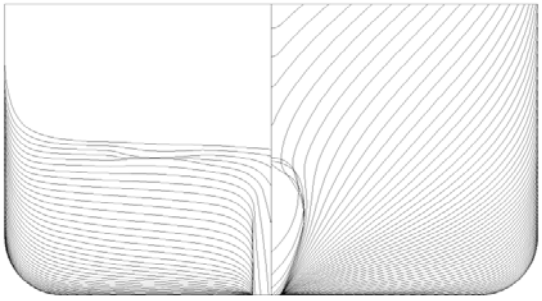

EUGD01-C2

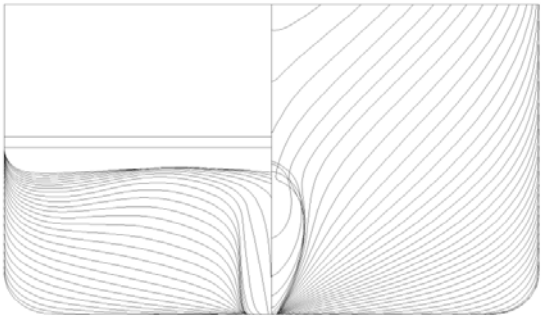

EUGD01-R1

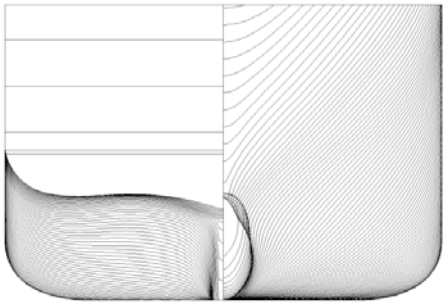

EUGD01-R2

Subdivision of EUGD01-C1

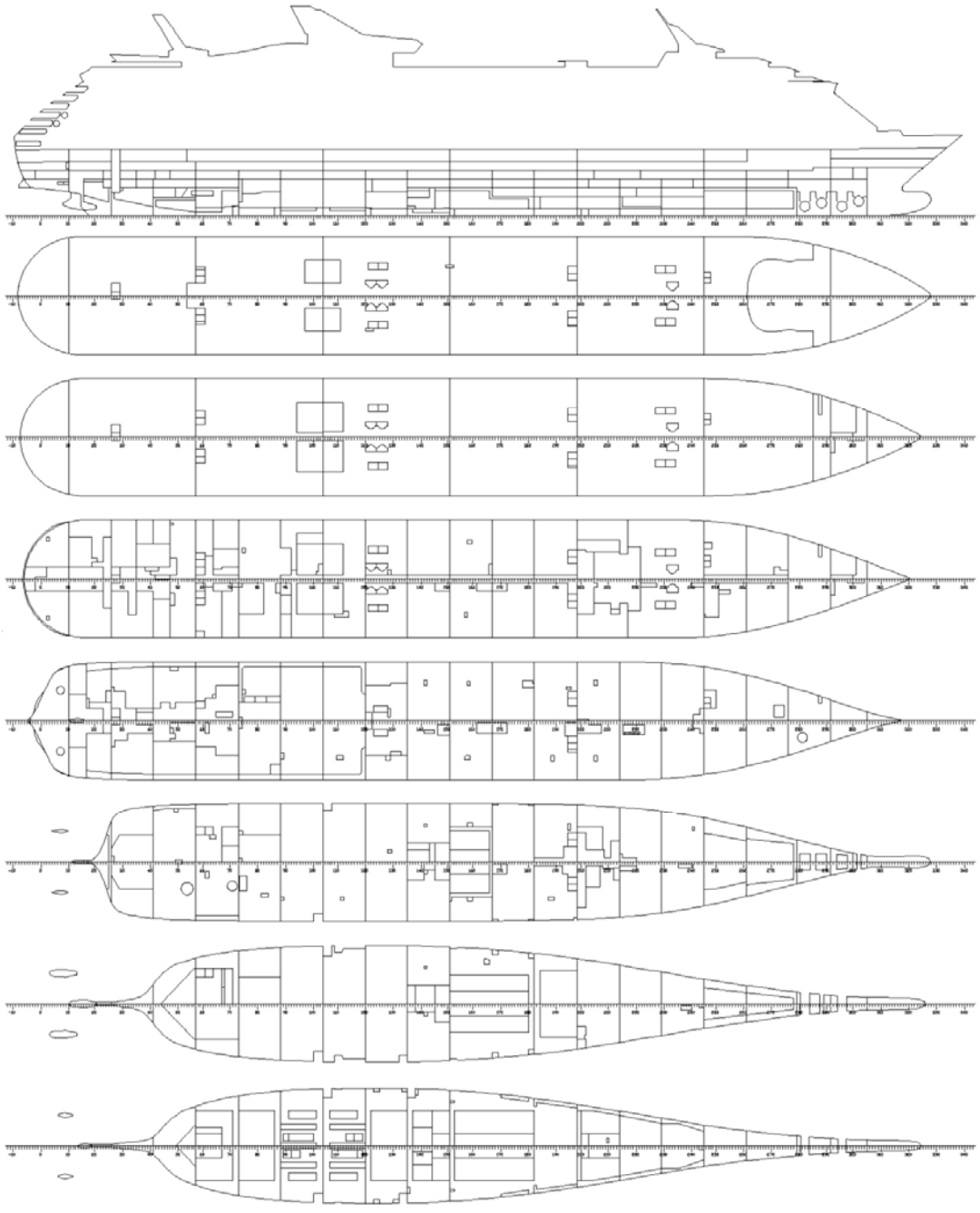

Subdivision of EUGD01-C2

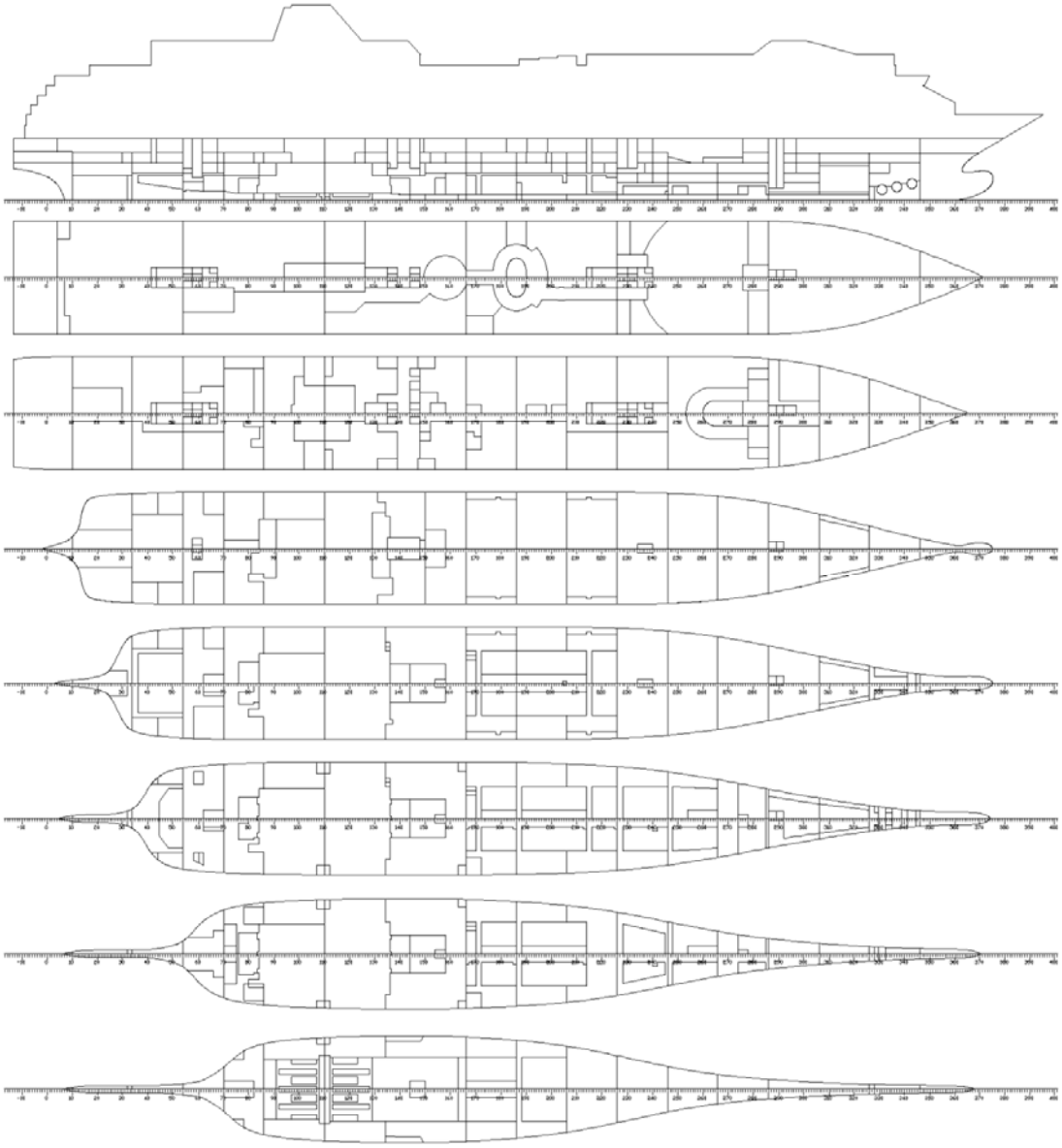

Subdivision of EUGD01-R1

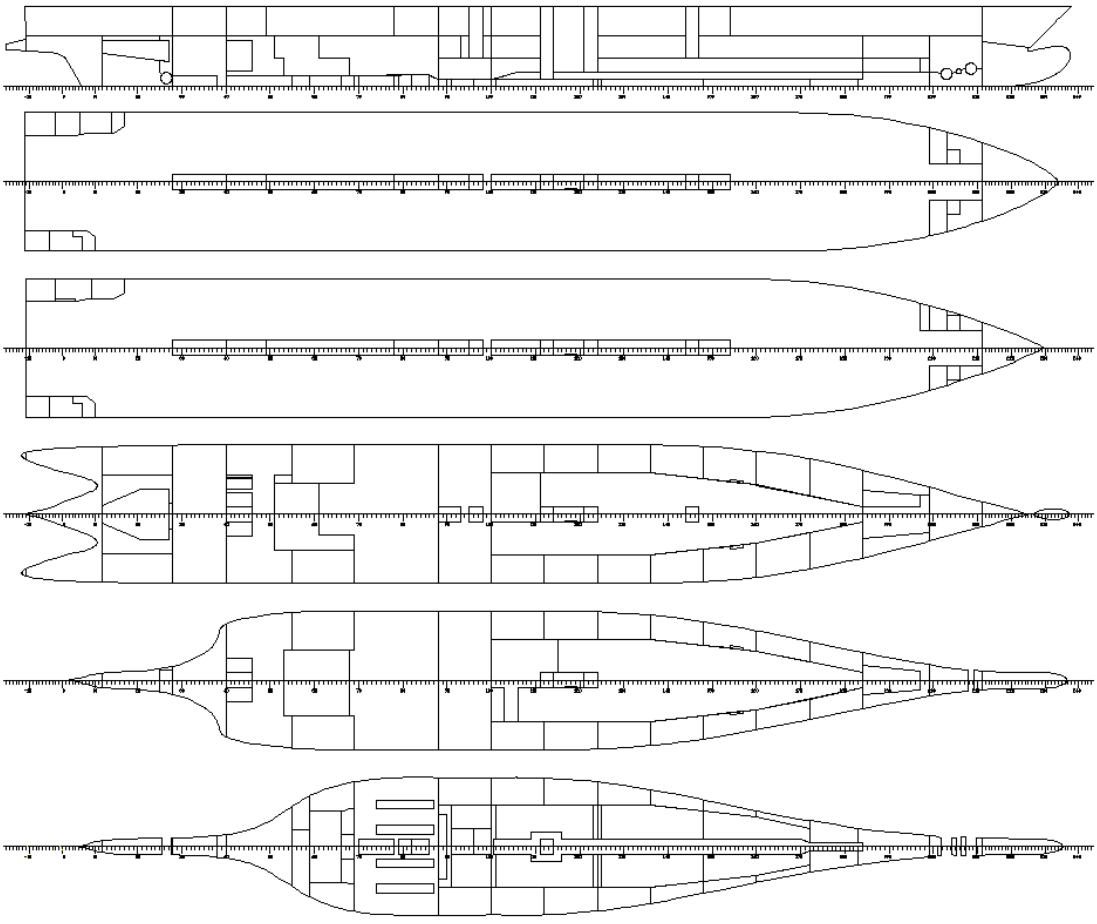

Subdivision of EUGD01-R2

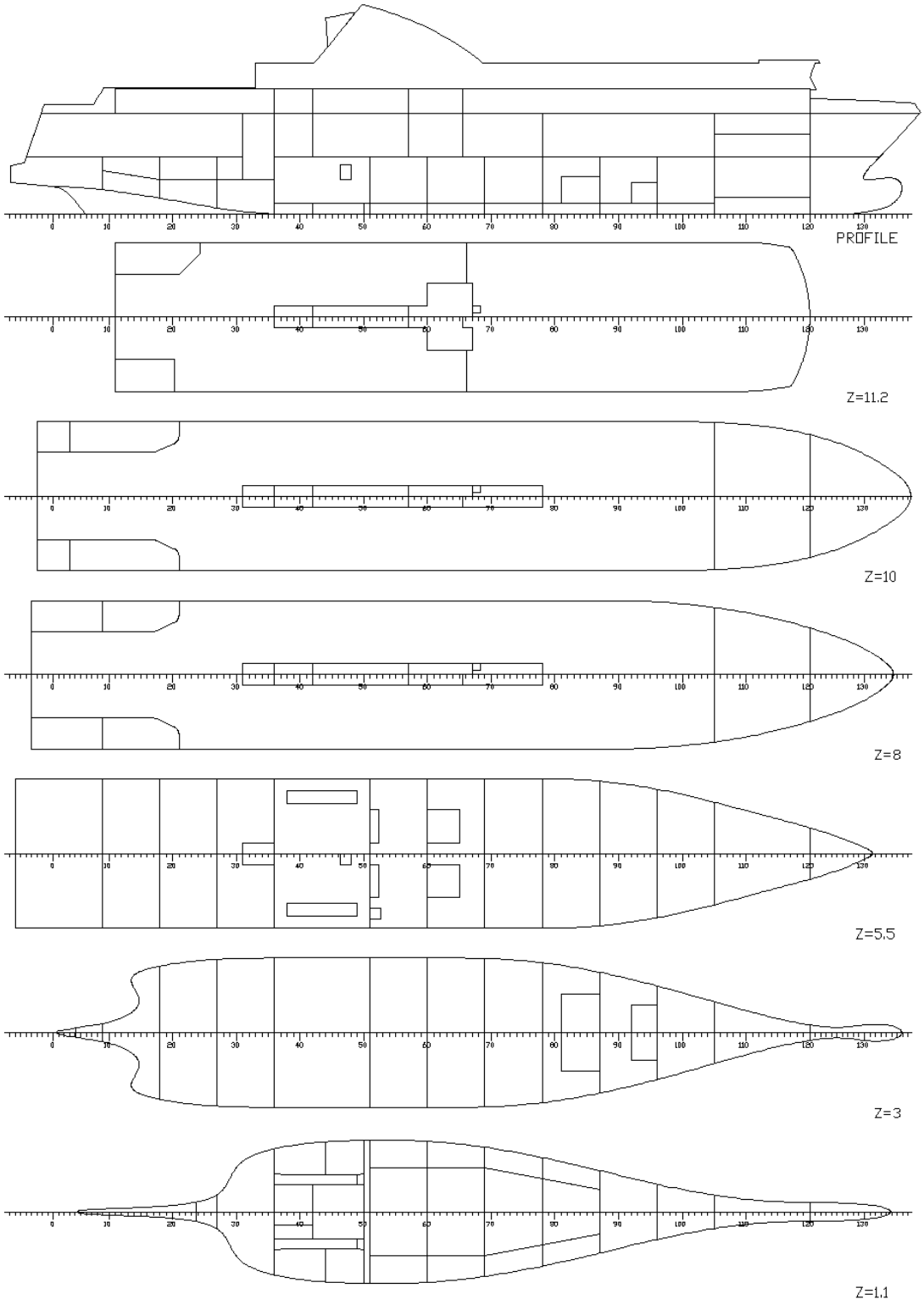

Appendix II – Evacuation completion curves

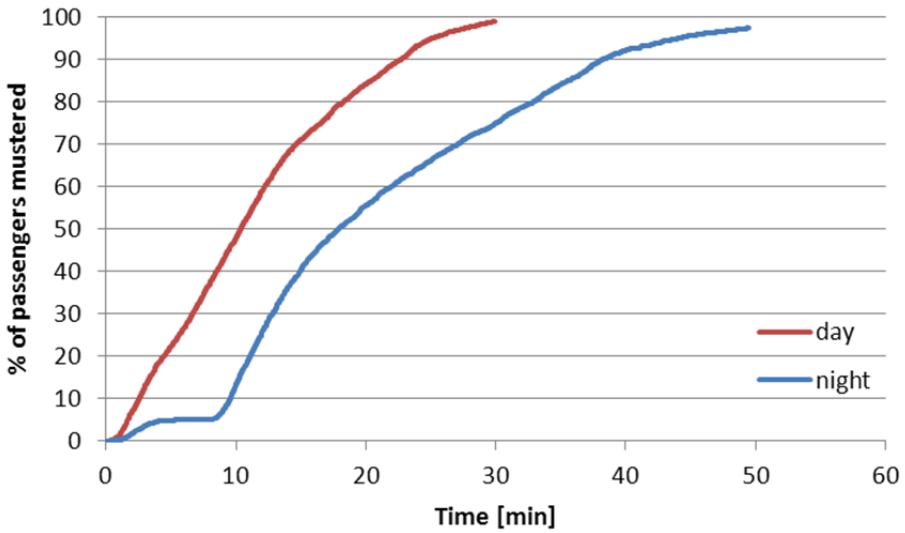

EUGD01-C1

3840 passengers

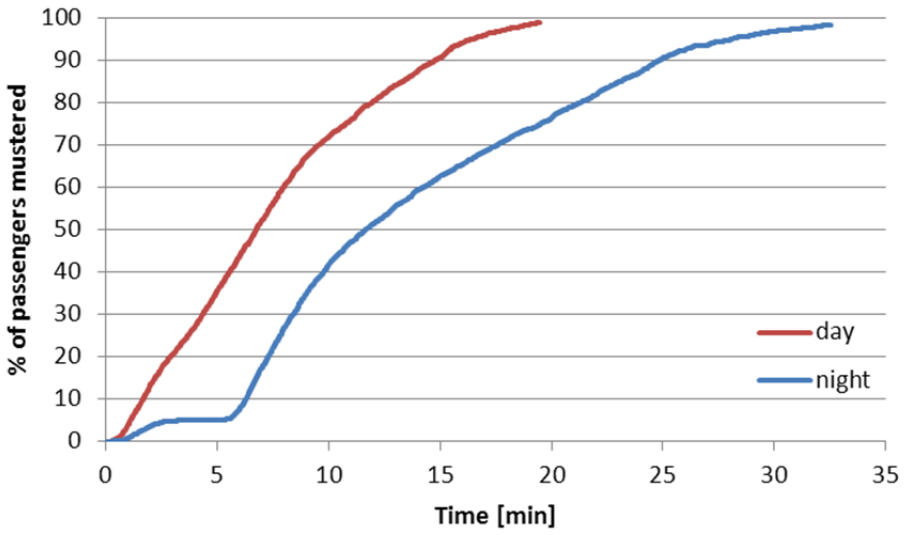

EUGD01-C2

2500 passengers

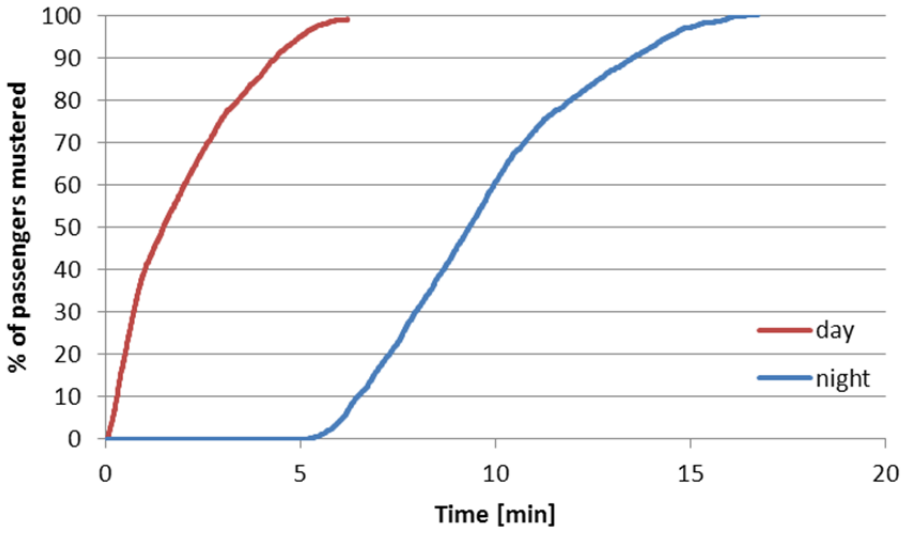

EUGD01-R1

1400 passengers

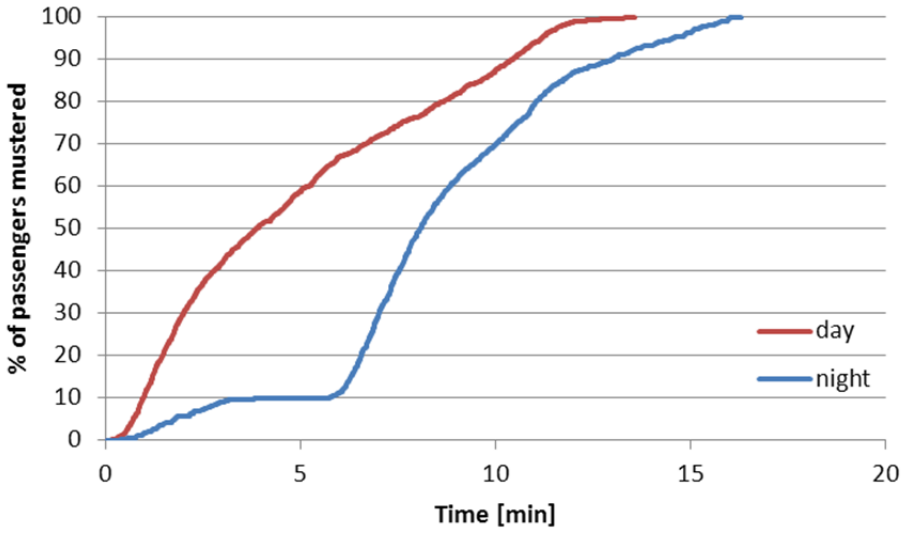

EUGD01-R2

800 passengers

Appendix III: Probability of time to capsize

The following figures show the probability of time to capsize as is given by UGD. Pr_T is the unconditional probability of time to capsize, while pr_T∩D_S,D_P,D_L is the conditional probability of time to capsize *and* loading condition according to SOLAS 2009 mass function for loading conditions (D_S:0.4, D_P:0.4, D_L:0.2). Pr_T|D_S,D_L,D_L is the conditional probability *given* loading condition occurred.

EUGD01-C1: L_{PP}=274.73m, B=38.2m, T_d=8.6m, 3840 passengers

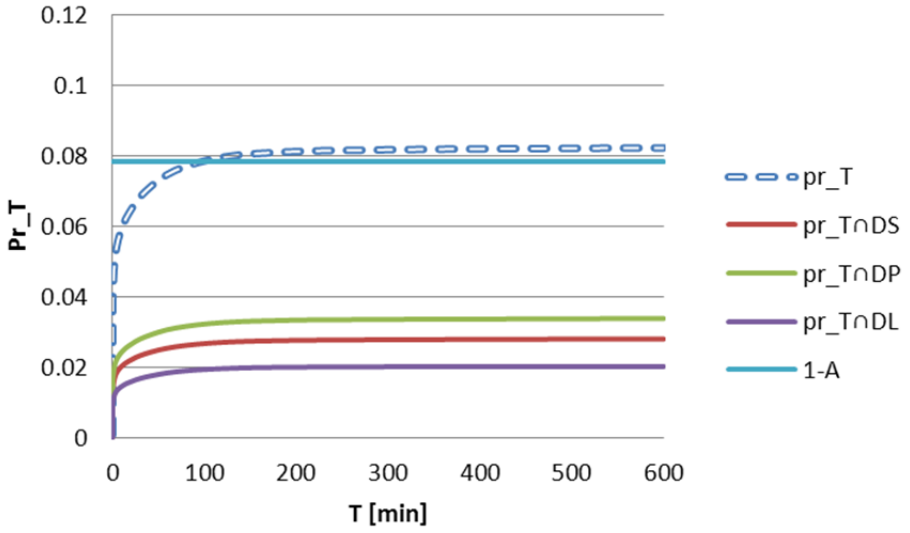

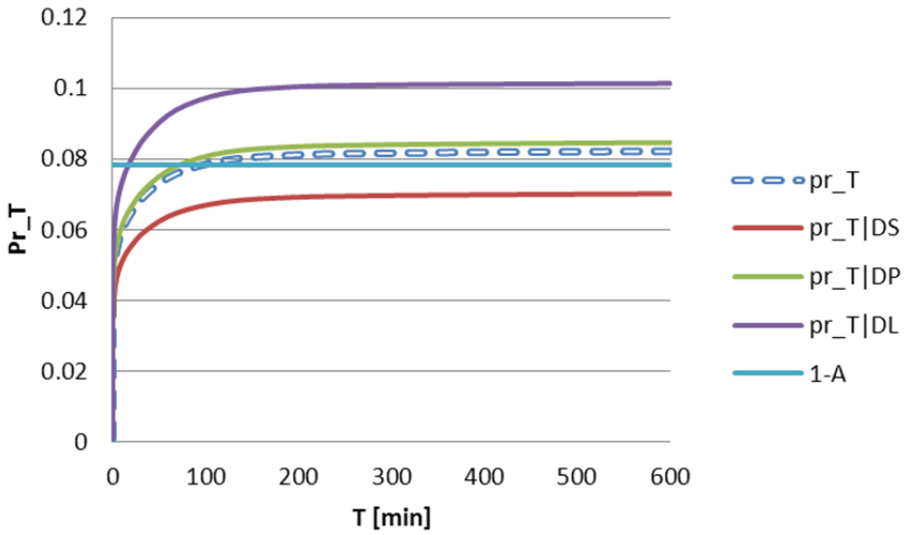

EUGD01-C2: L_{PP}=260.6m, B=32.2m, T_d=7.8m, 2500 passengers

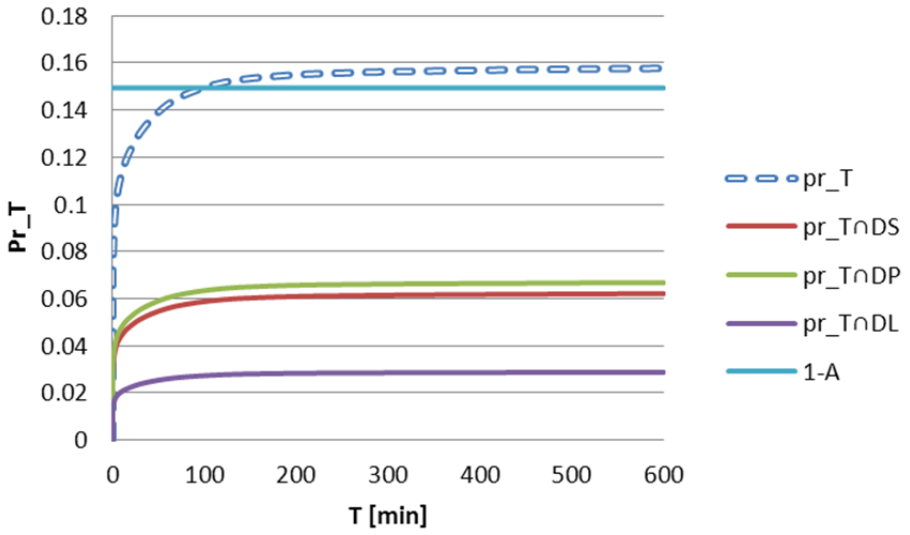

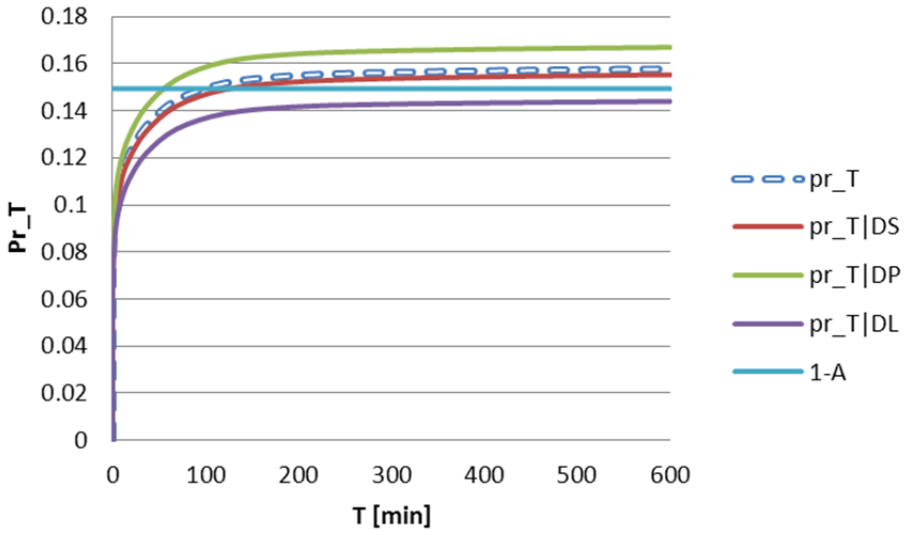

EUGD01-R1: L_{PP}=176.0m, B=25.0m, T_d=6.4m, 1400 passengers

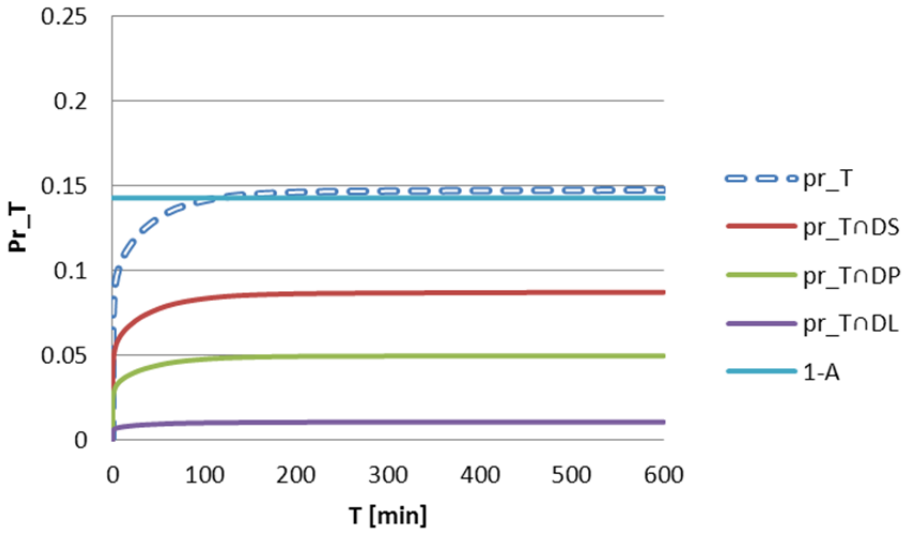

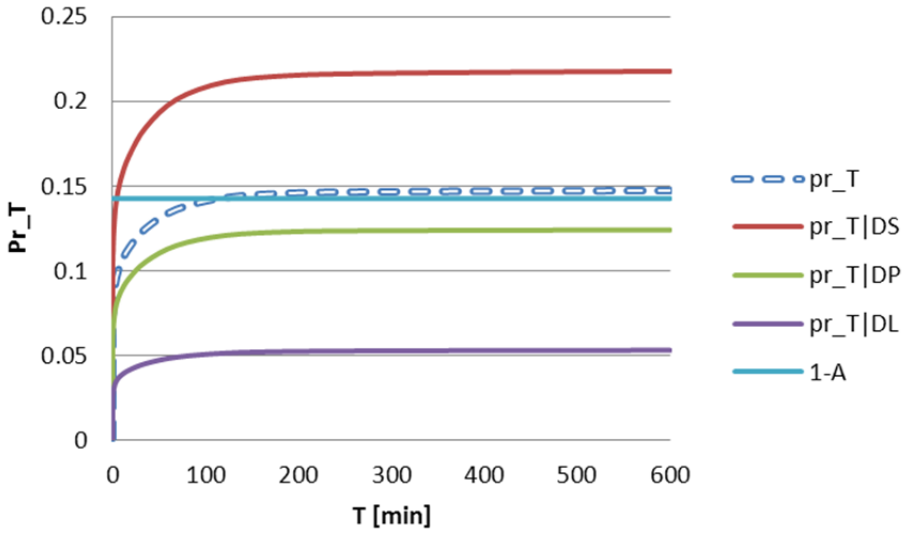

EUGD01-R2: L_{PP}=89.0m, B=16.4m, T_d=4.0m, 800 passengers

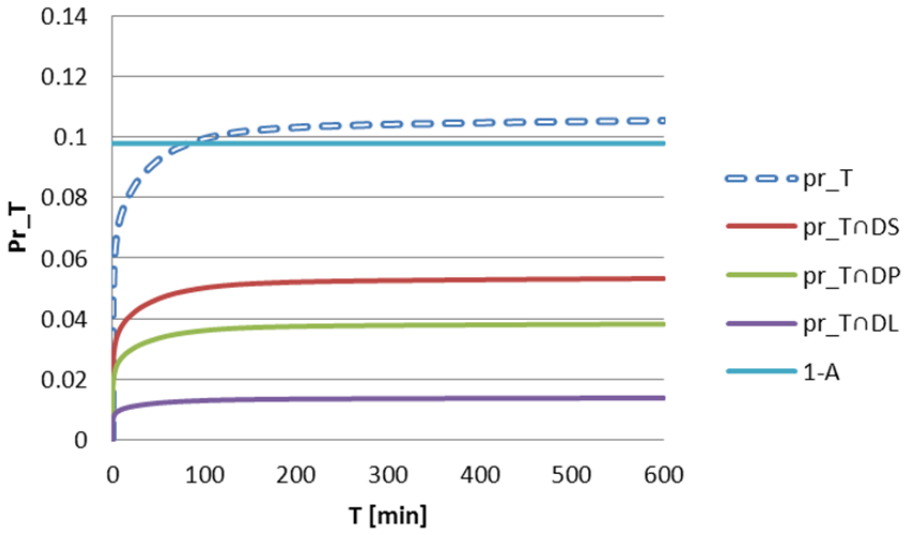

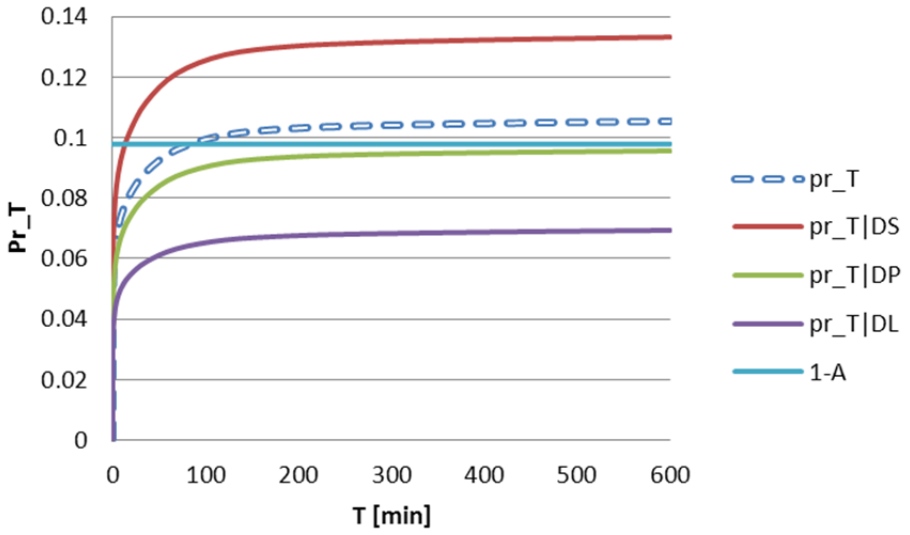

Appendix IV: MC simulations vs. UGD

EUGD01-C1

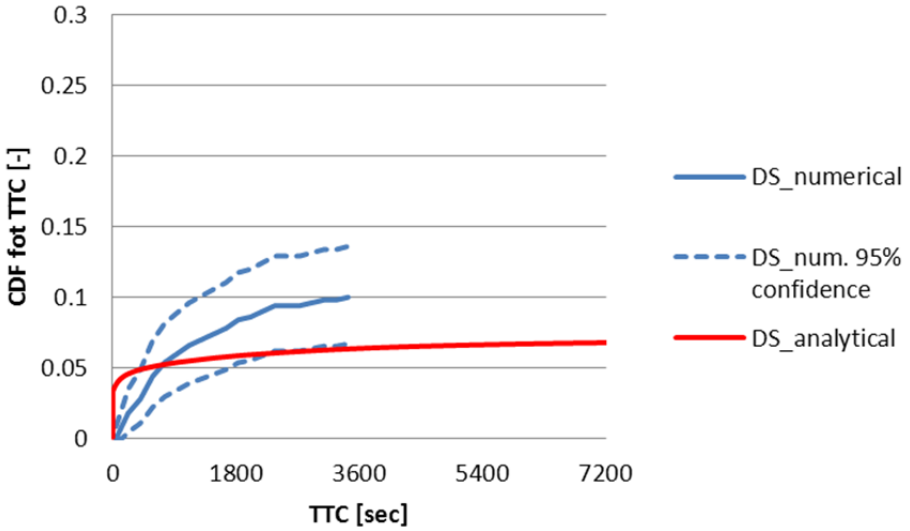

EUGD01-C2

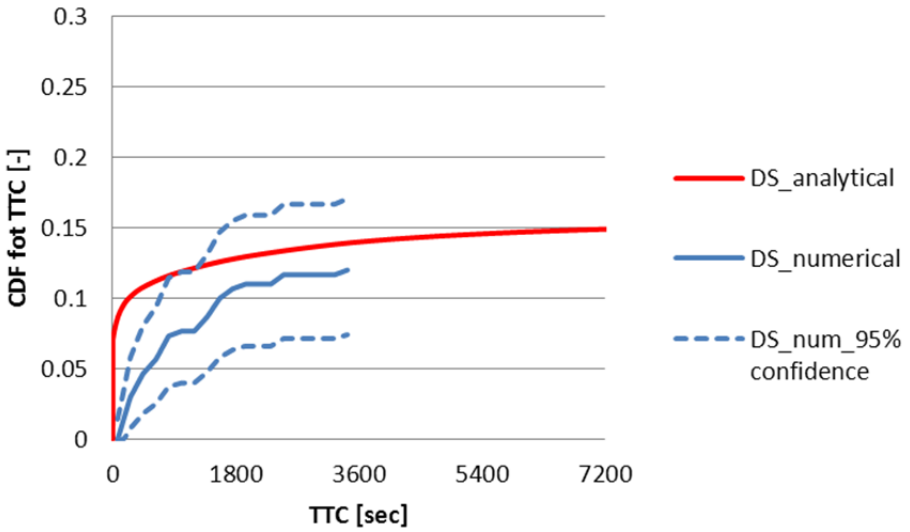

EUGD01-R1

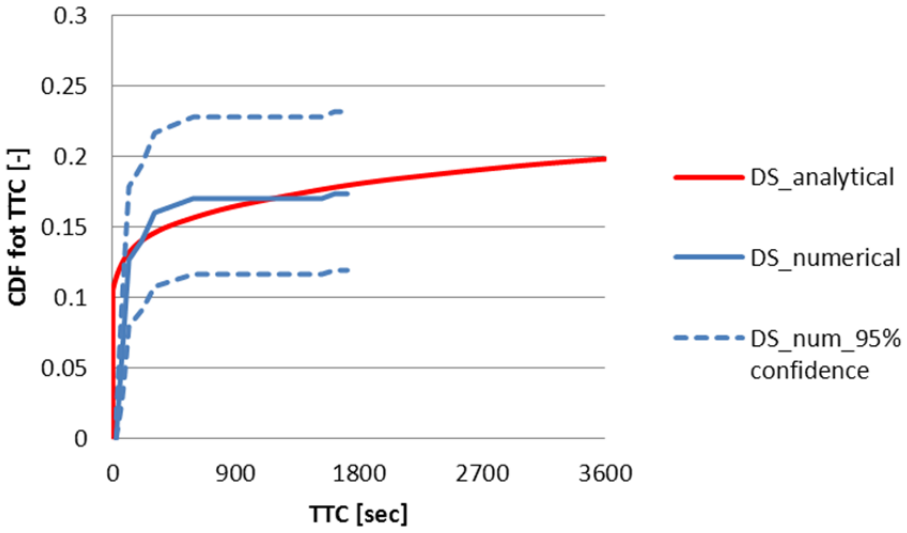

EUGD01-R2

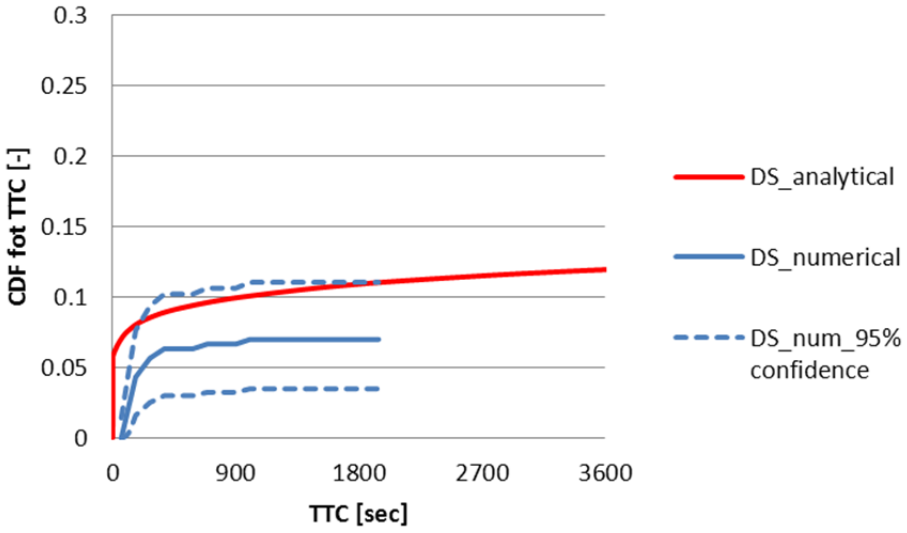

Appendix V: F-N curves

The resulting F-N curves for all the vessels and frequencies can be found in this appendix

Frequency = 1.0E-02

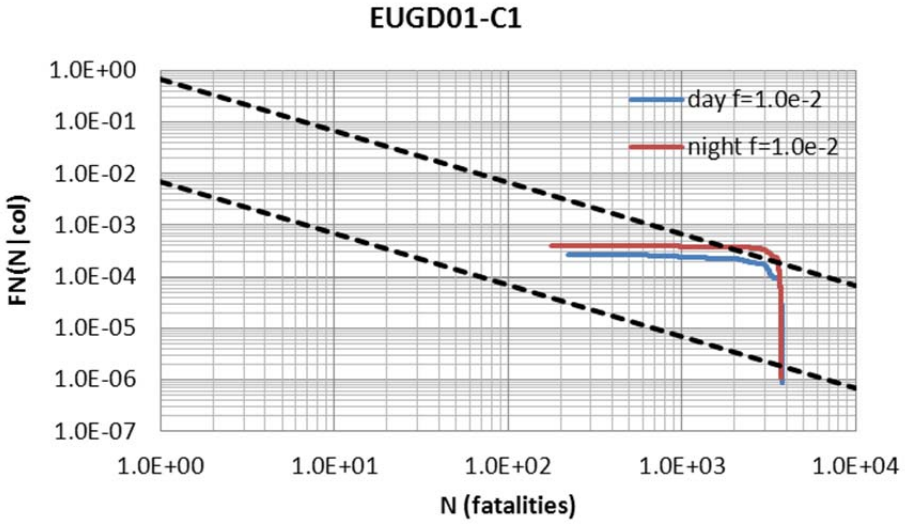

Frequency = 5.0E-03

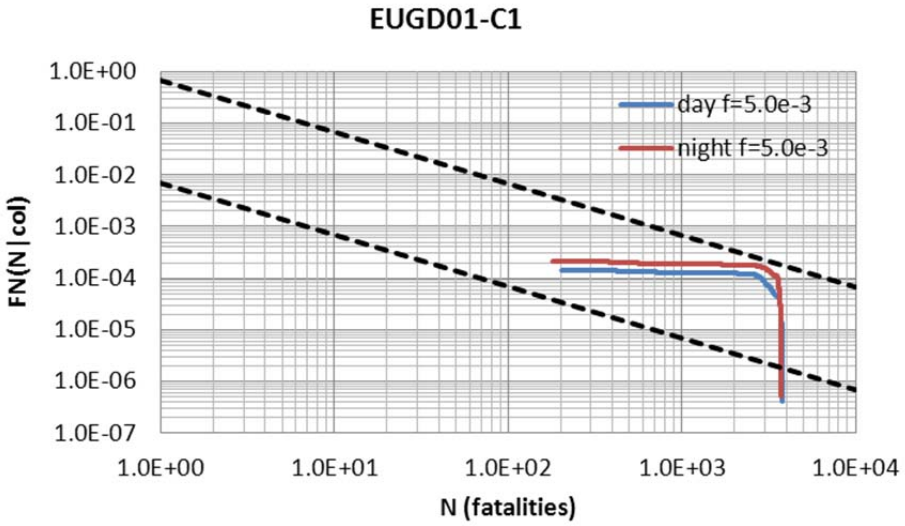

Frequency = 1.0E-03

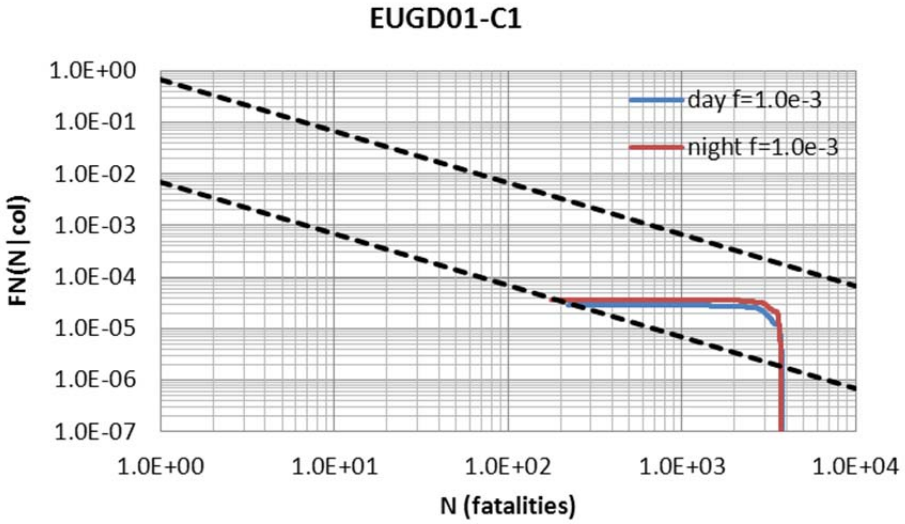

Frequency = 5.0E-04

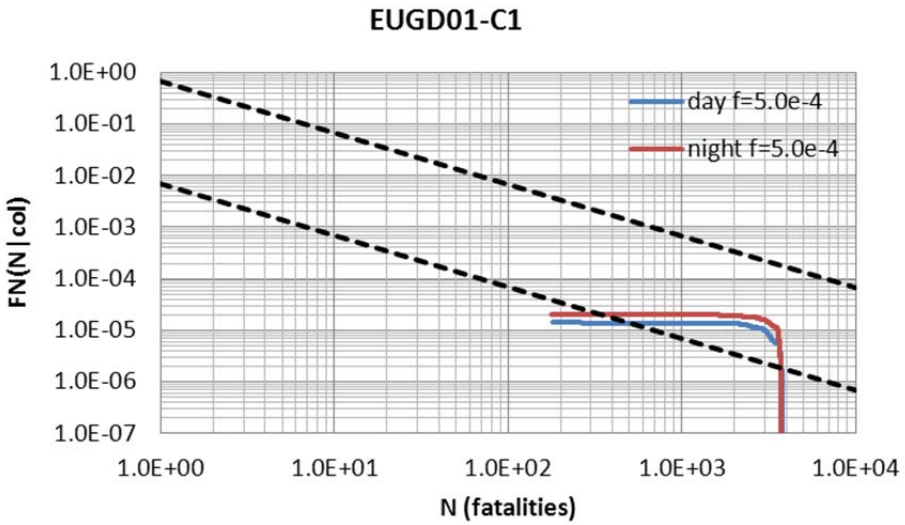

Frequency = 1.0E-02

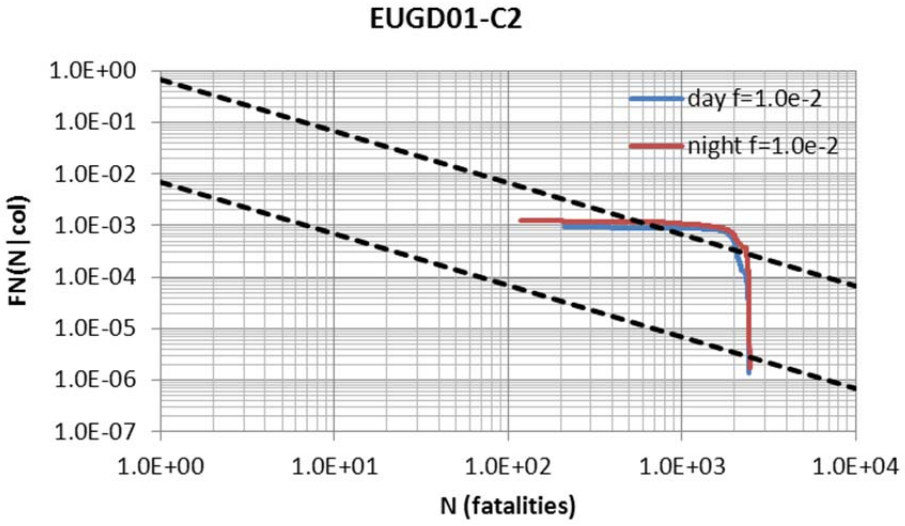

Frequency = 5.0E-03

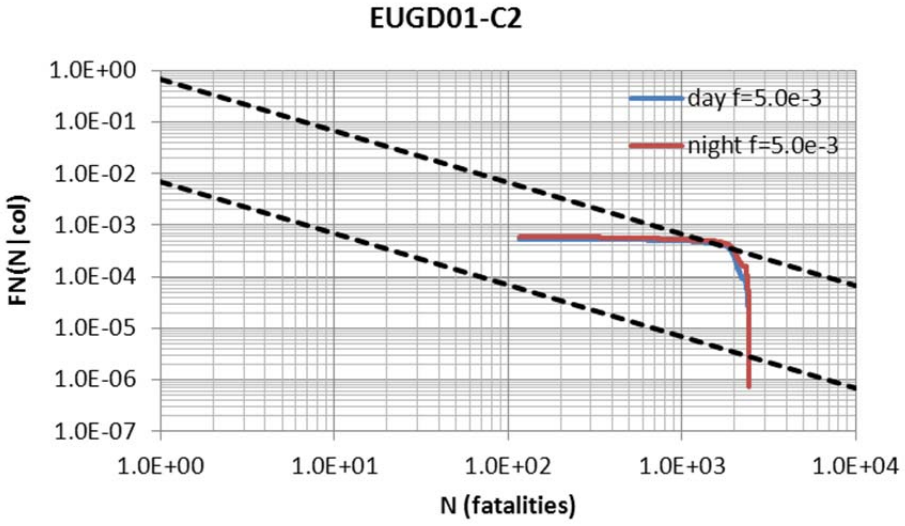

Frequency = 1.0E-03

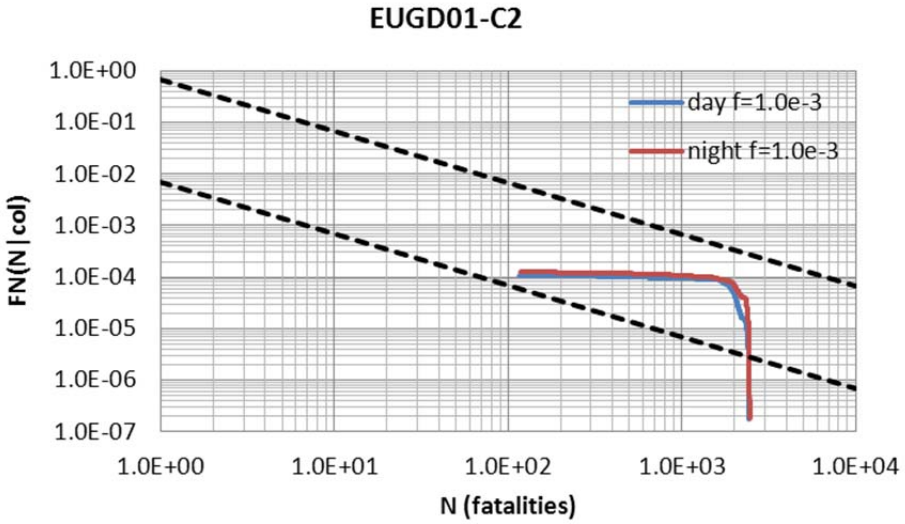

Frequency = 5.0E-04

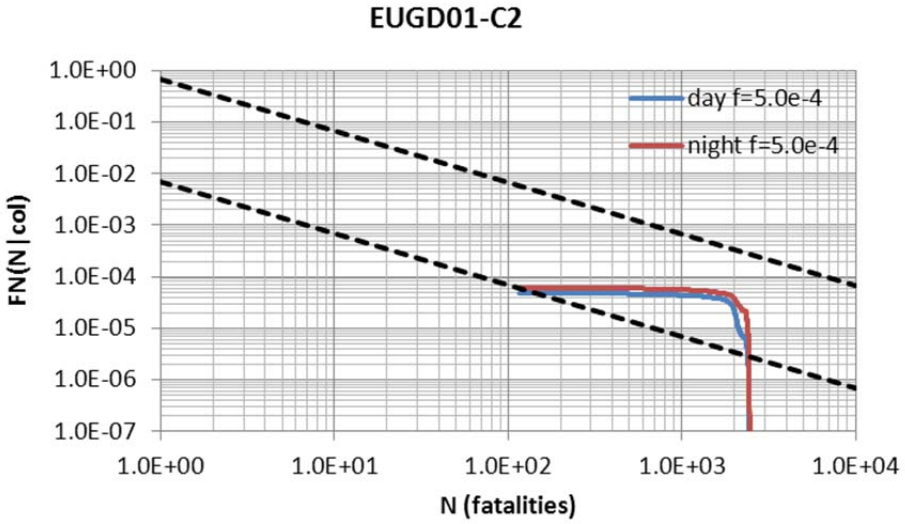

Frequency = 1.0E-02

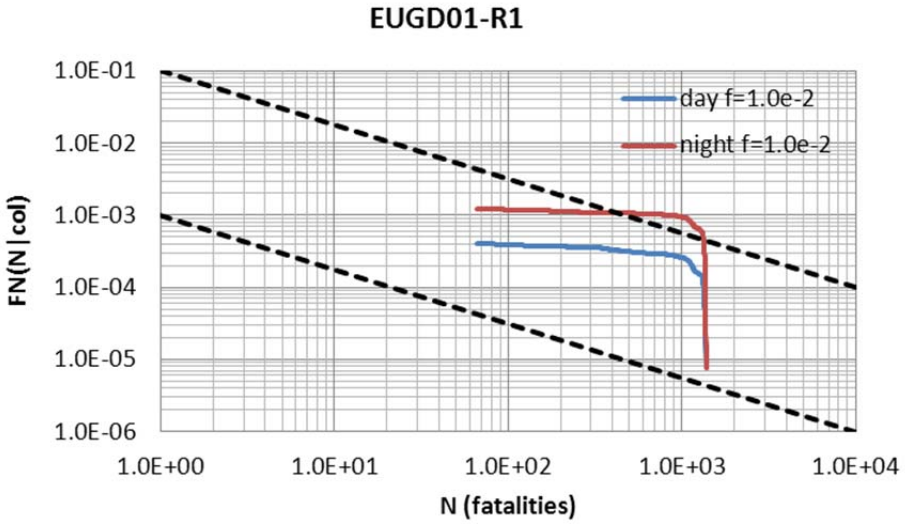

Frequency = 5.0E-03

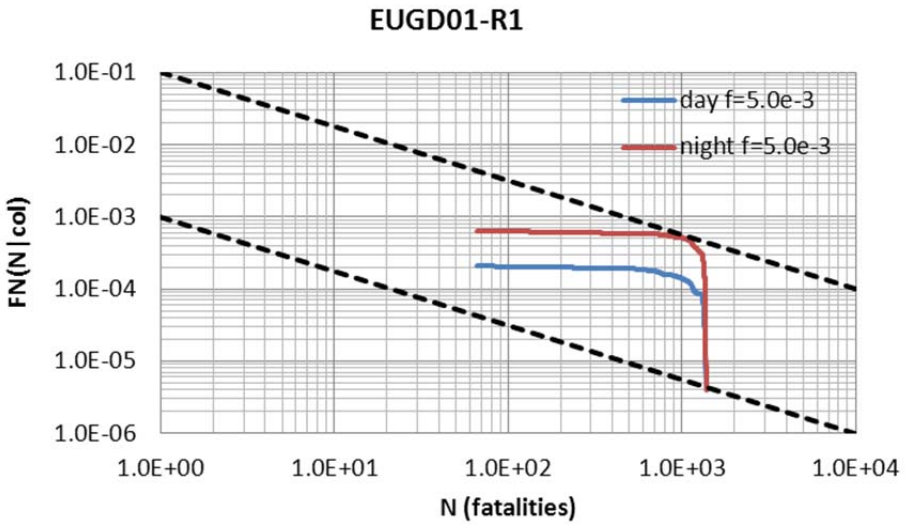

Frequency = 1.0E-03

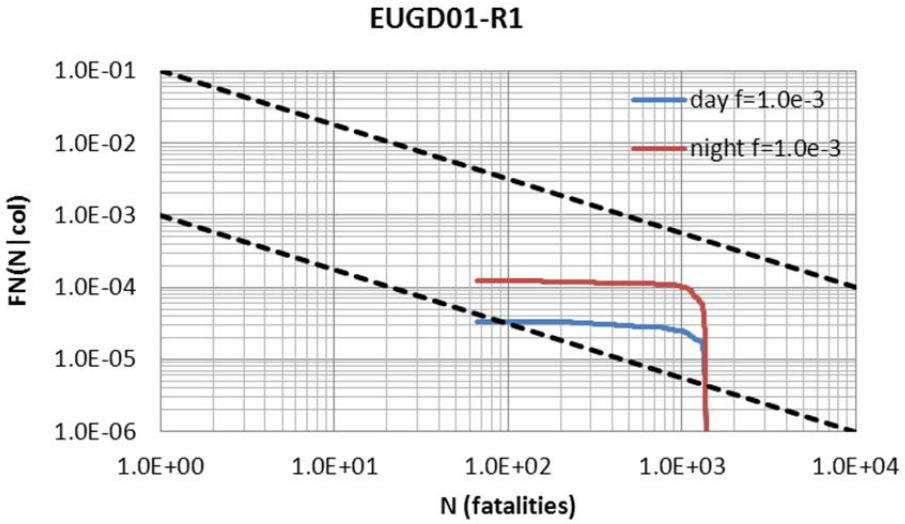

Frequency = 5.0E-04

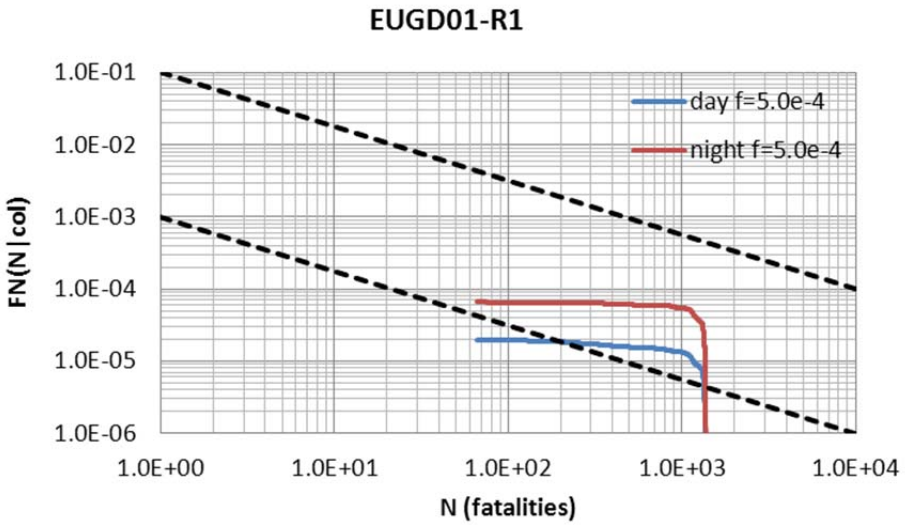

Frequency = 1.0E-02

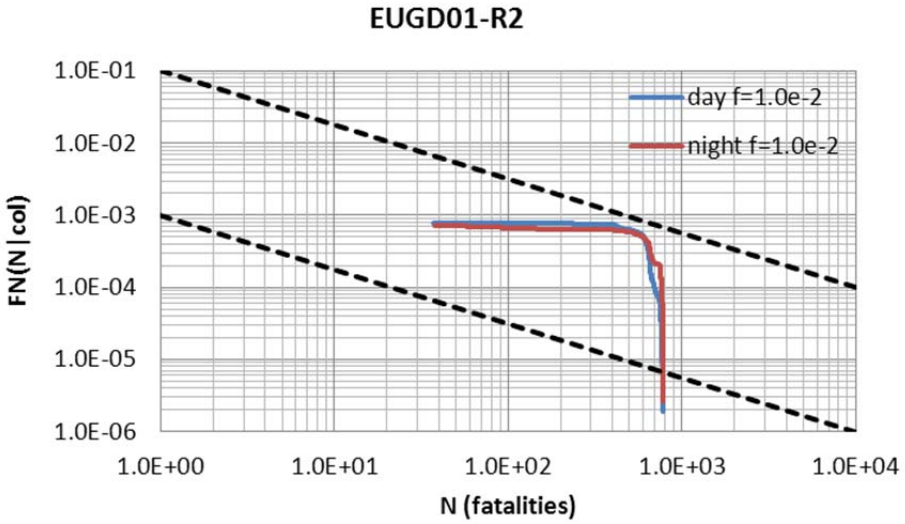

Frequency = 5.0E-03

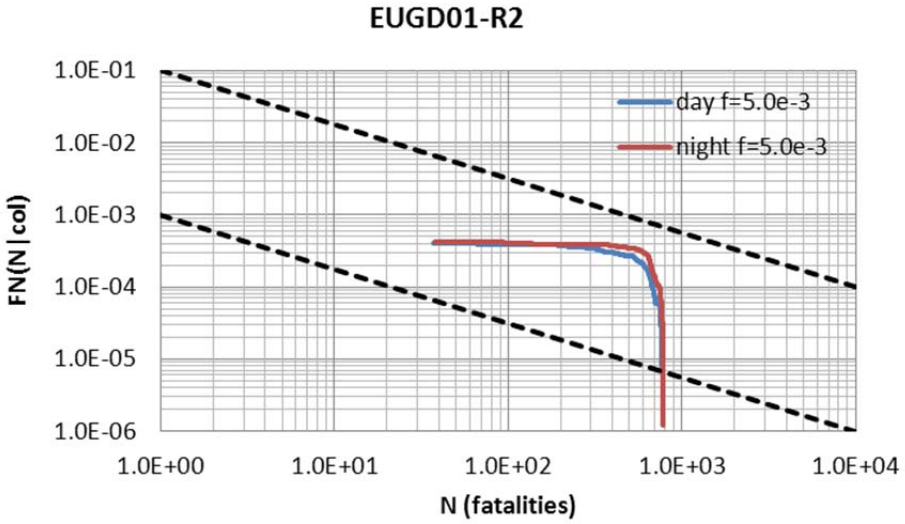

Frequency = 1.0E-03

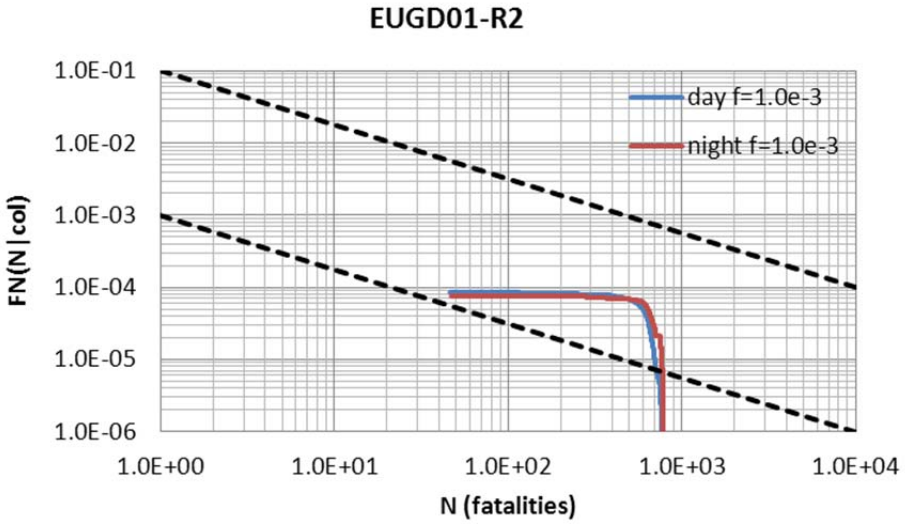

Frequency = 5.0E-04

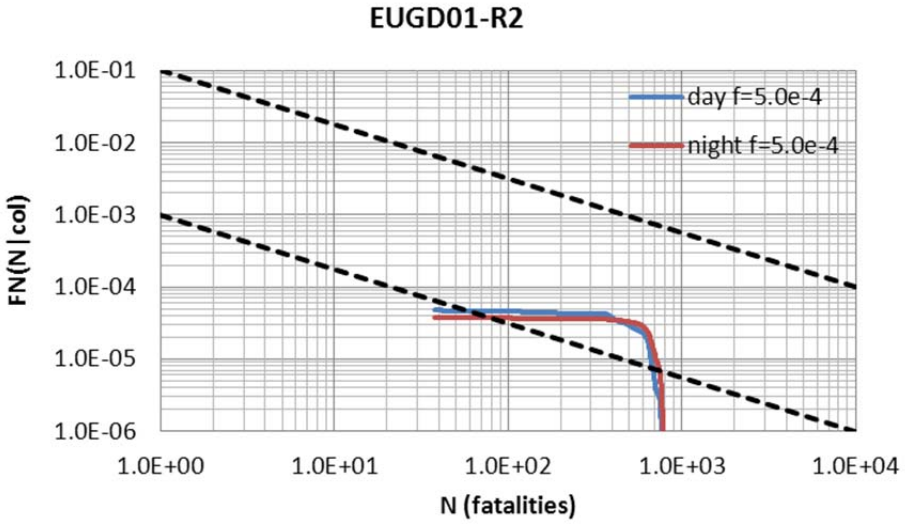

Appendix VI: MC simulation setups for grounding

EUGD01-C1: All

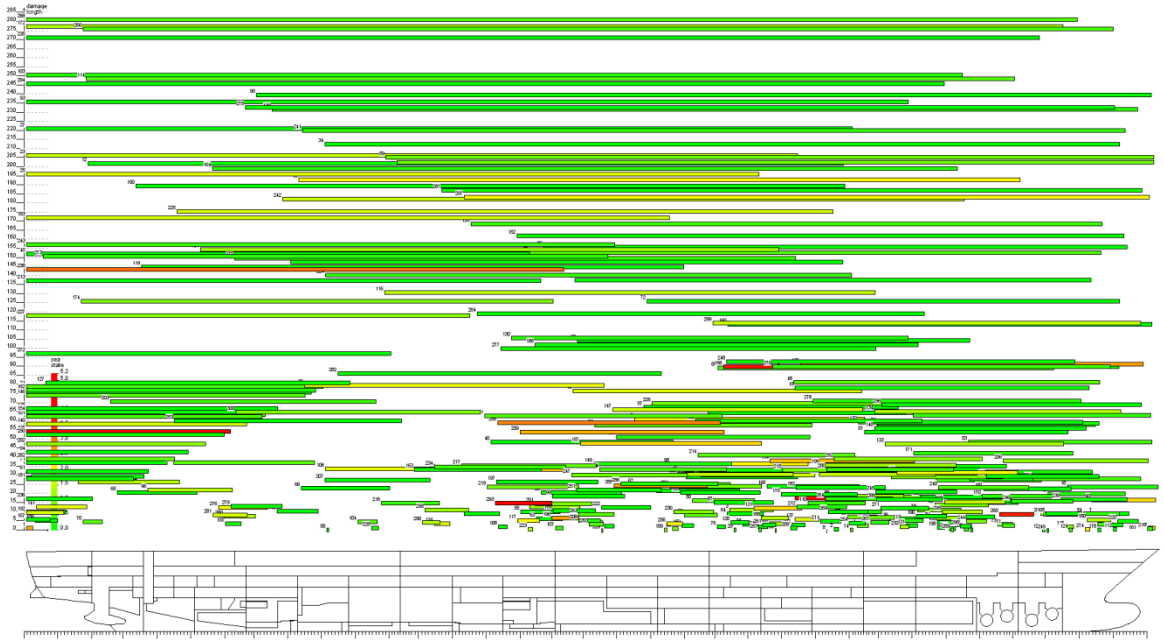

EUGD01-C1: Simulated

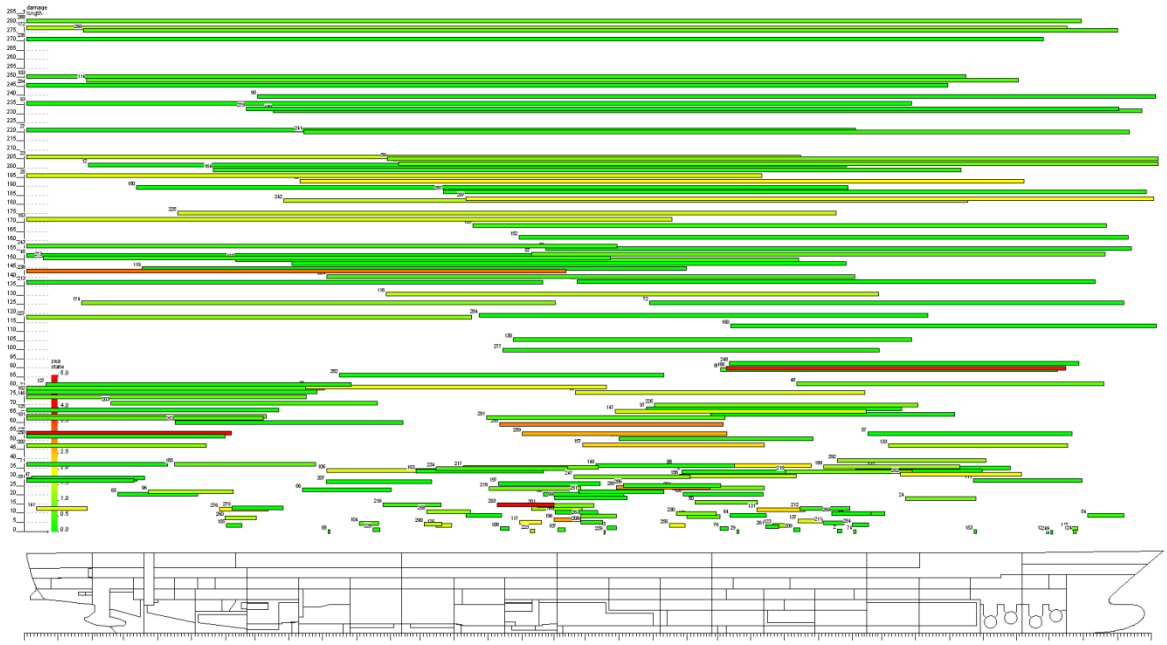

EUGD01-C1: Lost

EUGD01-C2: All

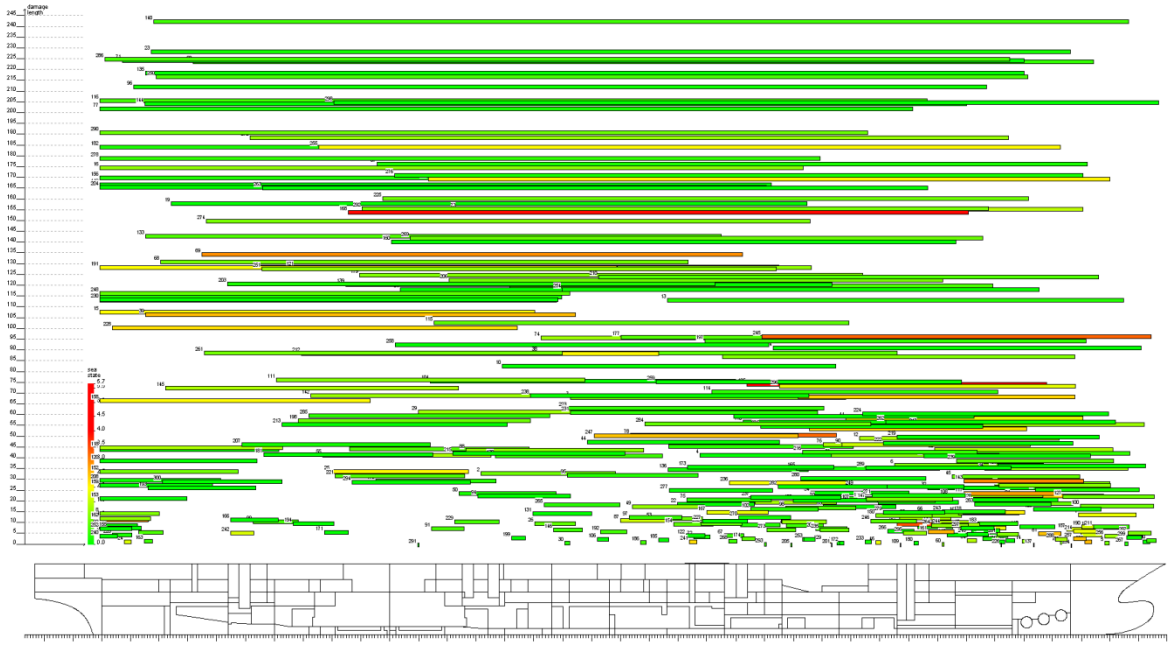

EUGD01-C2: Simulated

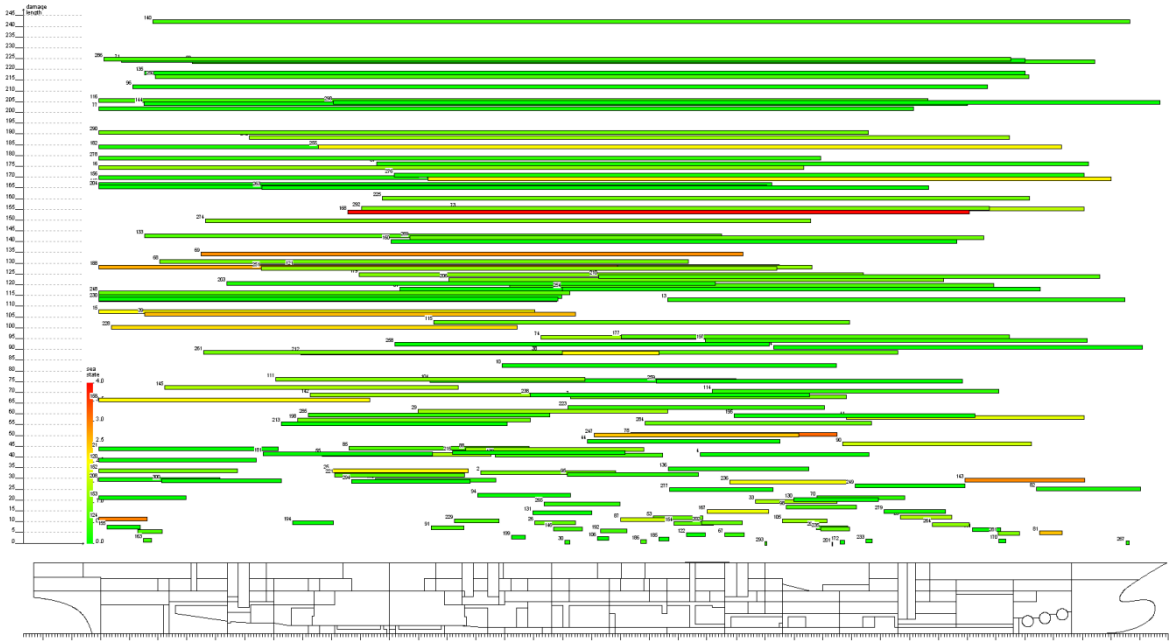

EUGD01-C2: Lost

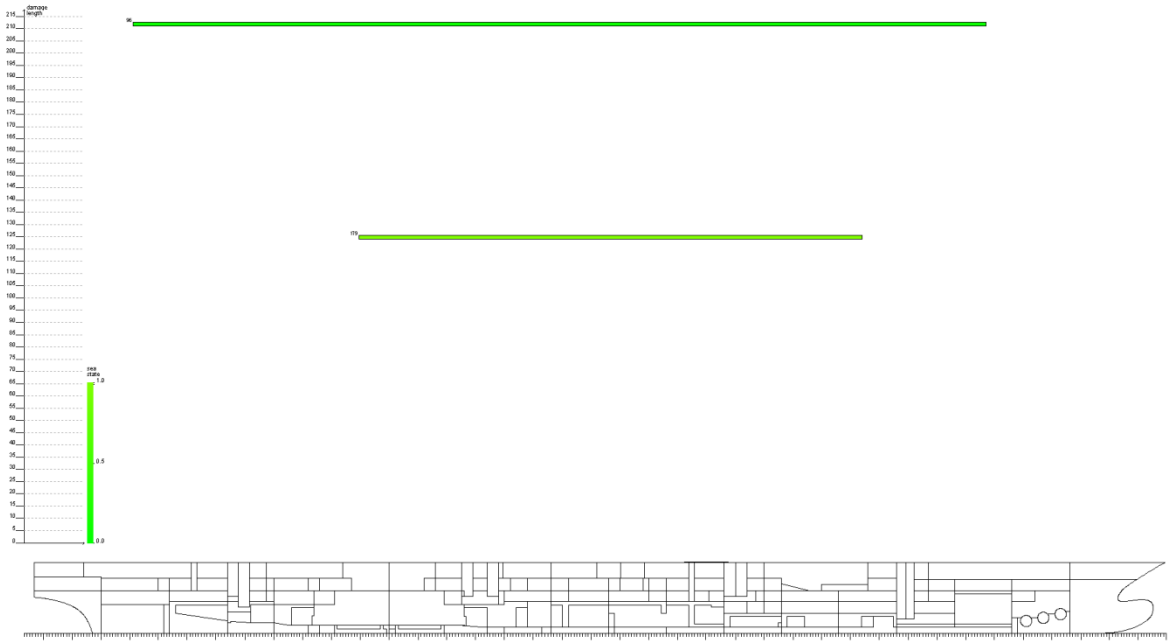

EUGD01-R1: All

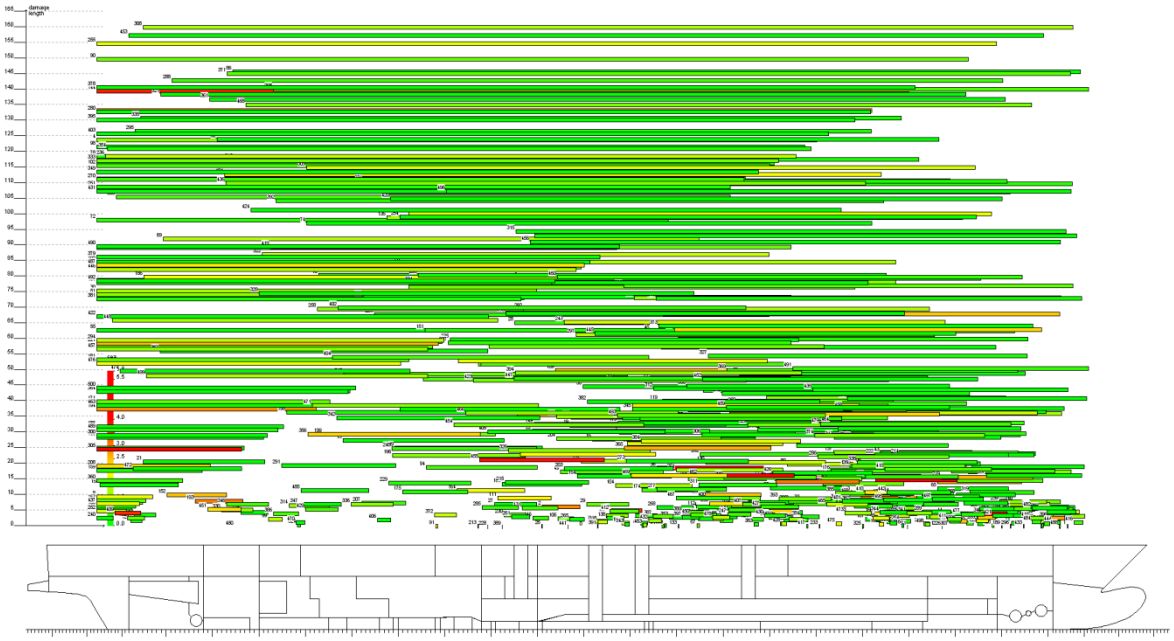

EUGD01-R1: Simulated

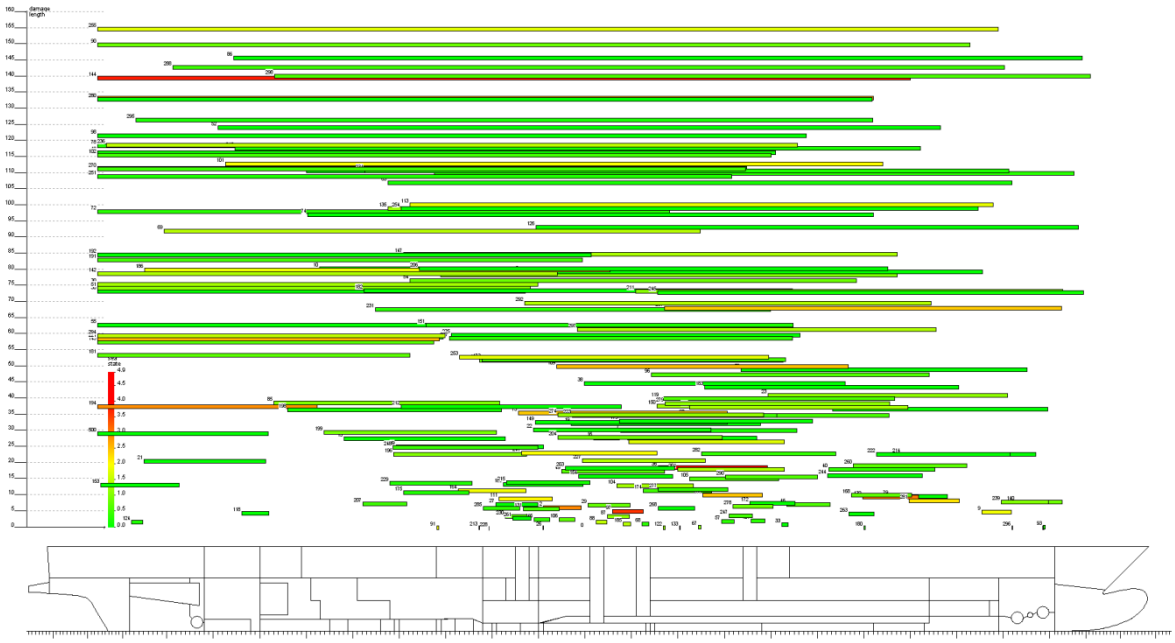

EUGD01-R2: All

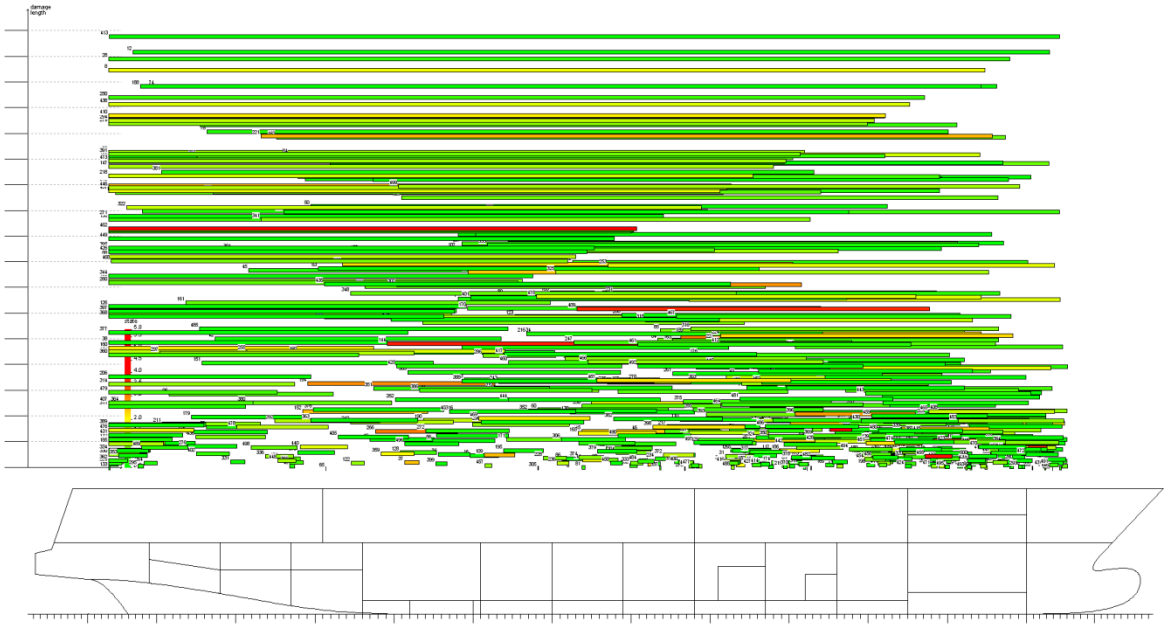

EUGD01-R2: Simulated

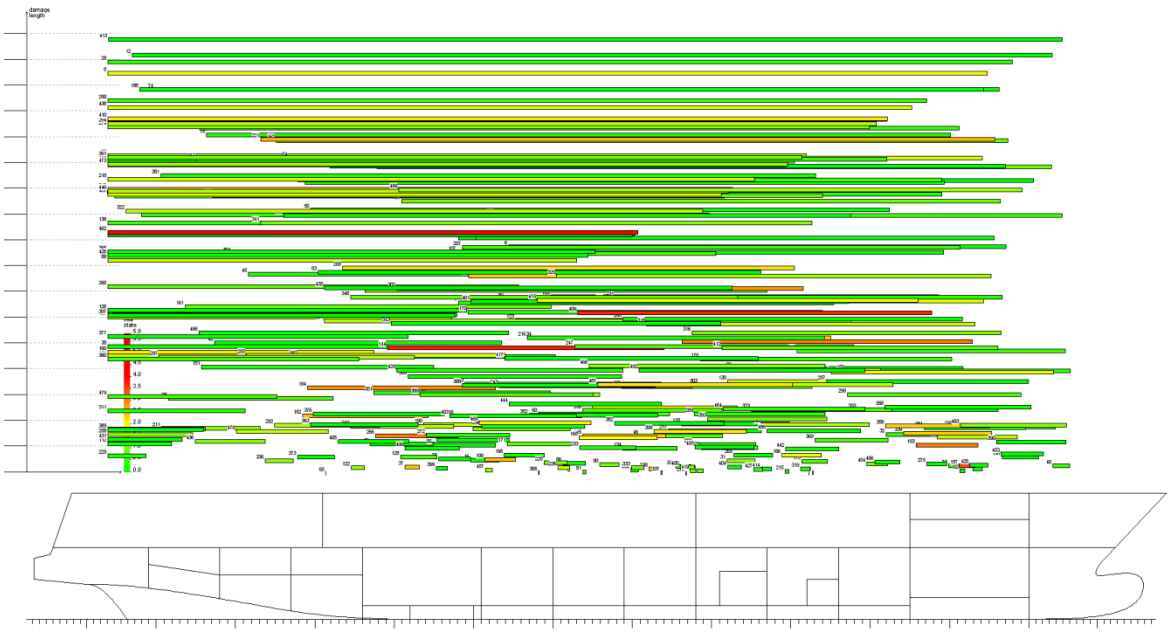

Appendix VII: PDFs for grounding damages

The following table shows the generated (sampled) CDFs (random) compared to the input ones (slender)

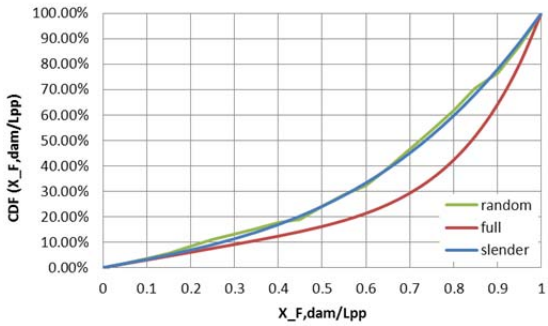

Location of leading edge of damage (CDF)

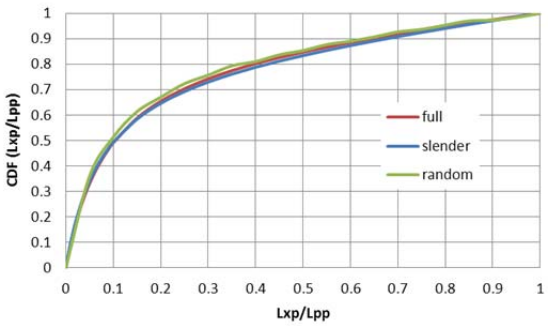

Length of damage (CDF)

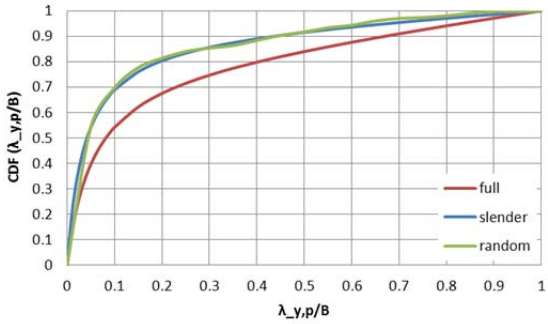

Width (CDF)

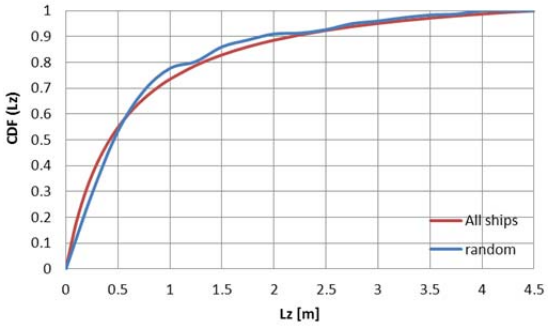

Penetration (CDF)

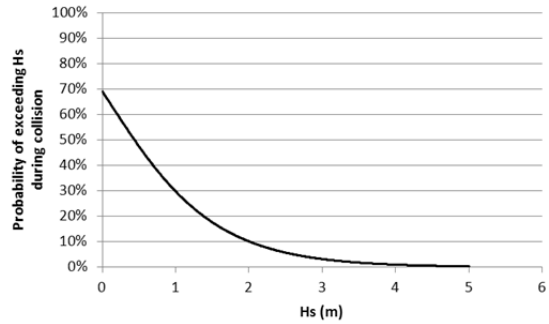

sea-state at time of collision / grounding (PDF)

Table below shows an example of how the final probability distribution functions (simulated) compare to the input ones (random)

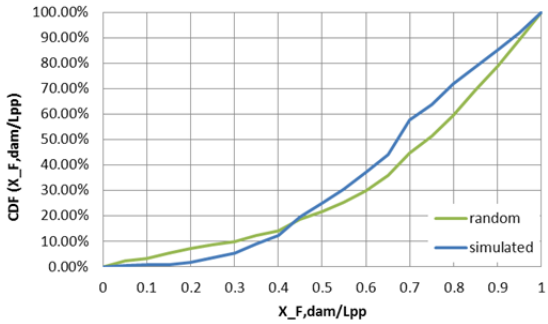

a. Location of leading edge of damage (CDF)

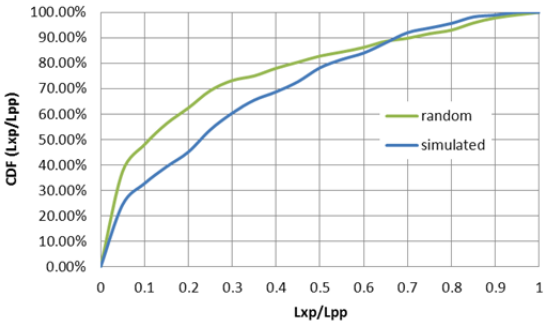

b. Length of damage (CDF)

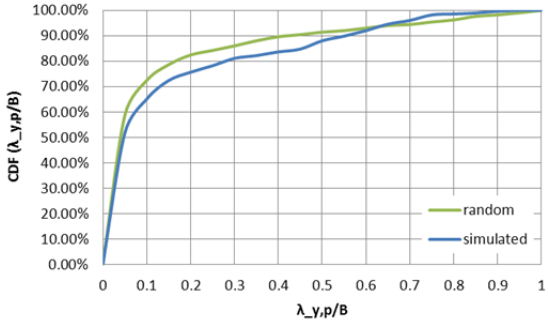

c. Width (CDF)

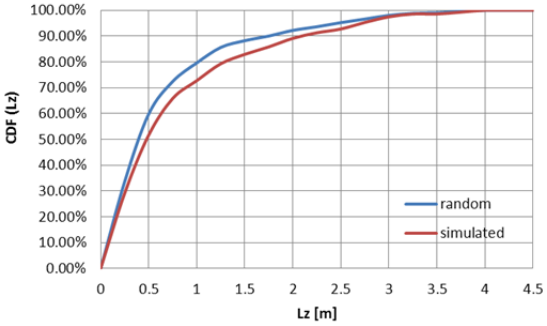

d. Penetration (CDF)

Appendix VIII: MC simulation setups for collision.

EUGD01-C1; 500 damages

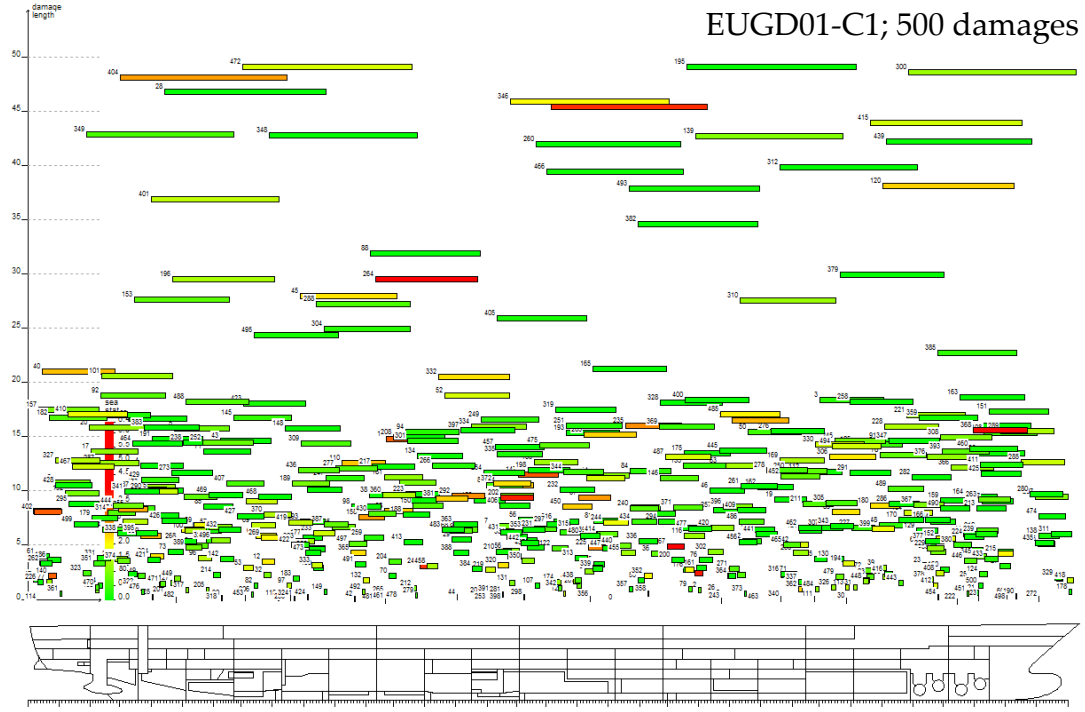

EUGD01-C2; 500 damages

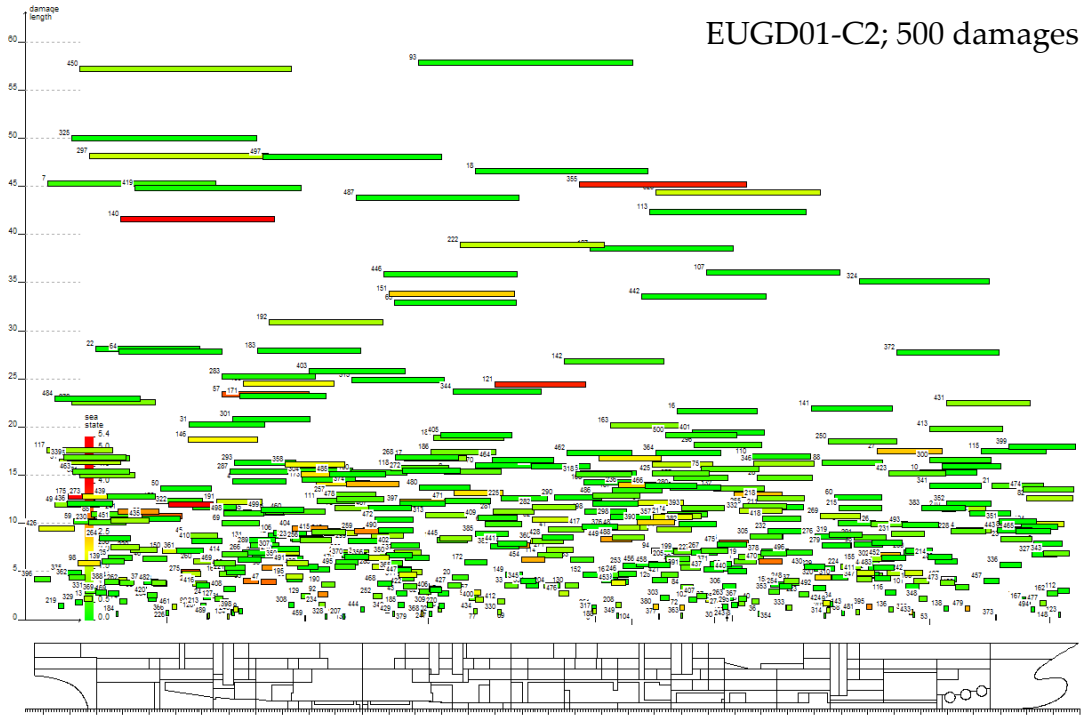

EUGD01-R1; 300 damages

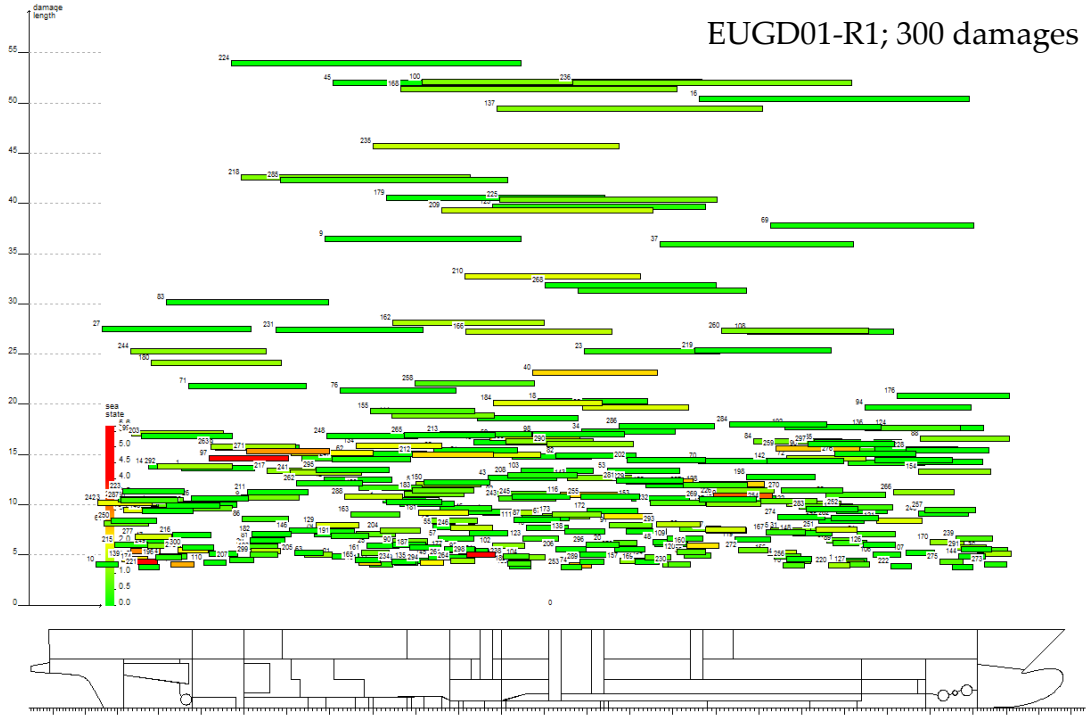

EUGD01-R2; 300 damages

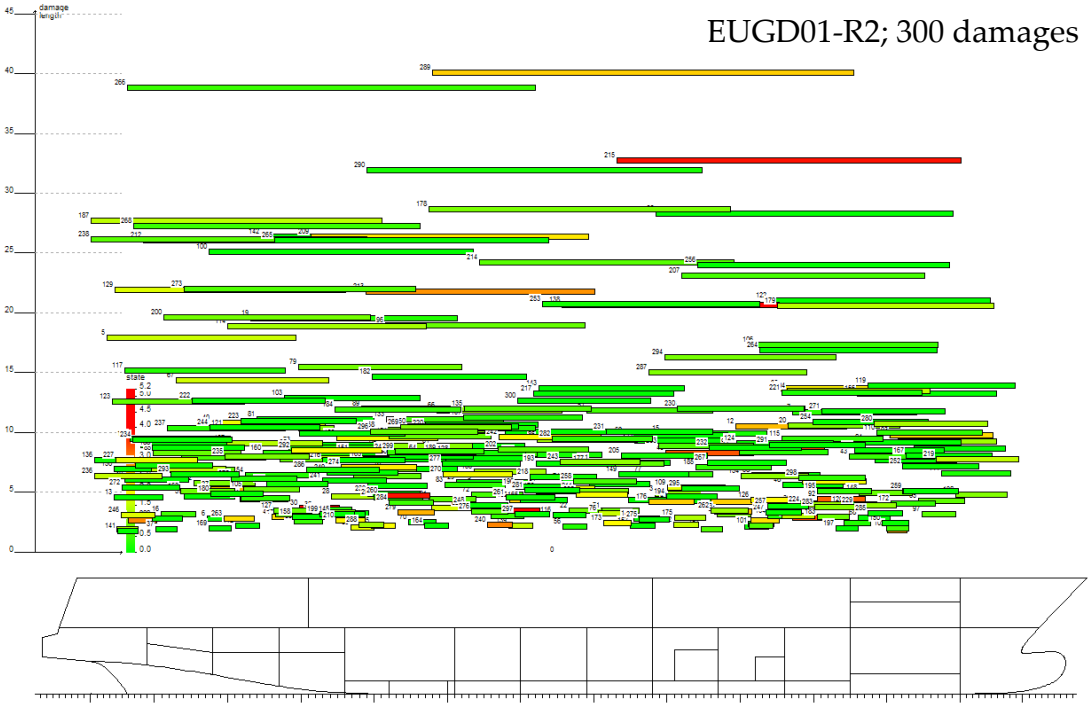

Appendix IX: RoPax vessels used in side casing study

EUGD01-R1 original

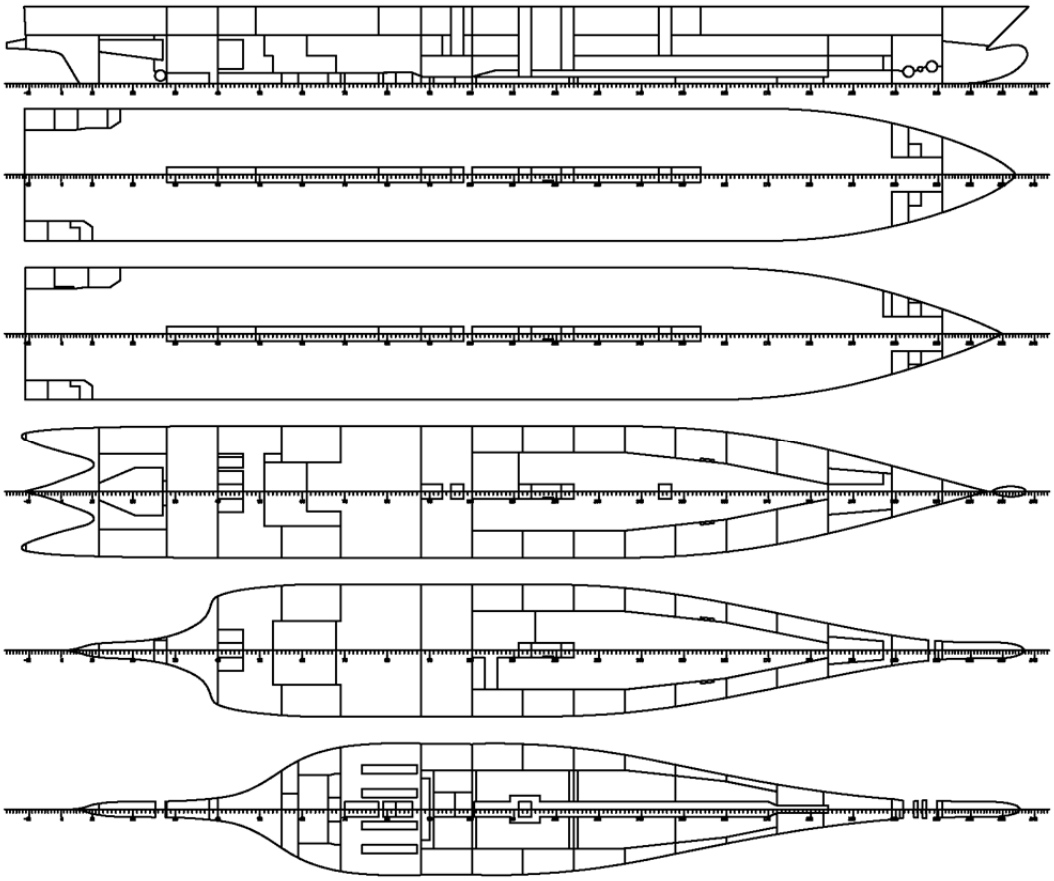

EUGD01-R1 modified

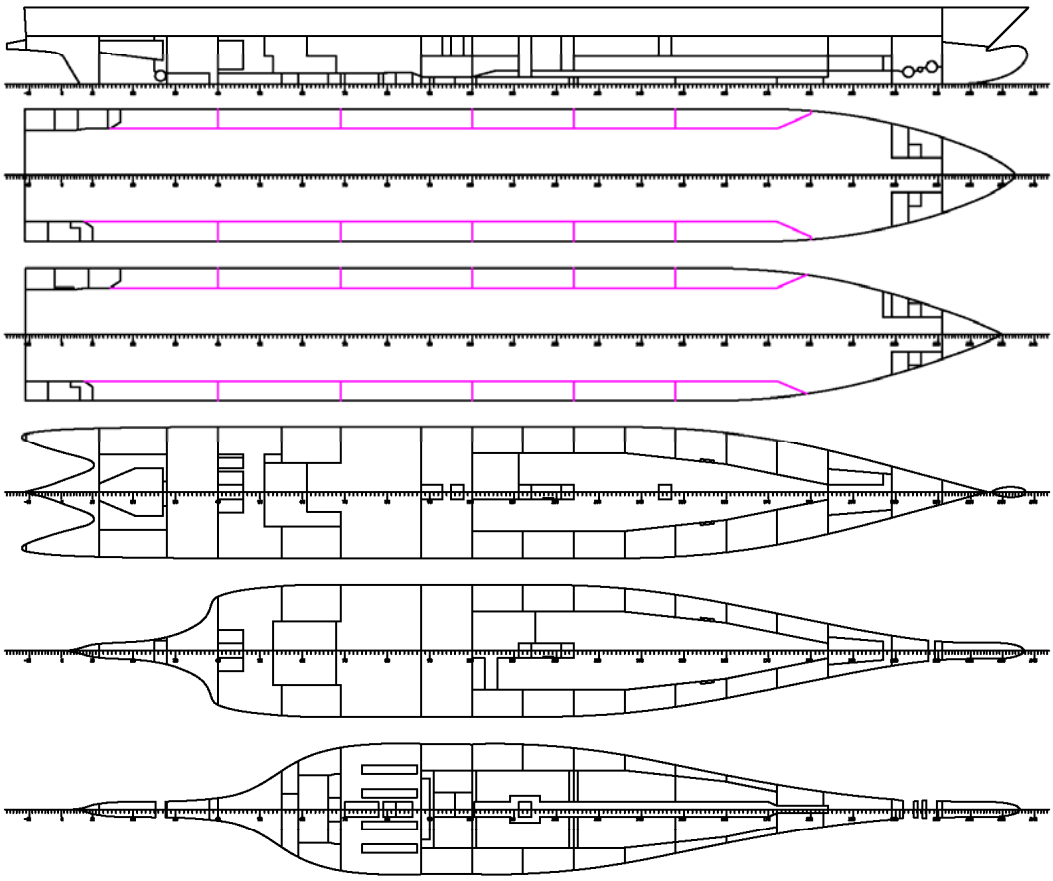

MCRP08-2B original

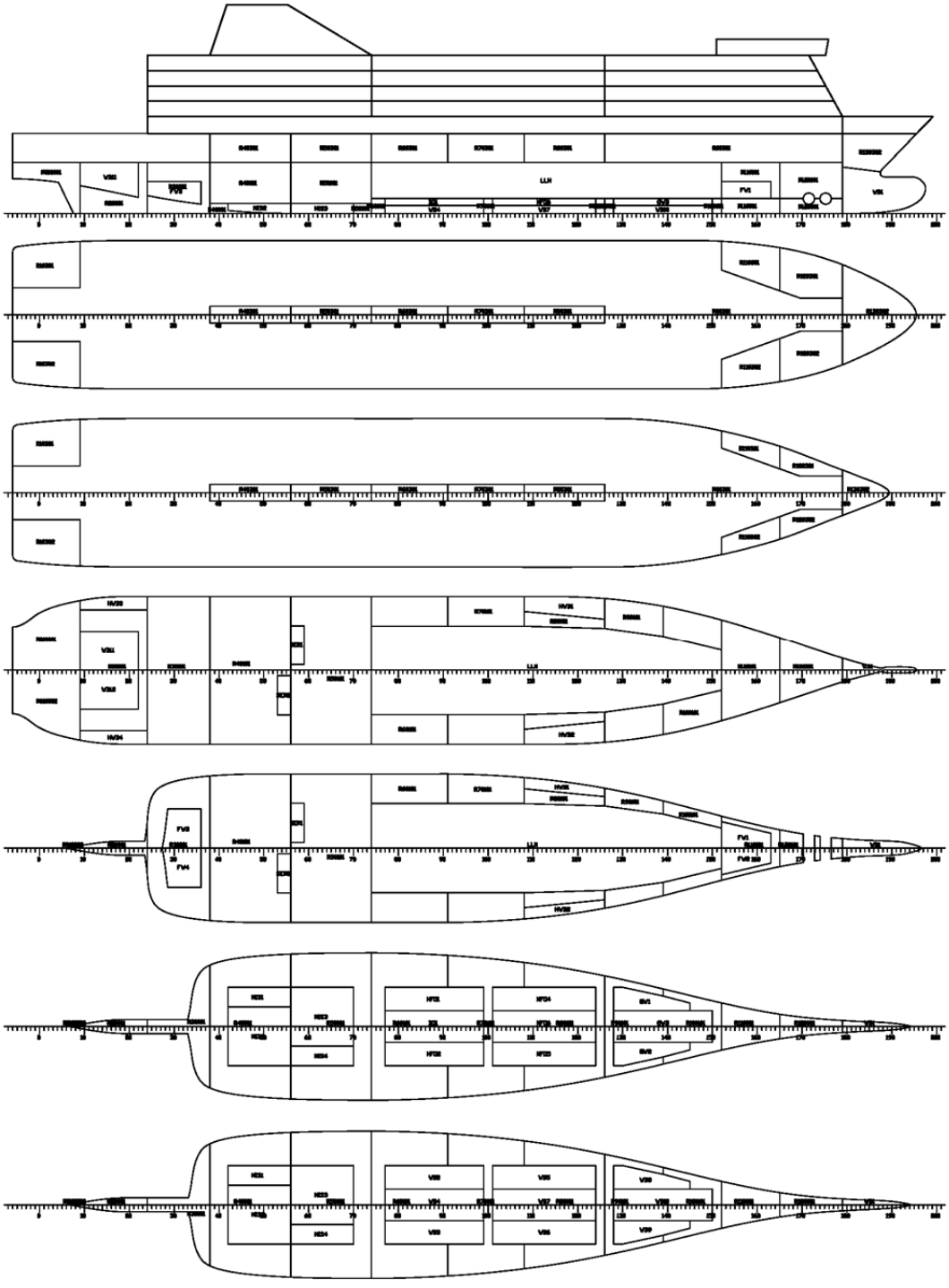

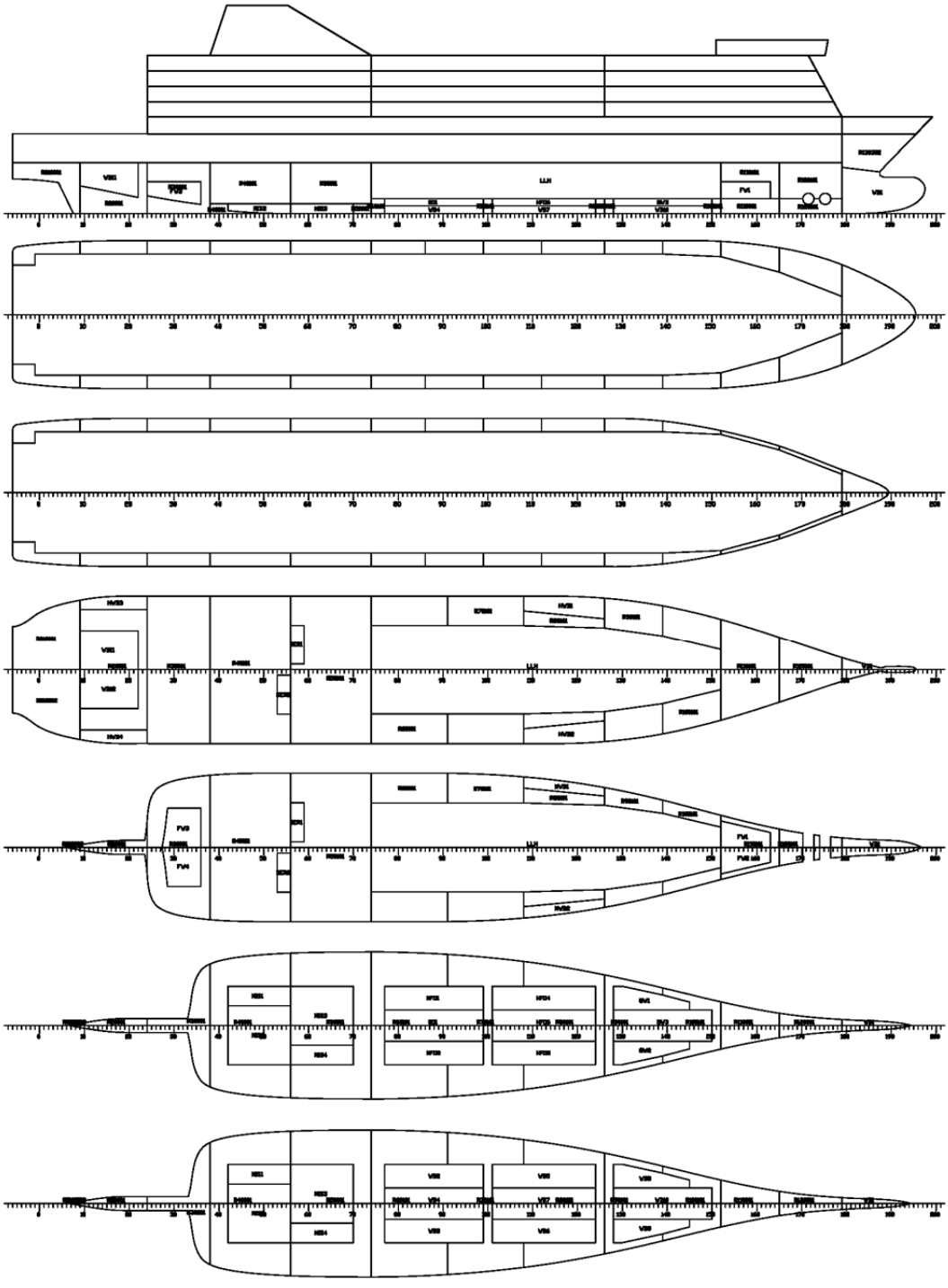

MCRP08-2B 2nd modified version

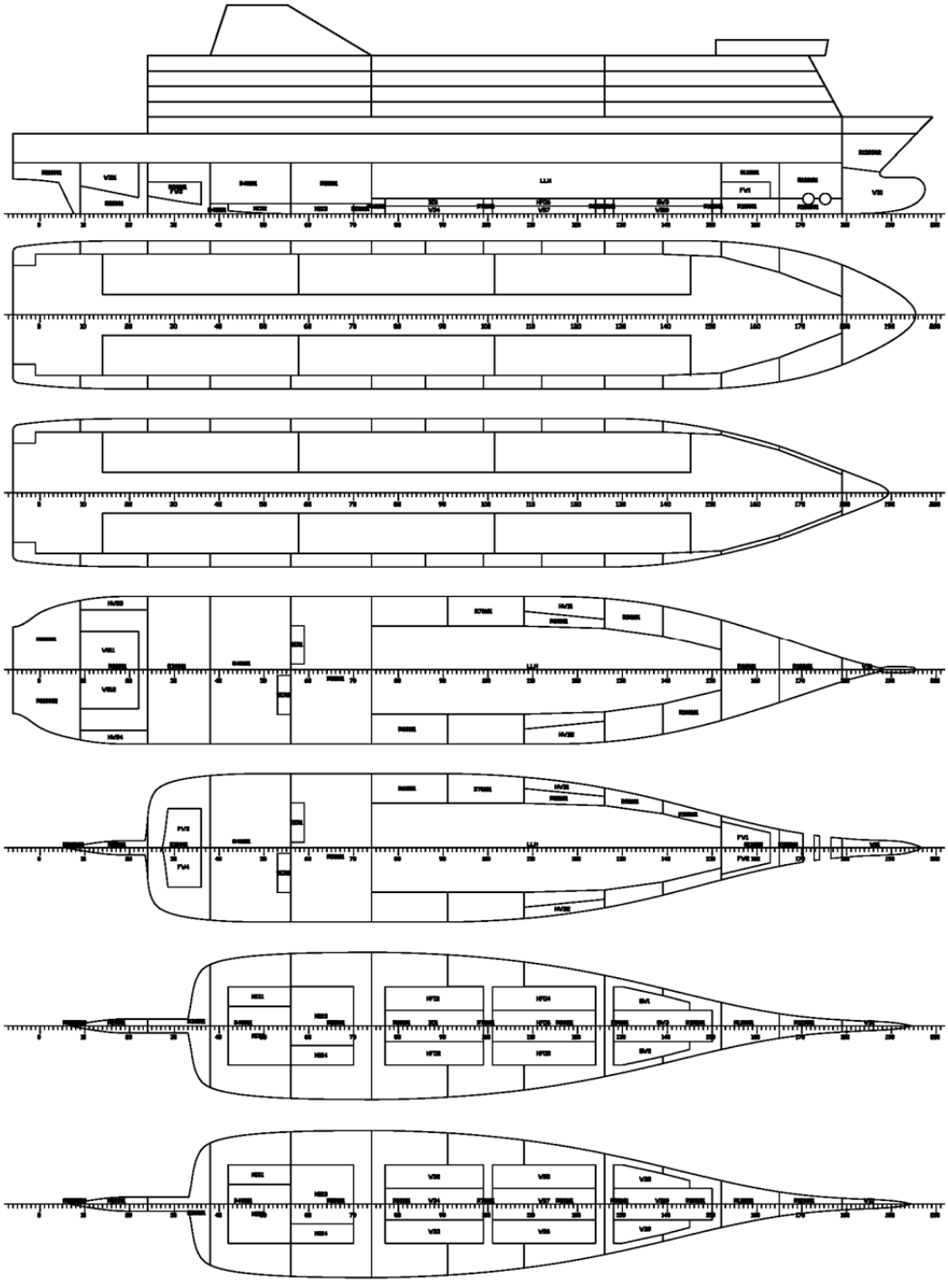

MCRP05-2A original

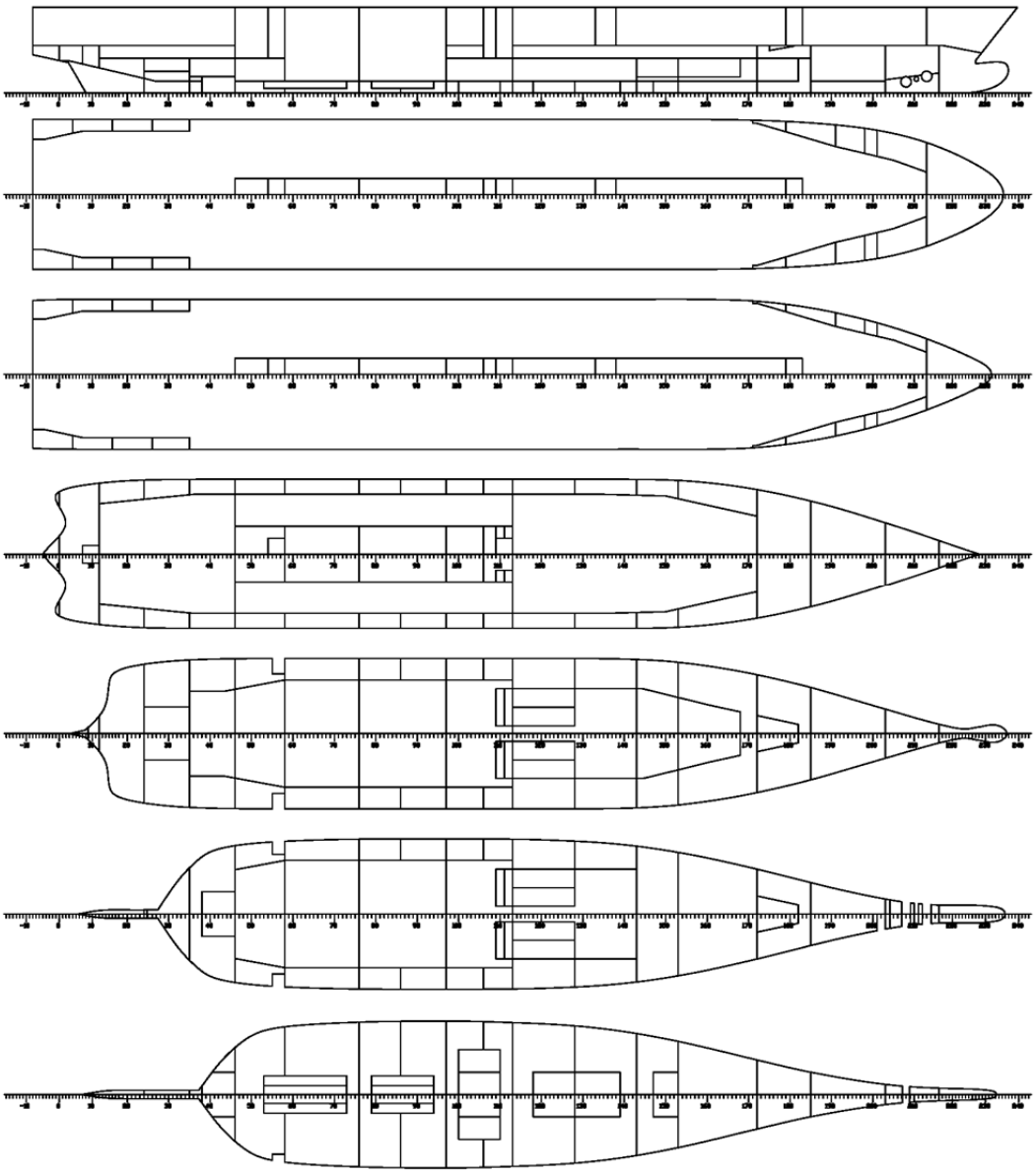

MCRP05-2A modified

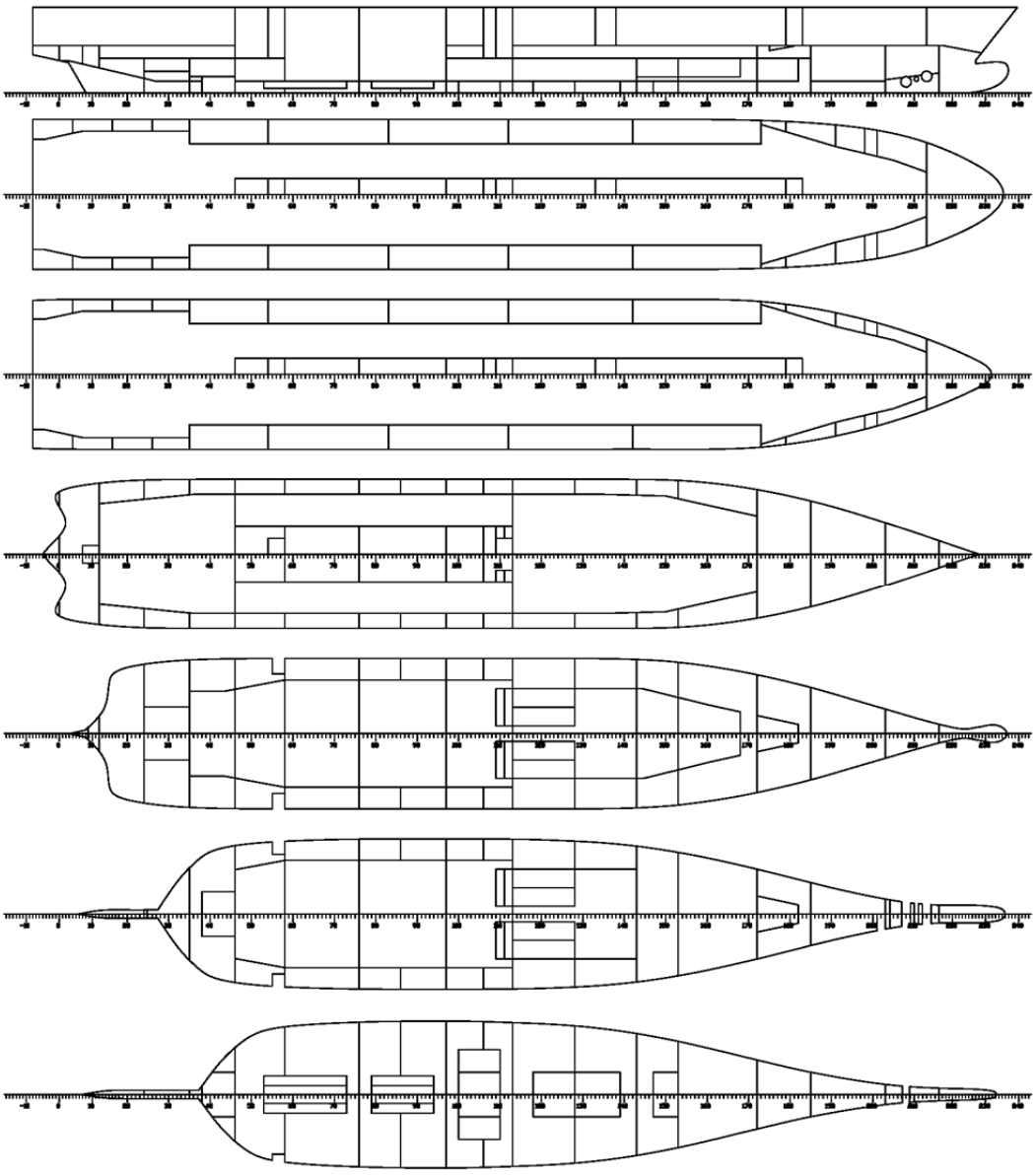

Appendix X: Nomenclature

FSA	Formal Safety Assessment
PBS	Performance-Based Survivability
SAFEDOR	SAFE Design and Operation
UGD	Univariate Geometric Distribution
HARDER	EC project "Harmonisation of Rules and Design Rationale"
GOALDS	EC project "GOAL-based Damage Stability"
SOLAS	Safety of Life at Sea
SA	Stockholm Agreement
SSRC	Ship Stability Research Centre
RoPax	Roll on/off Passenger vessels
Ro-Ro	Roll on/off vessel
EU	European Union
EC	European Commission
CDF	Cumulative Distribution Function
PDF	Probability Density Function
JONSWAP	Joint North Sea Wave Analysis Project
LLH	Long Lower Hold (RoPax)

SRtP	Safe Return to Port
s-factor	SOLAS 2009 formulation for survivability
p-factor	SOLAS 2009 formulation for probability of damage extent
Index-A	SOLAS 2009 probabilistic index of subdivision
MCA	UK Maritime and Coastguard Agency
Pf	Probability to capsize
SWD	Semi-watertight doors
WTD	Watertight doors
SEM	Static Equivalent Method
LPP	Length between perpendiculars
B	Beam
BM	Moulded beam
D (or D1)	Depth at main deck
T	Draft
Td	Draft in damaged condition
FB	Freeboard